

ชุดลักษณะระดับจุลภาคของชั้นหินที่มีหอยกาบคู่จำพวกอะลาโทคอนคิต
อายุเพอร์เมียนตอนกลาง ในพื้นที่เขาสมโภชน์ จังหวัดลพบุรี
ประเทศไทยตอนกลาง

นายมงคล อุดชาชน

วิทยานิพนธ์นี้เป็นส่วนหนึ่งของการศึกษาตามหลักสูตรปริญญาวิทยาศาสตรดุษฎีบัณฑิต

สาขาวิชาชีววิทยาสิ่งแวดล้อม

มหาวิทยาลัยเทคโนโลยีสุรนารี

ปีการศึกษา 2550

**MICROFACIES OF MIDDLE PERMIAN
ALATOCONCHID-BEARING STRATA IN KHAO
SOMPHOT LOCALITY, LOPBURI PROVINCE,
CENTRAL THAILAND**

Mongkol Udchachon

A Thesis Submitted in Partial Fulfillment of the Requirements for the

Degree of Doctor of Philosophy in Environmental Biology

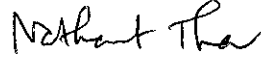
Suranaree University of Technology

Academic Year 2007

**MICROFACIES OF MIDDLE PERMIAN ALATOCONCHID-
BEARING STRATA IN KHAO SOMPHOT LOCALITY,
LOPBURI PROVINCE, CENTRAL THAILAND**

Suranaree University of Technology has approved this thesis submitted in partial fulfillment of the requirements for the Degree of Doctor of Philosophy.

Thesis Examining Committee



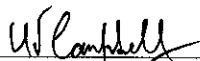
(Asst. Prof. Dr. Nathawut Thane)

Chairperson



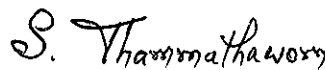
(Dr. Chongpan Chonglakmani)

Member (Thesis Advisor)



(Dr. Hamish Campbell)

Member



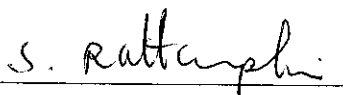
(Assoc. Prof. Dr. Sompong Thammathaworn)

Member



(Dr. Pongthep Suwanwaree)

Member



(Assoc. Prof. Dr. Saowanee Rattanaphani)

Vice Rector for Academic Affairs



(Assoc. Prof. Dr. Prapan Manyum)

Dean of Institute of Science

มงคล อุดชาชน : ชุดลักษณะระดับจุลภาคของชั้นหินที่มีหอยกาบคู่จำพวกอะลาโทคอนคิด
อายุเพอร์เมียนตอนกลาง ในพื้นที่เขาสม โภชน์ จังหวัดลพบุรี ประเทศไทยตอนกลาง

(MICROFACIES OF MIDDLE PERMIAN ALATOCONCHID-BEARING
STRATA IN KHAO SOMPHOT LOCALITY, LOPBURI PROVINCE,
CENTRAL THAILAND) อาจารย์ที่ปรึกษา : ดร.จงพันธ์ จงลักษณะณี, 233 หน้า.

การศึกษานี้มีจุดประสงค์เพื่อจำแนกชุดลักษณะระดับจุลภาคของหินคาร์บอนเนต บริเวณ
ตอนบนของหน้าตัดชั้นหินในพื้นที่เขาสม โภชน์พร้อมทั้งประเมินลักษณะสภาพแวดล้อมของการ
สะสมตัว และมีจุดประสงค์เพื่อจำแนกอนุกรมวิธานของหอยกาบคู่จำพวกอะลาโทคอนคิด และบ่ง
บอก ลักษณะสภาพแวดล้อมบรรพกาล ผลการศึกษาพบว่าหินคาร์บอนเนตในพื้นที่ศึกษา
ประกอบด้วยสปีชีส์หลักของชุดลักษณะระดับจุลภาค ประกอบด้วยหินโคลนเนื้อปูน/หิน
แวกสโตน หินไบด์สโตนที่มีลักษณะเป็นชั้นบาง หินแวกสโตน/แพคสโตนของสาหร่ายและฟอ
แรม หินแวกสโตน/แพคสโตนของฟิโลยและเศษชีวภาพ หินแวกสโตน/หินแพคสโตน/หิน
โฟลทสโตนของหอยกาบคู่จำพวกอะลาโทคอนคิด หินแวกสโตน/หินแพคสโตน/หินเกรนสโตน
ของฟิวซิลินิด หินเกรนสโตนของเศษชีวภาพพอกคลุม หินไบโอสโตรม/หินโฟลทสโตนของ
ปะการัง หินแพคสโตนของไครนอย และหินกรวดเหลี่ยม/กรวดมนของคาร์บอนเนต สภาพแวดล้อม
ของการสะสมตัวของชุดลำดับชั้นหินนี้ประกอบด้วยสภาพแวดล้อมรอบระดับน้ำขึ้น-ลง และได้
ระดับน้ำขึ้น-ลง ที่มีสันดอนใต้น้ำชั้นในของลานทะเลตื้นเขตร้อน อะลาโทคอนคิดประกอบไปด้วย
Shikamaia (Tanchintongia) cf. perakensis และ *Saikraconcha cf. tunisiensis* โดยมีถิ่นที่
อยู่บริเวณลากูนเปิดและลากูนกึ่งกึ่งแคบและมีพื้นทะเลอ่อนนุ่ม การพบฟิวซิลินิดสกุล
Lepidolina, Yabeina, Conodofusiella, Sumatrina และฟิวซิลินิดชนิด *Colania douvillei*
ซึ่งอยู่ในโซนของฟิวซิลินิด *Lepidolina-Yabeina* สามารถกำหนดอายุของชุดลำดับชั้นหินเป็น
ช่วงปลายของตอนกลางยุคเพอร์เมียน คือ Midian (Capitanian)

สาขาวิชาชีววิทยา

ปีการศึกษา 2550

ลายมือชื่อนักศึกษา _____

ลายมือชื่ออาจารย์ที่ปรึกษา _____

ลายมือชื่ออาจารย์ที่ปรึกษาร่วม _____

ลายมือชื่ออาจารย์ที่ปรึกษาร่วม _____

MONGKOL UDCHACHON : MICROFACIES OF MIDDLE PERMIAN
ALATOCONCHID-BEARING STRATA IN KHAO SOMPHOT
LOCALITY, LOPBURI PROVINCE, CENTRAL THAILAND. THESIS
ADVISOR : CHONGPAN CHONGLAKMANI, Ph.D. 233 PP.

MICROFACIES/ALATOCONCHIDS/ PALEOENVIRONMENT/LITHOFACIES
PERMIAN/ /MIDIAN/CARBONATE ROCKS/LIMESTONES/KHAO SOMPHOT/
THAILAND

The objective of this thesis is to describe and define microfacies of carbonate rocks in the uppermost section of the Khao Somphot locality with a view to evaluating their depositional environment. Additionally, it has been aimed at better determining the taxonomy of alatoconchid bivalves and clarifying their paleoenvironmental significance. As a result, carbonate rocks in the study locality are described in terms of ten major microfacies types including lime mudstone/wackestone, laminated bindstone, algal-foram wackestone/ packstone, bioclastic peloidal wackestone/ packstone, alatoconchid wackestone/ packstone/ floatstone, fusulinid wackestone/ packstone/ grainstone, coated bioclastic grainstone, coral biostrome/floatstone, crinoidal packstone, and carbonate breccia/ conglomerate. The depositional environment of this sequence is interpreted as peritidal and subtidal with internal shoaling of a tropical shallow marine platform. The alatoconchids are identified as *Shikamaia (Tanchintongia)* cf. *perakensis* and *Saikraconcha* cf. *tunisiensis*. Their habitat is interpreted as open lagoon and semi-restricted lagoon with soft substrate. The occurrence of fusulinids *Conodofusiella* sp., *Sumatrina* sp. and

Colania douvillei (Ozawa) which belong to the *Lepidolina-Yabeina* zone with the alatoconchids indicates that they are a Midian (Capitanian) age.

School of Biology

Academic Year 2007

Student's Signature _____

Advisor's Signature _____

Co-advisor's Signature _____

Co-advisor's Signature _____

ACKNOWLEDGEMENTS

The author would like to express his sincere appreciations to whom which have contributed to this thesis including his thesis advisor, Dr. Chongpan Chonglakmani for his encouragement for this research, the thesis co-advisor, Dr. Hamish Campbell for his enthusiastic support, continuous guidance and invaluable advice both in Thailand and New Zealand. These appreciations are also conveyed to Dr. Nathawut Thanee, the co-advisor and head of school of biology, for his effort to help and suggestion for methodology and event arrangements.

He is grateful to Mahsarakham University for three-year financial support. Thanks to Institute of Geological and Nuclear Science (GNS), Wellington for their welcome to access during the visit and University of Auckland for providing good resources at the library.

Many thanks are due to Dr. Jack Grant-Mackie and Diana for their supports and suggestions during the visit to Auckland. Sincere thanks are extended to Hamish's family members for their contribution during Wellington visit.

Special thanks to Ms. Hathaithip Thassanapak and Mr. Nitipon Noipow for their help during field observation, sampling and sample preparation.

Last but not least, his respect and love is expressed to his parent and his wife for their continuous inspiration, and financial support.

Mongkol Udchachon

CONTENTS

	Page
ABSTRACT IN THAI.....	I
ABSTRACT IN ENGLISH.....	II
ACKNOWLEDGMENTS.....	IV
CONTENTS.....	V
LIST OF TABLES.....	XI
LIST OF FIGURES.....	XII
LIST OF ABBREVIATIONS.....	XXIX

CHAPTER

I INTRODUCTION

1.1 Introduction.....	1
1.2 Research objectives.....	4
1.3 Scope and limitations.....	4
1.4 Research methodology.....	5

II GENERAL GEOLOGY

2.1 Permian tectonic history of Thailand.....	8
2.2 Permian lithostratigraphy of Thailand.....	11
2.2.1 Loei-Phetchabun region.....	14
2.2.2 Northern and Upper Western Region	28
2.2.3 Eastern Region	29
2.2.4 Lower Western and Southern Region.....	30

CONTENTS (Continued)

	Page
2.3 Geology of Khao Somphot and the study area.....	31
III LITHOSTRATIGRAPHY AND MICROFACIES	
3.1 Introduction.....	42
3.2 Lithostratigraphy.....	45
3.3 Microfacies.....	50
3.3.1 MF1: Lime mudstone/ wackestone.....	51
3.3.3.1 MF1a: Lime mudstone.....	51
3.3.3.2 MF1b: Fenestral mudstone.....	54
3.3.3.3 MF1c: Bioclastic wackestone.....	56
3.3.2 MF2: Laminated bindstone.....	58
3.3.2.1 MF2a: Laminated bindstone.....	58
3.3.2.2 MF2b: Fenestral bindstone.....	60
3.3.3 MF3: Algal-foram wackestone/packstone.....	62
3.3.3.1 MF3a: Algal-foram wackestone.....	63
3.3.3.2 MF3b: Algal-foram packstone.....	63
3.3.4 MF4: Bioclastic-peloidal wackestone/packstone.....	65
3.3.4.1 MF4a: Bioclastic-peloidal wackestone.....	65
3.3.4.2 MF4b: Bioclastic-peloidal packstone.....	66
3.3.5 MF5: Alatoconchid facies.....	68
3.3.5.1 MF5a: Alatoconchid floatstone/rudstone (coquinites).....	68
3.3.5.2 MF5b: Alatoconchid biostrome.....	79

CONTENTS (Continued)

	Page
3.3.6 MF6: Fusulinid facies (wackestone/packstone/grainstone).....	84
3.3.6.1 MF6a: Fusulinid wackestone	84
3.3.6.2 MF6b: Fusulinid packstone	86
3.3.6.3 MF6c: Fusulinid grainstone	88
3.3.7 MF7: Coated bioclastic grainstone	90
3.3.8 MF8: Coral biostrome/ floatstone	92
3.3.8.1 MF8a: Coral biostrome	92
3.3.8.2 MF8: Coral floatstone	96
3.3.9 MF9: Crinoidal packstone (encrinites)	97
3.3.10 MF10: Limestone breccia/conglomerate	98
3.3.10.1. MF10a: Mass-flow breccia	98
3.3.10.2 MF10b: Intraformational conglomerate/breccia	100
3.3.10.3 MF10c: Polymict channel conglomerate	100
3.3.10.4 MF10d: Solution-collapse breccia	102
IV PALEONTOLOGY	
4.1 General background on alatoconchid bivalves	117
4.2 Morphology and taxonomy of alatoconchids	119
4.3 Key foraminifers and algae.....	123
V INTERPRETATION AND DISCUSSION	
5.1 Depositional environments	125
5.1.1 Peritidal domain.....	127

CONTENTS (Continued)

	Page
5.1.1.1 Depositional environment of lime mudstone (MF1a).....	127
5.1.1.2 Depositional environment of fenestral mudstone (MF1b).....	129
5.1.1.3 Depositional environment of wackestone (MF1c).....	129
5.1.1.4 Depositional environment of laminated bindstone (MF2a).....	130
5.1.1.5 Depositional environment of fenestral bindstone (MF2b).....	131
5.1.1.6 Depositional environment of algal-foram wackestone (MF3a).....	131
5.1.1.7 Depositional environment of intraformational conglomerate/breccia (MF10b).....	132
5.1.1.8 Depositional environment of polymict channel conglomerate (MF10c).....	132
5.1.1.9 Depositional environment of solution-collapse breccia (MF10d).	133
5.1.2 Subtidal domain.....	133
5.1.2.1 Depositional environment of algal-foram packstone (MF3b).....	134
5.1.2.2 Depositional environment of bioclastic-peloidal wackestone/packstone (MF4a; b).....	134
5.1.2.3 Depositional environment of thin-shell alatoconchid rudstone (MF5a1).....	135
5.1.2.4 Depositional environment of thick-shell alatoconchid rudstone (MF5a2).....	136

CONTENTS (Continued)

	Page
5.1.2.5 Depositional environment of thick-shell alatoconchid floatstone (MF5a3).....	136
5.1.2.6 Depositional environment of alatoconchid biostrome with peloidal wackestone matrix (MF5b1).....	138
5.1.2.7 Depositional environment of fusulinid wackestone (MF6a).....	139
5.1.2.8 Depositional environment of fusulinid packstone/ grainstone (MF6b; c).....	140
5.1.2.9 Depositional environment of coated bioclastic grainstone (MF7).....	140
5.1.2.10 Depositional environment of coral biostrome (MF8a).....	141
5.1.2.11 Depositional environment of coral floatstone (MF8b).....	142
5.1.2.12 Depositional environment of crinoidal packstone (encrinites) (MF9).....	142
5.1.2.13 Depositional environment of mass-flow breccia (MF10a).....	143
5.2 Age constraints.....	143
5.3 Paleoenvironment of alatoconchids.....	144
5.4 Sequence stratigraphy and relative sea-level fluctuation.....	151

CONTENTS (Continued)

	Page
5.5 Diagenesis.....	156
5.5.1 Mechanical compaction.....	156
5.5.2 Pressure solution and stylolitization.....	158
5.5.3 Dolomitization.....	159
5.5.4 Silicification.....	162
5.5.5 Micritization.....	163
5.6 Benefit of this study and suggestion for the next research.....	164
VI CONCLUSION.....	165
REFERENCES.....	169
APPENDICES	
APPENDIX A ALATOCONCHID BIVALVES.....	188
APPENDIX B KEY FUSULINIDS AND SMALLER FORMINIFERS.....	213
APPENDIX C KEY ALGAE.....	230
CURRICULUM VITAE.....	233

LIST OF TABLES

Table	page
2.1 Lithostratigraphic correlation of Upper Paleozoic rocks in Thailand.....	16
2.2 Lithostratigraphic correlation of the Permian System in central and northeastern Thailand.....	20
3.1 Summary of microfacies types, subfacies, their characteristics and key fossils.....	108
5.1 Summary of lithologic units with brief explanations, microfacies types, some fusulinids and algae, and their depositional environment interpretation.....	126
5.2 Chronostratigraphic subdivision scheme for the Permian system. (modified after Jin et al., 1997).....	145

LIST OF FIGURES

Figure	Page
<p>1.1 Map of Thailand showing tectono-stratigraphic zones and alatoconchid localities. These localities are particularly well exposed intensively in the Phetchabun zone from Loei through Srakaeo. Other localities are located in Ratburi and Kiu Lom of different zones. (modified after Barr and MacDonald, 1991).....</p>	3
<p>1.2 Flow chart showing summary of the study methodology.....</p>	7
<p>2.1 Paleogeographic maps of the world Carboniferous through Triassic. In the Early Permian, Paleotethyan Ocean is located between Pangea supercontinent and the Cathaysian domain. During Late Permian, Cimmerian continent including Shan-Thai (S) and others translated to tropical realm close to Indochina (I), and South China (SC) of the Cathaysian domain. (after Wakita and Metcalfe, 2005).....</p>	9
<p>2.2 A: Tectonic map of Thailand and neighboring area. Nan Suture is marked by ophiolite. I=Indochina Block, SC=south China Block , K=Khorat Plateau, ST=Shan-Thai Block. B: Lithostratigraphic map of Thailand. It is composed of seven belts (see detail in C). C: Summary of Shan-Thai and Indochina components with geological time scale. Shan-Thai terrane consists of stratigraphic belts 1-5 while Indochina includes belts 6 and 7. These Blocks are divided by the Nan Suture. (after Bunopas, 1992).....</p>	10

LIST OF FIGURES (Continued)

Figure	Page
2.3	Tectonic map of mainland Southeast Asia showing proposed location between western edge of the subtropical climate terrane and eastern margin of the Gondwanan (glacial-marine) (after Helmcke, 1994).....12
2.4	A: Geographic map of Asia showing distribution of the Cimmerian continent (dash area). This continent is interpreted as Gondwana derived. In Thailand, this continent is located in the western part along Thai-Myanmar border. B: The Middle Permian paleogeographic map (after Wang et al., 2001). C: Geographic map showing tectonic subdivision of mainland Thailand (after Ueno, 2003).....13
2.5	Map of Thailand showing lithostratigraphic distribution of Permian rocks. These rocks can be categorized into 8 units that are exposed throughout Thailand except in the area of Northeastern Thailand. (modified after DMR, 1987)15
2.6	Simplified geologic map showing the Permian carbonate platform and siliciclastic basin along the western portion of the Khorat plateau (Indochina Block). The study locality is located in the southern part of the Khao Khwang platform in Lam Narai vicinity (Chai Badan) of Lopburi province. (modified after Chonglakmani and Fontaine, 1990).....24
2.7	Carbonate depositional environments and sub-environments of a carbonate platform in northeastern Thailand. (after Wielchowsky and Young, 1985).....25

LIST OF FIGURES (Continued)

Figure	Page
2.8	Schematic stratigraphic section of the Phetchabun-Lam Narai region. (after Chonglakmani and Fontaine, 1990).....27
2.9	Topographic map showing location of the study area. (modified after Royal Thai Survey Department, 1986).....32
2.10	Geologic map of the study area. The study area is occupied by Permian limestone. This map shows clastic rocks of the Khorat Group located to the east of the study area while the main area of volcanic rocks is located to the north. (modified after Nakornsri, 1976).....34
2.11	Stratigraphic log of Khao Somphot section. Alatoconchid-bearing strata are located in the upper most part of the section in strata of middle Guadalupian to late Guadalupian age. (after Wielchowsky and Young, 1985).....35
2.12	Topographic map showing study area which is located in the eastern foothill of Khao Somphot mountain range as shown in box. (modified after Royal Thai Survey Department, 1992).....40
2.13	Field photograph showing the study area and study sections. A: Study section 1-3. B: Study section 4 and 5. C: Part of topographic map showing limestone hills of the study locality with sections.....41
3.1	Lithostratigraphic units of the alatoconchid-bearing limestone sections, Khao Somphot locality.....49

LIST OF FIGURES (Continued)

Figure	Page
3.2 Outcrop photographs of limestones from Unit A with thin shell alatoconchid coquinite beds (MF5a1). A: Field photograph showing various limestone beds ranging from thin to thick bedded. B: Sketch of A, alatoconchid found in bed 2 and 4 while bed 3 contains MF1a, b. C: Field photograph maximized from A (as shown in box of B). D: Sketch of C. E; Magnification of C (as shown in box of D), showing densely packed thin-shell alatoconchid fragments embedded in thin bed of the middle part of photograph. F: Sketch of E, alatoconchid fragments shown in dark gray color in bed 4. (ruler for scale=15 cm).....	52
3.3 A: Field photograph of limestones. Lime mudstone with fenestral fabric occur in the upper part of this limestone succession (ruler as scale=15 cm). B: Photograph of rock slab showing medium gray mudstone with light brown dolomitic texture on top. C: Photomicrograph of lime mudstone (MF1a) showing mud dominated texture almost absent of fossils. D: Photomicrograph of fenestral mudstone (MF1b) from the transition between lime mudstone and true fenestral mudstone. Fenestral fabric is partly developed. E: Photomicrograph of fenestral mudstone showing well developed fenestral fabric with geopetal structure. F: Photomicrograph of fenestral mudstone showing open void of fenestral fabric which is occluded mainly by coarse calcite spar on top and floored by micrite. (All scale bar=500 μ m).....	55

LIST OF FIGURES (Continued)

Figure	Page
3.4 A: Photograph of rock slab of wackestone (sample no. M05). B: Photomicrograph showing bioclastic wackestone texture (MF1c, sample no 710). Allochems include miliolids (m), calcareous algae (c), fecal pellets (f), and fragments of <i>Vermiporella nipponica</i> (v). C: Photomicrograph of wackestone (sample no. 740). Geopetal structure is shown in gastropod (g) and in open void. Brachiopod fragment (b) is at top of view. D: Photomicrograph of wackestone from the same sample as C showing <i>Vermiporella nipponica</i> on the lower left with miliolids. Fecal pellet is occluded mainly in burrow. (All scale bar=500 μ m).....	57
3.5 A: Field photograph of bed containing bindstone (ruler=15 cm). B: Photograph of rock slab of bindstone. C: Photomicrograph of packed laminated bindstone (MF2a, sample no. 729). D: Photomicrograph of packed bindstone showing algal tube (<i>Vermiporella nipponica</i>) associated with peloids and bioclastic fragments (sample no. 753c). E: Photomicrograph of packed bindstone showing flattened algal tube (<i>Vermiporella nipponica</i>) arranged parallel to bedding plane with bioclastic fragments and peloids (sample no. 743sc1). F: Photomicrograph of bindstone (magnification of E). (All scale bar = 500 μ m).....	59
3.6 A: Field photograph showing limestone bed that contains fenestral bindstone. B. Photograph of rock slab with lamination in lower part (sample no. 729). C: Photomicrograph of fenestral bindstone (MF2b) showing irregular fenestral fabric in light gray layer. D:	

LIST OF FIGURES (Continued)

Figure	Page
<p>Photomicrograph of fenestral bindstone (magnification of C). (All scale bar=500 μm).....</p>	61
<p>3.7 A: Rock slab of algal-foram facies showing medium to dark gray with sand-size fossils embedded in matrix. B: Photomicrograph of algal-foram wackestone (MF3a, sample no. 704) showing miliolids associated with <i>Vermiporella nipponica</i>. C: Photomicrograph from the same sample as B showing meandering and branching forms of <i>Vermiporella nipponica</i>. D: Photomicrograph of algal-foram packstone (MF3b, sample no. 704b) showing densely packed texture of miliolids and calcareous algae with fusulinids (<i>Nankinella</i> sp.). (All scale bar=500 μm).....</p>	64
<p>3.8 A: An outcrop photograph of thickly bedded limestone containing bioclastic peloidal wackestone. B: Rock slab of bioclastic peloidal packstone (MF4b, sample no. 703c). C: Photomicrograph of bioclastic peloidal wackestone. D: Photomicrograph of the same sample as C. Smaller foraminifers (<i>Globivalvulina</i> sp.) are dominant in this view. E: Photomicrograph of bioclastic packstone (MF4b, sample no. 703c) showing packed bioclastic texture with geopetal structure in center. Smaller foraminifers (s), small gastropods (g) and ostracods (o) are common in this facies. F: Photomicrograph of bioclastic packstone (MF4b, sample no. 703a). (All scale bar=500μm).....</p>	67
<p>3.9 A: Field photograph of thin-shell alatoconchid beds (MF5a1). B: Field photograph of thin-shell alatoconchid facies (MF5a1). C:</p>	

LIST OF FIGURES (Continued)

Figure	Page
<p>Photomicrograph of densely packed peloidal bioclastic texture with black filamentous matter (sample no. 739). D: Magnification of C. E: Photomicrograph of bioclastic calcisiltite matrix from alatoconchid floatstone facies (sample no. 779). F: Photomicrograph of calcisiltite matrix of alatoconchid floatstone facies (sample no. 784). (C, E, F, scale bar =500 μm; D, scale bar=100 μm).....</p>	70
<p>3.10 Alatoconchid coquinite or tempestite. A: Field photograph showing large amount of alatoconchid fragments scattered in matrix (marker pen for scale=15 cm). B: Sketch of A, alatoconchid fragments shown in dark gray gastropod in spiral shape on right of bed 3 and 4. C; Field photograph of the same outcrop showing wavy undulation in upper part of bed (pen for scale=15cm). D: Sketch of C, showing alatoconchid fragments in dark gray, gastropod on left as spiral conch.....</p>	72
<p>3.11 A: Field photograph of alatoconchid rudstone (MF5c2). B: Rock slab of alatoconchid rudstone from A. C: Photomicrograph of bioclastic calcisiltite matrix of alatoconchid rudstone (sample no. 0537) with dispersed fragments and debris. D: Photomicrograph of bioclastic calcisiltite matrix of alatoconchid rudstone showing larger shell debris floated in calcisiltite with black micrite matrix (sample no. 0537). E: Photomicrograph showing another view of calcisiltite matrix of alatoconchid rudstone (sample no. 787).</p>	

LIST OF FIGURES (Continued)

Figure	Page
F: Photomicrograph showing bioclastic calcisiltite matrix of alatoconchid rudstone. (All scale bar=500µm).....	73
3.12 Field photograph of alatoconchid floatstone bed overlying fusulinid limestone and underlying non-laminated limestone (measuring tape for scale=2 m). B: Sketch of A, 6=alatoconchid floatstone bed; alatoconchids as dark gray specimens; blue patches indicate nodular cherts, 5=fusulinid limestone bed, 7=non-laminated limestone bed. C: Enlargement of field photograph from A. D: Sketch of C, showing alatoconchids in dark gray floated in matrix with various directional arrangements with eroded undulatory base. E: Alatoconchid bed (maker pen for scale=15 cm). F; Sketch of E, 4=non-laminated limestone, 5-7 same as above.....	75
3.13 A: Field photograph of alatoconchid-bearing beds. B: Sketch of A, alatoconchids occur in 2, 3 and 4, abundant fusulinids occur in 1, laminated limestone in 5 and 6. C: Field photograph, magnification of bed 2. D: Sketch of C showing alatoconchid with good preservation at top, alatoconchid fragments (in dark gray) floated with massive coral fragments (lower right) and other shelly fragments. E: Enlargement field photograph of bed 3. F: Sketch of E, showing densely packed alatoconchid rudstone or coquinite bed, alatoconchid in dark gray fragments. (ruler for scale=15cm).....	76

LIST OF FIGURES (Continued)

Figure	Page
3.14 Alatoconchid floatstone bed. A: Field photograph of outcrop. B: Sketch of A, 1=non-laminated limestone with lenticular cherts in blue color, 2=alatoconchid floatstone bed with nodular chert at top, 3=non-laminated bed with laminated thin layer intercalation (notebook for scale=17 cm). C: Details of bed 2, showing alatoconchid floatstone. D: Sketch of C, most alatoconchids are displayed in double-valved condition.....	77
3.15 A-B: Photomicrograph of calcisiltite matrix of alatoconchid floatstone (sample no. 760). Larger fragments including micritic fusulinids, brachiopods, and alatoconchid shell fragments are floated in calcisiltite matrix. C: Photomicrograph of alatoconchid shell showing granular calcite of internal layer on left and prismatic calcite external layer on right (PPL). D: Photomicrograph of alatoconchid shell (XPL). (All scale bar=500 μm).....	78
3.16 Alatoconchid-bearing limestone beds with alatoconchids in life-position. A: Field photograph showing nearly vertical bedded limestones. B: Sketch of A, alatoconchid beds observed in 1 and 2, lenticular and nodular cherts in blue color. C: Alatoconchid in growth-position showing wing-like flanges and large internal chamber, lenticular chert developed at top. D: Sketch of C. E: alatoconchid biostrome with alatoconchid in growth position with some alatoconchid fragments. F: Sketch of E. (ruler for scale=15 cm).....	81

LIST OF FIGURES (Continued)

Figure	Page
3.17 Field photographs of alatoconchid biostrome and alatoconchid floatstone beds. A: Photograph of alatoconchid biostrome bed, random sections of double- and single-valved alatoconchids in life position embedded with alatoconchid fragments. B: Sketch of A, alatoconchids displayed in dark gray. C: Field photograph of alatoconchid floatstone bed overlain on non-laminated limestone bed. D: Sketch of C, alatoconchid shown in dark gray fragments and single valves. (ruler for scale=15 cm).....82	82
3.18 A: Rock slab of alatoconchid biostrome facies (sample no. 705). B: Rock slab of alatoconchid biostrome facies (sample no. 721). C: Photomicrograph of bioclastic peloidal matrix of alatoconchid biostrome (sample no. 722b). Part of alatoconchid shell in lower part of view. Smaller foraminifers and algae are shown at top of view. D: Photomicrograph of bioclastic peloidal matrix of alatoconchid biostrome (sample no. 755). E: Photomicrograph of peloidal matrix of alatoconchid biostrome (sample no. 705) showing smaller foraminifer in peloidal- rich texture. F: Photomicrograph of bioclastic peloidal matrix of alatoconchid biostrome (sample no. 721). Gastropods and algae are common. (All scale bar=500 μ m).....83	83
3.19 A: Field photograph of fusulinid wackestone bed (ruler=15 cm). B: Photograph of rock slab of fusulinid wackestone facies (MF6a). C: Photomicrograph of bioclastic wackestone texture of fusulinid	

LIST OF FIGURES (Continued)

Figure	Page
<p>wackestone facies showing fusulinid with smaller foraminifers, algae, and peloids sparsely distributed in micrite. D: Photomicrograph of the same sample as C showing smaller foraminifers bioclasts and peloids in micrite matrix with partly sparry calcite cement. E: Photomicrograph of fusulinid wackestone (sample no. 747). F: Photomicrograph of fusulinid wackestone (sample no. 778b) showing algal fragments (<i>Undarella</i> sp.) associated with peloidal wackestone texture. (All scale bar=500 μm).....</p>	85
<p>3.20 A: Field photograph of fusulinid packstone bed. B: Photograph of rock slab from A. C: Photomicrograph of fusulinid packstone (sample no. 773) showing abraded and micritised fusulinid tests in bioclastic peloidal calcisiltite matrix. D: Photomicrograph of fusulinid packstone (same sample as C) showing well preserved smaller foraminifer in shell debris-rich matrix. E: Photomicrograph of fusulinid packstone (sample no. 782) showing debris compared with F. Photomicrograph of fusulinid packstone (sample no. 783) with well preserved fusulinid tests (<i>Lepidolina</i> sp.) and debris in comparison to D. (All scale bar=500 μm).....</p>	87
<p>3.21 A: Field photograph of limestone beds containing fusulinid packstone/grainstone. B: Field photograph of fusulinid grainstone. C: Slab of fusulinid grainstone (MF6c). D: Photomicrograph of fusulinid grainstone showing fusulinids in sparry calcite cement (sample no. A25). Micritised fusulinids and algae with oncolitic structure</p>	

LIST OF FIGURES (Continued)

Figure	Page
<p>are conspicuous. Fusulinid (on right of view) shows lobate shape and oncolitic structure. E: Photomicrograph of fusulinid grainstone (sample no. A31) showing fusulinid (<i>Lepidolina</i> sp.) with round oncolitic structure and algae (<i>Mizzia</i> sp.) without oncolitic structure. F: Photomicrograph of fusulinid grainstone showing composite grains with oncolitic structure. (All scale bar=500 μm).....</p>	89
<p>3.22 A: Photomicrograph of bioclastic grainstone from Unit B showing micritised and coated bioclastic grains, peloids with aggregate grains, and calcareous algae in sparry calcite cement (sample no. 809). B: Photomicrograph of bioclastic grainstone from Unit B (same sample as A) showing another view of this facies. C: Photomicrograph of bioclastic grainstone (sample no. 777) showing red algal fragment (<i>Undarella</i> sp.) floated in grainstone texture. D: Same as B, showing small cortoids. (All scale bar=500 μm).....</p>	91
<p>3.23 Limestone outcrop from upper part of Unit B. A: Coral biostrome interval, showing as massive corals in middle part which are overlain by alatoconchid fragments and tabulate corals in ascending order. B: Sketch of A, 1=thickly bedded limestones, 2=alatoconchid bed with alatoconchid fragments shown as undulating solid lines, massive corals (purple patches with straight solid lines inside) in lower part, 3=coral biostrome bed with tabulate corals in growth-position. C: Field photograph of limestone beds that underlie fissure structure</p>	

LIST OF FIGURES (Continued)

Figure	Page
<p>and collapse breccias. D: Sketch of C, single coral head shown in purple patch, 1=non-laminated limestone bed. 2=coral bed with reworked coral heads. (ruler for scale=15 cm).....</p>	94
<p>3.24 A: Field photograph of an outcrop with coral biostrome (MF8). B: Enlargement coral biostrome (pen=15 cm). C: Photomicrograph of matrix in coral biostrome facies showing profound encrusting structure by microbial organisms in dark gray laminae (sample no. 802). D: Photomicrograph showing calcareous algae in micrite matrix of coral biostrome (sample no. A56). E: Photomicrograph of bioclastic wackestone matrix with <i>Tubiphytes</i> and debris (sample no. 802). F: Photomicrograph of bafflestone showing stalk shaped tabulate coral in growth position with peloidal wackestone matrix (sample no. 923). (All scale bar=500 μm).....</p>	95
<p>3.25 A Field photograph of thickly to very-thickly crinoidal packstone beds. B: Rock slab of crinoidal facies (sample no. A50). C: Rock slab of crinoidal facies with massive coral fragment at base (sample no. A52) D: Photomicrograph of crinoidal packstone showing densely packed crinoid elements (sample no. A50) with distinct twin laminae. E: Photomicrograph of crinoidal facies showing poorly sorted, loosely packed crinoidal elements in diagenetic groundmass with dolomite rhombs (sample no. A52). F: Photomicrograph of crinoidal facies showing crinoid elements with dark gray micrite and diagenetic</p>	

LIST OF FIGURES (Continued)

Figure	Page
groundmass. (All scale bar=500 μ m).....	99
3.26 A: An outcrop photograph of depositional breccia (MF10a1) from Unit E. B: Breccia from Unit E showing more fitted clasts in comparison to Unit G. Clast components are of intraformational origin with varieties of microfacies type. C: Photomicrograph of breccia showing wackestone clast on left, grainstone on top with variation. They compose of fusulinid wackestone/packstone, limestone clasts with coral fragments, fragments and debris forming as matrix in lower part. D: Photomicrograph of breccia showing lithoclast fragments and fusulinid fragment (<i>Sumatrina</i> sp.) embedded in groundmass. (All scale bar=500 μ m).....	101
3.27 A: Rock slab of breccia from lower part of Unit G. B: Photomicrograph of intraformational conglomerate/breccia showing periphery cracking of clast (sample no. A47). C: Photomicrograph of intraformational conglomerate/breccia showing sparry calcite cement between clasts (sample no. A48). D: Photomicrograph of intraformational conglomerate/breccia showing calcareous algae with other fossils in lithoclasts (same sample as B). (All scale bar=500 μ m).....	103
3.28 A: Field photograph of limestone conglomerate/breccia outcrop of Unit G. B: Outcrop photograph from Unit G showing poorly sorted, polymict conglomerate floated in red matrix. C: Well-rounded clasts in conglomerate from Unit G (marker pen=15 cm). D: Subangular to subrounded clasts from the same unit as C.....	104

LIST OF FIGURES (Continued)

Figure	Page
3.29	A: An outcrop of fissure-bearing limestone interval; fissure-fill material is brown in colour with irregular shape. B: Fissure-fill sediment showing lamination with poorly sorted grains texture. C: Another view of an irregular fissure truncated into limestone bed. (ruler=15 cm).....105
3.30	A: An outcrop of non-depositional breccia (MF10b1) of Unit C. Braccia is exposed in the lower part of view. B: Blocks of limestone clasts floated in groundmass showing the high angularity of the clasts. C: Clasts in breccia showing variety of limestone facies with platform fossils such as coral (lower left).....106
3.31	Stratigraphic log of section 1.....112
3.32	Stratigraphic log of section 2.....113
3.33	Stratigraphic log of section 3.....114
3.34	Stratigraphic log of section 4.....115
3.35	Stratigraphic log of section 5.....116
4.1	Reconstruction of alatoconchids (<i>Shikamaia (Tanchintongia) perakensis</i>). A: Dorsal view. B: Lateral view. C: Internal view with terminology. (after Yancey and Boyd, 1983).....118
5.1	Microfacies types and depositional model of the study area in upper most part of Khao Somphot sections. A=supratidal; B=intertidal; C= shallow subtidal with restricted condition; D= subtidal with semi-restricted condition; E=internal bioclastic shoal or barrier bar; F=sheltered lagoon with open marine circulation; MSL=

LIST OF FIGURES (Continued)

Figure	Page
<p>mean sea-level; FWWB=fair-weather wave base; SWB=storm wave base. Explanation of microfacies types and symbols see in text.....</p>	128
<p>5.2 A: Relative sea-level curve with stratigraphic unit from this thesis study. B: Coastal-onlap chart of the Permian showing relative sea-level fall during late Middle Permian. (modified after Wielchowsky and Young, 1985). C: Coastal-onlap curve and eustacy curve of the Permian showing two events of relative sea-level fall (marked by arrows) during Capitanian (Midian) time. (modified after Ross and Ross, 1985). Sea-level fall in A can be correlated with B and C.....</p>	153
<p>5.3 Parasequence types observed in the upper part of the Khao Somphot sections. Abbreviations and symbols as in Fig. 5.2 and Fig. 3.31.....</p>	154
<p>5.4 An ideal Lofer cycle showing subtidal deposit capped by intertidal deposit. Disconformity is located on top of subtidal deposit with or without basal conglomerate (after Fischer, 1964).....</p>	155
<p>5.5 A: Photomicrograph of horse-tail spray of insoluble seams caused by compaction in mud-supported limestone texture. B: Photomicrograph showing crushed miliolid tests cause by strong compaction. C: Photomicrograph showing sutured stylolite. D: Photomicrograph showing stylobreccia. E: Photomicrograph of selective silicification in the internal chamber of fusulinid tests. F: Authigenic quartz crystal. (All=PPL). (All scale bar=500 μm).....</p>	157

LIST OF FIGURES (Continued)

Figure	Page
5.6 A-B: Photomicrograph of fine-grained inequigranular hypidiotopic dolomite (PPL). C: Photomicrograph of selective silicification and inequigranular rhombic poikilotopic dolomite. D: Photomicrograph of inequigranular rhombic poikilotopic dolomite. E: Photomicrograph of fusulinid grainstone facies showing micrite envelopes at grain margins of algae and fusulinids. F: Photomicrograph of coated grain facies showing cortoids and peloids. (All scale bar=500 μ m; under PPL for all except D, XPL).....	160

LIST OF ABBREVIATIONS

%	percent
mm	millimeter
cm	centimeter
m	meter
μm	micrometer
pp	pages
p	page
et al	et alia (and others)
PPL	plane polarized light
XPL	cross polarized light

CHAPTER I

INTRODUCTION

1.1 Introduction

Alatoconchid bivalves are an extinct group of marine benthic epifauna belonging to Family Alatoconchidae (Yancey and Ozaki, 1986). These organisms are restricted in occurrence to tropical marine Permian strata within the North Africa, Middle East and Asia. Wallowaconchids (Family Wallowaconchidae) which display a similar morphology at first glance, are placed within a different group on the basis of their detailed morphology and shell structure. Moreover, the latter are restricted in occurrence to tropical marine Triassic sequence in western North America (Yancey and Stanley, 1999).

The alatoconchids are bizarre in shape and size in comparison to all other bivalves. Accordingly, they are of great interest. Paleogeographically, alatoconchids have been observed only along the margins of the Permian Paleotethys Ocean within sequence exposed in Africa, Europe and Asia. They have never been observed in the American continent or in high latitude regions.

Within the Paleotethyan province, they have been reported in shallow marine sequence of the Cimmerian continent, occurring in Tunisia, Yugoslavia, Afghanistan, Malaysia, and Thailand (Yancey and Boyd, 1983; Kochansky-Devide, 1978; Termier et al., 1973; Runnegar and Gobbet, 1975; Baird et al., 1993). In the Cathaysian region, they have been found in Japan, Thailand, the Philippines (Yancey and Ozaki, 1986;

Campbell, 1997; Kiessling and Flügel, 2000; Isozaki, 2006). However, it has never been reported in China and eastern Pacific region of the U.S.A (Yancey and Stanley, 1999). These works provide some information on shell morphology, taxonomy, systematics, paleoenvironment and paleobiogeographic distribution. However, their paleoenvironment has been interpreted in several ways unless these organisms have a wider environmental habitat than previously thought. The study of lithofacies of the rocks containing these organisms and paleontology of associated fossils would be meaningful for evaluating their paleoenvironmental condition.

In Thailand, there are numerous localities of alatoconchid-bearing strata some of which are exceptionally well exposed. The rocks of these strata are comprised mainly of Middle Permian limestones. They occur within the Shan-Thai Block, Indochina Block (Cathaysian) and Sibumasu/ Phuket Terrane (Cimmerian) (Fig. 1.1). For the Indochina Block, they have been explored in Loei, Nam Nao, Tak Fa, Saraburi, Pak Chong, Khao Yai and Khao Ta Ngok areas along the western and southern edges of the Khorat plateau. In the Shan-Thai Block, they are represented by limestones of Ngao Group in the vicinity of Kiu Lom Dam (Chonglakmani and Intarawichitr, 1996). In the Phuket Terrane, there are alatoconchid-bearing limestones reported in Ratchaburi province. The limestones belong to the Ratburi Group (Baird et al., 1993). Detailed study relating to paleoenvironment and taxonomy of alatoconchids in Thailand has never been conducted. The occurrence at Khao Somphot locality is the finest known so far. Khao Somphot is located to the east of Chai Badan district (Lam Narai), Lop Buri Province. The study sections are situated on two small hills east of Khao Somphot range. The thesis objectives with scope and limitation and methodology are stated as follows.

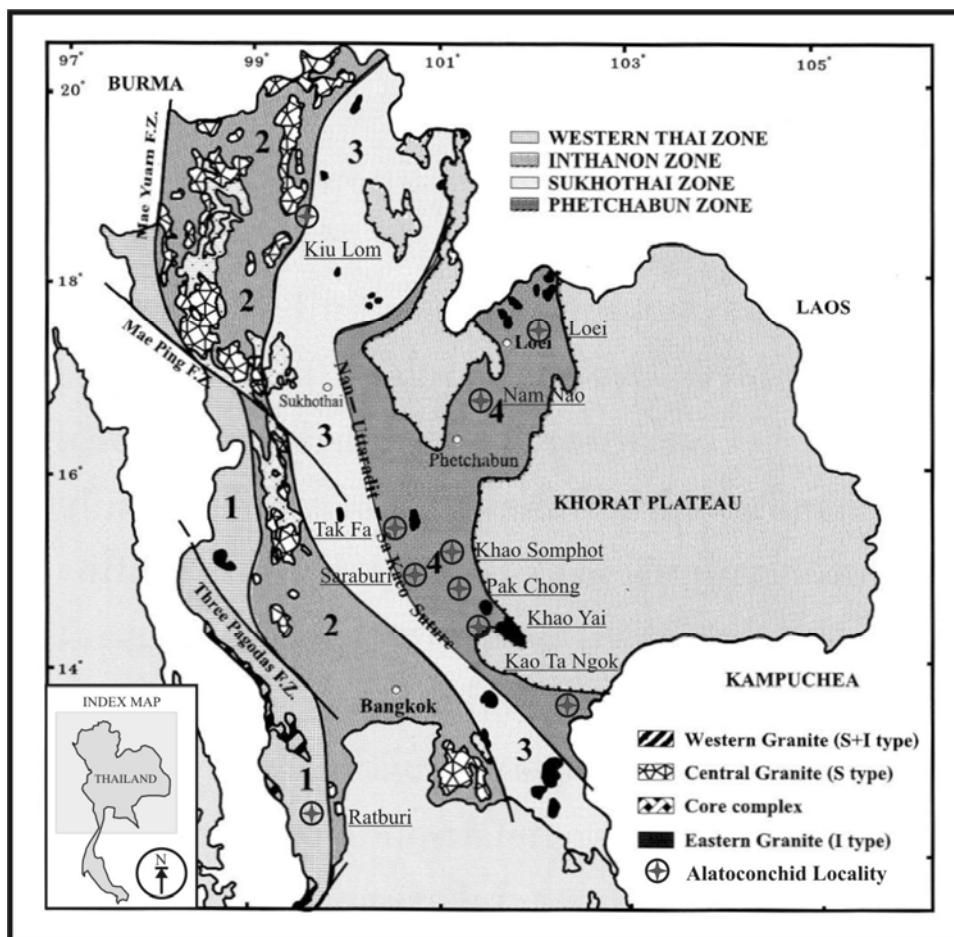


Figure 1.1 Map of Thailand showing tectono-stratigraphic zones and alatoconchid localities. These localities are particularly well exposed intensively in the Phetchabun zone from Loei through Srakaeo. Other localities are located in Ratburi and Kiu Lom of different zones. (modified after Barr and MacDonald, 1991)

1.2 Research objectives

The thesis has four main objectives: firstly, to define microfacies of carbonate rocks in the uppermost section of the Khao Somphot area; secondly, to evaluate depositional environment of these carbonate rocks; thirdly, to determine taxonomy of alatoconchid bivalves in this area; fourthly, to clarify paleoenvironment of these alatoconchids.

1.3 Scope and limitations

The study is concerned mainly with the paleontology and lithofacies of alatoconchid-bearing strata in the uppermost succession of the Permian carbonate rocks in the Khao Somphot area. Accordingly, the paleontology consists mainly of taxonomic description and classification of alatoconchids. However, it is difficult to extract fossils for complete morphological investigation. The taxonomy of alatoconchids depends largely on the condition of observed specimen. Identification and classification of these bivalves is based mainly on Moore (1969), Yancey and Ozaki (1986) and Yancey and Boyd (1983). Note that taxonomic interpretation of these bivalves is limited because there are so few references and research available on this topic. For other fossils in the study area, there is abundant previous research available in the literature. Some of them such as fusulinids and algae are determined to taxonomic levels that reveal accurate biostratigraphic age and some paleoenvironmental interpretation of the rock strata. However, taxonomy of other fossils (except alatoconchids) is beyond the scope of this thesis.

According to lithofacies study of the carbonate rocks, the study sections are comprised mainly of limestone that is in approximately 400 meters thick. Mapping of

lithofacies and lithostratigraphy was carried out in the field and was supported more detailed by laboratory-based microfacies analysis. This involved detailed preparation and examination of polished slabs and thin-sections of rock samples in the laboratory. Microfacies classification is based mainly on Dunham (1962) and Folk (1959; 1962). Interpretation of microfacies will be discussed and correlated with several previous works.

1.4 Research methodology

The thesis study was planned in terms of several stages including desk study, field reconnaissance, detailed field study (lithostratigraphy, paleontology, and sampling), sample preparation (alatoconchid extraction, polished slab and thin-section of rocks), microfacies classification, field checking, interpretation, discussion and conclusion (Fig. 1.2). The desk study was carried out in order to collect some preliminary data. For this stage, all previous information relating to the thesis study were collected and prepared, such as articles, textbooks, geologic and topographic maps, etc. Detailed field investigations and sampling were planned in order to collect geological and paleontological data. Firstly, detailed stratigraphic observation, measurement and lithological sampling was conducted for lithostratigraphic mapping purposes. Relative abundance, size, and taphonomic conditions (e.g. preservation, arrangement, orientation) of alatoconchids were investigated and recorded. In addition, other information related to paleontology of associated fossils in the field were examined especially foraminifers and calcareous algae. Some specimens of rocks and fossils were sampled for further detailed investigation in the laboratory. In the laboratory, specimens of alatoconchids were extracted in an attempt to reveal their

morphology for further taxonomic study. Polished slabs and thin sections were made and studied using a binocular microscope. Then, all information was integrated and rechecked in the field to confirm that all stratigraphic information has been correctly represented and interpreted.

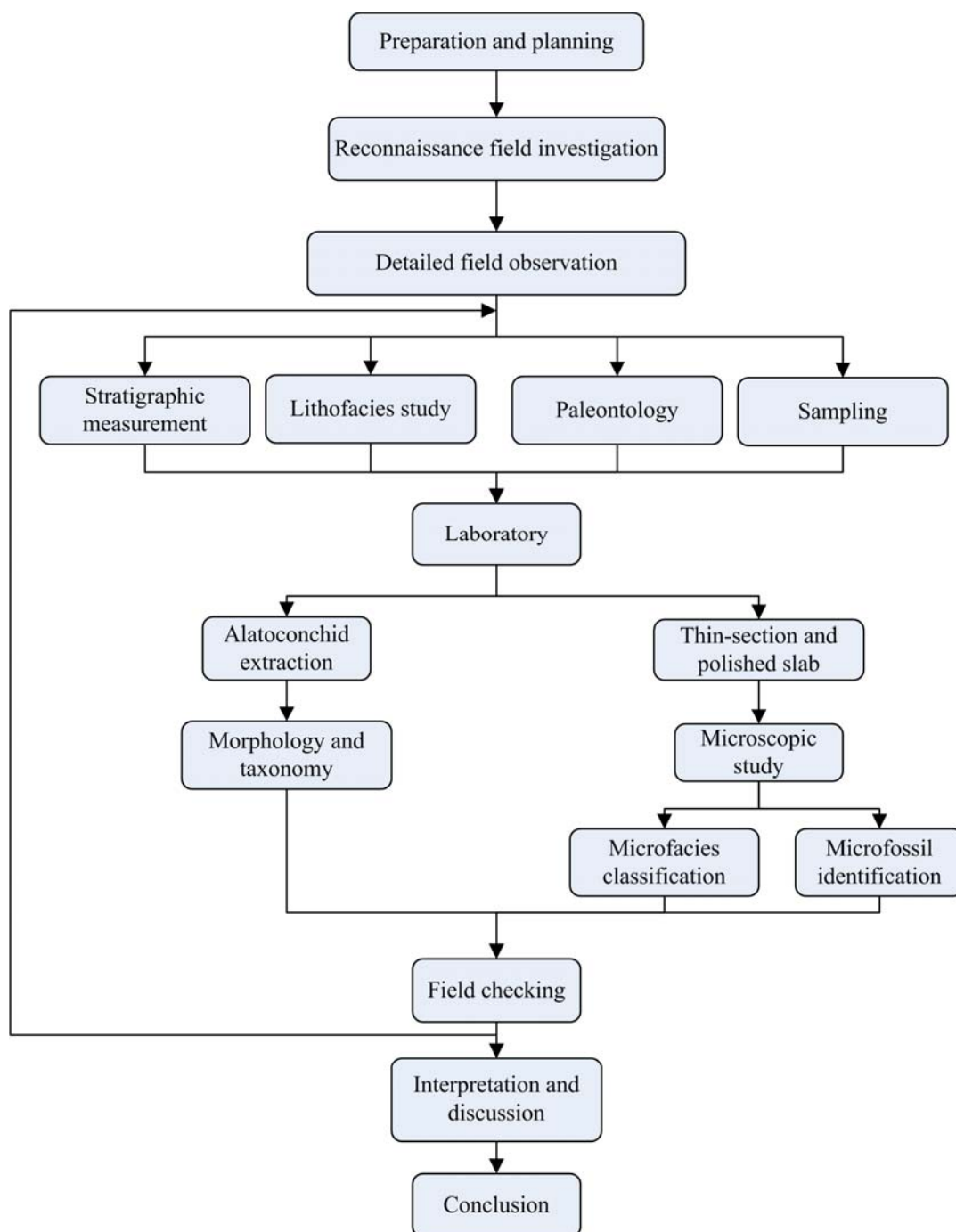


Figure 1.2 Flow chart showing summary of the study methodology.

CHAPTER II

GENERAL GEOLOGY

2.1 Permian tectonic history of Thailand

During the last few decades, there has been some controversy on topics relating to the tectonic history of Thailand. Much of the debate has been focused mainly on location and closing time of the Paleotethys in this region. Some information and background on this topic are briefly reviewed in this section.

Paleogeographically, in the Devonian, the Paleotethys Ocean was opened when some continental terranes were separated from north Gondwanaland (Bunopas, 1981, Metcalfe, 1990; 2002). These terranes include South China, North China, Tarim and Indochina. Later on, in the late Early Permian, the Cimmerian continental strip was also rifted from Gondwanaland (Fig. 2.1). Consequently, this continental strip moved to the north amalgamated with former derived terranes around the tropical Tethyan province.

Generally, Thailand and the neighboring region is composed of two continental terranes that are divided by the Nan Suture (Bunopas, 1992). They include Indochina and Shan-Thai located to the east and the west of that suture respectively (Fig. 2.2). This suture has traditionally been inferred as a remnant of Paleotethys. The Indochina Block comprises eastern Thailand, Laos, Cambodia and parts of Vietnam. This terrane is composed mainly of middle Paleozoic rocks and Permian carbonate and siliciclastic rocks. The Shan-Thai Block consists of eastern Malaysia, western

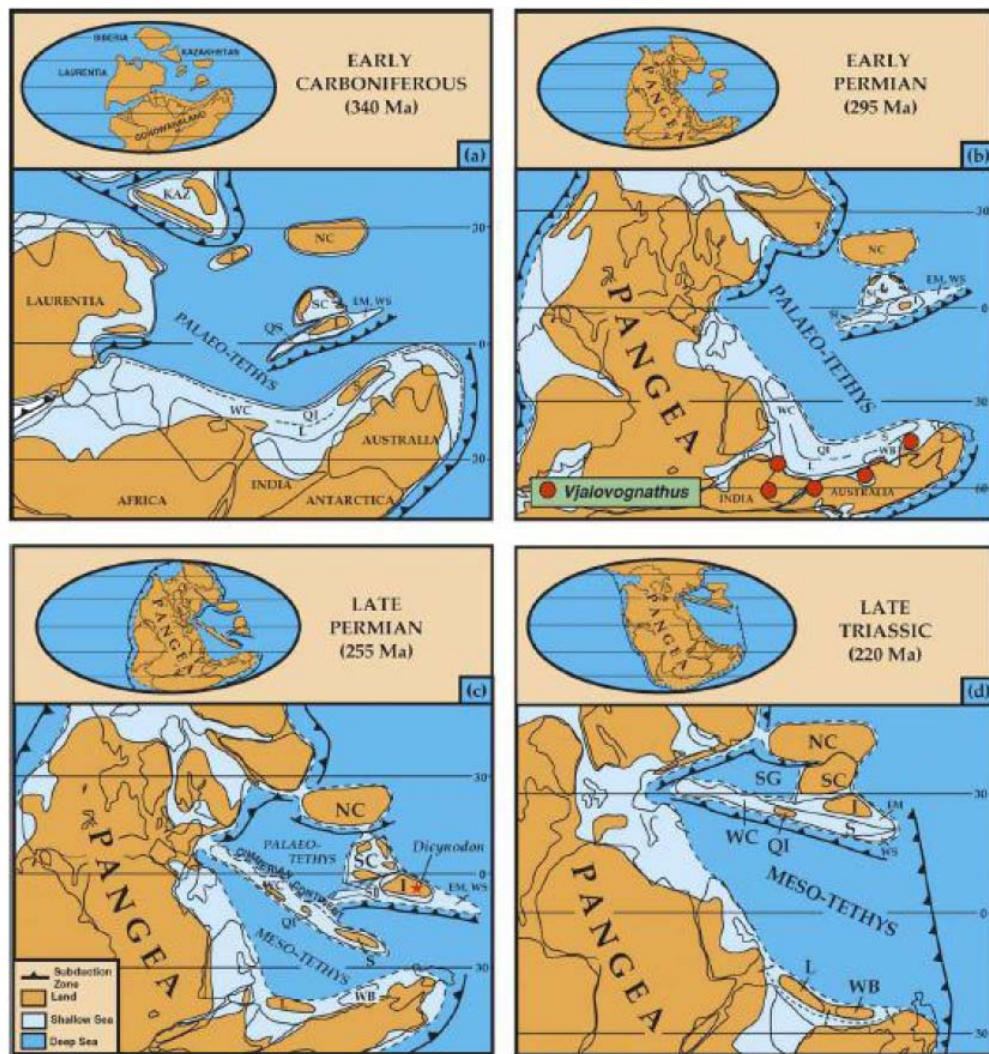


Figure 2.1 Paleogeographic maps of the world Carboniferous through Triassic. In the Early Permian, Paleotethyan Ocean is located between Pangea supercontinent and the Cathaysian domain. During Late Permian, Cimmerian continent including Shan-Thai (S) and others translated to tropical realm close to Indochina (I), and South China (SC) of the Cathaysian domain. (after Wakita and Metcalfe, 2005)

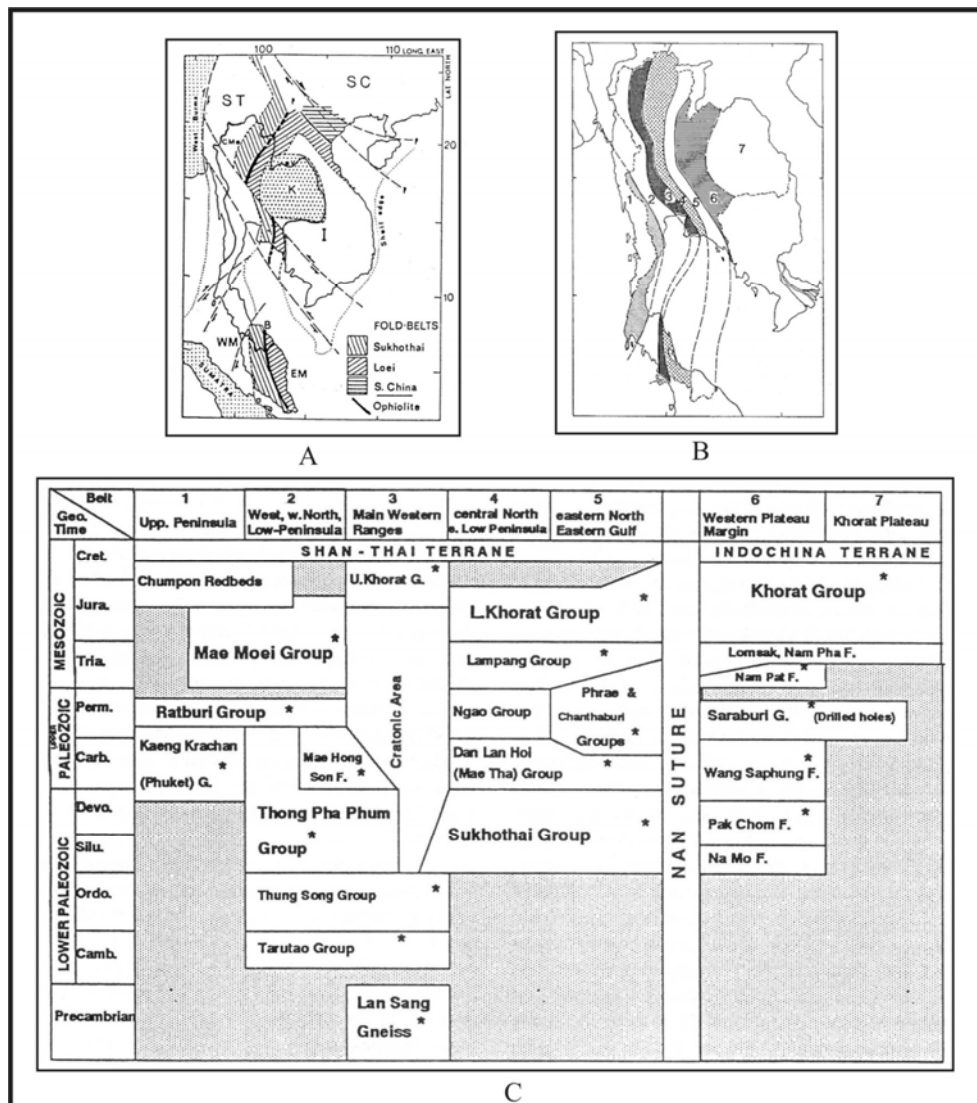


Figure 2.2 A: Tectonic map of Thailand and neighboring area. Nan Suture is marked by ophiolite. I=Indochina Block, SC=south China Block, K=Khorat Plateau, ST=Shan-Thai Block. B: Lithostratigraphic map of Thailand. It is composed of seven belts (see detail in C). C: Summary of Shan-Thai and Indochina components with geological time scale. Shan-Thai terrane consists of stratigraphic belts 1-5 while Indochina includes belts 6 and 7. These Blocks are divided by the Nan Suture. (after Bunopas, 1992)

Thailand, western Peninsular Malaysia and northern Sumatra. It consists of Precambrian granitoids, high grade metamorphic rocks. These rocks are overlain by Paleozoic and Mesozoic rocks. The Shan-Thai has been interpreted as part of Gondwanaland that was located in the Southern Hemisphere during Early Permian time before it rifted and drifted to the north in late Early Permian time (e.g. Wakita and Metcalfe, 2005). Indochina was located in tropical regions as part of the Cathaysian domain during this time.

The amalgamation of these terranes along the Nan Suture occurred during Triassic time (Metcalfe, 1990; Bunopas and Vella, 1978; 1983; Gatinsky et al., 1978; Chaodumrong, 1992). However, other opinions on suturing time have been variously suggested including Devonian-Carboniferous (Hahn et al., 1986; Alterman, 1991), Middle to Late Carboniferous (Wolfart, 1987), Late Permian to Early Triassic (Thanasuthipitak, 1978; Cooper et al., 1989; Piyasin, 1991) and Middle Permian (Helmcke and Lindenberg, 1983; Helmcke, 1985; 1994). Moreover, it was suggested (Helmcke, 1994) that the main Paleotethys should be located further to the west of the Nan Suture along the Thai-Myanmar (Burma) border (Fig. 2.3). Recently, this suggestion has been widely accepted; new information on paleontology and geology supports this interpretation (Ueno, 2003; Wang et al., 2001; Chonglakmani, 1999; 2002) (Fig. 2.4).

2.2 Permian lithostratigraphy of Thailand

The Permian rocks in Thailand are characterized predominately by carbonate rocks. However, other Permian rocks such as clastics, siliciclastics and volcanics have also been reported. Geographically, Permian strata can be found in all regions except

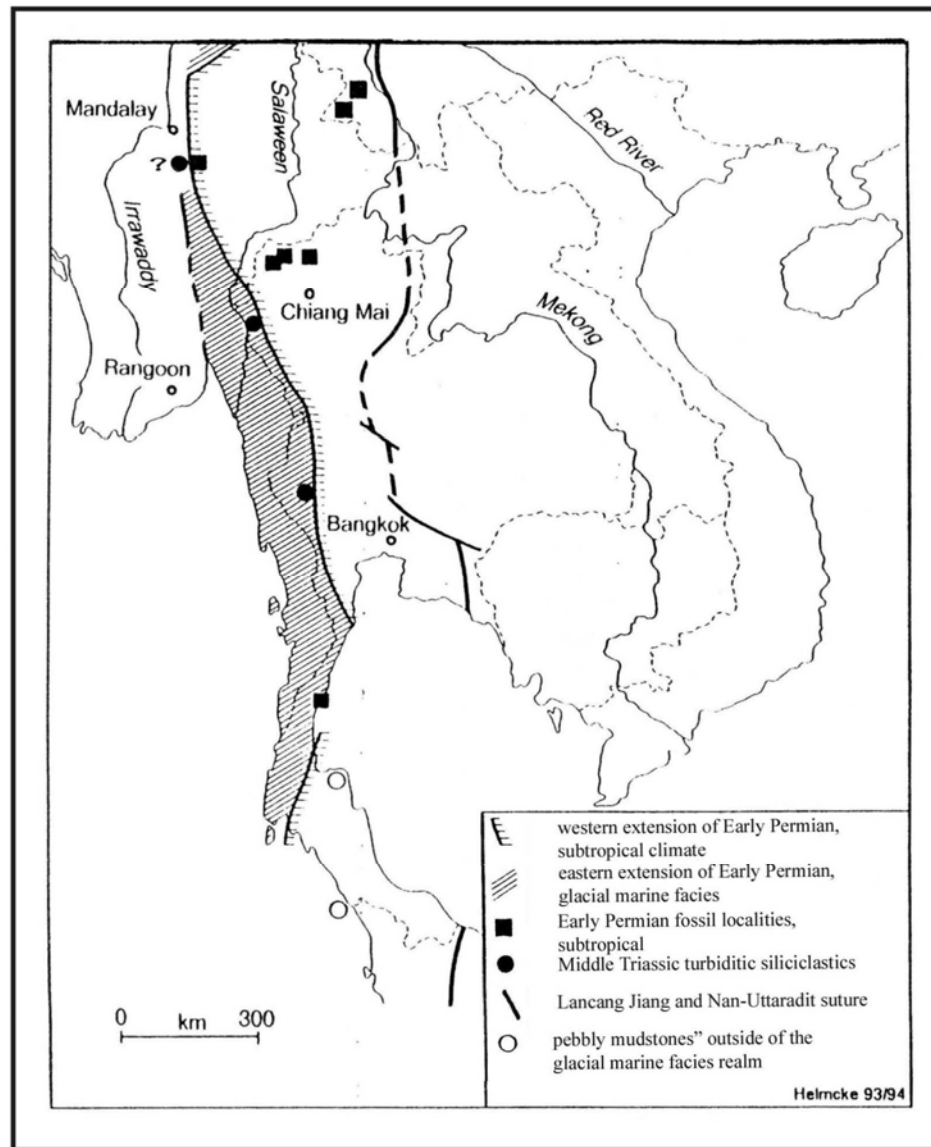


Figure 2.3 Tectonic map of mainland Southeast Asia showing proposed location between western edge of the subtropical climate terrane and eastern margin of the Gondwanan (glacial-marine). (after Helmcke, 1994)

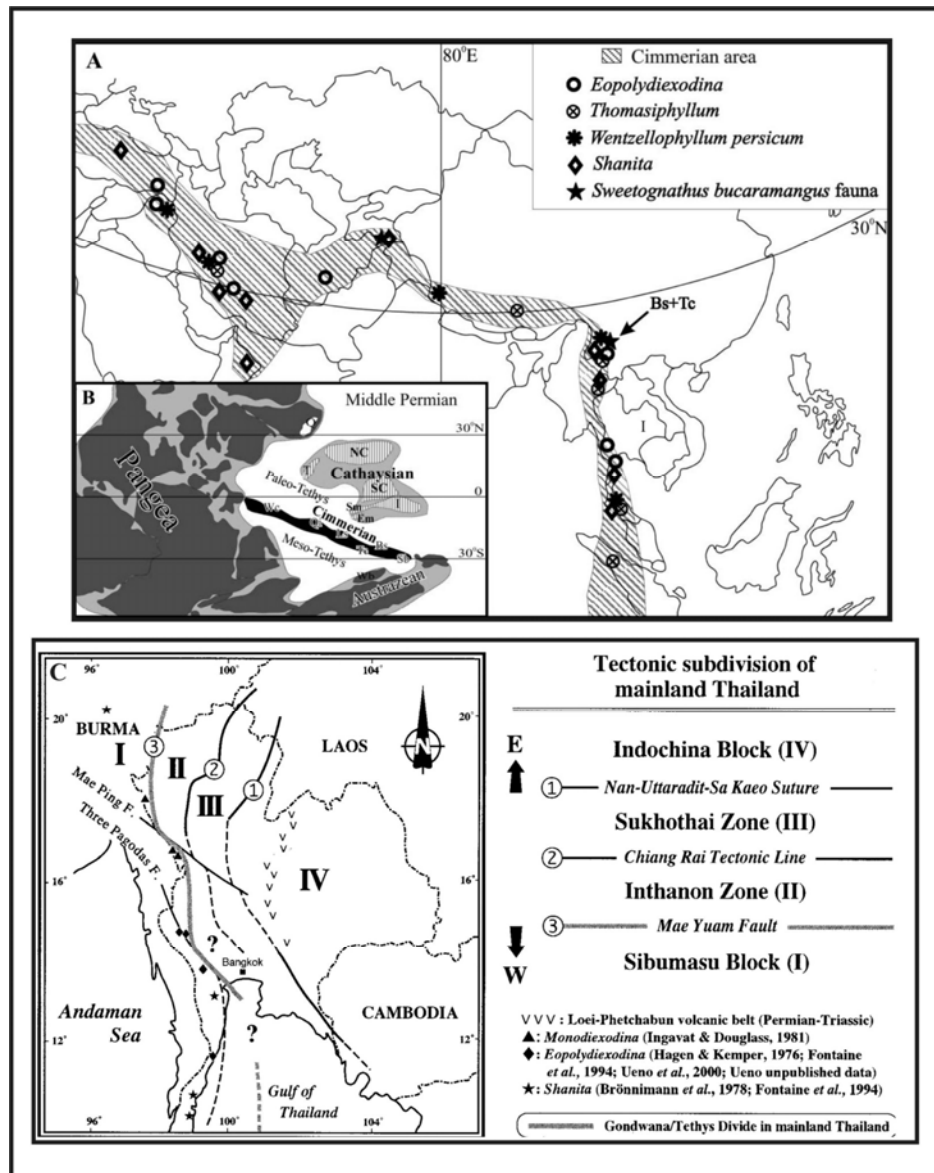


Figure 2.4 A: Geographic map of Asia showing distribution of the Cimmerian continent (dash area). This continent is interpreted as Gondwana derived. In Thailand, this continent is located in the western part along Thai-Myanmar border. B: The Middle Permian paleogeographic map (after Wang et al., 2001). C: Geographic map showing tectonic subdivision of mainland Thailand (after Ueno, 2003).

in the Northeastern region of the Khorat Plateau (Fig. 2.5). In other different regions, these rocks have been assigned different lithostratigraphic nomenclature (Tab. 2.1). In Loei-Petchabun region, it is occupied by Saraburi Group. In the north and upper western region, the Permian strata are assigned as Ngao Group. In the eastern region, Chantaburi Group is predominant. In lower western and southern regions, Permian rocks include Ratburi Group and the upper part of Kaeng Krachan Group (Phuket Group). Details of these rocks are summarized as follows.

2.2.1 Loei-Phetchabun region

This region occupies a slightly longitudinal area tracing northwardly from Saraburi to Phetchabun, and beyond to Loei. The rocks in this region are mainly of carbonate but with some additional clastic rocks. In the past, the rock in this region was assigned as Ratburi Group. It was later renamed as Saraburi Group by Bunopas (1981). The Saraburi Group was consequently revised by Hinthong and other (1985). According to Hinthong and others (1985), the Saraburi Group can be divided into six formations, namely, Phu Phe, Khao Khwang, Nong Pong, Pang Asok, Khao Khad, and Sap Bon in ascending order. Lithologic summarization of these formations is provided below.

Phu Phe Formation

This formation is placed in the lowermost part of the Saraburi Group. It is characterized mainly by dark to very dark gray, thickly to very thickly bedded limestones with nodular cherts. They occur with intercalations of light brown to brownish gray shale and slaty shale in the lower part of the formation. According to fusulinids including *Pseudoschwagerina* sp. and *Triticites* sp., this formation is of Early Permian (Asselian to Sakmarian) age. It contains about 600 meters thick.

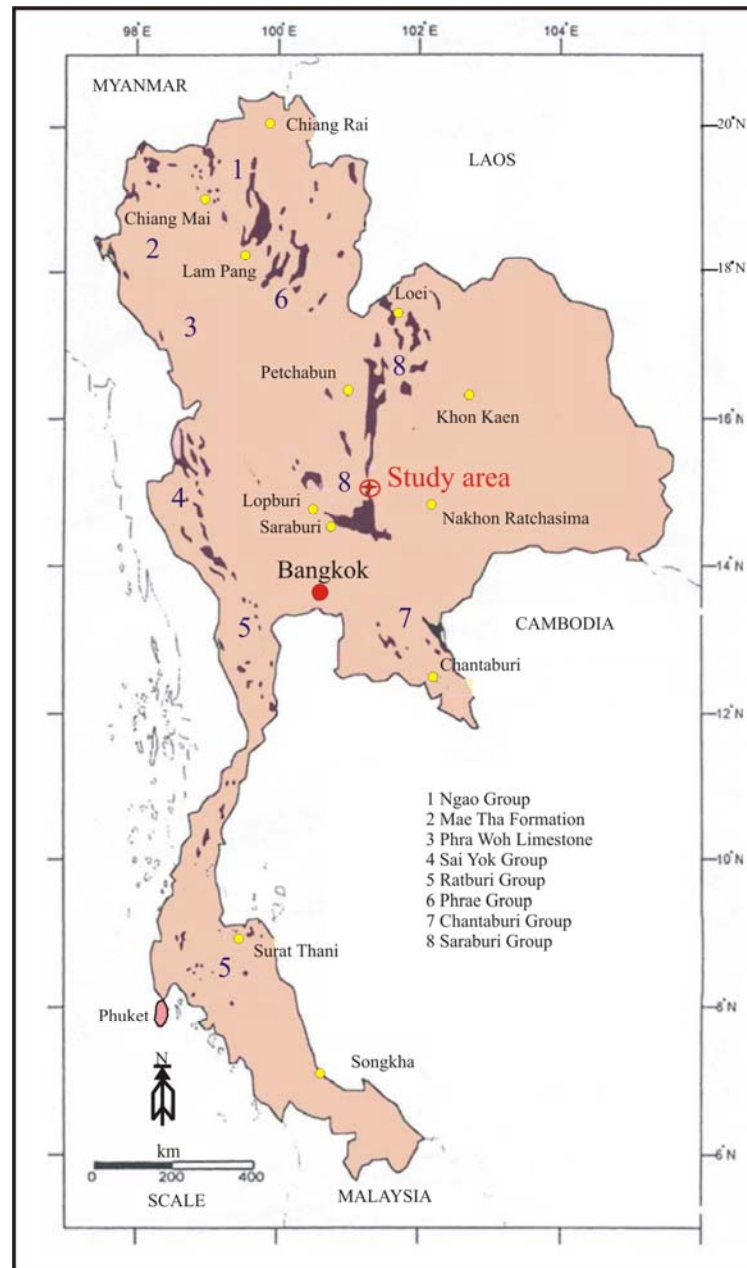


Figure 2.5 Map of Thailand showing lithostratigraphic distribution of Permian rocks. These rocks can be categorized into 8 units that are exposed throughout Thailand except in the area of Northeastern Thailand. (modified after DMR, 1987)

Table 2.1 Lithostratigraphic correlation of Upper Paleozoic rocks in Thailand. (after Raksaskulwong, 2002)

Age (Ma)	Era	Period	Northern & Upper Western		Loei - Pechabun Ranges		Eastern		Lower Western & Southern	
			Group	Formation	Group	Formation	Group	Formation	Group	Formation
245	Mesozoic	Triassic	Lampang					Pong Nam Ron		Si Bon Chai Buri
		Permian	Ngao	Upper	Huai Tak	Saraburi	Sap Bon (Nam Duk) Khao Khad	Chantaburi	Khao Chakan (Khao Ta Ngok)	Ratburi
Middle	Pha Huat			Pang Asok (Hua Na Kam) Nong Pong (E-ler)	Sra Kao (Wang Nam Yen)		Phab Pha Thung Nang Ling			
Lower	Kiu Lom			Khao Khwang (Nam Ma Ho Ran Pha Nok Khao) Phu Phe			Kaeng Krachan (Phuket)		Khao Phra (Ko Yao Noi)	
285	Upper Paleozoic	Carboniferous	Dan Lan Hoi (Mae Tha, Phrae)	Upper	Khao Luang Pyroclastic (Rong Kwang)	Wang Sa Phung (Huai Som)		C2		Ko He Spill way
				Middle	Lan Hoi (Fang Redbed, Doi Kong Mu)					Khao Wang Kradat
				Lower	Khao Khi ma Pyroclastic Mae Sai					
360	Lower Paleozoic	Devonian	Sukhothai (Musur)	Mae Hong Son		Nong Dok Bua (Dok Du)		C1	Tong Pha Phum	Khuan Klang (Ya Ha)
									Tanaosri	
410						Pak Chom				

Khao Khwang Formation

Lithology of this formation is composed of dark to light gray, thinly to thickly well bedded limestones. Nodular cherts are abundant and scattered throughout the sequence. Dolomites, sandstones, tuffaceous sandstone, volcanic rocks and shale intercalations have also been observed in some intervals. Fossils in the sequence consist of brachiopods, bryozoans, crinoid stems, and fusulinids. According to fossils, this formation is assigned an Early Permian (Sakmarian) age. Total thickness of the formation is about 490 meters.

Nong Pong Formation

It is composed predominately of brownish gray to light gray shales. These rocks are interbedded with limestones. The limestones are characterized by medium to dark gray, bedded, banded to well laminated and argillaceous in some interval. Bedded cherts are intercalated in the upper part of the sequence. Fossil assemblages consist of ammonoids (*Agathiceras* sp.) and fusulinids. This formation is of Early Permian (Artinskian to Kungurian) age. Total thickness is about 670 meters.

Pang Asok Formation

This formation consists mainly of shales, slaty shales, and sandstones. In the lower part, it contains light greenish gray to pale reddish-brown sandstones intercalated with shales. This interval is overlain by pale reddish-brown shales interbedded with light greenish gray arkosic sandstone and brownish gray limestones. The middle part is composed of gray to grayish brown shales. The upper part is brown to dark shales, slaty shales and greenish gray lenticular arkosic sandstone. Some limestone lenses contain fossils including bivalves, crinoid stems, and coral fragments. The age of this formation is obtained from *Agathiceras* sp. which indicates

an Early Permian (Artinskian to Kungurian) age. It is about 360 meters total thickness.

Khao Khad Formation

This formation contains predominant dark gray limestones and dolomites. Nodular and bedded cherts are common. In some intervals, there are shales and sandstones intercalated with limestones. Marble, calcsilicate rocks, hornfels and volcanic rocks are locally exposed. This formation contains fossiliferous rocks in several areas. The age of the formation is Early Permian (Artinskian to Kungurian) to upper Middle Permian (Midian or Capitanian). The formation is about 1,800 meters in total thickness.

Sap Bon Formation

The Sap Bon Formation consists mainly of gray to brown tuffaceous sandstones, shales, cherts, and thinly bedded limestones. In some place, the rocks are metamorphosed to slaty shale, phyllite and schist. This formation is assigned a Middle Permian (Kungurian to Roadian) age on the basis of the ammonoid (*Agathiceras* sp.). Total thickness of this formation is approximately 1,100 meters.

Saraburi Group is the official lithostratigraphic name attributed to Permian rocks of the Loei-Phetchabun region by DMR (1992). Type sections of the rock formations are located in Saraburi and adjacent areas and are representative of the rock in this area in particular. However, in Phetchabun and Chaiyaphum area, Chonglakmani and Sattayarak (1984) proposed a different lithostratigraphic division of the Permian rocks, namely, Pha Nok Khao, Hua Na Kham, and Nam Duk Formations, in ascending order. In addition, Chareonprawat and others (1984) also assigned the Permian rocks in Loei and Nong Bua Lamphu area into three formations,

namely, Nam Mahoran, E-Lert, and Pha Dua Formations, in ascending order. In Nakhorn Sawan and Lopburi area, the Permian rocks have been divided into two formations including Khao Luak and Tak Fa Formations (Nakornsri, 1976; 1981). Lithostratigraphic correlation of the Permian rocks in this region is summarized in Table. 2.2. Some details on these lithostratigraphic nomenclatures are stated as follows.

Phetchabun and Chaiyaphum area

Pha Nok Khao Formation

It contains thickly to very thickly bedded, gray limestones with nodular and lenticular cherts. These rocks are intercalated with shales. The formation can be correlated with the Nam Mahoran Formation in Loei area and Khao Khwang Formation of the Saraburi Group. Fossils in the Pha Nok Khao Formation include fusulinids and corals that indicate Early to Middle Permian age.

Loei and Nong Bua Lamphu area

Nam Mahoran Formation

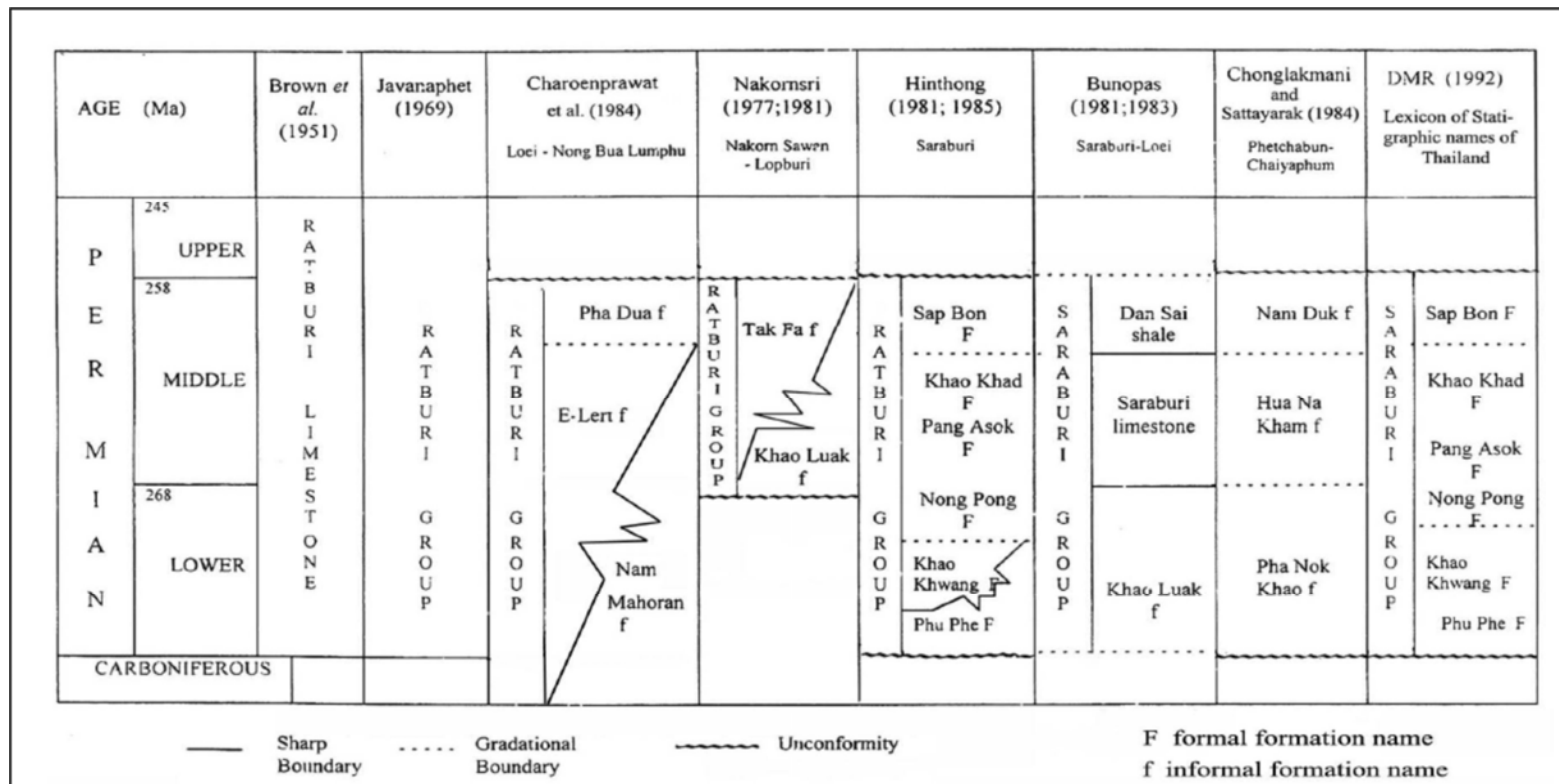
It contains gray, thickly bedded limestones with nodular and lenticular cherts. These rocks are found intercalated with gray, thinly bedded shales. Fossil assemblages in this formation include corals, brachiopods, crinoid stems, fusulinids and algae. These fossils indicate Gzhelian (Late Carboniferous) to Murgabian (early Middle Permian).

E-Lert

This formation is shown as brownish gray shale, yellowish brown sandstones and dark gray, thinly bedded limestones and cherts. Cross-bedding and

Table 2.2 Lithostratigraphic correlation of the Permian System in central and northeastern Thailand.

(after Assavapatchara, 1997)



wavy lamination in clastic rocks maybe an indication of Bouma-sequence. Fossils include fusulinids (*Parafusulina* sp.), ammonoids (*Agathiceras* sp.) The age of the formation is Early Permian (Asselian to Kubergandian). This formation can be correlated with Pang Asok Formation.

Pha Dua Formations

It consists of brown to brownish micaceous sandstones, siltstones, and shales. Fossils include ammonoids (*Agathiceras* sp.) and plant fossils. The fossils indicate a middle Middle Permian age. This formation might be correlated with the Sap Bon Formation of the Saraburi Group.

Nakhorn Sawan and Lopburi area

Khao Luak Formation

It is dominated by greenish to gray, well bedded sandstones, brownish gray shales and banded limestones. Fossils include corals such as *Pseudohuangia* sp., and fusulinids. The fusulinid *Verbekina verbeeki* indicates an early Middle Permian age.

Tak Fa Formation

The Tak Fa Formation is characterized mainly by gray to bluish gray, medium to very thickly bedded fossiliferous limestone. Nodular cherts are common. Sandstones and shales are the minor components in this formation. Fossil assemblages include brachiopods, bryozoans, fusulinids (e.g. *Neoschwagerina* sp., *Pseudodoliolina* sp., *Sumatrina* sp., *Yabeina* sp., and *Lepidolina* sp.). The age of the formation is Middle Permian.

Based on regional facies variations of the Permian rocks along the Phetchabun Fold belt (Wielchowsky and Young, 1985), the rocks in this belt can be

grouped into three main paleogeographic provinces ranging in age from Early to Middle Permian. They are composed of the Khao Kwang carbonate platform located to the west, the Pha Nok Khao mixed carbonate-siliciclastic platform located to the east and the central Nam Duk mixed siliciclastic and carbonate basin located between these two platforms (Fig. 2.6). Depositional environments in the carbonate platform include restricted platform, platform interior and platform margin (Fig. 2.7). These environments can be further divided into ten sub-environments based on their microfacies characteristics. Details of these platforms and basins are described below.

The Khao Khwang Platform

This platform covers an area from north of Saraburi to north of Phetchabun. This platform is dominated mainly by carbonate rocks of the Permian Saraburi Group, however, siliciclastic and volcanic-clastic sedimentary rocks are also observed as minor parts. The rock strata in this platform accumulated in three main depositional environments including outer platform, platform interior and restricted platform. These environments can be further divided into nine depositional sub-environments (Wielchowsky and Young, 1985). The platform ranges in age from Asselian to Midian (Altermann, 1989; Chonglakmani and Fontaine, 1990). The underlying and overlying rocks of the Khao Khwang platform comprise Carboniferous and Late Triassic rocks respectively. The Carboniferous rocks include shales and limestones exposed around Ban Bo Nam (Fontaine et al., 1999). These are probably the oldest marine rocks underlying the Khao Khwang platform. The Late Triassic rocks are composed of basal conglomerates of Hui Hin Lat Formation and are found closed to the Carboniferous locality. These basal conglomerates seem to directly overlies Permian rocks of the Khao Khwang platform with significant unconformity. Both

localities are situated within a few kilometers to the north of Khao Somphot range. The Khao Khwang platform was probably terminated by the influence of a marine regression event in late Late Permian time. Wood fossils (without growth ring structure) are evidence for this interpretation. These wood fossils belong to *Glossopteris* and they are well-known in Late Permian floras of China. Sedimentary succession of the Khao Khwang platform in the Phetchabun-Lam Narai area is shown in Figure 2.8 (Chonglakmani and Fontaine, 1990). In the southern part of this platform, carbonate facies are similar to that found in Khao Somphot. Dawson and Racey (1993) recognized six main biofacies in this area from a 1,400 meter-thick section exposed along highway number 21 north of Saraburi at about latitude 14° 41'N to 14° 44' N and longitude 100° 55' E. Age of this sequence ranges from Artinskian (Yahtasian) to early Midian. These biofacies include facies 1) slope and turbidite deposits; facies 2) algal reef complex and marginal platform; facies 3) back reef/ middle platform; facies 4) inner platform with patch reefs; facies 5) protected lagoon/ inner platform; facies 6) peritidal flats. Based on my field observations, there are several areas containing alatoconchid-bearing rocks within the Khao Khwang platform including Nam Nao, Saraburi, Takfa, and Khao Yai areas. The most excellent alatoconchid locality is at Khao Somphot.

The Nam Duk Basin

This basin is located within a longitudinal area from northeast of Saraburi in the south to southwest of Loei in the north. It is situated between Pha Nok Khao and Khao Khwang Platforms. The basin is characterized mainly by the rocks of Nam Duk Formation. The term Nam Duk Formation was named after the type locality along Ban Nam Duk in Lom Sak area by Chonglakmani and Sattayarak (1984). The rock

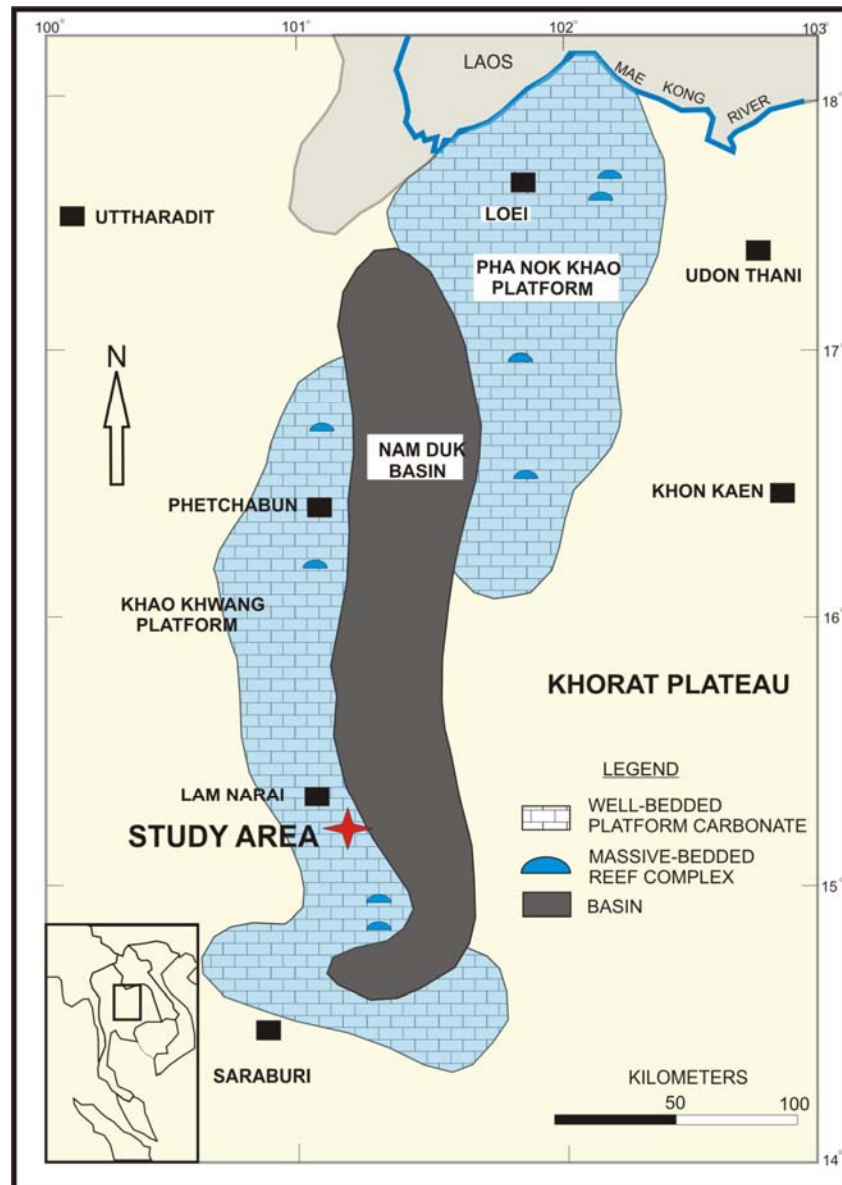


Figure 2.6 Simplified geologic map showing the Permian carbonate platform and siliciclastic basin along the western portion of the Khorat plateau (Indochina Block). The study locality is located in the southern part of the Khao Khwang platform in Lam Narai vicinity (Chai Badan) of Lopburi province. (modified after Chonglakmani and Fontaine, 1990)

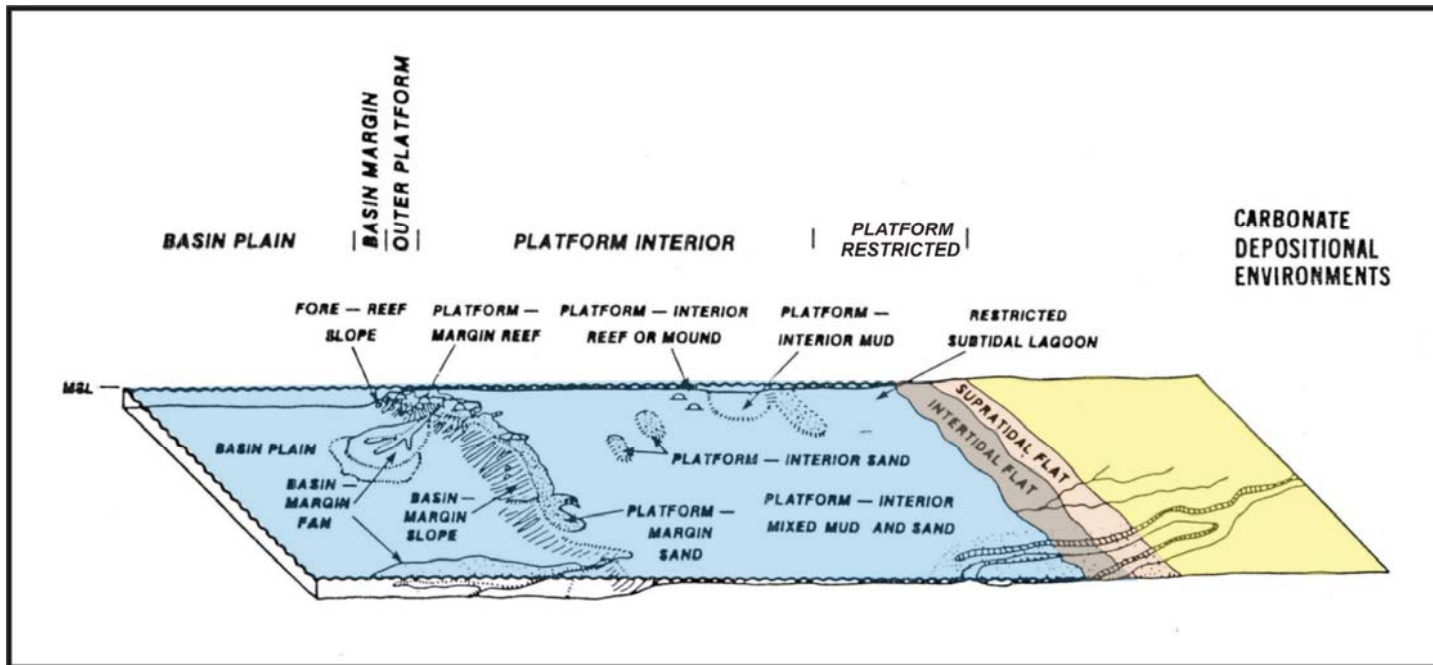


Figure 2.7 Carbonate depositional environments and sub-environments of a carbonate platform in northeastern Thailand.

(modified after Wielchowsky and Young, 1985)

includes pelagic, flysch and molasse types of orogenic sedimentary succession. All of these successions are believed to be related to Late Variscan orogenic event (Helmcke, 1986). They are folded inclined to the west with east-vergent folds and in places are overthrust on younger strata. The pelagic sediments include shales (gray to greenish), banded chert (dark gray to whitish), allodepic limestones redeposited by turbidity current, and volcani-clastic sediments. They are interpreted as pre-flysch succession ranging in age from Early to Middle Permian (Kuberkandiana to possibly early Murghabian). The flysch type sediments are characterized by clastic turbidite sequence and are interpreted as the beginning of an orogenic event. The clastic sequence with autochthonous limestone intercalations in the upper part of the sequence is interpreted as the molasse type, characteristic of a subsiding basin that became more and more shallow and indicates the final stage of orogeny.

The Pha Nok Khao Platform

The Pha Nok Khao platform covers the area of Chum Phae in the south, Loei in the center and Chiang Khan in the north. This carbonate platform developed on a distally steepened ramp-like margin. It contains several lithologies that accumulated in three environments; restricted platform, platform interior and outer platform. These lithologies compose of bird's eye carbonate mudstone, massive algal boundstone, evaporites, massive carbonate mudstone, skeletal and peloidal wackestone and packstone, bedded and nodular cherts and limestone, skeletal grainstones and packstones and limestone conglomerate and breccia (El Tabakh and Utha-aroon, 1998). Based on fusulinids, the age of this platform succession is early Asselian to late Guadalupian (Kozur et al., 1992; Wielchowsky and Young, 1985).

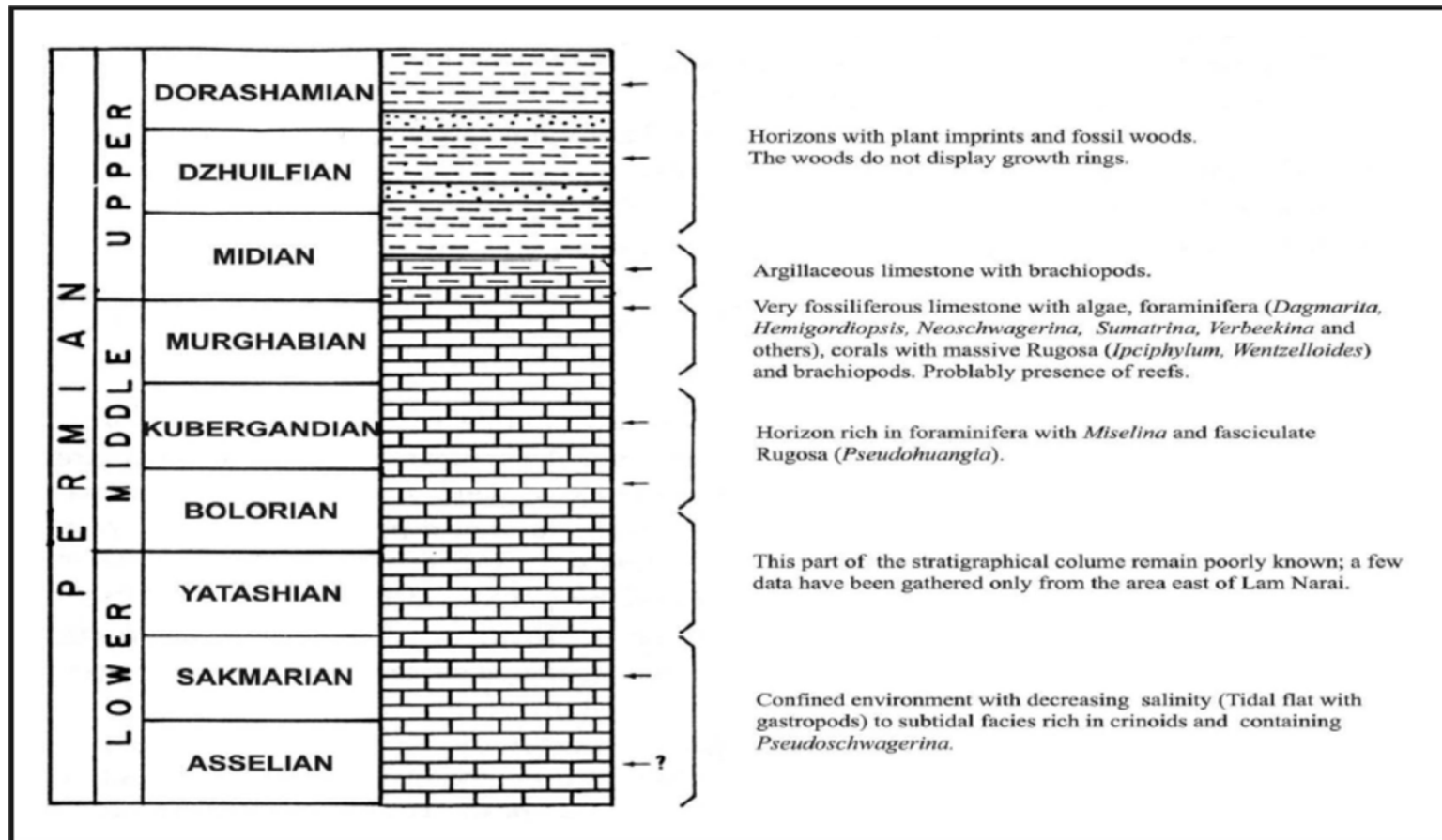


Figure 2.8 Schematic stratigraphic section of the Phetchabun-Lam Narai region. (after Chonglakmani and Fontaine, 1990)

2.2.2 Northern and Upper Western Region

The Permian strata in this region have been assigned as Ngao Group (Bunopas, 1981). It can be divided into three formations including Kiu Lom, Pha Huat and Huai Tak in ascending order. Lithologic information of these formations is described below.

Kiu Lom Formation

This formation overlies conformably on Dan Lan Hoi Group of the Carboniferous age. The formation is composed of clastic and pyroclastic sedimentary rocks with thin bedded limestone intercalations. Fossil assemblages include fusulinids (*Triticites* sp., *Pseudoschwagerina* sp.), brachiopods (*Linoproductus* sp., *Juresania* sp.), gastropods and crinoids. These fossils indicate Early Permian age. Total thickness of this formation is more than 200 meters.

Pha Huat Formation

This formation consists predominantly of thickly to very thickly bedded crystalline limestone with locally nodular cherts. The limestone is intercalated with tuffaceous sandstone in some intervals. The fossils include fusulinids (*Neoschwagerina* sp.), brachiopods (*Martinia* sp., *Dielasma* sp.), bryozoans (*Fenestella* sp., *Polypora* sp.), smaller foraminifers and crinoids. Fusulinids indicate Middle Permian age. The total thickness of the formation is about 600 meters.

Huai Tak Formation

It contains dark gray shales, laminated and thin bedded sandstone, limestone and conglomerates. This formation contains fossils of brachiopods (*Leptodus* sp., *Neospirifera* sp.), ammonoids, fusulinids (*Palaeofusulina sinensis*, *Colaniella parva*) and smaller foraminifers. The age of this formation is assigned as

Late Permian mainly on the basis of fusulinids. It consists of about 760 meters in total thickness.

2.2.3 Eastern Region

The Permian strata in this region are assigned as Chantaburi Group (Bunopas, 1981; 1992). This group contains the Srakaeo Formation and the Khao Chakarn Formation in ascending order. Additionally, Chaodumrong (1992) proposed two further formations of Permian age in this area, namely, Wang Nam Yen and Pang Asok in ascending order. These formations can be correlated with the Srakaeo Formation and the Khao Chakarn Formation respectively.

Srakaeo Formation

This formation is composed of cherts, limestones and ultramafic rocks (ophiolite suite). Radiolarians from cherts provide Middle to Late Permian ages for the formation.

Khao Chakarn Formation

It consists predominantly of very thickly bedded fossiliferous limestones. These limestones can be divided into two parts: western and eastern. These limestones differ in age which is dated mainly by fusulinids. The western limestone contains *Cancellina* sp. and *Neoschwagerina simplex* indicating a Kubergandian to early Murghabian age. The eastern limestone contains fusulinids (*Yabeina* sp., *Lepidolina* sp.) and corals (e.g., *Pseudohuangia* sp., *Waagenophyllum* sp., *Multimurinus* sp., and *Ipciphyllum* sp.) which provide a Midian (Capitanian) age (Fontaine and Salyapongse, 1997).

2.2.4 Lower Western and Southern Region

The region include mainly Ratburi Group with the upper part of Kaeng Krachan Group (Phuket Group). The Ratburi Group was first proposed by Javanaphet (1969) and revised by Bunopas (1981; 1992). It is conformably overlain clastic rocks of the Kaeng Krachan Group. This group is comprised predominantly of thinly bedded and very thickly bedded limestones with clastic rock intercalations, and is approximately 800 meters thick. Fossil assemblages include bryozoans, fusulinids, smaller foraminifers, brachiopods and algae. The age of the rocks obtained from these fossils is Middle to Late Permian. According to Fontaine and Sutheethorn (1988), the Ratburi Group shows six distinctive characteristics including: 1) fossils are neither rich nor diverse; 2) corals are restricted to a few localities; 3) the age range of the limestone is Middle to Late Permian; 4) underlying clastic sedimentary rocks are of early Permian age; 5) boron content of mudstone (especially close to Carboniferous-Permian boundary); this data is incompatible with glacial event data; 6) the Ratburi limestone accumulated on a shelf platform relatively far from the coast; it contains rare, small and mainly planktonic fossils. In addition, the Ratburi Group can be divided into four formations, namely, the Thung Nang Ling, the Prab Pha, the Pa Nom Wang, and the Um Luk Formation in ascending order (Harrison et al., 1997).

Thung Nang Ling Formation

This formation is characterized by dark, pale gray, medium to thickly bedded fossiliferous limestone. It has a total thickness of about 80 meters. This formation lies on the upper part of Kaeng Krachan Group.

Prab Pha Formation

It include dark gray thin to medium bedded limestone intercalated with calcareous mudstones and shales. Nodular cherts are occasionally observed within limestones. This formation is about 200 meters thick.

Pa Nom Wang

The Pa Nom Wang Formation consists mainly of coarse-grained medium to thickly bedded limestones, dolomitic limestone and dolomites. Nodular cherts are common. Total thickness of this formation is about 80 meters.

Um Luk Formation

This formation displays pale gray very thickly bedded limestones. It is more than 200 meters thick.

2.3 Geology of the Khao Somphot and the study area

The Khao Somphot mountain range is located at about 20 km east of Chai Badan district (Lam Narai), Lopburi province and at the western margin of the Khorat Plateau (Fig. 2.9). This mountain range and some parts of the surrounding areas are under the protection of the Khao Somphot Non-Hunting Office. It The range has a northwest-southeast trend and stand above a low plain of terra rossa sediments. A prominent feature of this mountain range is karstification of the upper part. Maximum height is 658 meters above sea level for the highest peak. Limestone exposure occur around foothill on the east and southeast of the mountain range. Additionally, there is another limestone hill located at about 10 km northeast of the Khao Somphot range namely Khao Ta Mon mountain. This mountain also shows prominent karstification with steep creek features. However, it has different lithologies to the limestones of

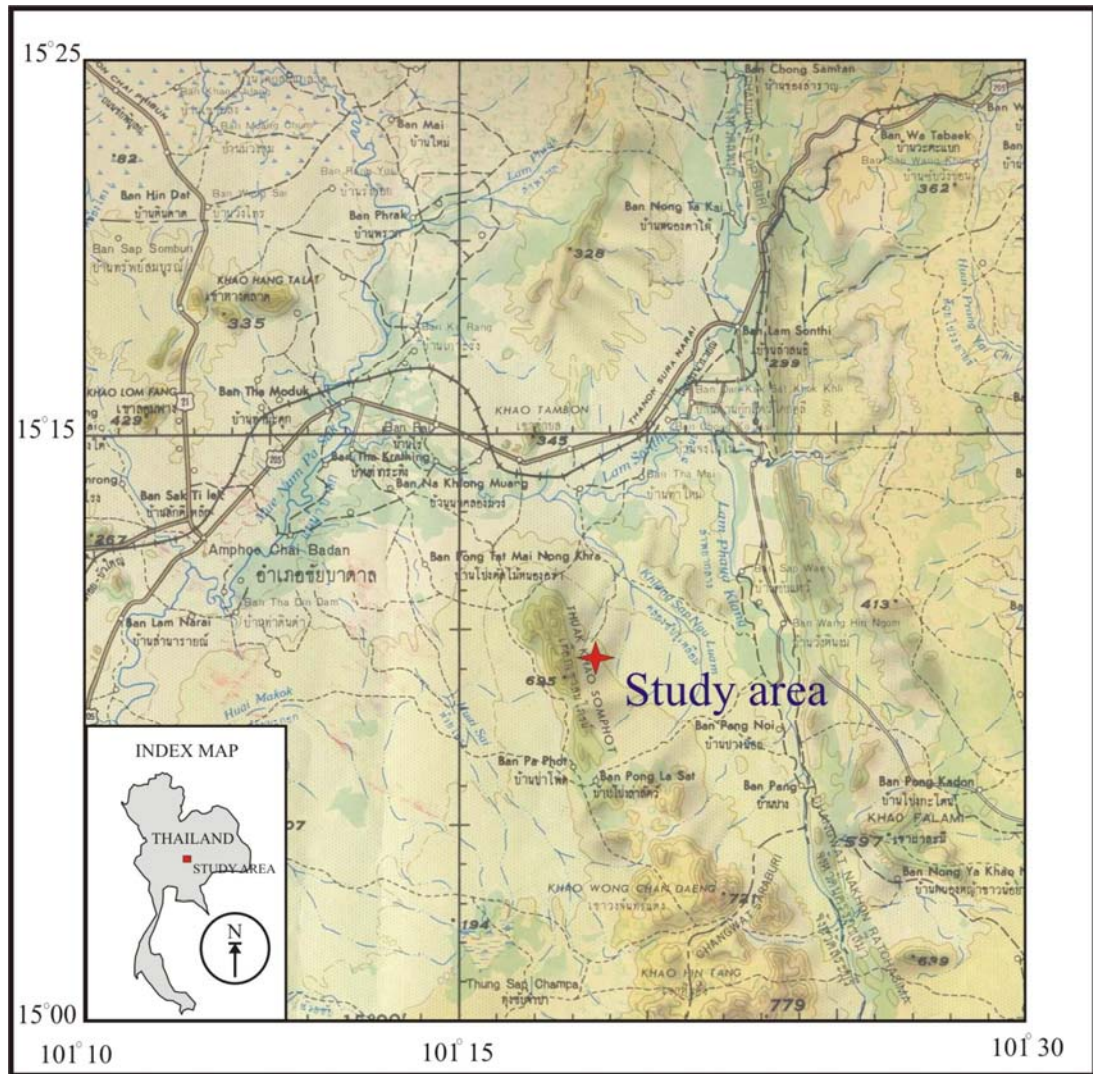


Figure 2.9 Topographic map showing location of the study area.

(modified after Royal Thai Survey Department, 1986)

Khao Somphot.

Geologically, the Khao Somphot is located to the south of the Khao Khwang platform. It belongs to Tak Fa Formation which might be correlated to Khao Khad Formation of the Saraburi Group (Nakornsri, 1976; DMR, 1992). Permian rocks of Khao Luak Formation are located a few kilometers to the north of Khao Somphot. Volcanic rocks including basalts and rhyolites are located mainly to the west of this area. To the east, Tak Fa Formation is bounded by clastic rocks of the Mesozoic Khorat Group. The low plain is covered mainly by Quaternary sediments (terra rossa) (Fig. 2.10).

The rocks in the Khao Somphot range are mainly limestones and dolomites which are aligned in slightly north-south trend. The limestones were deposited mainly within the carbonate platform interior environment and are approximately 1,200 meters thick (Fig. 2.11). Based on fusulinids, these rocks range in age from Asselian, Sakmarian, and early through late Guadalupian time. Dolomite occurs in age range between Asselian and late Sakmarian and is approximately 200 meters thick (Wielchowsky and Young, 1985). Additionally, Kubergandian-Murghabian strata composed of limestones and limestone conglomerates occur in the eastern foot hill of Khao Somphot range (Altermann, 1987).

According to Wielchowsky and Young (1985), the age of carbonate rocks in Khao Somphot range was established as Asselian through to late Guadalupian. This data is based mainly on fusulinid zonation from a 1,260 meter- thick measured section, between $15^{\circ} 06' - 07.5' N$, $101^{\circ} 18'-19' E$. Depositional environments along this section comprise three out of four sub-environments of platform interior including platform carbonate-interior lagoon, platform-interior mixed-mud and sand

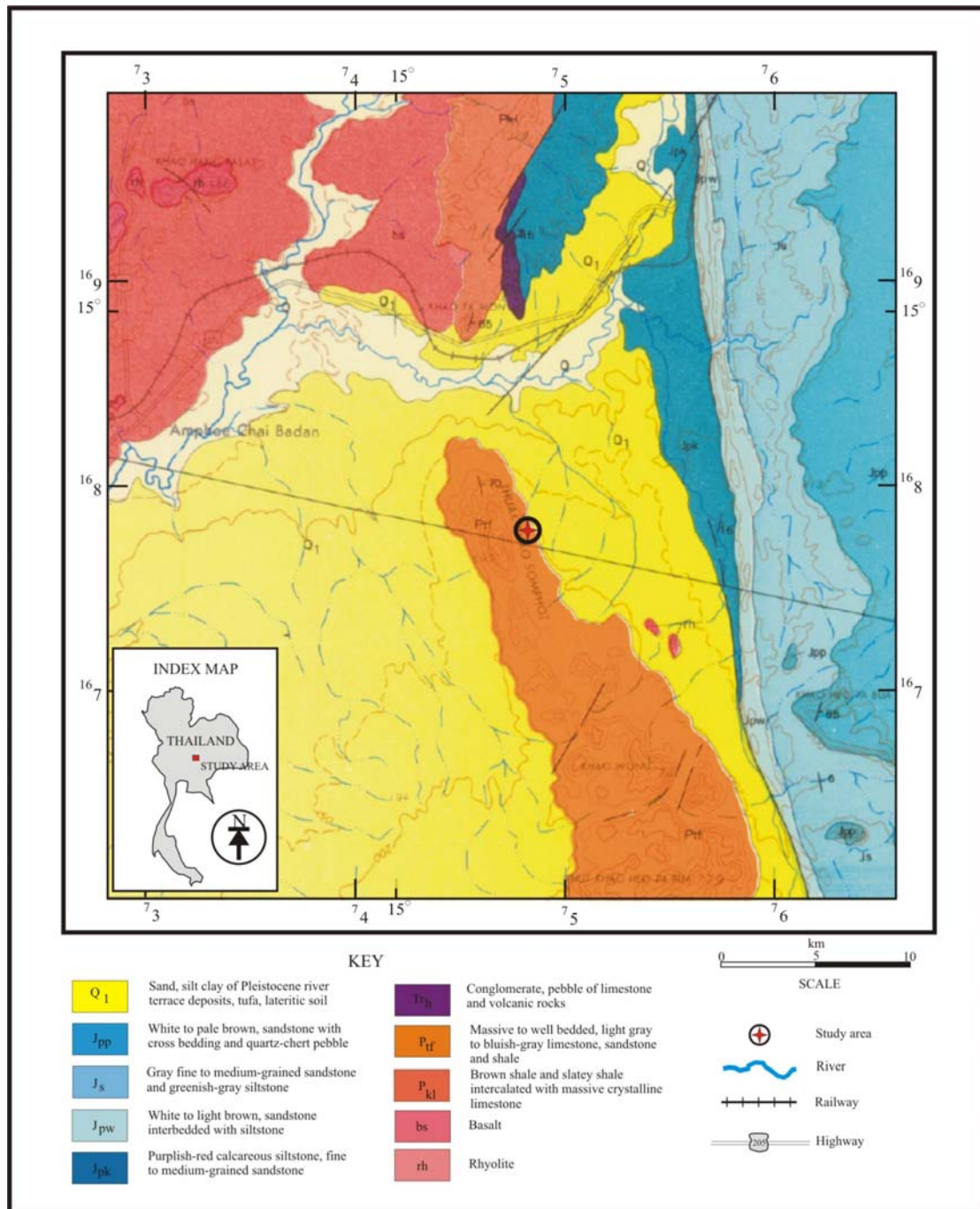


Figure 2.10 Geologic map of the study area. The study area is occupied by Permian limestone. This map shows clastic rocks of the Khorat Group located to the east of the study area while the main area of volcanic rocks is located to the north. (modified after Nakornsri, 1976)

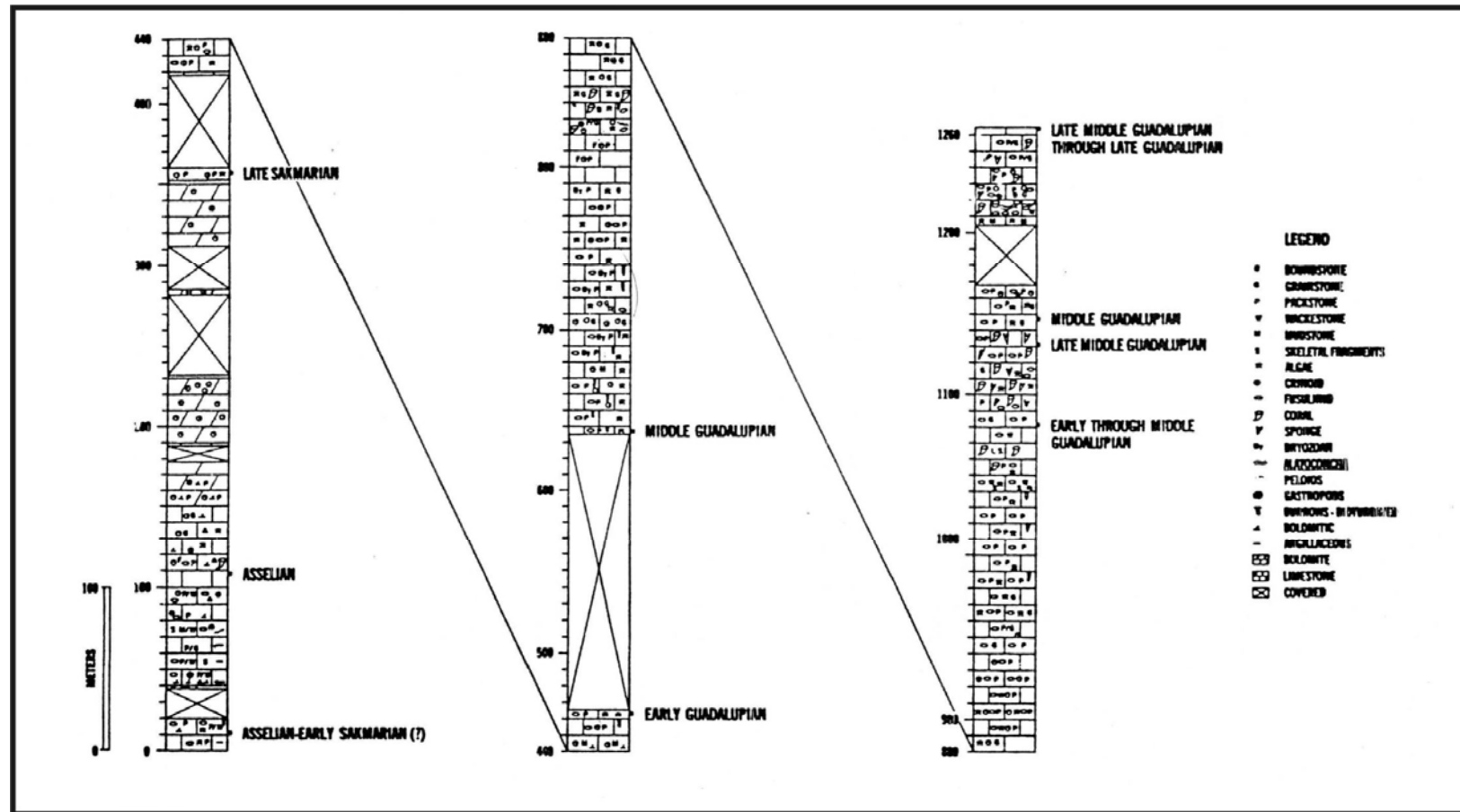


Figure 2.11 Stratigraphic log of Khao Somphot section. Alatoconchid-bearing strata are located in the upper most part of the section in strata of middle Guadalupian to late Guadalupian age. (after Wielchowsky and Young, 1985)

complex, and platform-interior sand shoal. These sub-environments are interpreted from the observation of shoaling-upward sequence of the carbonate beds. In term of lithology, the sequence includes medium-bedded carbonate mudstones, skeletal wackestones, and skeletal packstones and grainstones in ascending order. This lithofacies succession is similar to that found in the north of Saraburi area (Tittirananda, 1976). According to data from Khao Somphot, not only platform-interior environment is represented but restricted platform environment also. In addition, restricted platform environment is also characterized by shallowing-upward sequence. This sequence mostly shows dark gray thin-bedded mudstones and wackestones with thin laminations and small pieces of carbonaceous matter (charcoal fragments) on top of the sequence. Birdseye structures (fenestrae) are also observed from these rocks. Dolomitizations are common and occur locally at a meter-scale. Nodular and lenticular cherts are common and they contain some fossils in some cases. Altermann (1989) discovered oncoidal limestones which are interpreted as shallow, intertidal environment as well.

Light reddish limestone conglomerate is observed along the eastern foothills of Khao Somphot range. This conglomerate occurs within Kubergandan-Murghabian strata. It is matrix-supported, medium grained (pebble to cobble size), with clasts embedded in sparitic calcite matrix. The clasts are subangular to rounded and consist mainly of unfossiliferous micrite or microsparite facies often with a dark, iron-rich coating. Skeletal fragments are scattered in the matrix. On the basis of these observation and the lack of fossils in clasts and matrix, Altermann (1989) interpreted this conglomerate as a reworked former supratidal deposit rather than a reef slope deposit. Other conglomerates and breccias in this area are located along the lower part

of Khao Somphot (15° 11'N). They also show reddish color, are matrix-supported and include clasts of pebble and cobble sizes. The matrix is clastic and coarse grained. About 50% of clasts are of limestones and the other 50% is reworked conglomerate. Foraminifers from the layers of wackestones, packstones and grainstones indicates Midian age. Depositional environment is interpreted as high energy tidal channel and tidal shelf (Altermann, 1989).

For this thesis, two localities of conglomerate and breccias were observed and studied. Based on sedimentology and stratigraphy, one locality is interpreted as a local collapse breccia. The second locality is interpreted as tidal channel deposits. This outcrop is probably the same interval of Altermann (1989) mentioned above. More details on these conglomerate and breccias are presented in the following chapter.

Along the eastern foothills in the northern part of Khao Somphot range, there is coral patch reef exposed with individual colonies of 0.5 to 1.0 meters in diameter. In addition, limestones containing crinoidal fine debris and up to 10 cm crinoid stems and abundant brachiopod shells were found interfingering with that coral reef. Foraminiferal biomicrites and sparites (packstones) are common with age ranging from Bolorian to Kubergandian. These findings indicate a shoal shelf with small reefs and mounds, affected by wave action, and protected lagoon. This interpretation is compatible with Wielchowsky and Young (1985)'s interpretation (Altermann, 1989).

Fossils in Khao Somphot area are abundant and diverse. They include fusulinids, corals, brachiopods, bivalves, algae, gastropods, sponges and crinoids. Alatoconchid bivalves occur in strata ranging late middle Guadalupian and late Guadalupian (Wielchowsky and Young, 1985). Fusulinids include include *Lepidolina multiseptata* (Deprat) and *Verbeekina verbeeki* (Geinitz) found in skeletal grainstones

and packstone, and *Metadolina* cf. *gravitesta* (Kanmera), *Verbeekina douvillei*, *Kahlerina* sp., *Boultonia* sp., *Chusenella* sp., *Nankinella* sp. in skeletal grainstones. These lithologies indicate a platform interior environment.

In the small hill at an abandoned quarry southeast of Khao Somphot range, there are alatoconchids associated with massive corals, fusulinids, gastropods, brachiopods and algae. The massive corals are *Ipciphyllum* and *Wentzelloides*. Fusulines included *Colania douvillei* and *Verbeekina verbeeki* which occur abundantly in wackestone/packstone. These faunas are associated with calcispheres and small foraminifers such as Nodosariidae, *Globivalvulina*, *Hemigordiopsis*, *Climacammina*, *Pachyphloia*, *Dagmaria* and *Pseudovermiporella nipponica*. These faunas indicate shallow, warm marine environments of late Murghabian age (Chonglakmani and Fontaine, 1990).

It should be noted that, the occurrence of *Lepidolina* in this area is not common whereas in Cambodia and around the Thai-Cambodian border *Lepidolina* is prolific. Additionally, the observation of *Lepidolina* in Khao Tam Yai further north of this area supports a Midian age for the shallow marine Khao Khwang platform as well (Fontaine et al., 2002).

The study area of this thesis is part of Khao Somphot mountain located in the vicinity of Ban Sap Kradon of Chai Badan district. It include two limestone hills located in the eastern foothills of this mountain with highest points at 297 and 258 meters above mean sea level (Fig. 2.12). This is primarily based on measured five sections located within these two limestone hills (Fig. 2.13). Section one to section four lie approximately 7685/4690 and 7685/4722 (latitude/longitude). Section five lies approximately between 7685/4725 and 7685/4750 (latitude/longitude). The rocks

involved are mainly of light to dark gray, well bedded limestones which are situated stratigraphically within the uppermost available exposure of Permian strata in this area. The limestone beds are exposed along a slightly north-south strike trend and are steeply inclined at about 75 degree to the east. In general, these limestones are mostly fossiliferous with relative abundant fossils such as alatoconchids, massive corals, fusulinids, gastropods, brachiopods, sponges, crinoids, etc.

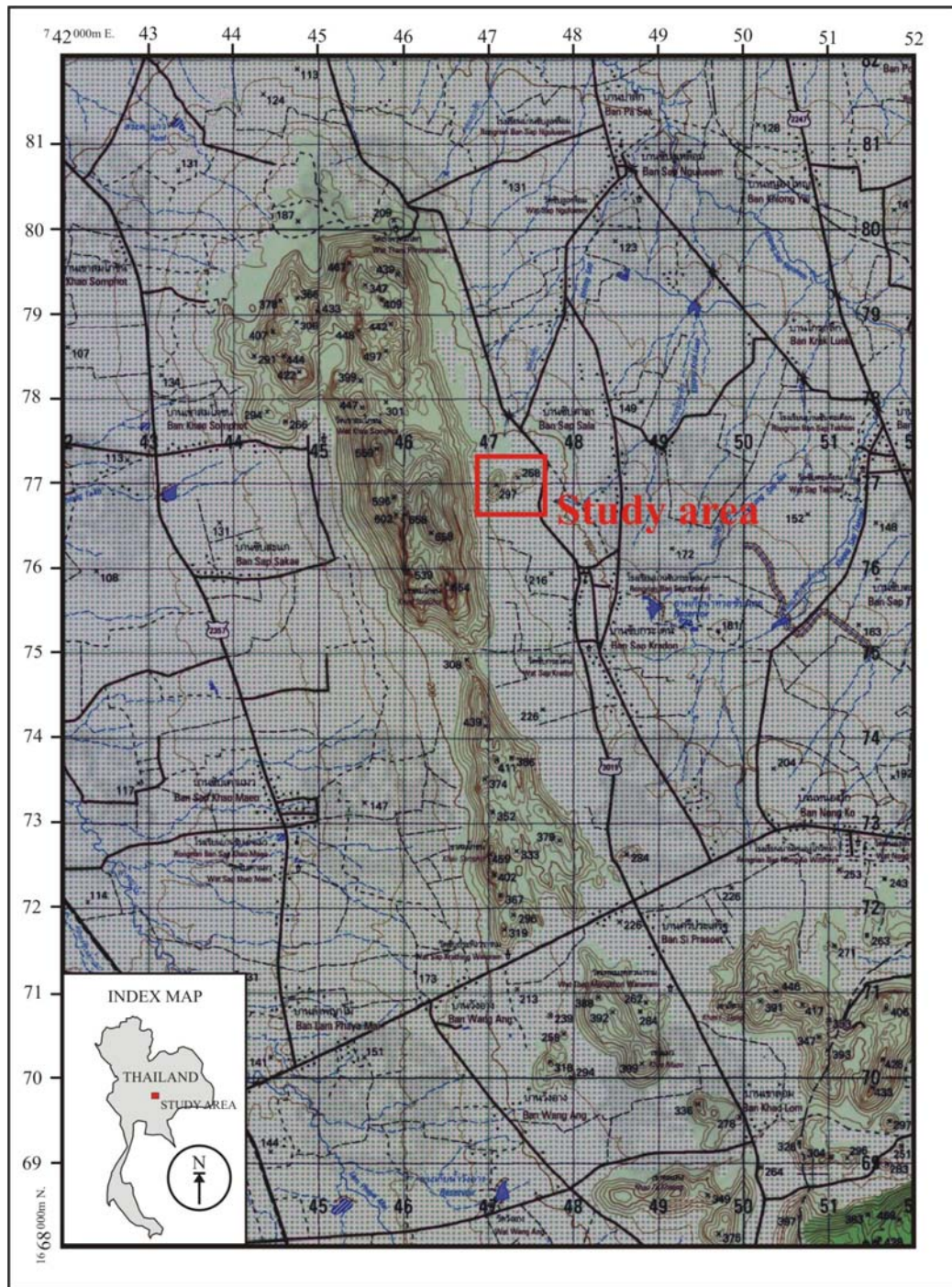


Figure 2.12 Topographic map showing study area which is located in the eastern foothill of Khao Somphot mountain range as shown in box. (modified after Royal Thai Survey Department, 1992)

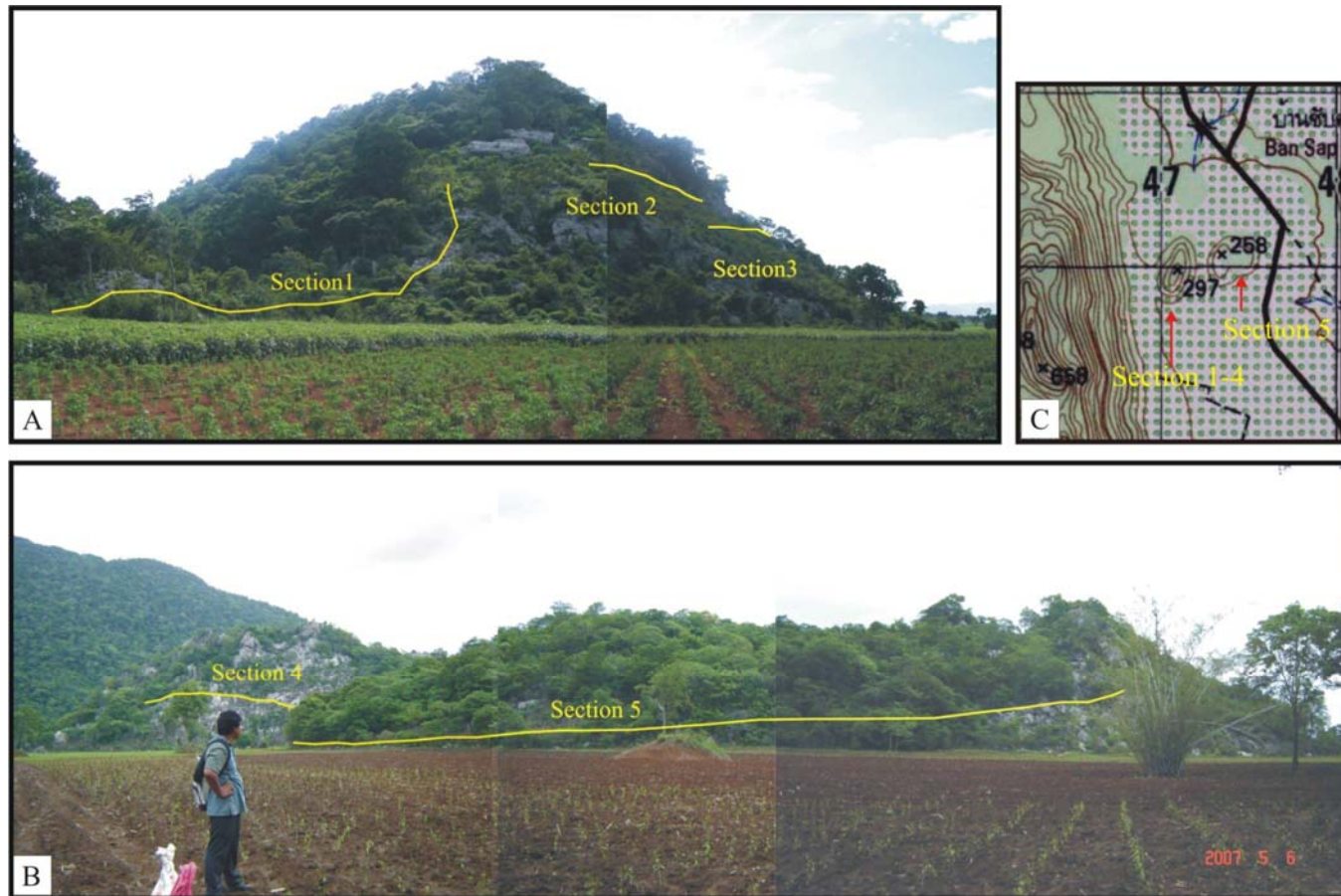


Figure 2.13 Field photograph showing the study area and study sections. A: Study section 1-3. B: Study section 4 and 5. C: Part of topographic map showing limestone hills of the study locality with sections.

CHAPTER III

LITHOSTRATIGRAPHY AND MICROFACIES

3.1 Introduction

Geologically, the term facies has been used in several ways. For example, it is used as a descriptive term for a body of rock with specified characteristics. In sedimentary rocks, these characteristics include lithology, composition, color, geometry, physical, chemical or biological sedimentary structures, and fossil content. Additionally, in some cases the term “facies” can be alternatively used either in a genetic sense or as interpreted depositional environment (Pirrie, 1998). In this thesis study, two terms of “facies” are used including lithofacies and microfacies. The term “lithofacies” is used for describing facies that are primarily based on lithological data. While the term “microfacies” has been used to refer to the total or sum of all sedimentological and paleontological data that can be described and classified from thin sections, peel, polished slabs or rock samples (Flügel, 1982; 2004). Lithostratigraphy is a major branch of stratigraphy and involves the subdivision of rock succession into units based mainly on gross lithology or rock type (Cox and Sumbler, 1998).

In this thesis, the study locality is dominated by carbonate rocks especially limestones. Lithologic differentiation of these rocks into units is a primary objective of field investigation. Lithological data and lithologic unit recognition then lead to formal lithostratigraphic description. Details of the lithology of these rocks are largely

determined in the laboratory by microfacies study. Both field information and microfacies data are the basis of carbonate classification and interpretation of depositional environment.

Classification of carbonate rocks has been discussed and proposed by various authors before World War II. It was begun by Pia (1933) with carbonate classification based on present day environmental conditions and depositional settings. His classification criteria of carbonate rocks related to water energy. This concept was later used for almost all recent carbonate classification. However, more interest in carbonate classification began with increasing carbonate research and its application for oil exploration in the early 1960s (Carozzi, 1993). Today, the most well known limestone classification schemes include those of Folk (1959; 1962), Dunham (1962), Dunham (1962) with modification by Embry and Kovan (1971), Strohmenger and Wirsing (1991), Wright (1992), and Carozzi (1989). Some concepts and information relating to selected classifications are described below.

The limestone classification proposed by Folk (1959; 1962) is based conceptually mainly on water energy in relation to limestone components. Generally, in low-water energy conditions, carbonate mud (micrite) with or without grains is likely to be accumulated whilst in higher-energy environments fine-grained material is winnowed away into lower energy settings. In this high-energy case, sparry cement later fills in interstitial space between grains. According to this classification, limestones are composed of three end members including allochems, micrite and sparry cement. These rocks are divided into two broad categories based on the interstitial materials which are micrite and sparite. Both of these can be further subdivided into four subclasses depending on predominating allochemical

constituents. These constituents include bioclast, ooid, peloid and intraclast. They are briefly assigned as bio, oo, pel and intra respectively. These assignments are then used as an adjective extension of micrite and sparite types.

According to the limestone classification of Dunham (1962), and Dunham (1962) with modification by Embry and Kovan (1971), the primary emphasis is most concerned with limestone depositional fabric. Two types of carbonates are distinguished. They include carbonate in which the original components were not bound during deposition (allochthonous) and carbonate with whose original components bounded during deposition (autochthonous). The first type is further divided into four categories including mudstone, wackestone, packstone and grainstone. The first three categories contain mud with different mud/grain ratio. There is mud-supported texture in mudstone and wackestone while grain-supported texture is found in packstone. Mudstone contains less than 10% allochems while wackestone has more than 10% allochems. Grainstone is characterized by grain-supported texture without mud. This allochthonous fabric can be separately classified into floatstone and rudstone if size of allochems exceeds 2 mm. Allochems are floated in floatstone but densely packed in rudstone. Autochthonous deposits can be separated into bindstone, bafflestone and framestone. Organically binding organisms serve as the main constructor in bindstone. Branching or stalk-shaped organisms play a baffling role in bafflestone. Framstone has rigid framework organisms as main reef-builders.

Carozzi (1983; 1989) proposed a carbonate classification based on grain-size in combination with texture (mud-supported or grain-supported). This classification requires a long sentence or paragraph in order to provide more descriptive details on

that carbonate rock. They include all constituents and textural-diagenetic relationships. Practical classification consists of calcilutite, calcisiltite, mud-supported calcarenite, grain-supported calcarenite, matrix-supported calcirudite, clast-supported calcirudite, bioaccumulated limestone and bioconstructed limestone.

In this thesis study, the principal concern is interpretation of the depositional environments of alatoconchid-bearing limestones. The results will provide insight on the depositional environment and natural habitat of alatoconchid bivalves. In order to acquire this information, field study and microfacies analysis including carbonate classification and interpretation is conducted.

3.2 Lithostratigraphy

On the basis of field observations, seven lithostratigraphic units (Unit A-G) have been recognized from five measured sections as shown in Figure 1. These units were differentiated on the basis of lithologic and physiographic characteristics. They consist mainly of bedded limestones which are disrupted by limestone breccias and conglomerate in some intervals. In this locality, the sections are exposed within two main limestone hills. These hills are located at the eastern foothill of Khao Somphot Mountain. They are informally erected as Western hill and Eastern hill. They are located to the west and the east in relation to the other respectively. Unit A to Unit E occur in the Western hill while Unit F and Unit G occur in the Eastern hill. Limestone beds in both hills are within a homoclinal sequence that is steeply dipping to the east and is eastwardly younging. Details on field-oriented lithologic units are described below in ascending order.

Unit A: this unit is located at base of the study sections. It starts from western foothill of the Western hill. It is exposed from the ground surface with a few meters of relief. The unit can be traced continuously to higher elevation with about ten meters height in an easterly direction. Total thickness of this unit is up to approximately 25 meters.

Unit A consists predominantly of medium to thickly bedded limestones. These limestones are mainly intercalated with thinly to medium bedded argillaceous limestone and laminated limestone. The alternation of limestone beds and these intercalation beds are profound in the field. It shows stratigraphic repetition of this pattern up-sequence, indicative of a regular cyclicity. In addition, there are up to seven alatoconchid coquinite beds presented in Unit A. Alatoconchids can be observed in both life position and in displaced or reworked position. Fusulinids were found dispersed in some beds with less than 10% of rock volume. In the lower part of the Unit A, they were found concentrated in a single layer. Gastropods and brachiopods were separately observed in relatively high concentration within single layers. Diagenetic textures including dolomitic patches, chert nodules and bands, and stylolites are common.

In summary, this Unit A is characterised by strong and conspicuous alternation of limestone and argillaceous limestone, or limestone and laminated limestone.

Unit B: this unit conformably overlies Unit A. The base of Unit B is a distinctive fusulinid-bearing bed. The top of Unit B is capped by fissure-bearing limestones and collapse breccias of Unit C. Unit B is up to 97 meters thick. However, lithological data not available from a zone of non-exposure about 25 meters thick in

the central part of the unit. This interval is covered by a debris cover of loose blocks of limestone.

Unit B is characterised mainly by thickly bedded fusulinid-bearing limestone, coral-bearing limestone, and alatoconchid-bearing limestone. Nodular cherts are common while dolomites are less common in comparison with Unit A. Fusulinid-bearing limestone can be observed throughout the unit. They are characterised by scattered fusulinid tests in the rock. Fusulinids can be estimated to comprise more than 10% of total rock volume. Furthermore, they are concentrated with densely packed texture in some thin layers. Coral-bearing limestones were observed with corals in both growth position forming biostromal structure, and as displaced and/or reworked blocks of coral heads. Massive corals are dominant over other coral types. Solitary and fasciculate corals are rare. Fasciculate coral includes *Sinopora* sp. Tabulate corals were found in two beds. They exhibit as life position corals forming decimetre thick biostromes. These coral-bearing limestones are more obvious in the upper part of Unit B. Alatoconchid beds appear with both growth- (in situ) and reworked- positions of alatoconchid bivalves up to 20 beds were observed throughout the unit. Argillaceous limestone and laminated limestone are present, mostly near the base of this unit but they are not conspicuous as in Unit A.

Unit C: this unit is characterized by fissures with fissure-fill sediments in pre-existing limestone beds and collapse- breccias. The former lithology occurs in the lower part of the unit while the latter is situated in the upper part. Total thickness is approximately 8 meters.

Unit D: crinoidal limestone or encrinite is the dominant lithology in this unit. It occurs directly overlying Unit C and extended up to the base of Unit E.

It is up to 17 meters in total thickness. Unit D is mostly thick to very thickly bedded limestone. It is predominantly comprised of crinoidal elements with fragments of bryozoans and other skeletal fragments. Some beds show distinctive elephant skin texture indicative of dolomitic recrystallisation.

Unit E: this unit is located in the eastern most part of the Western hill. It immediately overlies Unit D and underlies Unit F. However, there is discontinuous exposure of limestone beds between this unit and Unit F. It is largely obscured cover. Unit E has a total thickness of about 40 meters. However, there is a debris cover of loose blocks of limestone and soil in the lower to middle parts of this unit, an interval of about 17 meters thickness. Lithofacies of Unit E are characterized mainly by thickly bedded fusulinid-bearing limestone and alatoconchid-bearing limestone. Fusulinid beds are dominated by more than 10% of fusulinids scattered in the rocks. These beds were observed throughout almost all intervals of this unit. Massive coral-bearing limestone was found in four beds, all located in the lower half of the unit. Alatoconchid beds are intercalated with fusulinid beds in the upper half of Unit E. Polymict breccia is exposed as a single discontinuous layer in the middle part of the unit. Chert nodules were observed also, mainly in the middle part of the unit.

In general, lithologic characteristics of this unit are similar to those found in the upper part of Unit B. However, it differs in having different fusulinid assemblages and lacking any conspicuous dolomitic texture.

Unit F: fusulinid-bearing limestone is the most dominant lithofacies in this unit. The base of Unit F is at the western end of the Eastern hill. It is about 155 meters thick. This thickness is more than 66% total thickness of the sequence exposed in Eastern hill. Unit F is overlain by Unit G. In Unit F, fusulinid beds were

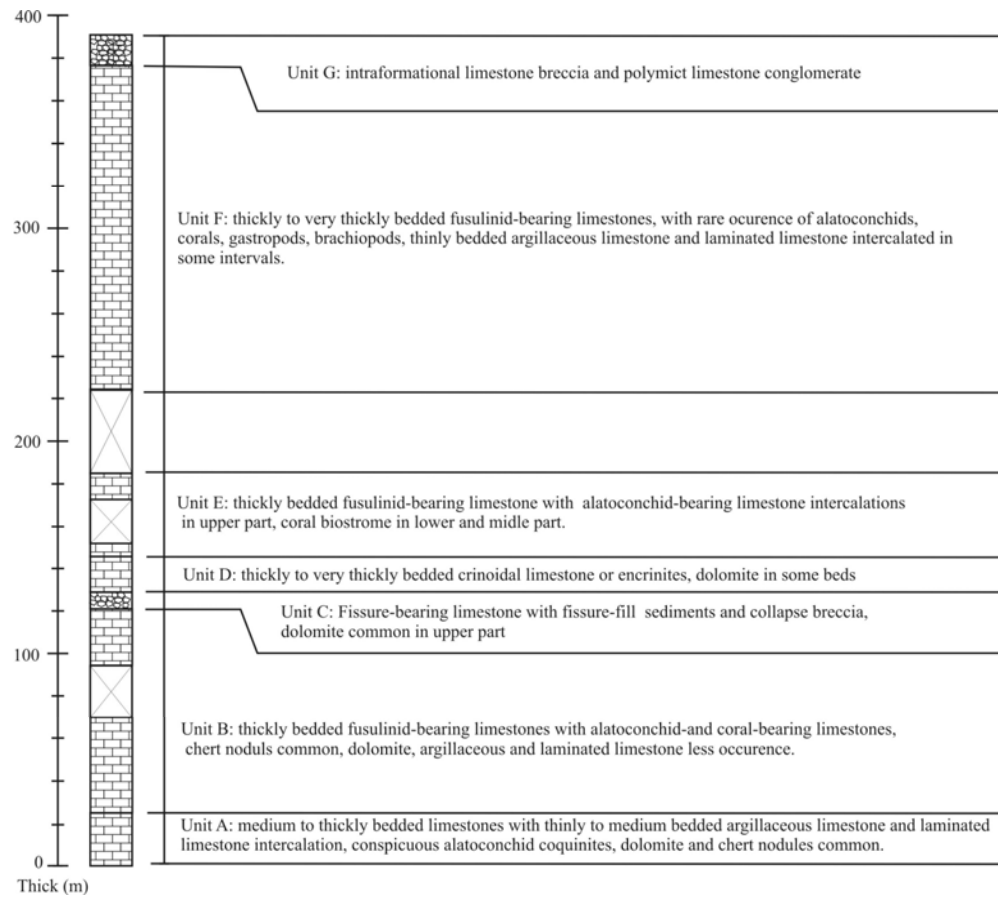


Figure 3.1 Lithostratigraphic units of the alatoconchid-bearing limestone sections, Khao Somphot locality.

found mainly as thick to very thickly bedded limestones. These beds are mostly characterized by more than 10% of fusulinids floated in limestones. In some cases, fusulinid beds show high concentration of fusulinid content with densely packed texture. This texture is effectively clast-supported with fusulinid tests in contact with each other. Most of these beds were thin to medium bedded but there are some rare thick beds.

Other lithofacies in this unit include thinly bedded argillaceous and laminated limestones and limestone breccias. These limestones are occasionally observed in some intervals. Additionally, three alatoconchid-bearing beds were observed in the lower and middle parts of this unit. Massive corals are nearly absent in this unit. They were found associated with *Sinopora* sp. and fusulinids overlying an alatoconchid bed in the middle part of the unit.

Unit G: this unit is located in the topmost of the study sections. It directly overlies Unit F. Unit G includes with two distinct lithofacies of limestone breccia and conglomerate. They include intraformational breccia and polymict conglomerate respectively. Intraformational breccia strata are about 5 meters thick. These strata are underlain by 10 meters of polymict conglomerate.

3.3 Microfacies

In order to confirm field data, more than 227 samples were prepared for thin-section and rock slabs. Based mainly on Dunham (1962), Folk (1959; 1962) and Flügel (2004), these samples were classified and summarized into ten major microfacies types (MF). Comparison charts for visual percentage estimation proposed by Baccelle and Bosellini (1965) were used for percentage estimation of allochemical

components in microfacies. Charts for visual estimation of degree of sorting based on Pettijohn and others (1972) were used for sorting designation of allochems. Microfacies types are summarized in Table 3.1 at the end of this section. Microfacies types and field information are presented in stratigraphic logs as shown in Figures 3.31-3.35. The ten microfacies types (MF1-10) are as follows:

1. Lime mudstone/wackestone
2. Laminated bindstone
3. Algal-foram wackestone/packstone
4. Bioclastic peloidal wackestone/packstone
5. Alatoconchid wackestone/packstone/floatstone
6. Fusulinid wackestone/packstone/grainstone
7. Coated bioclastic packstone/grainstone
8. Coral biostrome/floatstone
9. Crinoidal packstone
10. Carbonate breccias/conglomerate

Details of these microfacies types are described as follows:

3.3.1 MF1: Lime mudstone/ wackestone

This microfacies can be further divided into three sub-facies including lime mudstone facies, fenestral mudstone facies and wackestone facies. Details of all microfacies are described below.

3.3.1.1 MF1a: Lime mudstone

Description: The rock is characterized by thin to medium bedded limestone in the field (Fig. 3.2). It occur as non-laminated limestone. It is light gray in

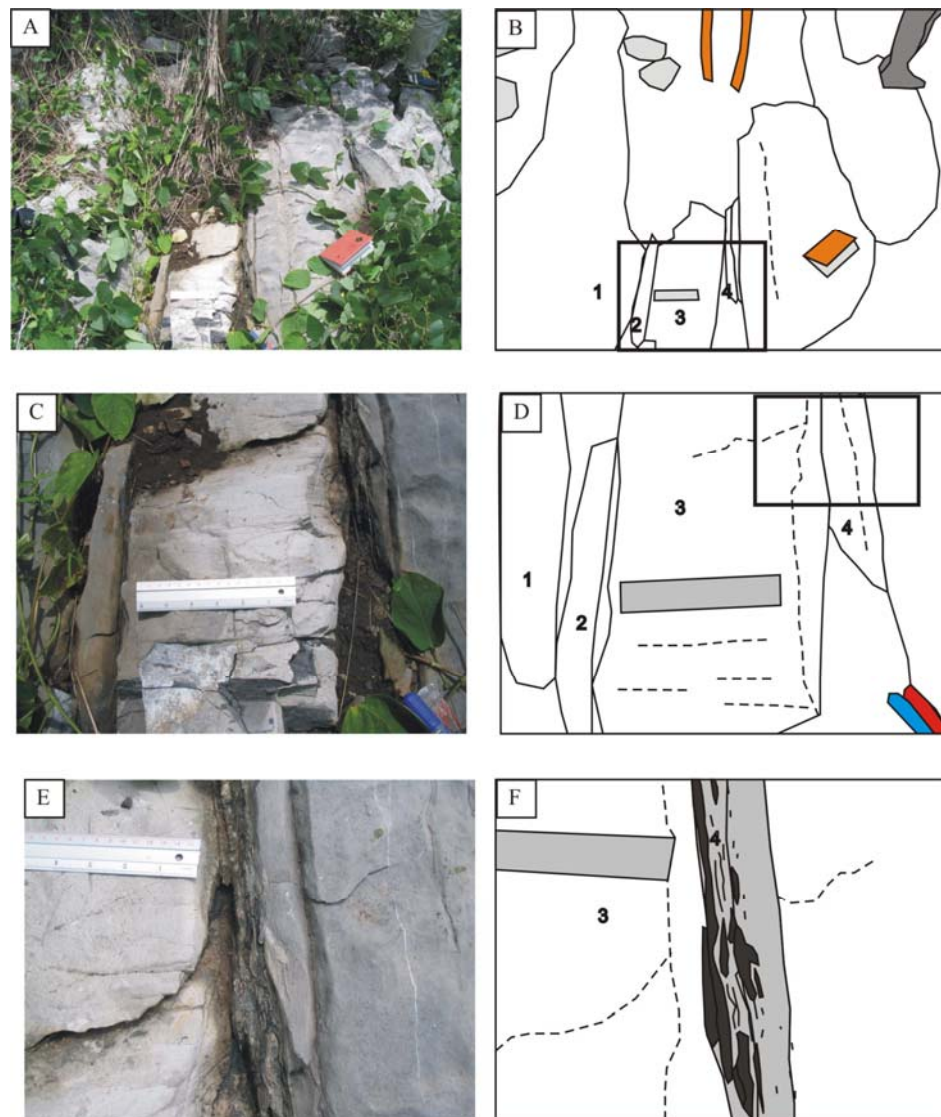


Figure 3.2 Outcrop photographs of limestones from Unit A with thin shell alatoconchid coquinite beds (MF5a1). A: Field photograph showing various limestone beds ranging from thin to thick bedded. B: Sketch of A, alatoconchid found in bed 2 and 4 while bed 3 contains MF1a, b. C: Field photograph maximized from A (as shown in box of B). D: Sketch of C. E; Magnification of C (as shown in box of D), showing densely packed thin-shell alatoconchid fragments embedded in thin bed of the middle part of photograph. F: Sketch of E, alatoconchid fragments shown in dark gray color in bed 4. (Ruler for scale=15 cm)

weathered surface and medium gray in fresh color. This rock was found commonly intercalated with thickly bedded algal-foram facies, laminated facies and non-laminated facies. In some intervals, it occurs locally as dolomitic limestone or dolomite.

Petrographically, this facies is generally characterized by mud with an absence or nearly absence of bioclastic grains (e.g. sample no. 701, 740, and 742) (Fig. 3.3). It can be classified as mudstone (Dunham, 1962) or fossiliferous micrite (Folk, 1959; 1962). Allochemical constituents are comprised of peloids, coarse intraclasts with less than 10% of bioclastic components. Peloids occur in two main groups: light gray coarse-grained peloids and dark gray fine-grained peloids. The first group is the most common type of peloid and is commonly found in other microfacies types. It is observed with peloid diameter of between 20 μm and 50 μm . The common fine grained of peloid is generally smaller in size, with less than 20 μm diameter. It is found scattered throughout the rock texture and accumulated in fenestral fabric as well. Intraclasts are prominent by virtue of their color, with slightly darker color than groundmass. Although it is easy to differentiate boundaries between them, texture and internal composition of intraclast and groundmass are similar. Bioclastic grains include ostracods, smaller foraminifers, algal fragments, shell fragments and other indeterminate shelly debris. Filamentous matter is also observed with orientation sub-parallel to bedding plane. Ostracods are commonly preserved as single-valves and fragments. Double-valved ostracods are rarely observed. Smaller foraminifers have been identified as *Langella* sp., *Globivalvulina* sp., *Neohemigordius grandis*, *N. japonica*, *Hemigordius* sp., *Agathammina* sp.

In sample no. 742-1, thin laminoid fenestral fabric is conspicuous and maybe a dominant feature of this facies. It is relatively smaller in size than a similar fenestral fabric observed in sample no. 742-2. The fenestrae present as elongate cavities with parallel to sub-parallel arrangement to the bedding plane. Internal cavities are occluded mainly by equant calcite cement and partly by dark-gray peloids.

3.3.1.2 MF1b: Fenestral mudstone

Description: This fenestral fabric is found locally overlying mudstone facies. In some intervals, mudstone facies grades into fenestral mudstone facies. In general, fenestral mudstone can not be differentiated in the field if the fenestral pore size is too small. However, it can be clearly observed under microscope.

Petrographically, the texture is characterized by irregular fenestral fabric (sample no. 742-2) (Fig. 3.3). The sedimentary framework consists of bioclastic grains and peloids. This facies can be designated to dismicrite (Folk, 1959; 1962) or fenestral mudstone (Dunham, 1962). Fenestral cavities exhibit an irregular shape infilled by coarse equant calcite cement, peloids and isolated grains. Isolated grains and stromatactoid fabric are common inside fenestral structures. Fossils are normally rare but common in some samples. They include algae, ostracods, smaller foraminifers, calcispheres, and small gastropods. Algae are found mainly as *Pseudovermiporella* sp., and *Vermiporella nipponnica*. Smaller foraminifers are *Hemigordius* sp., *Agathammina* sp., *Nodosaria* sp., *Calcitornella* sp. and *Globivalvulina* sp. Ostracods are found in both double-valved and single-valved conditions.

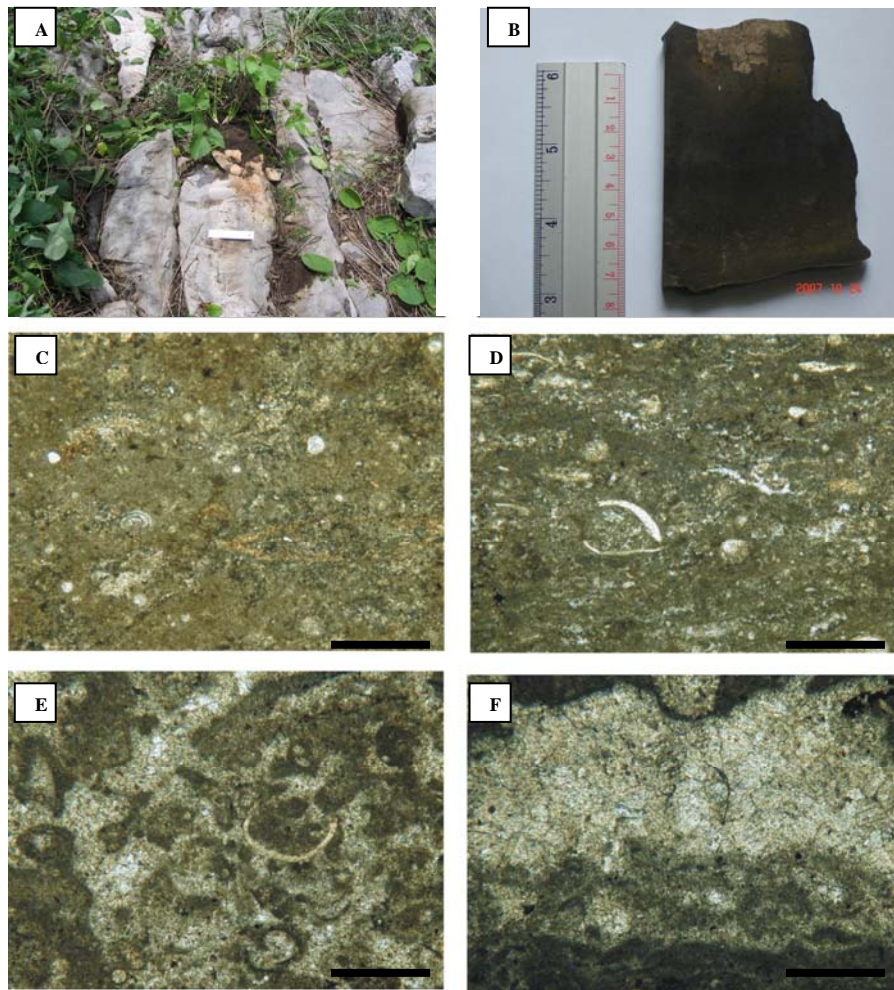


Figure 3.3 A: Field photograph of limestones. Lime mudstone with fenestral fabric occur in the upper part of this limestone succession (ruler as scale=15 cm). B: Photograph of rock slab showing medium gray mudstone with light brown dolomitic texture on top. C: Photomicrograph of lime mudstone (MF1a) showing mud dominated texture almost absent of fossils. D: Photomicrograph of fenestral mudstone (MF1b) from the transition between lime mudstone and true fenestral mudstone. Fenestral fabric is partly developed. E: Photomicrograph of fenestral mudstone showing well developed fenestral fabric with geopetal structure. F: Photomicrograph of fenestral mudstone showing open void of fenestral fabric which is occluded mainly by coarse calcite spar on top and floored by micrite. (All scale bar=500 μm)

3.3.1.3 MF1c: Bioclastic wackestone

Description: The rock is characterized by medium to thick bedded limestones. It can be found in the field as non-laminated limestones. Weathered color is light gray and fresh color is medium to dark gray. The weathered surface is slightly rough with prominent lithoclasts embedded in the rocks. Lithoclasts are approximately 1.0 cm to 2.0 cm in diameter. The upper part of this rock is grades into dolomitic limestone or dolomites in some intervals.

Petrographically, allochemical content in this microfacies is found over 10% and less than 50% (e.g. sample no. M05 and 710) (Fig. 3.4). They contain bioclastic grains, lithic peloids and intraclasts dispersed in mud matrix without any sign of compaction. It can be assigned as sparse biomicrite (Folk, 1959; 1962) or bioclastic wackestone (Dunham, 1962). The rock texture is lacking sparry cement. Drusy and blocky calcite cements are observed only in intragranular spaces of bioclastic grains. Evidence of aggrading neomorphism including microsparite and blocky calcite cement is clearly observed such as inside gastropod whorls. Peloids are round and common in the rock. Most of them show the same color and texture as intraclasts. Bioclastic grains are composed of smaller foraminifers, calcispheres, algae, ostracods, gastropods, brachiopods, corals and fine-grained comminuted shell debris. Geopetal structure is common in this facies and can be found mainly in gastropods. Smaller foraminifers consist of *Agathammina* sp., *Hemigordius* sp., *Globivalvulina* sp., *Calcitornella* sp., and *Pseudoendothyra* sp. Ostracods are found in both single- and double-valved conditions. Algae are *Pseudovermiporella* sp. and most of them are fragmented. Small gastropods are common. Corals are rare and occur as small fragments. Lithoclasts are common but their texture is different from

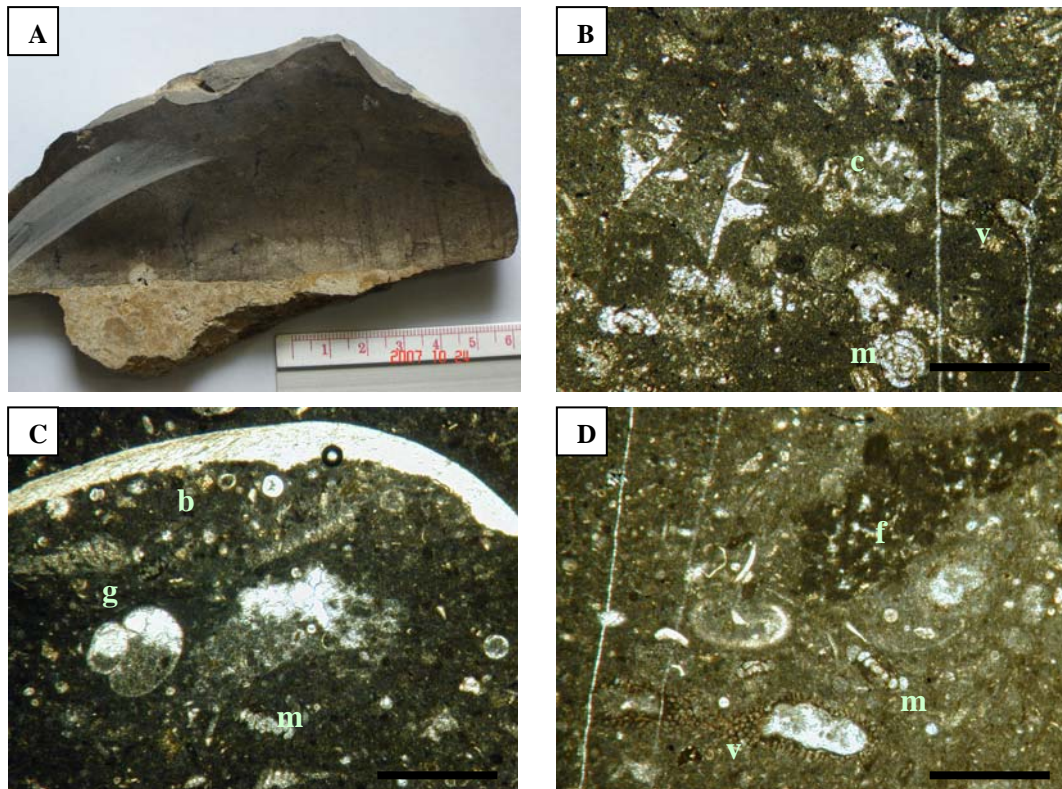


Figure 3.4 A: Photograph of rock slab of wackestone (sample no. M05). B. Photomicrograph showing bioclastic wackestone texture (MF1c, sample no 710). Allochems include miliolids (m), calcareous algae (c), fecal pellets (f), and fragments of *Vermiporella nipponica* (v). C: Photomicrograph of wackestone (sample no. 740). Geopetal structure is shown in gastropod (g) and in open void. Brachiopod fragment (b) is at top of view. D: Photomicrograph of wackestone from the same sample as C showing *Vermiporella nipponica* on the lower left with miliolids. Fecal pellet is occluded mainly in burrow. (All scale bar=500 μ m)

the host-rock (sample no. 740). They are subangular to subrounded with size ranging from 50 μm up to 200 μm . Fine lamination and original texture is obvious within the intraclasts.

3.3.2 MF2: Laminated bindstone

3.3.2.1 MF2a: Laminated bindstone

Description: In the field, this limestone has a distinctive prominent lamination. The rock is mostly thin to medium bedded. It exhibits light gray in weathered color and medium to dark gray in fresh color. Lamination is of planar type, aligned sub-parallel to parallel along the bedding plane. Fusulinid tests and small shell fragments are occasionally observed. These grains and fragments are arranged in sub-parallel to parallel orientation to bedding plane. Commonly, this rock is intercalated with thickly bedded fusulinid facies and medium to thickly bedded non-laminated limestones. It can be found intercalated with other facies as well but to lesser extent.

Petrographically, the rock texture contains moderately to densely packed allochemical components with rare micrite and lacking sign of cement (e.g. sample no.729 and 753) (Fig. 3.5). It can be designated as laminated bindstone with bioclastic-peloidal packstone matrix (Dunham, 1962; Embry and Klovan, 1971) or laminated biolithite with packed biomicrite matrix (Folk, 1959; 1962). The rock texture shows grain orientation sub-parallel to parallel along the bedding plane. More than 50% of allochems were observed in this sample. Allochems are dominated by skeletal fragments and peloids. Peloids are abundant with diameters ranging from 20 μm to 100 μm and characterized as rounded grains with sub-spherical to cylindrical shape. Skeletal grains are abraded and composed of calcareous green algae, smaller

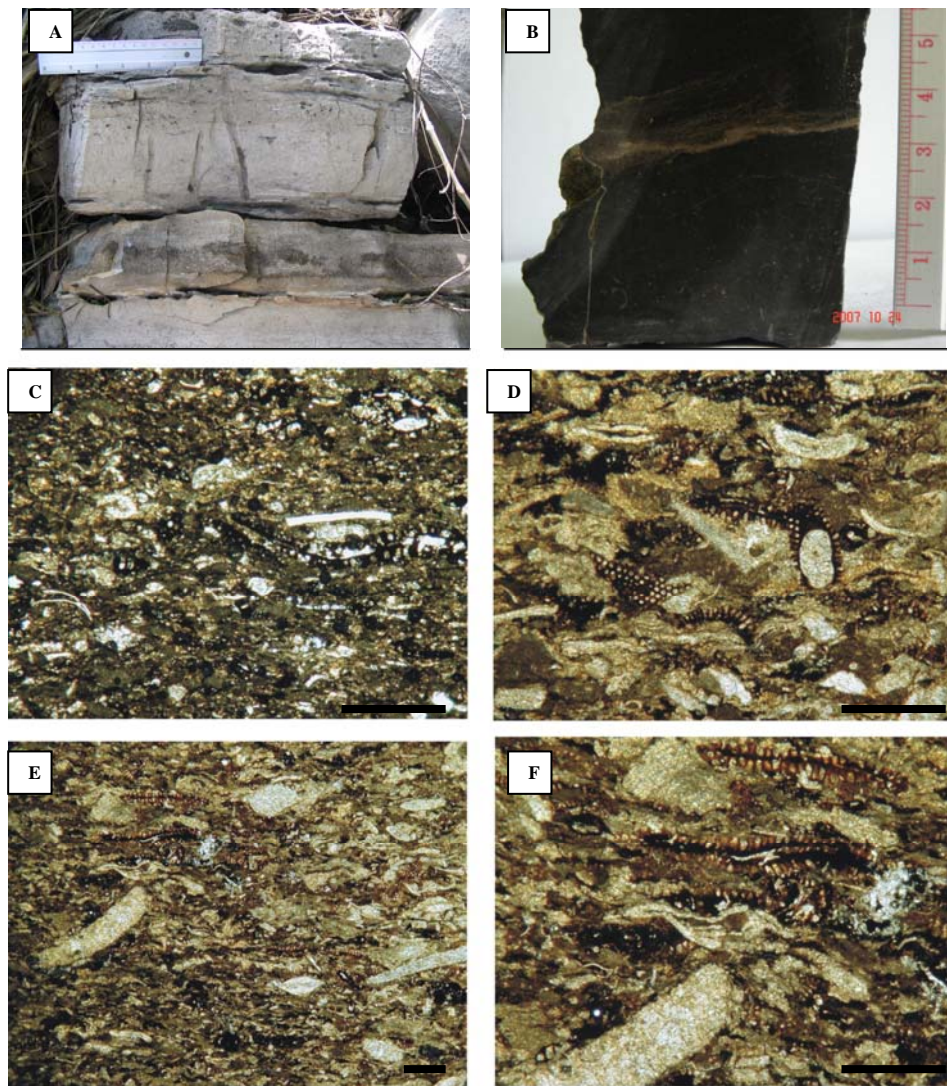


Figure 3.5 A: Field photograph of bed containing bindstone (ruler=15 cm). B: Photograph of rock slab of bindstone. C: Photomicrograph of packed laminated bindstone (MF2a, sample no. 729). D: Photomicrograph of packed bindstone showing algal tube (*Vermiporella nipponica*) associated with peloids and bioclastic fragments (sample no. 753c). E: Photomicrograph of packed bindstone showing flattened algal tube (*Vermiporella nipponica*) arranged parallel to bedding plane with bioclastic fragments and peloids (sample no. 743sc1). F: Photomicrograph of bindstone (magnification of E). (All scale bar = 500 μ m)

foraminifers, alatoconchid fragments, shell and algal debris. Algae consist of *Mizzia* sp. and *Pseudovermiporella* sp. Most algal thalli are flattened especially in *Pseudovermiporella* sp. Some skeletal grains such as calcareous algae and bivalve fragments have been encrusted by black filamentous laminae. Smaller foraminifers are found mainly as miliolids but rare hyaline test was occasionally observed. Milionids are poorly preserved as weathered and recrystallised tests. Fusulinids are rare with strongly micritised and crushed tests (sample no. 754). Skeletal fragments are dominated by thin alatoconchid shells which characterize as floated shell in matrix. Shell and algal debris are common. Shell debris composes of alatoconchid and unidentified shells. Algal debris is black in color and can be determined by its remnant of wall structure. Algal debris can be found as fine irregular fragments scattered throughout the rock. Interstitial void space is occluded mainly by micrite matrix. However, blocky sparry cement is occasionally observed as partly infilling in intergranular void of bioclasts.

3.3.2.2 MF2b: Fenestral bindstone

Description: In the field, this facies was found in very thin to thin beds. General texture can be compared to laminated bindstone facies. Most occurrences of this facies grades from laminated bindstone (e.g. sample no. 729). It can also be observed within laminated bindstone in some intervals. This facies is rare in comparison with the other facies.

Petrographically, the facies is characterized by laminated alternation of light-gray and dark-gray laminae (Fig. 3.6). It can be classified as fenestral bindstone with wackestone matrix (Dunham, 1962; Embry and Klovan, 1971). It can be compared to dismicrite or fenestral laminated biolithite (Folk, 1959; 1962). Fenestral

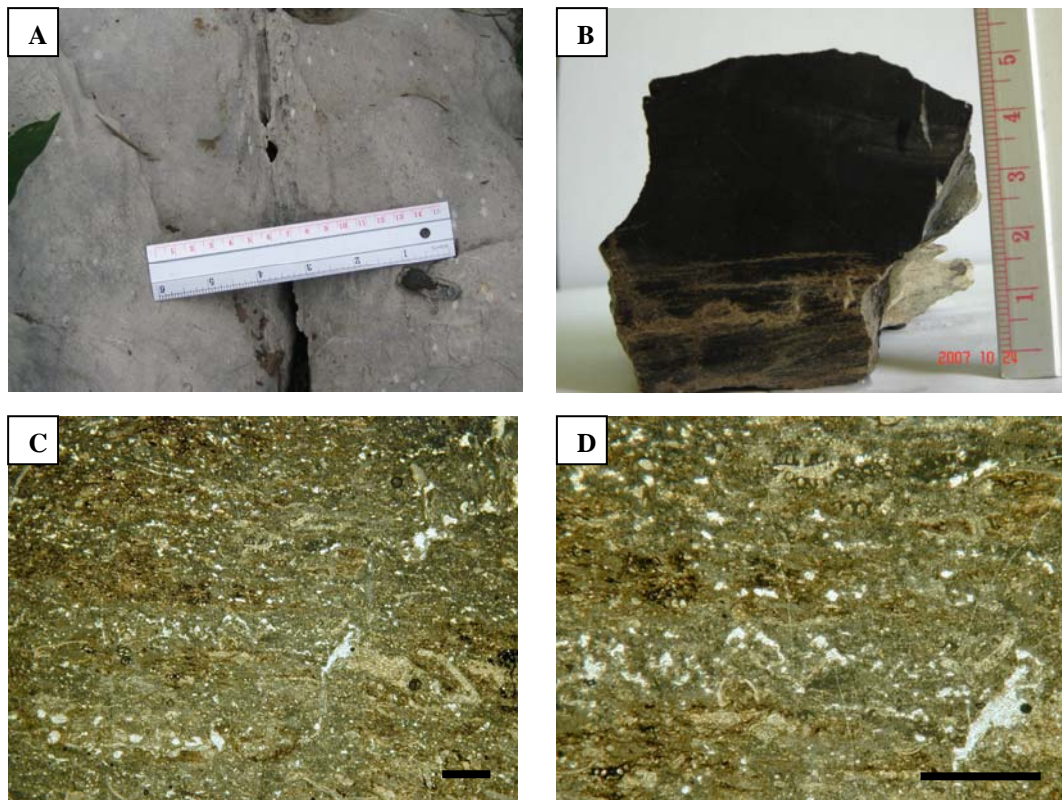


Figure 3.6 A: Field photograph showing limestone bed that contains fenestral bindstone. B: Photograph of rock slab with lamination in lower part (sample no. 729). C: Photomicrograph of fenestral bindstone (MF2b) showing irregular fenestral fabric in light gray layer. D: Photomicrograph of fenestral bindstone (magnification of C). (All scale bar=500 μm)

fabric is found mainly in light gray layers. In these layers, fenestral structure is characterised as laterally extended irregular, laminar fenestral cavities. The internal cavities are floored by sediment matrix and spar filled cement. Note that vertical cavities can also be observed. The sedimentary framework in this layer is characterized by allochems arranged in sub-horizontal to horizontal layers. Allochems consist of peloids predominating over bioclastic grains, with the relic of filamentous matter in groundmass. Calcisiltite and micritic mud form the matrix. Microsparite cement is partly observed. Peloids are rounded sub-spherical to ellipsoidal in shape. Bioclastic grains are miliolid smaller foraminifers, algal fragments, ostracods and shell debris. Algae are mainly *Pseudovermiporella* sp. For the dark layer, allochemical constituents are the same as that found in the light layer, but it differs in that it has higher numbers of algal fragments (*Pseudovermiporella* sp.). Algal filaments are abundant in this layer.

3.3.3 MF3: Algal-foram wackestone/ packstone

This facies is found mostly in the lower part of Unit A. It is characterized by medium bedded limestone with light-gray weathered surface and medium- to dark-gray fresh surface. This facies was commonly found intercalated with non-laminated and laminated limestones. In some cases, it was observed intercalated with alatoconhid biostrome as well. On the basis of petrographic study, this facies can be further divided into two subfacies including algal-foram wackestone and algal-foram packstone. These facies share common bioclastic components but differ in their texture. In some cases, this facies is grades into dolomitic limestone in the upper part of beds. Burrows are present in some intervals. Nodular and lenticular cherts are common.

3.3.3.1 MF3a: Algal-foram wackestone

Description: Petrographically, allochemical components range between 10 and 50% of total rock. Matrix is occluded mainly by micrite over sparry calcite cement (e.g. sample no. 704) (Fig. 3.7). Drusy calcite spar mosaic shows crystal size increasing toward center of void spaces. This sample can be assigned as algal-foram wackestone (Dunham, 1959) or sparse algal-foram biomicrite (Folk, 1959; 1962). Allochems are mainly of smaller foraminifers and algae with peloids. Algae in this facies are predominantly *Pseudovermiporella* sp.; *Mizzia* sp. is rare. Branch thallus can be observed in *Pseudovermiporella* sp. Micritised external walls are common in algae. Smaller foraminifers are dominated by miliolids including *Hemigordius* sp., *Agathammina* sp., and *Kamurana* sp. Other foraminifers are *Pseudoendothyra* sp., *Globivalvulina* sp., *Ichthyolaria* sp., *Eotuberitina* sp., and *Pachyphloia* sp. Ostracods are rare and most occur as fragments. Peloids are abundant composed of poorly sorted, sub-angular to sub-rounded clasts ranging in size from 10 um to 30 um. Interstitial space is occluded mainly by micrite. Pseudomicrosparite is common and drusy calcite cement is also observed.

3.3.3.2 MF3b: Algal-foram packstone

Description: Petrographically, this facies contains more than 50% allochemical components. The texture is characterized by packed, grain-supported, poorly to moderately sorted grains, with peloids in micrite matrix (e.g. sample 704b) (Fig. 3.7). Based on texture and composition of allochemical constituents this microfacies can be assigned as algal-foram packstone (Dunham, 1962). Additionally, it can be regarded as packed biomicrite (Folk, 1959; 1962). Allochems show no significant trace of arrangement and some grains show point- contact. Micrite exhibits

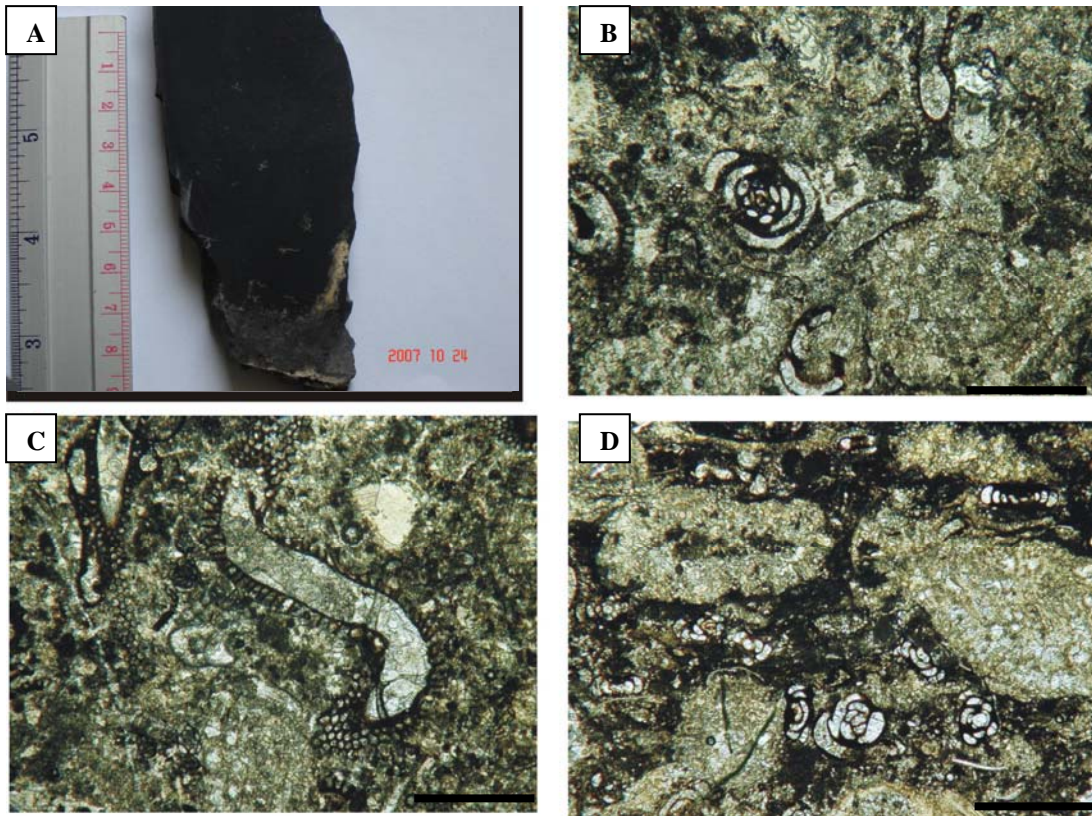


Figure 3.7 A: Rock slab of algal-foram facies showing medium to dark gray with sand-size fossils embedded in matrix. B: Photomicrograph of algal-foram wackestone (MF3a, sample no. 704) showing miliolids associated with *Vermiporella nipponica*. C: Photomicrograph from the same sample as B showing meandering and branching forms of *Vermiporella nipponica*. D: Photomicrograph of algal-foram packstone (MF3b, sample no. 704b) showing densely packed texture of miliolids and calcareous algae with fusulinids (*Nankinella* sp.). (All scale bar=500 μm)

some relicts of squeezing deformation parallel to bedding plane. Geopetal structure can be found in ostracod shells. Calcareous green algae and miliolid foraminifers are dominant in this facies. Other allochems consist of ostracods, brachiopods, and peloids. Coarse skeletal grains including *Mizzia* sp., and *Nankinella* sp. are recrystallised but smaller grains such as miliolids are well preserved. Smaller foraminifers include *Hemigordius* sp., *Agathammina* sp., *Kamurana* sp. and *Pseudoendothyra* sp. Ostracods mostly occur as fragments but deformed articulate shells are also observed. These deformed particles show relicts of plastic deformation with wavy parallel arrangement to the bedding plane. Peloids are variable in size, subangular to subrounded. Interstitial space is occluded by micrite and calcisiltite. Microstylolite formation can be observed within crushed miliolid tests.

3.3.4 MF4: Bioclastic-peloidal wackestone/packstone

Most limestones containing this facies are thick to very thick bedded. It is recognizable in the field in association with non-laminated limestones. This rock facies shows weathered surface in light gray while fresh color is medium to dark gray. It is common in the lower parts of Unit A and Unit B. In some intervals, it occurs intercalated with alatoconchid facies, algal-foram facies and mudstone facies.

3.3.4.1 MF4a: Bioclastic-peloidal wackestone

Description: Petrographically, this facies is characterized by more than 10% but less than 50% allochems in the matrix. Both skeletal and non-skeletal grains are poorly sorted and sparsely distributed in the rock (e.g. sample no. 708, A3) (Fig. 3.8). According to Dunham (1962), this facies can be classified as bioclastic-peloidal wackestone. It can be named as sparse biopelmicrite based on Folk (1959; 1962). Non-skeletal grains are composed of peloids which dominate this facies. They

are dark gray, irregular in shape, and their sizes range between 5 and 10 μm . Skeletal grains are normally eroded or corroded into bioclastic grains or fragments. They include algal thallus and fragments, smaller foraminifers, ostracods and other bioclastic fragments or shell debris. Algae are common in this facies and are dominated by calcareous green algae (or problematica) as *Vermiporella* sp. and red algae (*Undarella* sp.). Algal thalli (*Vermiporella* sp.) are black in color and normally decayed and eroded. Internal chambers of algae are occluded by coarse isopacouse mosaic sparry cement. Black algal fragments are found scattered throughout in this microfabric. Most fusulinid tests are worn or without outer volutions. Spirothical fragments and crushed tests are also present in this facies.

Smaller foraminifers are abundant and diverse. They include *Pachyphloia* sp. and others. Most miliolids are strongly recrystallised with obliterated original structure. Ostracods were found as fragments but articulated specimens are rarely observed. Micrite is predominant in interstitial spaces over sparry calcite cement. However, sparry calcite is commonly found infilling central stems of algal fragments, within internal cavities of smaller foraminifers and other shelly material. Some skeletal grains show micritisation around external walls and/or within internal chambers. In some cases, selective dolomite and dispersed fine dolomitic grains were found in bioclasts and in micrite matrix, respectively (e.g. sample no. 708).

3.3.4.2 MF4b: Bioclastic-peloidal packstone

Petrographically, this subfacies has a similar allochemical component to MF4a but differs in texture. This facies is defined by grain-supported texture with abundant peloids. Grains are mostly in contact with poorly to moderately sorted

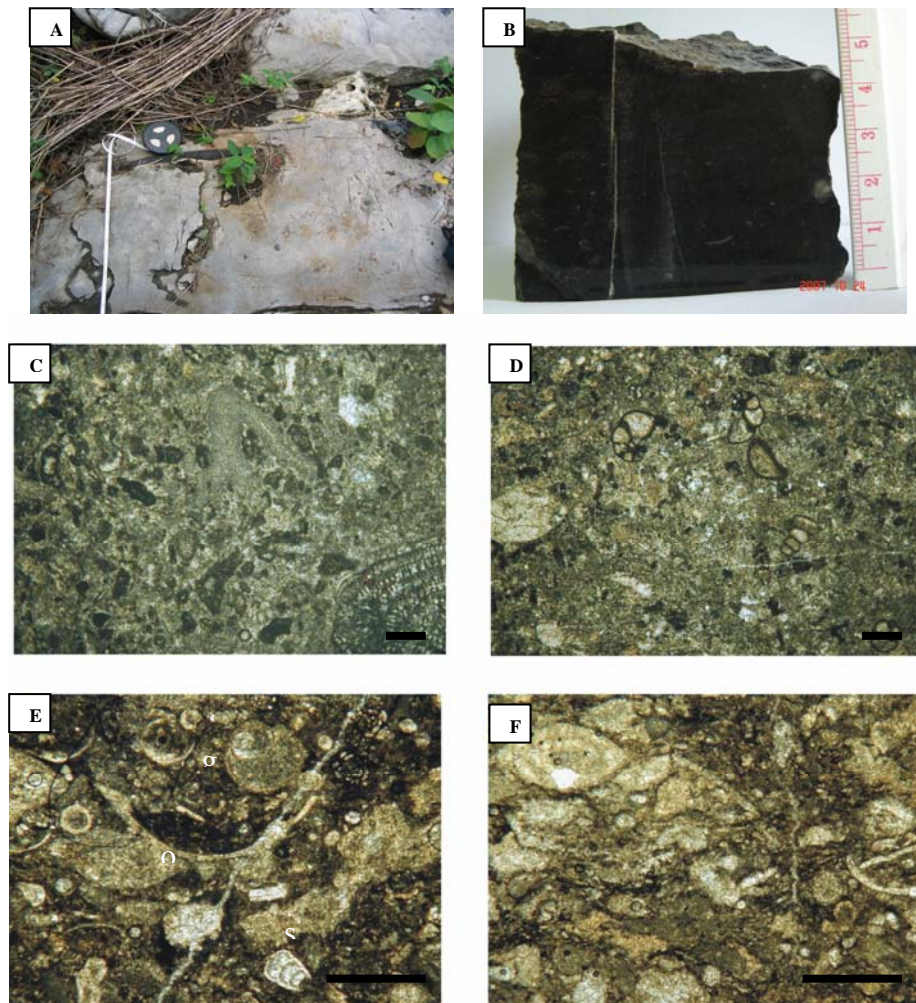


Figure 3.8 A: An outcrop photograph of thickly bedded limestone containing bioclastic peloidal wackestone. B: Rock slab of bioclastic peloidal packstone (MF4b, sample no. 703c). C: Photomicrograph of bioclastic peloidal wackestone. D: Photomicrograph of the same sample as C. Smaller foraminifers (*Globivalvulina* sp.) are dominant in this view. E: Photomicrograph of bioclastic packstone (MF4b, sample no. 703c) showing packed bioclastic texture with geopetal structure in center. Smaller foraminifers (s), small gastropods (g) and ostracods (o) are common in this facies. F: Photomicrograph of bioclastic packstone (MF4b, sample no. 703a). (All scale bar=500 μ m)

grains (e.g. sample no. 703c and 756) (Fig. 3.8). Interstitial space is occluded mainly by micrite. Other allochems in this facies include bioclastic grains and fragments. They consist of smaller foraminifers and calcareous algae. Among the algae, *Mizzia* sp. is prevalent while the fusulinids are dominated by *Nankinella* sp. Coated and micritic grains, some with encrusting layers are common.

In some samples, this facies shows densely packed texture (e.g. sample no. 752). It consists of poorly sorted bioclastic grains in micrite mud matrix but lacking calcite cement. These grains are worn or abraded. They include calcareous algae, miliolids, fusulinids and some calcareous fragments. Miliolids are prolific in this facies, occurring as infiltration grains with mud in the spaces between larger grains. Larger grains show imbrication structure with preferred grain orientation in some directions.

3.3.5 MF5: Alatoconchid facies

Based on preservation state of alatoconchid fossils in the field and microfacies from thin section, this facies can be divided into two subfacies. They are referred to here as Alatoconchid floatstone/rudstone (coquinites) (e.g. Figs. 3.9, 3.11, and 3.13) and Alatoconchid biostrome (e.g. Figs. 3.15 and 3.16).

3.3.5.1 MF5a: Alatoconchid floatstone/rudstone (coquinites)

Based on alatoconchid size and shell thickness, this facies can be further subdivided into two groups as thin-shell alatoconchid rudstone and thick-shell alatoconchid rudstone. These subfacies have a common matrix type but differ in alatoconchid shell size. Details of these facies are described below.

3.3.5.1.1 MF5a1: Thin-shell alatoconchid rudstone

Description: In the field, this rock is characterized as thin to medium bedded (Figs. 3.2 and 3.9). The color of weathered surfaces is light gray and fresh color is dark gray. This rock shows fitted grains of thin alatoconchid fragments. There are two thinly bedded limestones with densely-packed thin alatoconchid shell fragments found intercalated within wackestone facies in Unit A. The first bed is underlain by wackestone is overlain by bioclastic-peloidal wackestone bed. The second bed overlies this same wackestone bed. These alatoconchids beds are located in the middle of Unit A (e.g. sample no. 739). In addition, other thin-shell alatoconchid rudstone beds are found as thin layers within non-laminated limestones, such as in the upper part of Unit B (e.g. sample no. 773a and 774). Shell thickness of these alatoconchids is 0.3 cm on average. Some of these shell fragments are more than 10 cm long. However, it is difficult to estimate total length or width because most specimens occur as fragments in random cross section.

Petrographically, this microfacies is composed of over 80% densely packed allochemical constituents (Fig. 3.9). Allochemicals include peloids and bioclastic fragments with very rare micrite. This microfacies can be classified as bioclastic peloidal packstone (Dunham, 1962) or densely packed biopelmicrite (Folk, 1959; 1962). As a lithofacies, it can be regarded as thin-shell alatoconchid rudstone with bioclastic peloidal packstone matrix. Most grains are arranged parallel to bedding plane. Peloids exhibit ellipsoidal shape ranging in size from 20 μm to 200 μm long. Bioclastic fragments are algae, ostracods, smaller foraminifers and unidentified shelly fragments. Alatoconchid shell fragments exhibit double shell layers with a thick inner layer and thin outer layer.

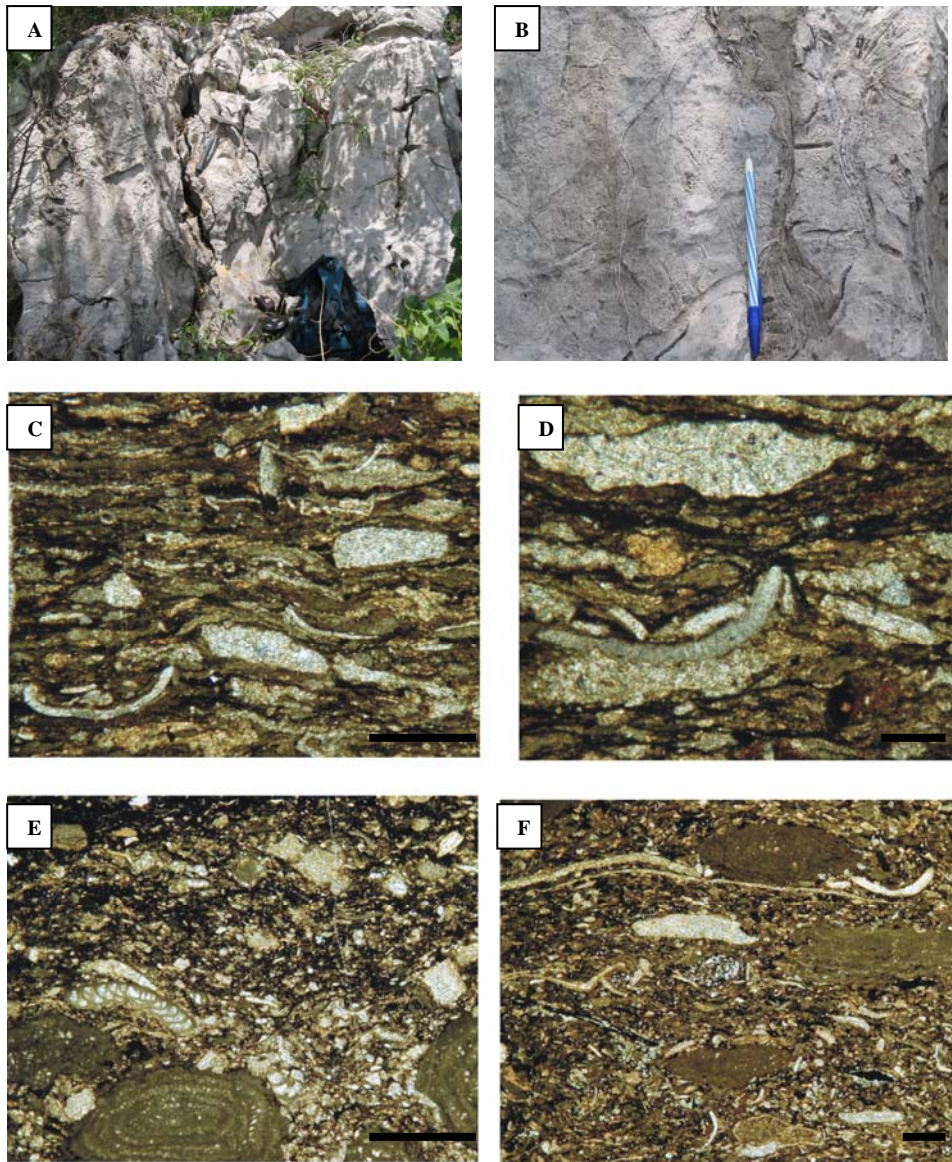


Figure 3.9 A: Field photograph of thin-shell alatoconchid beds (MF5a1). B: Field photograph of thin-shell alatoconchid facies (MF5a1). C: Photomicrograph of densely packed peloidal bioclastic texture with black filamentous matter (sample no. 739). D: Magnification of C. E: Photomicrograph of bioclastic calcisiltite matrix from alatoconchid floatstone facies (sample no. 779). F: Photomicrograph of calcisiltite matrix of alatoconchid floatstone facies (sample no. 784). (C, E, F, scale bar=500 μm ; D, scale bar=100 μm)

In terms of shell structure, prismatic calcite forms the external layer and granular calcite the internal larger. Black filamentous matter is prominent between grains.

3.3.5.1.2 MF5a2: Thick-shell alatoconchid rudstone

Description: In the field, this facies is characterized by spectacular abundance of large alatoconchid shells accumulated in densely packed condition (Fig. 3.10). Characteristics of alatoconchid shells and their preservation condition are described in more details in Chapter IV. This facies occur in limestone beds that are medium to thick bedded. Weathered surfaces are light brownish-gray and fresh surfaces are dark gray to bituminous black. The facies is commonly found intercalated with fusulinid facies such as found in the middle to upper part of Unit B (e.g. sample no. 781b, 782, M0558, 787, and M0537). Fusulinid tests and massive corals can be observed in this alatoconchid facies. Nodular chert is common.

Petrographically, this microfacies is characterized by abundant densely packed shell fragments and debris (Fig. 3.11). It shows prominent grains adhering to alatoconchid shells. According to Dunham (1962), this microfacies is classified as bioclastic packstone which is compatible with calcisiltite/calcarenite (Carozzi, 1989). It can be inferred to densely packed biomicrite (Folk, 1959; 1962). In terms of lithofacies, it is a thick-shell alatoconchid rudstone with bioclastic packstone or calcarenite matrix. Allochemical constituents are composed of shell debris, bioclastic fragments, peloids, ostracods, smaller foraminifers and carbonized or bituminous wood fragments. In some samples, wood fragments exhibit internal structure. Peloids are common and occur as silt size with subangular to rounded shape. Most bioclasts are fragmented or observed as debris. Black skeletal debris and filaments are also common in this facies. Alatoconchid shell

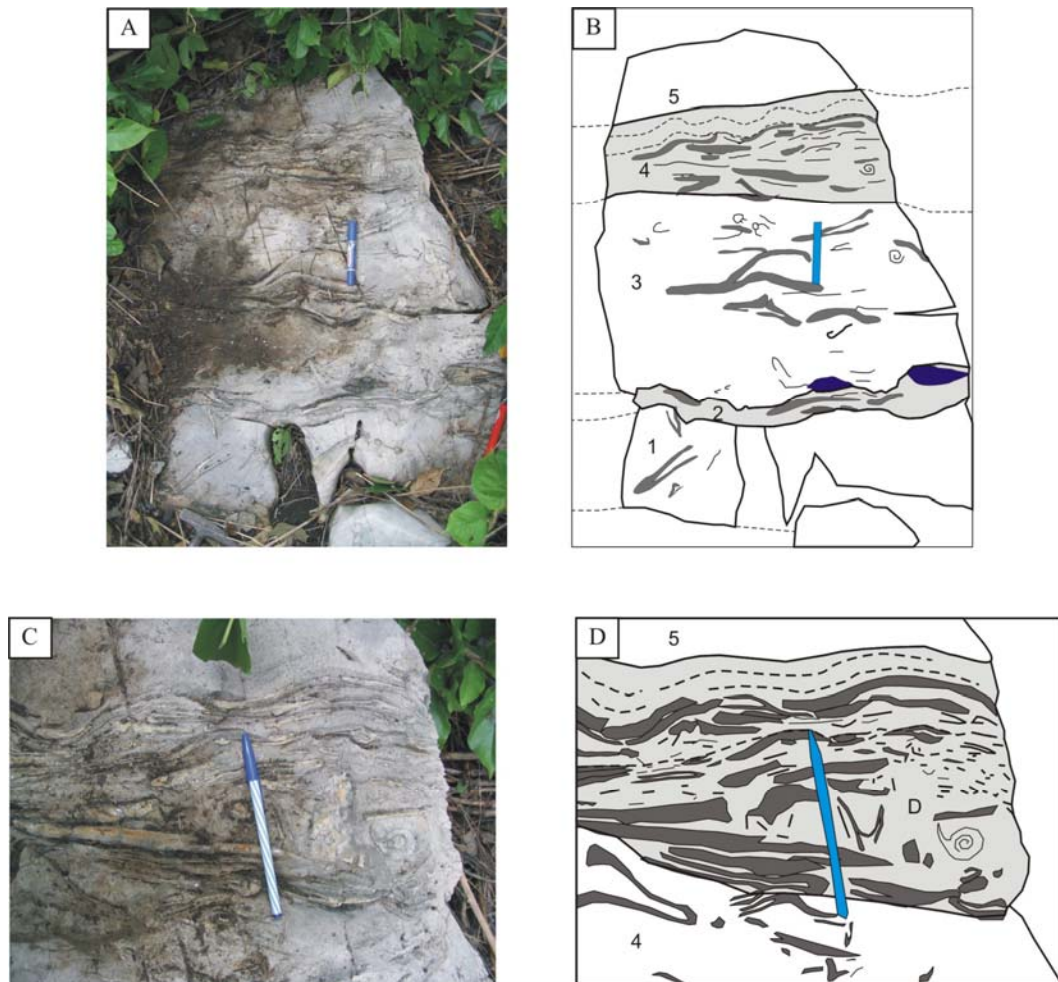


Figure 3.10 Alatoconchid coquinite or tempestite. A: Field photograph showing large amount of alatoconchid fragments scattered in matrix (marker pen for scale= 15 cm). B: Sketch of A, alatoconchid fragments shown in dark gray gastropod in spiral shape on right of bed 3 and 4. C; Field photograph of the same outcrop showing wavy undulation in upper part of bed (pen for scale=15cm). D: Sketch of C, showing alatoconchid fragments in dark gray, gastropod on left as spiral conch.

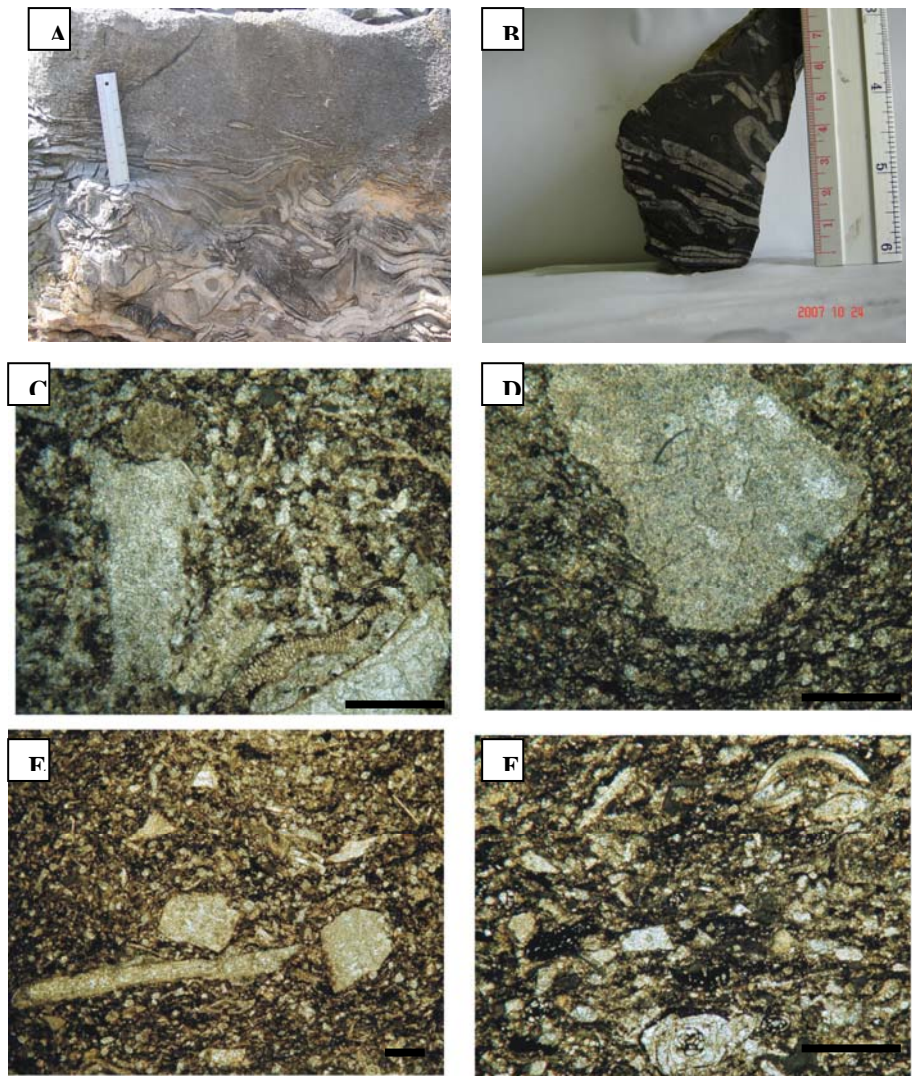


Figure 3.11 A: Field photograph of alatoconchid rudstone (MF5c2). B: Rock slab of alatoconchid rudstone from A. C: Photomicrograph of bioclastic calcisiltite matrix of alatoconchid rudstone (sample no. 0537) with dispersed fragments and debris. D: Photomicrograph of bioclastic calcisiltite matrix of alatoconchid rudstone showing larger shell debris floated in calcisiltite with black micrite matrix (sample no. 0537). E: Photomicrograph showing another view of calcisiltite matrix of alatoconchid rudstone (sample no. 787). F: Photomicrograph showing bioclastic calcisiltite matrix of alatoconchid rudstone. (All scale bar=500 μ m)

fragments and debris are recognized in the texture by floating or packing together with other allochems.

3.3.5.1.3 MF5a3: Thick-shell alatoconchid floatstone

Description: Alatoconchid floatstone occurs in medium to thickly bedded limestones. It is a dominant microfacies within Unit A and Unit B. Normally, the base of alatoconchid floatstone beds are shaped and undulating while the bed top is planar (Figs. 3.12, 3.13, 3.14, and 3.17). The first (lowest) alatoconchid floatstone bed in Unit A (Figs. 3.12) immediately overlies a bed with fusulinid facies and underlies a non-laminated limestone bed. In the lower part of this alatoconchid bed, some fusulinids are as found common as in the underlying bed and show imbrication. Nodular cherts are common in this bed. Alatoconchid shells occur in both single-valved and double-valved conditions with shell fragments. These shells are found arranged in various directions including normal, inclined and overturned orientations.

Petrographically, the microfacies of the matrix is bioclastic packstone (Dunham, 1962) and can be compared to densely packed biomicrite (Folk, 1959; 1962) (e.g. sample no. 912, 760, 779, and 784). It can be alternately designated as calcisiltite/calcarenite (Carozzi, 1989) (Fig. 3.12). As a result, lithofacies can be referred to as thick-shell alatoconchid floatstone with bioclastic packstone or calcarenite matrix. This microfacies consists mainly of shell fragments and debris. The various allochems are commonly adhered to alatoconchid shells. Intergranular space is occluded mainly by micrite. Fragments and debris are poorly sorted, angular to subangular in shape. Grains and fragments are comprised of smaller foraminifers, brachiopods, ostracods, alatoconchids, spicules and peloids. Some of smaller

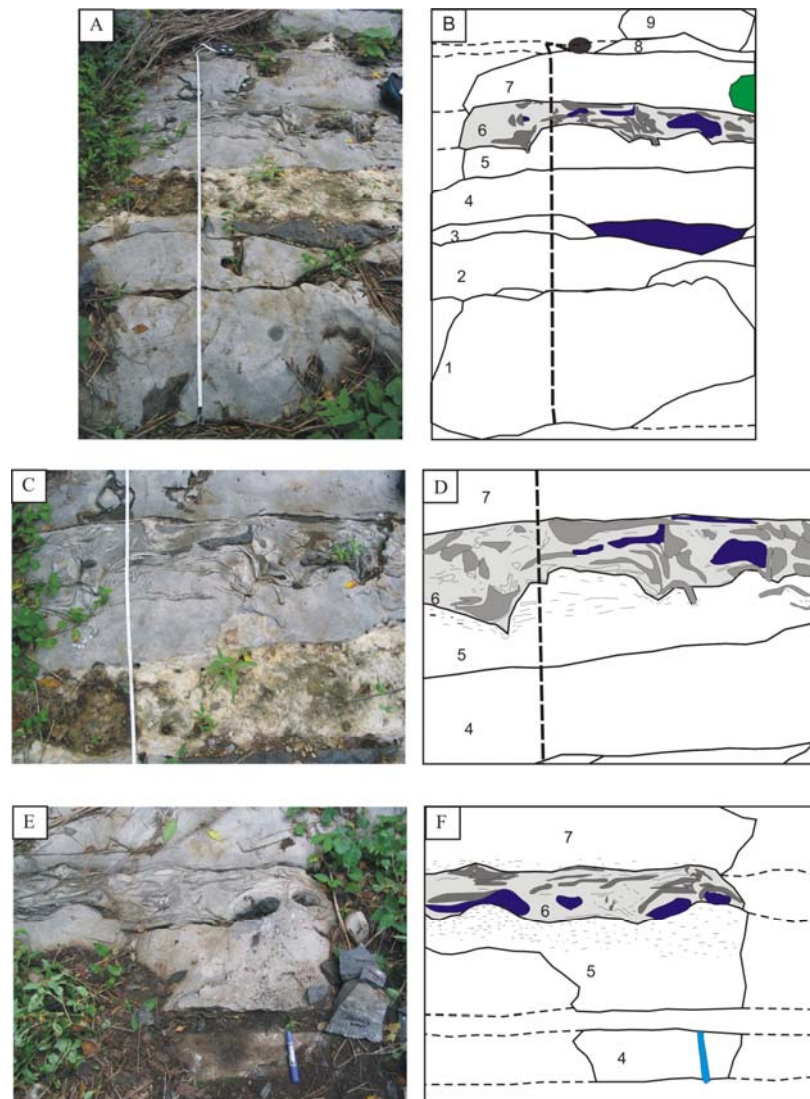


Figure 3.12 A: Field photograph of alatoconchid floatstone bed overlying fusulinid limestone and underlying non-laminated limestone (measuring tape for scale=2 m). B: Sketch of A, 6=alatoconchid floatstone bed; alatoconchids as dark gray specimens; blue patches indicate nodular cherts, 5=fusulinid limestone bed, 7=non-laminated limestone bed. C: Enlargement of field photograph from A. D: Sketch of C, showing alatoconchids in dark gray floated in matrix with various directional arrangements with eroded undulatory base. E: Alatoconchid bed (maker pen for scale=15 cm). F; Sketch of E, 4= non-laminated limestone, 5-7 same as above.

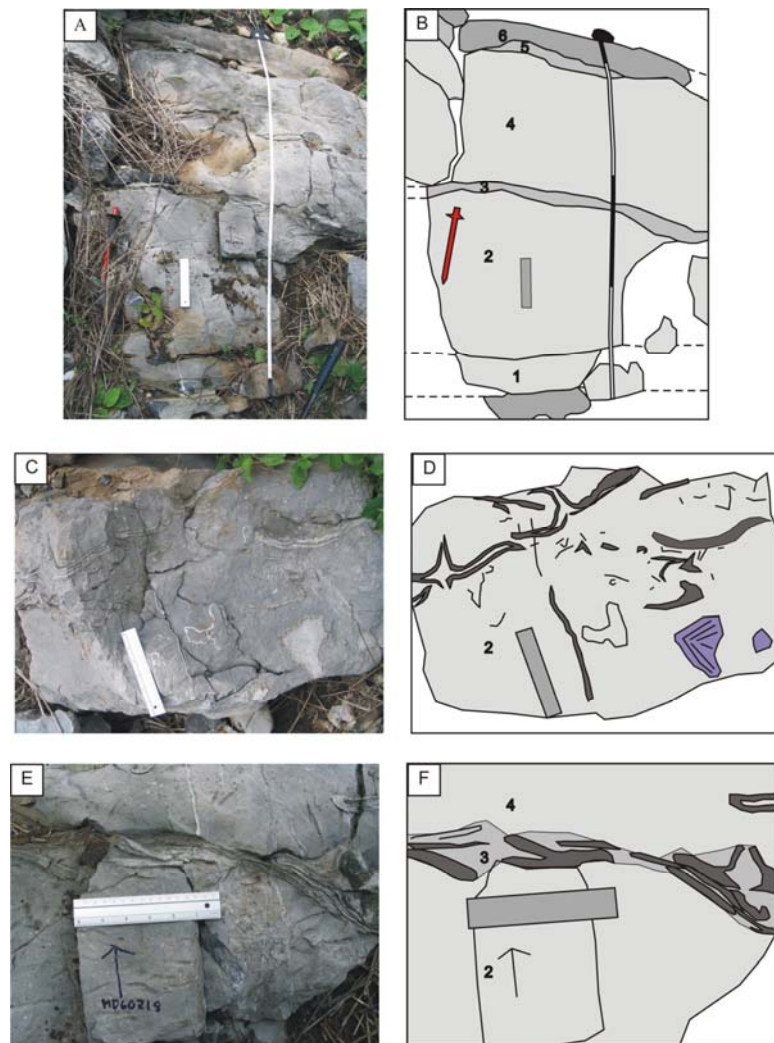


Figure 3.13 A: Field photograph of alatoconchid-bearing beds. B: Sketch of A, alatoconchids occur in 2, 3 and 4, abundant fusulinids occur in 1, laminated limestone in 5 and 6. C: Field photograph, magnification of bed 2. D: Sketch of C showing alatoconchid with good preservation at top, alatoconchid fragments (in dark gray) floated with massive coral fragments (lower right) and other shelly fragments. E: Enlargement field photograph of bed 3. F: Sketch of E, showing densely packed alatoconchid rudstone or coquinite bed, alatoconchid in dark gray fragments. (Ruler for scale =15cm)

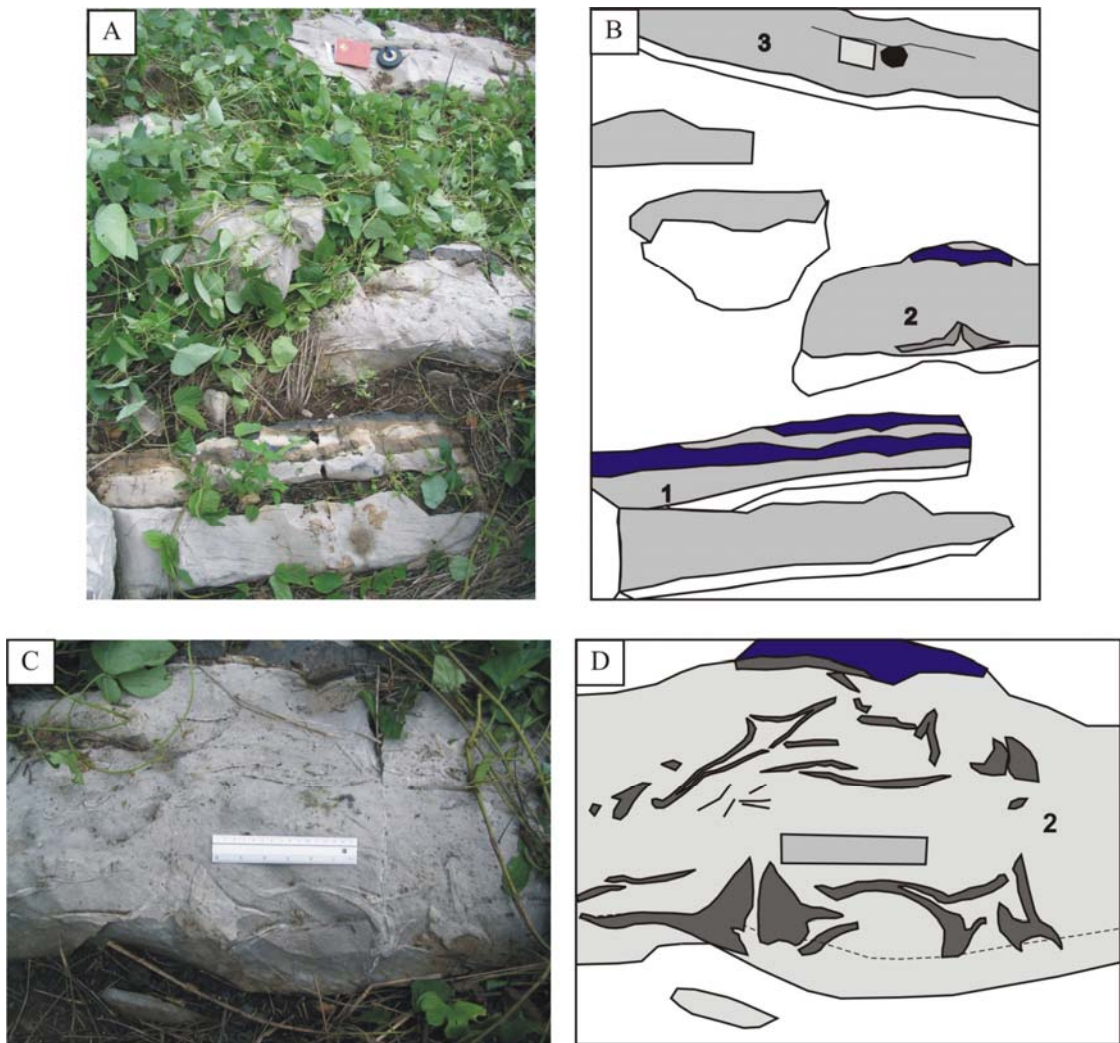


Figure 3.14 Alatoconchid floatstone bed. A: Field photograph of outcrop. B: Sketch of A, 1=non-laminated limestone with lenticular cherts in blue color, 2=alatoconchid floatstone bed with nodular chert at top, 3=non-laminated bed with laminated thin layer intercalation (notebook for scale=17 cm). C: Details of bed 2, showing alatoconchid floatstone. D: Sketch of C, most alatoconchids are displayed in double-valved condition.

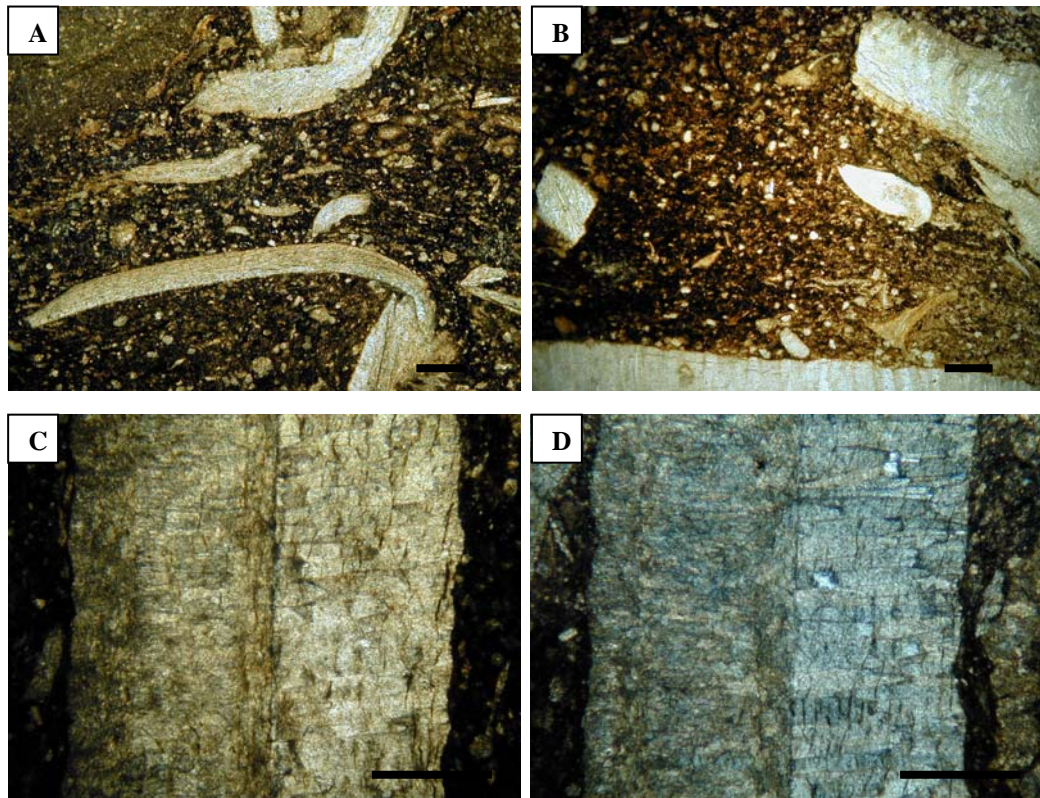


Figure 3.15 A-B: Photomicrograph of calcisiltite matrix of alatoconchid floatstone (sample no. 760). Larger fragments including micritic fusulinids, brachiopods, and alatoconchid shell fragments are floated in calcisiltite matrix. C: Photomicrograph of alatoconchid shell showing granular calcite of internal layer on left and prismatic calcite external layer on right (PPL). D: Photomicrograph of alatoconchid shell (XPL). (All scale bar=500 μm)

foraminifers are exceptionally well preserved, but not miliolids which exhibit worn and abraded tests. Black carbonized debris is scattered throughout. Algal thalli are found as fragments and in black color. Most ostracods are fragments but articulated condition is occasionally found. Brachiopods are observed in both single-valved and double-valved conditions.

3.3.5.2 MF5b: Alatoconchid biostrome

3.3.5.2.1 MF5b1: Alatoconchid biostrome

Description: Alatoconchid bivalve shells are found mainly in double-valved condition, but single valves and fragments are also observed. Shell orientations are sub-parallel or parallel to bedding plane (Figs. 3.16 and 3.17). Most of the alatoconchid shells observed in this bed are assumed to be adult shells with thick, large, and wing-like flange components. They exhibit the ventral side lying on the bottom and dorsal ridge pointing upward in growth position. Shell thickness is measured up to 1.0 cm with more than 30.0 cm measured for the width dimension of a single valve. Gastropods are large and common with more than 4.0 cm in diameter of the outer whorl.

Petrographically, this microfacies is dominated by peloids over skeletal grains in micrite matrix as shown in sample no. 705 (Fig. 3.18). The peloid content of this rock is approximately 20%. Micrite and calcite cement occupy intergranular void space to a similar percentage. This microfacies can be classified as peloidal wackestone (Dunham, 1962) or pelmicrite (Folk, 1959; 1962). The lithofacies can be referred to as alatoconchid biostrome with peloidal wackestone matrix. In terms of the rock matrix, allochems are sparsely distributed in a groundmass devoid of internal sedimentary structure. Peloids are irregular in shape

and diffuse in outline with diameters ranging from 20 μm to 100 μm . Bioclastic grains are rare and dominated by smaller foraminifers. They include some miliolids that mostly occur as small tests, *Tuberitina* sp., and *Globivalvulina* sp. Fusulinids are rare but are dominated by *Verbeekina verbeeki*. The other constituents consist of single-valved ostracods, fine-grained shell fragments, and algal fragments. Most skeletal grains are poorly to moderately preserved with either micritisation or recrystallisation. Intergranular materials consist of microsparite, drusy calcite cement and micrite. Note that micrite is observed as small patches.

Additionally, in samples no. 721 and 722b, allochems in this facies range between 10 to 50%. Peloids are predominant over bioclastic grains. Intergranular material is filled mainly by micrite over sparry cement. This microfacies can be designated as biosclastic peloidal wackestone (Dunham, 1962) or biopelmicrite (Folk, 1959; 1962). The lithofacies can be classified as alatoconchid biostrome with bioclastic peloidal wackestone matrix. Coarse sparry calcite is present mostly within intragranular chambers of some skeletal grains. Most peloids are rounded with diameters on average of about 20 μm . But, some single peloids can be found up to 100 μm . Skeletal grains include algae, smaller foraminifers, shell fragments and small gastropods. Algae and smaller foraminifers are more common over other bioclastic grains. Algae consist of calcareous green algae, mainly represented by *Psuedovermiporella* sp. Algal thalli are weathered and shown as either dark gray or brown colors. Smaller foraminifers include *Protonodosaria* sp., *Calcitornella* sp., *Nodosaria* sp., *Diplosasphaerina* sp., *Tuberitina* sp. and some miliolids. Shell fragments include fusulinid, ostracod, brachiopod, and bivalve fragments. Black, fine-grained, carbonized or bituminous matter is common in this facies as well. Some shell

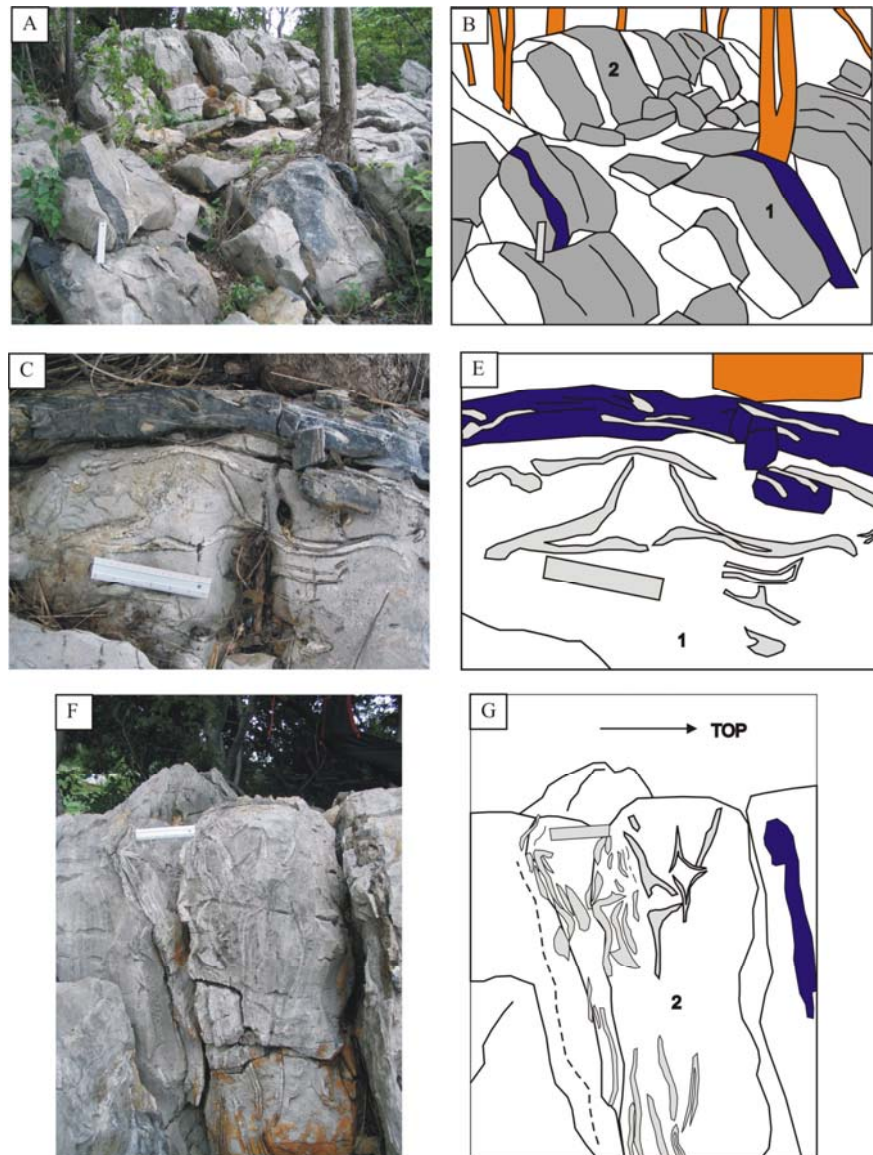


Figure 3.16 Alatoconchid-bearing limestone beds with alatoconchids in life-position. A: Field photograph showing nearly vertical bedded limestones. B: Sketch of A, alatoconchid beds observed in 1 and 2, lenticular and nodular cherts in blue color. C: Alatoconchid in growth-position showing wing-like flanges and large internal chamber, lenticular chert developed at top. D: Sketch of C. E: alatoconchid biostrome with alatoconchid in growth position with some alatoconchid fragments. F: Sketch of E. (Ruler for scale=15 cm)

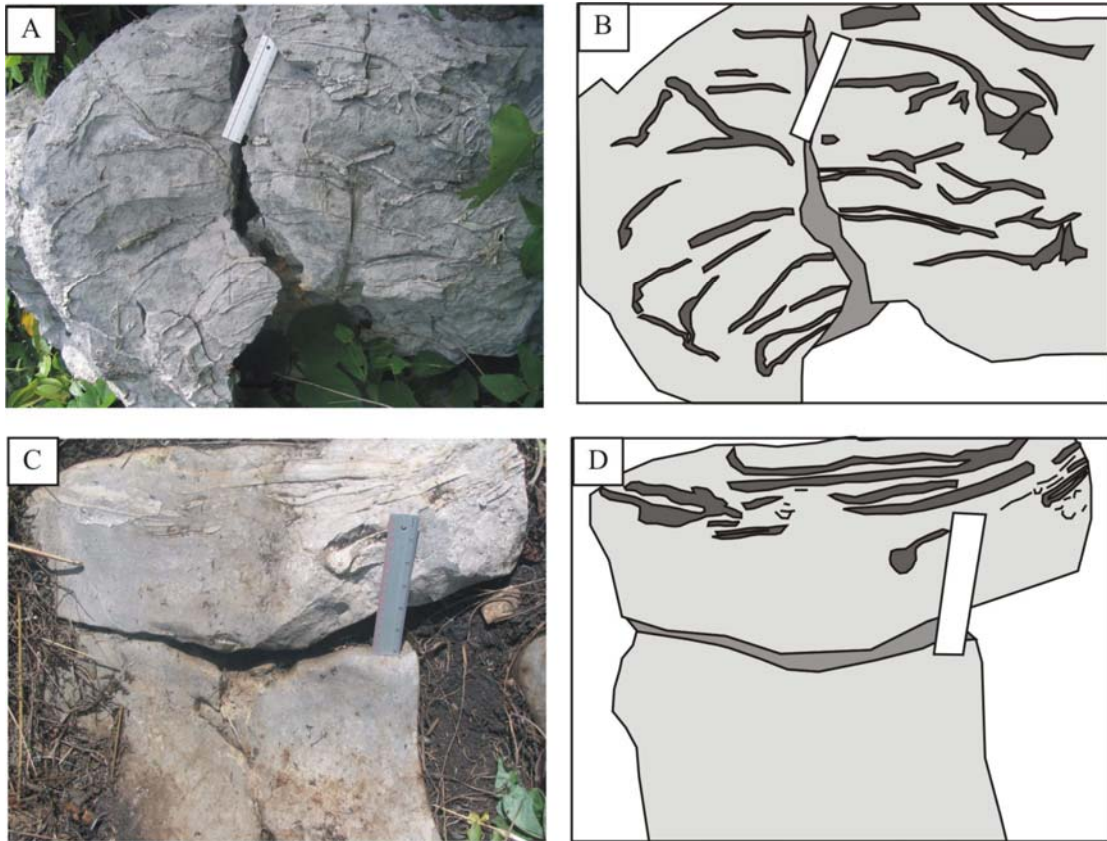


Figure 3.17 Field photographs of alatoconchid biostrome and alatoconchid floatstone beds. A: Photograph of alatoconchid biostrome bed, random sections of double- and single-valved alatoconchids in life position embedded with alatoconchid fragments. B: Sketch of A, alatoconchids displayed in dark gray. C: Field photograph of alatoconchid floatstone bed overlain on non-laminated limestone bed. D: Sketch of C, alatoconchid shown in dark gray fragments and single valves. (Ruler for scale=15 cm)

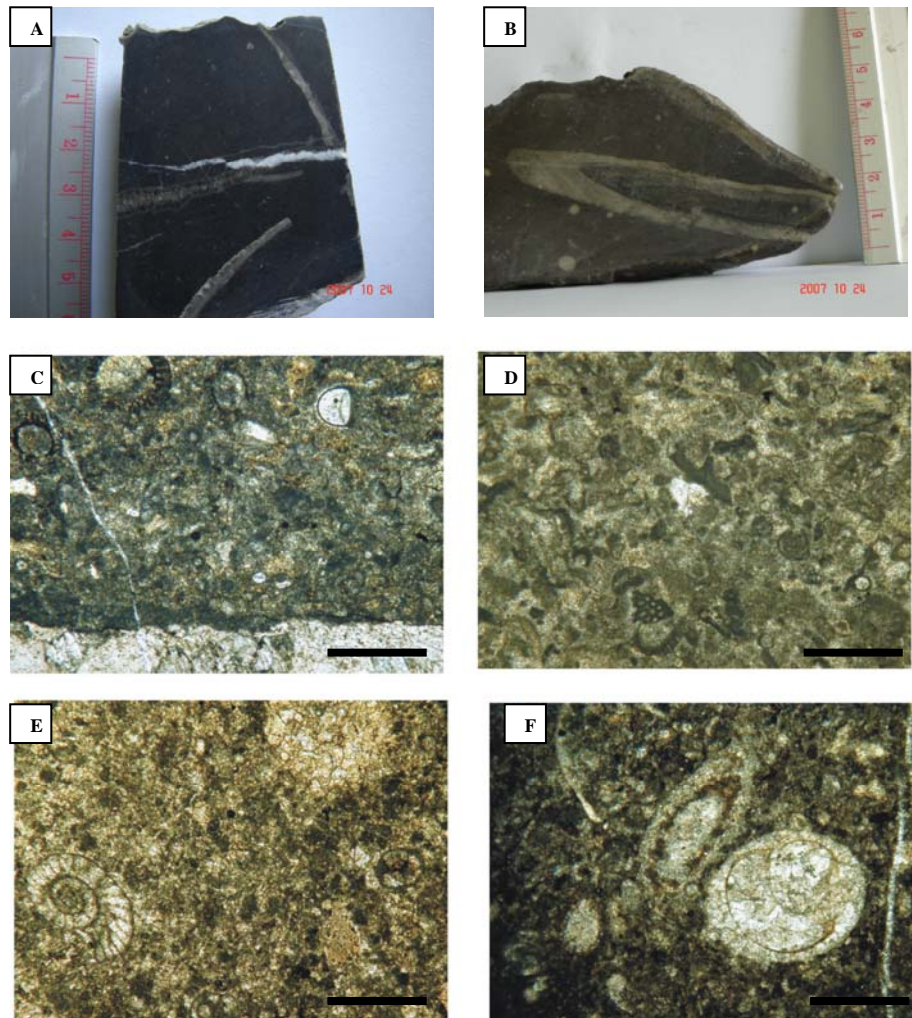


Figure 3.18 A: Rock slab of alatoconchid biostrome facies (sample no. 705). B: Rock slab of alatoconchid biostrome facies (sample no. 721). C: Photomicrograph of bioclastic peloidal matrix of alatoconchid biostrome (sample no. 722b). Part of alatoconchid shell in lower part of view. Smaller foraminifers and algae are shown at top of view. D: Photomicrograph of bioclastic peloidal matrix of alatoconchid biostrome (sample no. 755). E: Photomicrograph of peloidal matrix of alatoconchid biostrome (sample no. 705) showing smaller foraminifer in peloidal-rich texture. F: Photomicrograph of bioclastic peloidal matrix of alatoconchid biostrome (sample no. 721). Gastropods and algae are common. (All scale bar=500 μm)

fragments such as brachiopods and bivalves are coated by shelly encrusting organisms. Selective dolomitisation as shown by coarse rhombohedral dolomite crystals is found within the internal shell structure of some alatoconchids.

3.3.6 MF6: Fusulinid facies (wackestone/ packstone/ grainstone)

This microfacies is characterized in the field by more than 10% fusulinid tests present in the limestone bed. It is particularly common in the upper part of Unit A, in Unit B and Unit E but is most common in the lower to middle part of Unit F. This facies can be divided into three subfacies including fusulinid wackestone, packstone and grainstone on the basis of texture. Of these, fusulinid wackestone is most common while fusulinid grainstone is rare. Details of these subfacies are described below.

3.3.6.1 MF6a: Fusulinid wackestone

Description: This facies occurs in thick to very thick limestone beds. Fusulinids floating in the rock matrix are common. They can represent with more than 10% of total rock. This facies is found associated with fusulinid packstone but these two facies slightly differ in the field with the latter having greater abundance of fusulinids and densely packed texture. In some intervals, fusulinid wackestone facies grades into fusulinid packstone. Intercalation of these facies is common.

Petrographically, this microfacies is characterized by poorly sorted and sparse distribution of allochemical constituents in micrite (e.g. sample no. 747 and 778b) (Fig. 3.19). Allochemical components are approximately less than 50%. Intersitial space is occupied by micrite in comparable amount to microsparite. This microfacies can be classified as fusulinid floatstone with peloidal bioclastic wackestone matrix (Dunham, 1962) or sparse pelbiomicrite (Folk, 1959; 1962). Some

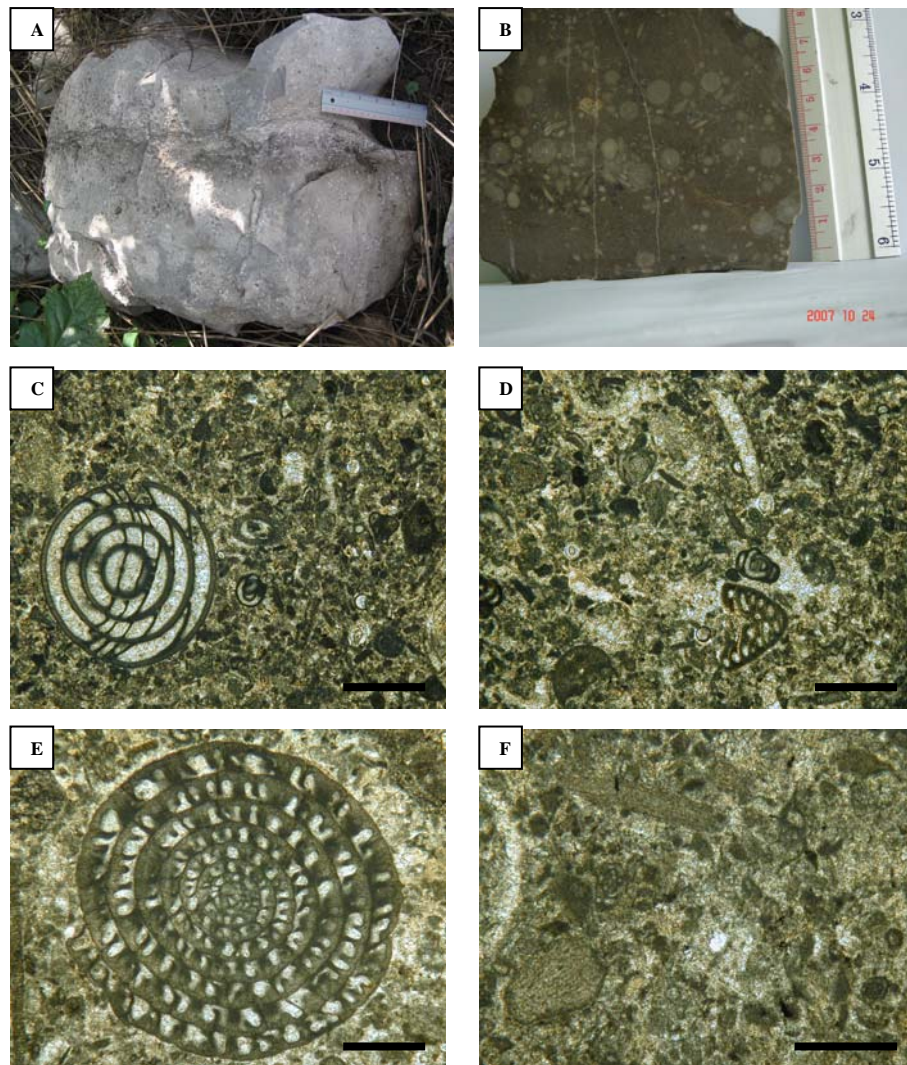


Figure 3.19 A: Field photograph of fusulinid wackestone bed (ruler=15 cm). B: Photograph of rock slab of fusulinid wackestone facies (MF6a). C: Photomicrograph of bioclastic wackestone texture of fusulinid wackestone facies showing fusulinid with smaller foraminifers, algae, and peloids sparsely distributed in micrite. D: Photomicrograph of the same sample as C showing smaller foraminifers bioclasts and peloids in micrite matrix with partly sparry calcite cement. E: Photomicrograph of fusulinid wackestone (sample no. 747). F: Photomicrograph of fusulinid wackestone (sample no. 778b) showing algal fragments (*Undarella* sp.) associated with peloidal wackestone texture. (All scale bar=500 μ m)

fusulinids exhibit some degree of test weathering and erosion including test fragmentation, crushed tests and micritised tests. However, some fusulinids are well preserved. Smaller foraminifers are common but ostracods and algal fragments are relatively rare. Fusulinids include *Verbeekina verbeeki*, *Neoschwagerina* sp. and *Nankinella* sp. Smaller foraminifers include *Tetrataxis* sp., *Pseudoendothyra* sp., *Globivalvulina* sp., *Agathammina* sp., *Hemigordius* sp., *Eotuberitina* sp., and others. Algae were found as algal fragments. Ostracods are represented by only a single double-valved specimen in this thin-section. It has a calcite-filled internal void. Non-skeletal grains are comprised mainly of peloids and cortoids. Peloids are more dominant with round outline and found mostly in silt size. Cortoids are rare showing micritised rim and sparry calcite infilling internal void space. Some single fragments were found encrusted by shelly epibiont encrusting organisms forming coated grains. These coated grains have a dark micritic rim with lobate outline.

In sample no. 746/2, fusulinid tests are abundant with densely packed texture in the upper part of the bed. This packed layer is up to 15 cm thick. In this sample, microstylolites are developed around fusuline tests and appear as a dark insoluble seam.

3.3.6.2 MF6b: Fusulinid packstone

Description: Field observations indicate that this limestone is characterized by more than 20% fusulinid tests. The rock is thick to very thickly bedded, light gray in weathered surfaces and light to medium gray in fresh color. Fusulinid-related sedimentary structure including fusuline sheets with imbrication, pocket and fill with fusulinids, and scour and fill with fusulinids are common in Unit G. Sutured stylolites are conspicuous with parallel orientation to bedding plane.

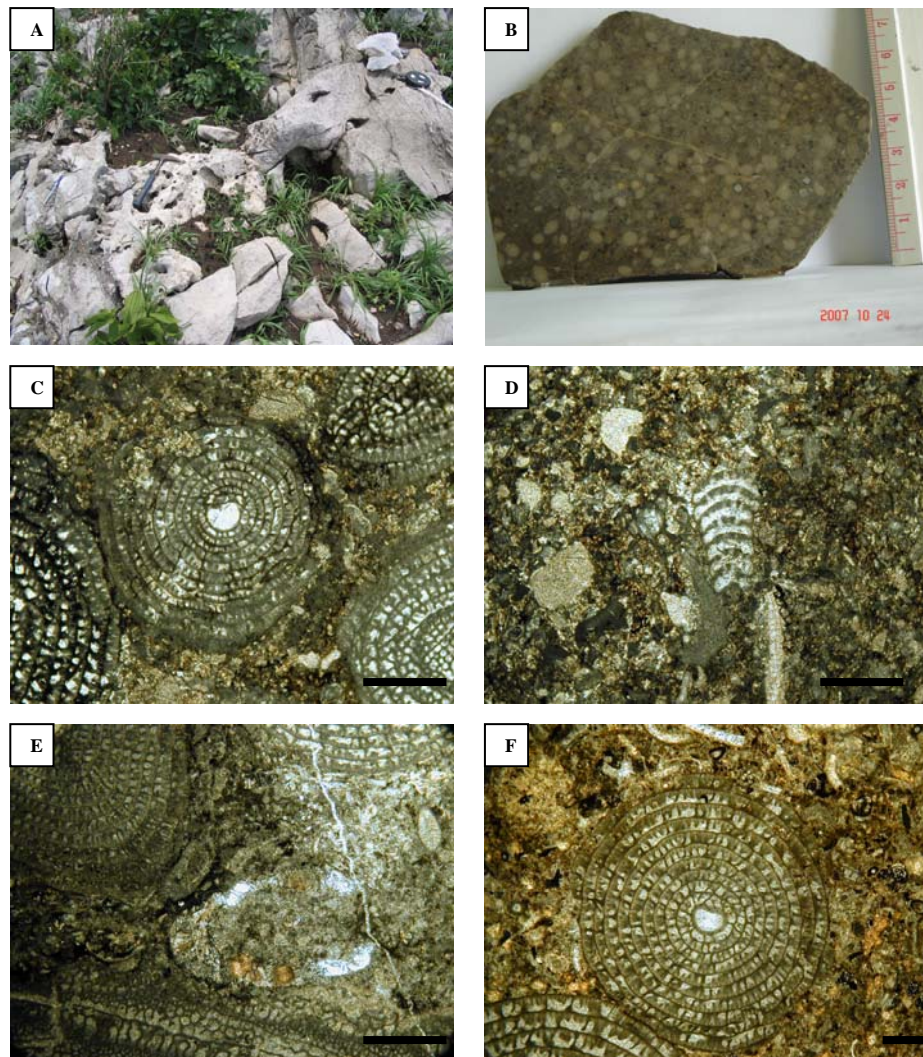


Figure 3.20 A: Field photograph of fusulinid packstone bed. B: Photograph of rock slab from A. C: Photomicrograph of fusulinid packstone (sample no. 773) showing abraded and micritised fusulinid tests in bioclastic peloidal calcisiltite matrix. D: Photomicrograph of fusulinid packstone (same sample as C) showing well preserved smaller foraminifer in shell debris-rich matrix. E: Photomicrograph of fusulinid packstone (sample no. 782) showing debris compared with F. Photomicrograph of fusulinid packstone (sample no. 783) with well preserved fusulinid tests (*Lepidolina* sp.) and debris in comparison to D. (All scale bar= 500 μ m)

Light gray weathered surfaces of small diagenetic patches caused by silicification and dolomitisation processes are locally common.

Petrographically, this microfacies contain more than 50% allochemical constituents (e.g. sample no. 773, 782, and 783) (Fig. 3.20). These allochems are immature or poorly sorted and are without preferred orientation. Contact between grains is very common in this facies. Allochems include prolific occurrence of fusulinids embedded with numerous of bioclastic fragments, debris and peloids. This microfacies can be classified as bioclastic packstone/grainstone (Dunham, 1962) or poorly washed biosparite (Folk, 1959; 1962). Most fusulinids exhibit good preservation. However, some of them are slightly worn, broken, or have lost their outer volution. Micritisation is common around peripheries of some fusulinid tests. Fusulinids include *Colania douvillei*, *Verbeekina verbeeki*, *Lepidolina* sp., and *Conodofusiella* sp. Other bioclastic grains are comprised of smaller foraminifers, ostracods, crinoids, small gastropods, algae, and bituminous or carbonized wood fragments. Smaller foraminifers include *Agathammina* sp., *Kamurana* sp., *Tuberlitina* sp. *Pachyphloia* sp., and *Cribogenerina* sp. Most algae occur as fragments. They can be classified as *Pseudovermiporella* sp., and *Undarella* sp. Crinoids are rare and characterized as crinoid ossicles.

3.3.6.3 MF6c: Fusulinid grainstone

In the field, two intervals of fusulinid grainstone were observed. Both of them are located around the middle part of Unit F. Two samples were collected from these intervals for petrographic study including sample no. A25 and A 31.

Petrographically, this subfacies is defined the common occurrence of fusulinids and calcareous algae with common grain-in-contacts (Fig. 3.21). Interstitial

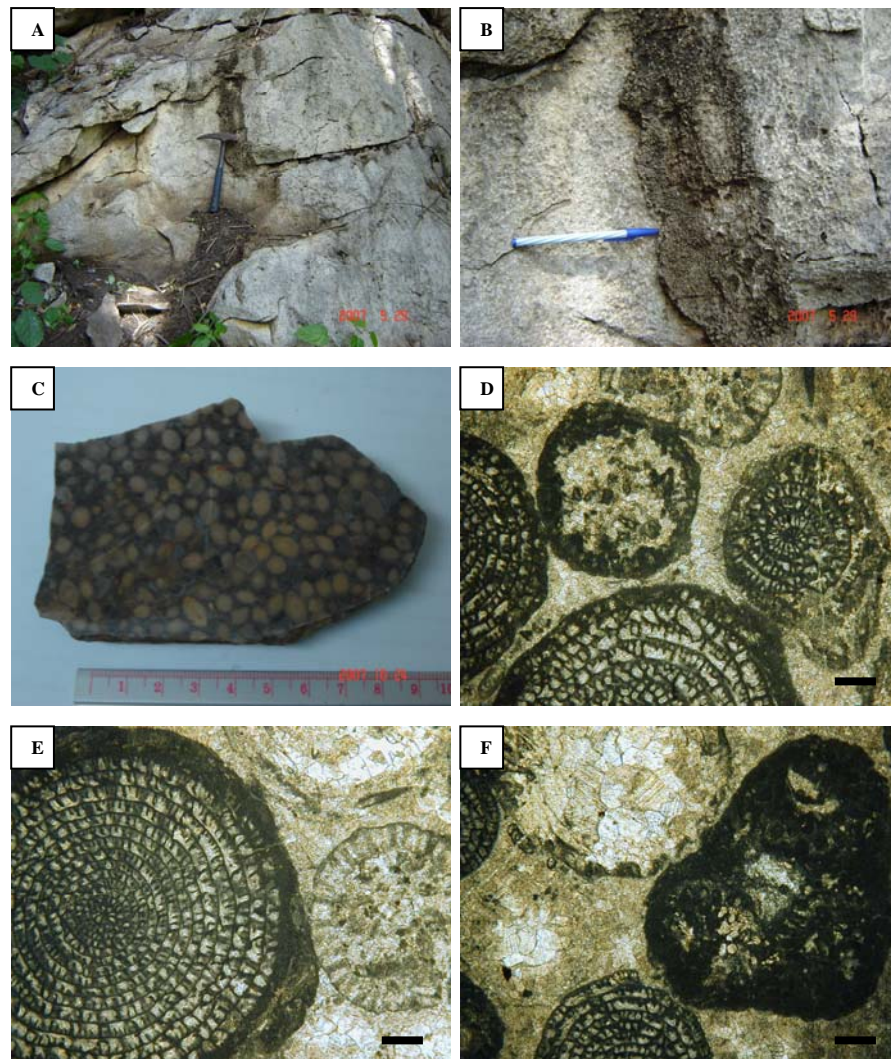


Figure 3.21 A: Field photograph of limestone beds containing fusulinid packstone/grainstone. B: Field photograph of fusulinid grainstone. C: Slab of fusulinid grainstone (MF6c). D: Photomicrograph of fusulinid grainstone showing fusulinids in sparry calcite cement (sample no. A25). Micritised fusulinids and algae with oncolitic structure are conspicuous. Fusulinid (on right of view) shows lobate shape and oncolitic structure. E: Photomicrograph of fusulinid grainstone (sample no. A31) showing fusulinid (*Lepidolina* sp.) with round oncolitic structure and algae (*Mizzia* sp.) without oncolitic structure. F: Photomicrograph of fusulinid grainstone showing composite grains with oncolitic structure. (All scale bar=500 μ m)

space is occluded mainly by coarse sparry cement. Oncoids are common in this facies. Most grains show oncolitic structure with dark gray micritic layers wrapping around them. Some of them are composite grains with oncolitic structure. This structure is mainly round in shape but lobate shape is occasionally observed. Fusulinids include *Lepidolina* sp., *Yabeina* sp, *Chusenella* sp. and *Conodofusiella* sp. Other fossil groups are less common in this facies. They include smaller foraminifers and ostracods.

3.3.7 MF7: Coated bioclastic grainstone

Description: This facies type is characterized in the field within medium to thickly bedded limestone and is typical of non-laminated limestones. This rock is light gray in weathered color and light to medium gray in fresh color. The rock surface is smooth with some small fossils scattered in the rock surface. Some of these fossils can be determined by the naked-eye. They include smaller foraminifers, fusulinids, small shell fragments and pieces of charcoal. Fusulinids in this facies are rare compared with fusulinid facies. In some cases, the underlying beds consist of fusulinid-bearing bed, alatoconchid bed or laminated limestone bed. Fusulinid beds commonly overlie this facies type.

Petrographically, this microfacies displays grain-supported fabric with common grain-in-contact. Most intergranular pores are occluded by calcite cement. Allochemical components occupy more than 50% of the rock texture (e.g. sample no. 768, 770, and 777) (Fig. 3.22). They are mainly silt-size, well rounded with good sorting. This microfacies can be referred to as coated bioclastic grainstone (Dunham, 1962) or fine-grain rounded biosparite (Folk, 1959; 1962). Grains are composed mainly of micritized or coated bioclasts with common micrite envelopes. The others are peloids, small cortoids, smaller foraminifers, and algae. Smaller foraminifers are

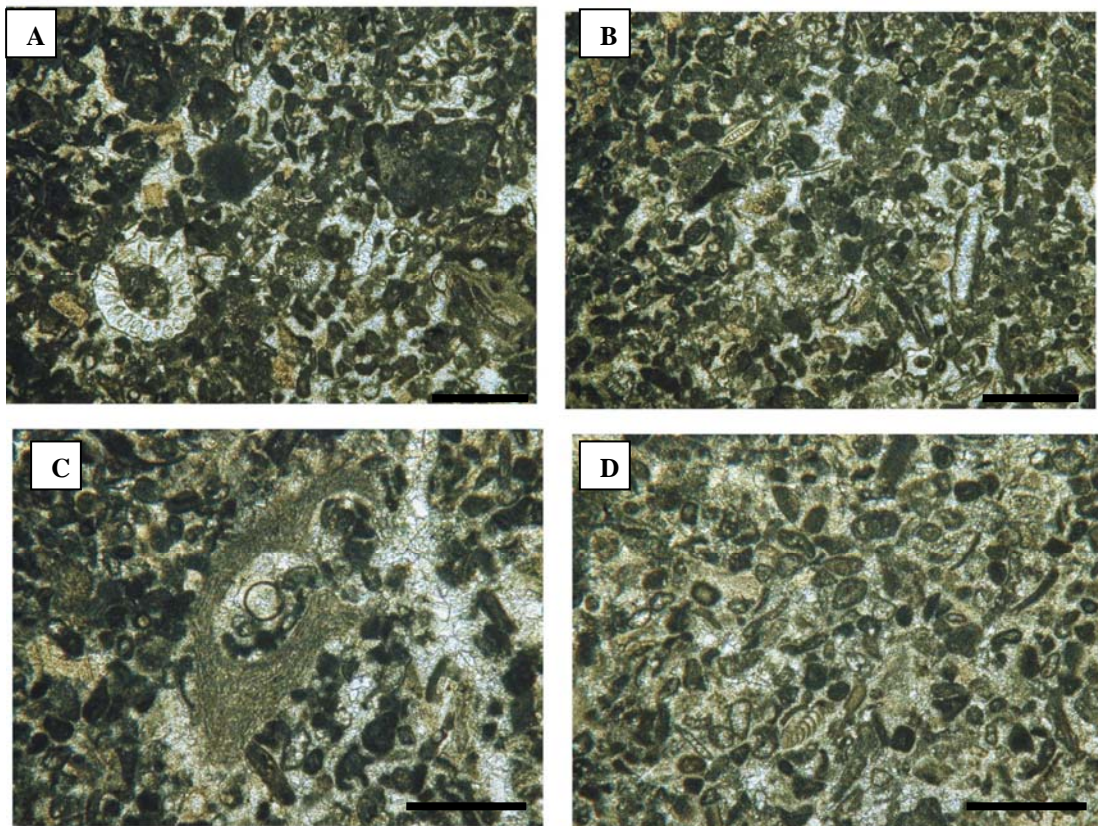


Figure 3.22 A: Photomicrograph of bioclastic grainstone from Unit B showing micritised and coated bioclastic grains, peloids with aggregate grains, and calcareous algae in sparry calcite cement (sample no. 809). B: Photomicrograph of bioclastic grainstone from Unit B (same sample as A) showing another view of this facies. C: Photomicrograph of bioclastic grainstone (sample no. 777) showing red algal fragment (*Undarella* sp.) floated in grainstone texture. D: Same as B, showing small cortoids. (All scale bar=500 µm)

common including miliolids, *Nodosaria* sp., *Protonodosaria* sp., *Pachyploia* sp., *Tuberitina* sp., *Calcitornella* sp., *Deckerella* sp., *Texturalia* sp., and *Globivalvulina* sp. Agglutinated foraminifers show traces of micritisation. Algae are found as algal fragments and are dominated by *Undarella* sp. Additionally, in some intervals, dacycladacean algae with small oncoids and mud lumps are present in this facies (e.g. sample no. 787b). This texture is that of a bimodally sorted grainstone.

3.3.8 MF8: Coral biostrome/ floatstone

This type is dominated by massive corals (e.g. sample no. 928). In addition, stalk shaped tabulate corals also in this facies at some intervals (e.g. sample no. 802 and 923). This facies formed as small buildups with decimeter- to meter-scale and up to a few meters in some intervals. The buildups are most common in Unit B and Unit E. Most of them occur as intercalations or interbeds with alatoconchid biostrome (e.g. sample no. 795 and 802). In addition, they underlie and overlie crinoidal grainstone beds (e.g. sample no. A56). Coral heads are characterized by lenticular shape, approximately 30 cm long and 10 cm high on average. However, some specimens are characterized as dome shape and up to 60 cm in diameter. Coral biostrome were constructed mainly by massive corals. Massive corals show two different modes of preservation. They are either in normal growth position or are in reworked position.

3.3.8.1MF8a: Coral biostrome

Description: For in-life-position cases (sample no. 802) (Fig. 3.23), coral biostrome occur as thickly bedded massive coral-bearing limestone bed that is overlain by thin bedded of tabulate coral layer. Alatoconchid beds are also observed in this interval in life-position (sample no. 801). However, limestone beds that contain

alatoconchids are distinct as alatoconchid facies (see detail in section 3.3.5). Intercalation between coral facies and alatoconchid facies is common.

Petrographically, as in sample A56, this microfacies is dominated by mudstone and bioclastic wackestone matrix (Fig. 3.24). Allochems are comprised of smaller foraminifers, echinoderm elements, calcareous algae, peloids, fragments and coated bioclasts. Cement fills the internal pores of algae and partly in shelter pores. This facies type can be classified as coral framestone with mudstone/bioclastic packstone matrix (Dunham, 1962; Embry and Klovan, 1971). It can be alternatively assigned as massive coral biolithite with fossiliferous micrite/sparse biomicrite matrix (Folk, 1959; 1962).

According to sample no. 802, the major allochemical constituent within the rock matrix is tabulate coral. Which has a thick wall with branching cylindrical corallites. The wall is strongly recrystallized. Encrustation in this facies is abundant. Encrusting organisms consist of smaller foraminifers and some red algae. Shelter pores are predominantly filled by sediment or matrix over cement. Matrix is bioclastic wackestone/packstone. Internal sediment within corallites of tabulate corals is bioclastic wackestone. Bioclastic grains in matrix include smaller foraminifers, red algae, small gastropods, shell fragments and debris. Smaller foraminifers are common such as *Pachyphloia* sp. and *Tuberitina* sp. Red algae are mainly *Tubiphytes* sp. This facies type is classified as bafflestone with bioclastic wackestone/packstone matrix (Dunham, 1962; Embry and Klovan, 1971). Alternatively, it can be erected as fasciculate coral biolithite with sparse biomicrite/packed biomicrite matrix (Folk, 1959; 1962).

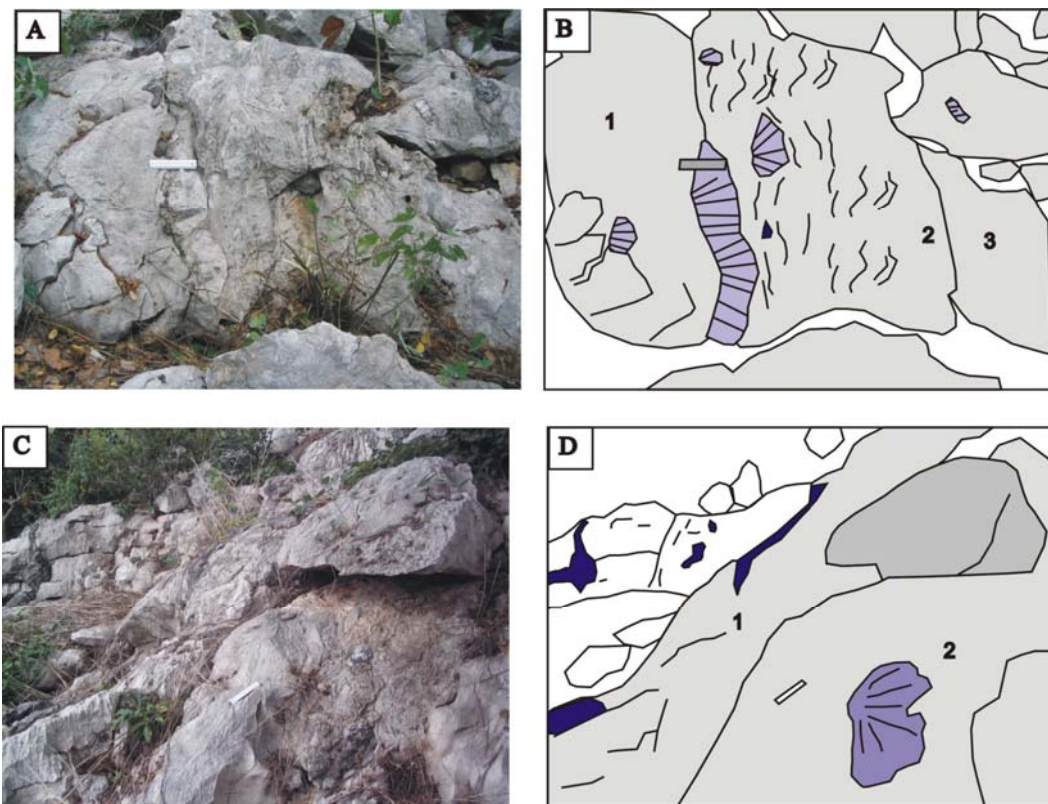


Figure 3.23 Limestone outcrop from upper part of Unit B. A: Coral biostrome interval, showing as massive corals in middle part which are overlain by alatoconchid fragments and tabulate corals in ascending order. B: Sketch of A, 1=thickly bedded limestones, 2=alatoconchid bed with alatoconchid fragments shown as undulating solid lines, massive corals (purple patches with straight solid lines inside) in lower part, 3=coral biostrome bed with tabulate corals in growth-position. C: Field photograph of limestone beds that underlie fissure structure and collapse breccias. D: Sketch of C, single coral head shown in purple patch, 1=non-laminated limestone bed. 2=coral bed with reworked coral heads. (Ruler for scale=15 cm)

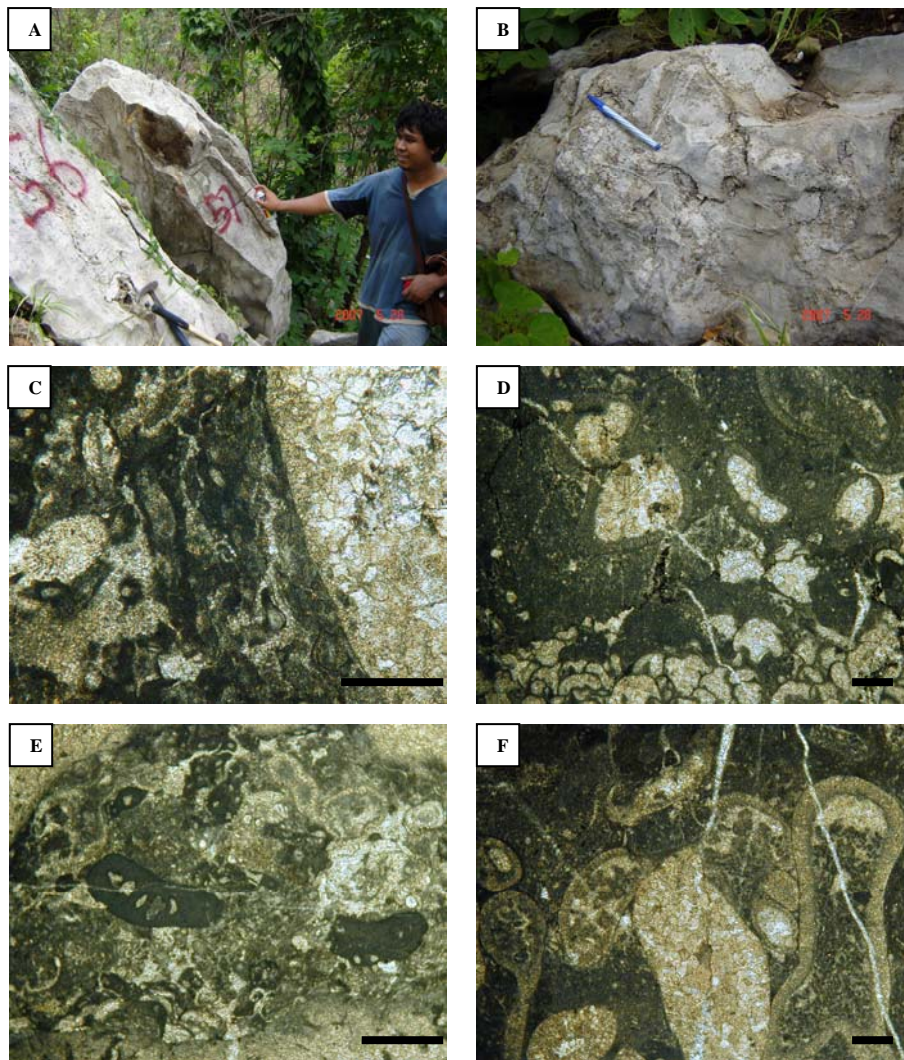


Figure 3.24 A: Field photograph of an outcrop with coral biostrome (MF8). B: Enlargement coral biostrome (pen=15 cm). C: Photomicrograph of matrix in coral biostrome facies showing profound encrusting structure by microbial organisms in dark gray laminae (sample no. 802). D: Photomicrograph showing calcareous algae in micrite matrix of coral biostrome (sample no. A56). E: Photomicrograph of bioclastic wackestone matrix with *Tubiphytes* and debris (sample no. 802). F: Photomicrograph of bafflestone showing stalk shaped tabulate coral in growth position with peloidal wackestone matrix (sample no. 923). (All scale bar= 500 μ m)

In sample no. 923, tabulate corals are predominant. Tabulate corals are observed in life-position with a stalk shape. Most of them are recrystallized. Geopetal structure is common in these corals. This structure formed by having mud matrix filling in the lower half of internal chambers and cements occupy the upper parts. In some specimens, rounded and well sorted peloids are occluded within internal chambers of these corals. Encrusting organisms include *Tuberitina* sp. microbials. *Tuberitina* sp. is common and well preserved in this facies. Most smaller foraminifer are found attached to the outer surface of tabulate corals. Encrusting microbials form as dark gray lobate shapes coating these corals. Shelter pores are occluded mainly by mudstone matrix over cements. Borrows are common in this sample and are infilled with well-sorted peloids. Laminated cement crusts are also observed in this facies but not common. Microstylolites are present in this sample. According to Dunham (1962) and Embry and Klovan (1971), this facies type is designated as coral bafflestone with mudstone matrix. Based on the carbonate classification of Folk (1959; 1962), this type can be classified as fasciculate coral biolithite with fossiliferous micrite matrix.

3.3.8.2 MF8: Coral floatstone

Description: In reworking-position cases (e.g. sample no. 810), this facies is recognized in the field by the common occurrence of massive corals that have obviously been reworked position (Fig. 3.23). The bed is characterized by thick bedded limestone. Coral heads are preserved in various positions ranging from inclined to up-side-down orientations. Small shell fragments and debris are found scattered in the rock. Silicification and dolomitization relicts are prominent as anastomosing patches throughout the rock surface. Discontinuous lenticular cherts

with up to 20 cm thick and more than 3 m wide occur at the base of the bed. In addition, nodular cherts are common within this bed.

Petrographically, this facies is comprised of more than 10% of allochems dispersed in mud matrix. Allochems include peloids, crinoid fragments, shell fragments, red algae fragments, smaller foraminifers, ostracods, and intraclasts. Authigenic quartz is common in this facies. This microfacies can be classified as bioclastic peloidal wackestone (Dunham, 1962) or biopelmicrite (Folk, 1962). As a result, this lithofacies is coral floatstone with bioclastic peloidal wackestone matrix (Dunham, 1962; Embry and Klovan, 1971).

3.3.9 MF9: Crinoidal packstone (encrinites)

Description: In the field, this facies type is characterized by densely packed crinoid elements (particles) in limestone beds within Unit D. Crinoid-bearing limestones in this interval are very thickly bedded. The weathered surface is light gray while the fresh color is lustrous brownish-gray. This interval is overlain and underlain by thickly bedded coral-bearing limestone beds. Note that the underlying coral-bearing bed is in turn underlain by collapse breccias of Unit C which is a good stratified marker for this locality. Rough surfaces developed on dolomitic patches and lenses are common throughout this interval. Nodular cherts are occasionally found. Associated fossils are very sparse in this interval with only some bryozoans are observed.

Petrographically, in sample no. A50, this microfacies exhibits densely packed crinoid elements (Fig. 3.25). These elements occur as fragments and are moderately sorted. Grain-contact between crinoid elements with stylolites are common. These characteristics are unique to this microfacies type. Fusulinid fragments are rarely

observed as are other unidentified fragments. Matrix is minimal in this facies. It consists of fine bioclastic fragments and debris with small patches of black substance. Twinning texture in crinoids is conspicuous. Dolomite rhombs formed between crinoid elements is partly observed.

According to sample A52, this facies is characterized by poorly sorted crinoid elements in matrix. Matrix is bioclastic packstone containing small bioclast fragments. In this facies type, crinoid fragments are floated in matrix. It differs from all other facies described herein (A50). Twinning character of crinoid particles is also conspicuous. Dolomite rhomb are observed in this facies type.

3.3.10 MF10: Limestone breccia/conglomerate

In this study area, limestone breccia and conglomerate include mass-flow breccias, intraformational conglomerate/breccia, polymict-channel breccia and solution collapse breccia. Details of these rocks are as follows.

3.3.10.1. MF10a: Mass-flow breccia

Description: This breccia was found overlain alatoconchid rudstone bed and underlain non-laminated limestone bed in Unit E. It was found in lenticular shape without lateral continuity. Maximum thickness of this bed is approximately 30 centimeter.

The rock is composed of different types of clasts. Colors of clasts are mostly in light to dark gray but others are black and red. The clasts are angular to rounded shape with sharp boundary between clasts and matrix. Fitting of clasts is low. It can be classified as polymict depositional carbonate breccia.

Petrographically, clasts contain several facies types (Fig. 3.26). They consist of fusulinid wackestone/packstone, coated bioclastic grainstone,

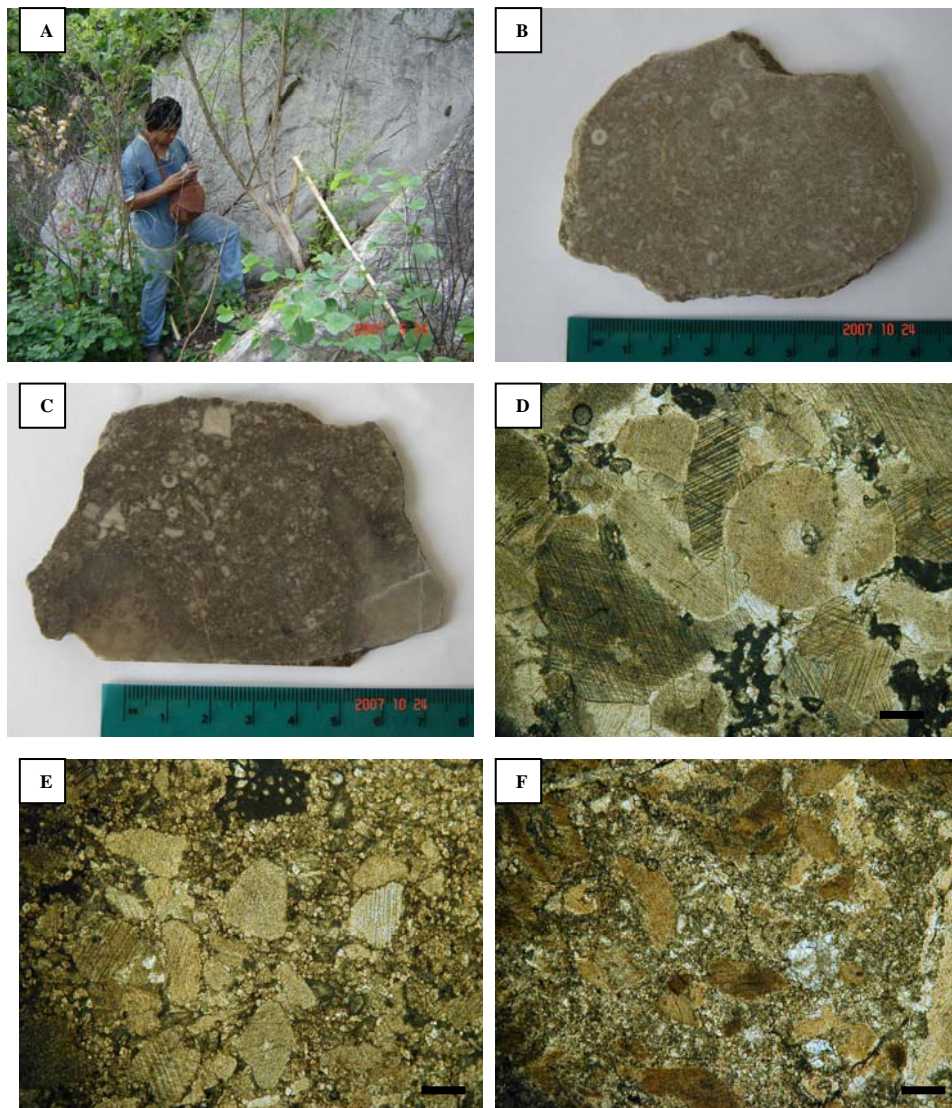


Figure 3.25 A Field photograph of thickly to very-thickly crinoidal packstone beds. B: Rock slab of crinoidal facies (sample no. A50). C: Rock slab of crinoidal facies with massive coral fragment at base (sample no. A52) D: Photomicrograph of crinoidal packstone showing densely packed crinoid elements (sample no. A50) with distinct twin laminae. E: Photomicrograph of crinoidal facies showing poorly sorted, loosely packed crinoidal elements in diagenetic groundmass with dolomite rhombs (sample no. A52). F: Photomicrograph of crinoidal facies showing crinoid elements with dark gray micrite and diagenetic groundmass. (All scale bar= 500 μm)

bioclastic wackestone/packstone, chert nodule fragments, dolomitic limestone and others. Reworked fossils including fusulinid fragments (e.g. *Sumatrina* sp.) and other shell fragments are common in calcarenite/doloarenite groundmass. Pressure solution features between clasts is prominent.

3.3.10.2 MF10b: Intraformational conglomerate/breccia

Description: This type was observed in the lower part of Unit G (e.g. sample no. A48 and A49). It is characterized by lithoclastic limestone breccia up to 5 meters thick. The rock is thickly to very thickly bedded with light gray weather color and medium gray fresh color. Lithoclasts are observed in centimeter size with subangular to rounded shape. They are noticeable in the field by virtue of their relatively darker color in comparison to groundmass. This stratum is overlain by limestone conglomerate.

Petrographically, lithoclasts are floated in matrix. They are comprised mainly of bioclastic wackestone/packstone clasts (Fig. 3.27). Fossils identified in these lithoclasts are compatible with fossils that are found in the underlying strata. They include *Dunbarulla* sp., *Mizzia* sp. and others. Circumgranular cracks around lithoclasts and veinlets are common. Groundmass is mainly calcisiltite matrix lacking fossils. It contains debris and fine lithoclasts floating in gray mud.

3.3.10.3 MF10c: Polymict channel conglomerate

Description: This deposit was found in the topmost section of this study area (Unit G) and is about 10 meters in total thickness. It is characterized as bimodal conglomerate with red color matrix (Fig. 3.28). Clasts are poorly sorted with mostly rounded shape. They are comprised of carbonate clasts with size ranging from cobbles to boulders. These clasts are polymict carbonates in origin with high

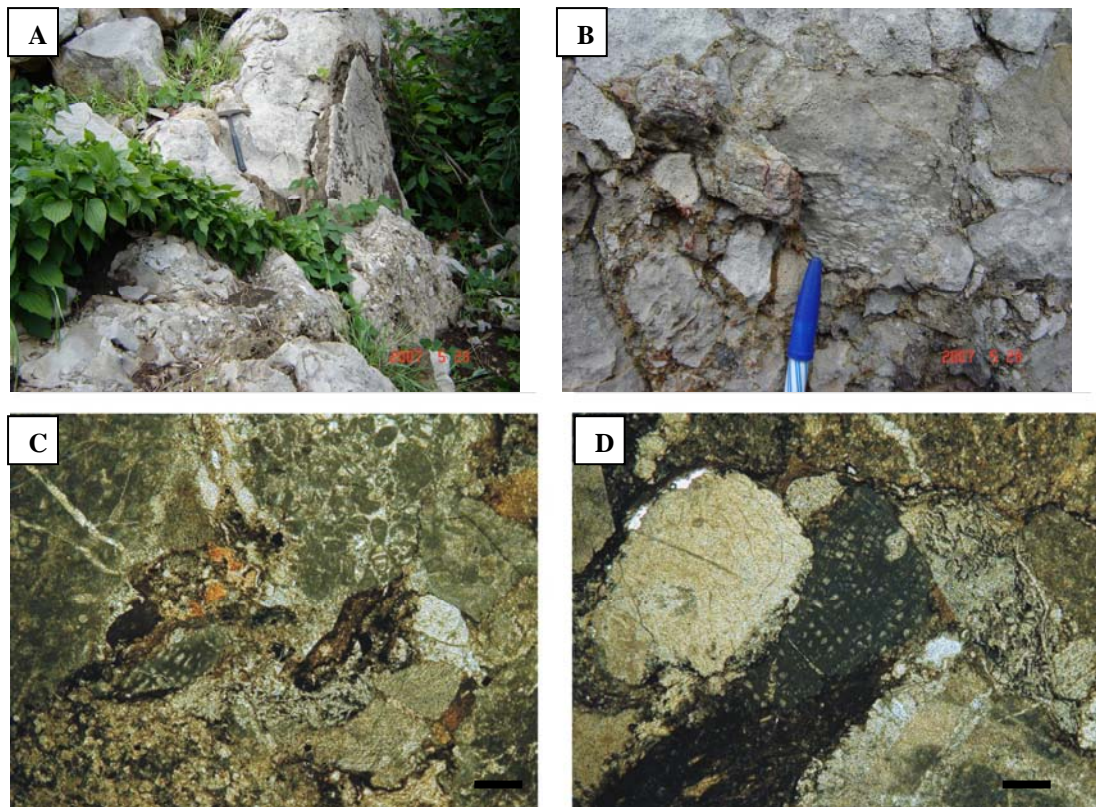


Figure 3.26 A: An outcrop photograph of depositional breccia (MF10a1) from Unit E. B: Breccia from Unit E showing more fitted clasts in comparison to Unit G. Clast components are of intraformational origin with varieties of microfacies type. C: Photomicrograph of breccia showing wackestone clast on left, grainstone on top with variation. They compose of fusulinid wackestone/packstone, limestone clasts with coral fragments, fragments and debris forming as matrix in lower part. D: Photomicrograph of breccia showing lithoclast fragments and fusulinid fragment (*Sumatrina* sp.) embedded in groundmass. (All scale bar=500 μm)

facies variation. They include fusulinid wackestone/packstone, limestone clasts with alatoconchids, dolomites and others. Groundmass consists mainly of pebble clasts in red color matrix. This unit overlies intraformational tidal-channel breccia. Matrix is lacking in fossils and composed mainly of calcisiltite and fine lithoclasts.

3.3.10.4 MF10d: Solution-collapse breccia

Description: In the field, this type of breccia is found exposed within Unit C. and is about 5 meters thick, however, the exposure is laterally discontinuous. This unit overlies thickly bedded non-laminated limestones. The overlying beds are thickly bedded coral biostrome and very thickly bedded crinoidal packstone. Boundaries between the breccia bed and underlying beds is irregular sharp and laterally discontinuous. These underlying beds exhibit a profound erosional surface. Evidence of truncation and infilling of preexisting rocks is common including sediment-infilling fractures, fissures, sills and coarse-calcite spar filled veins. This interval can be subdivided into two types of breccia. The first is fissure-infill breccia formed as internal sediments filling in fissures within underlying host rocks (Fig. 3.29). The second is collapse breccia which forms the main part of this Unit. This breccia is characterized by large breccia clasts overlying fissure-infill breccia.

In the main collapse breccia, clasts are mostly in light gray weathered color and light to medium gray fresh color. Groundmass is light grey to dark grey, light brown, and reddish brown (Fig. 3.30). Grain contact is moderate and the boundary between clasts and groundmass is prominent. The rock fabric can be classified as polymictic clast-supported breccia. The composition of the clasts reveals different lithologies such as bioclastic limestones, dolomites and chert fragments. Bioclastic limestones contain alatoconchid fragments, massive corals, gastropods, crinoid

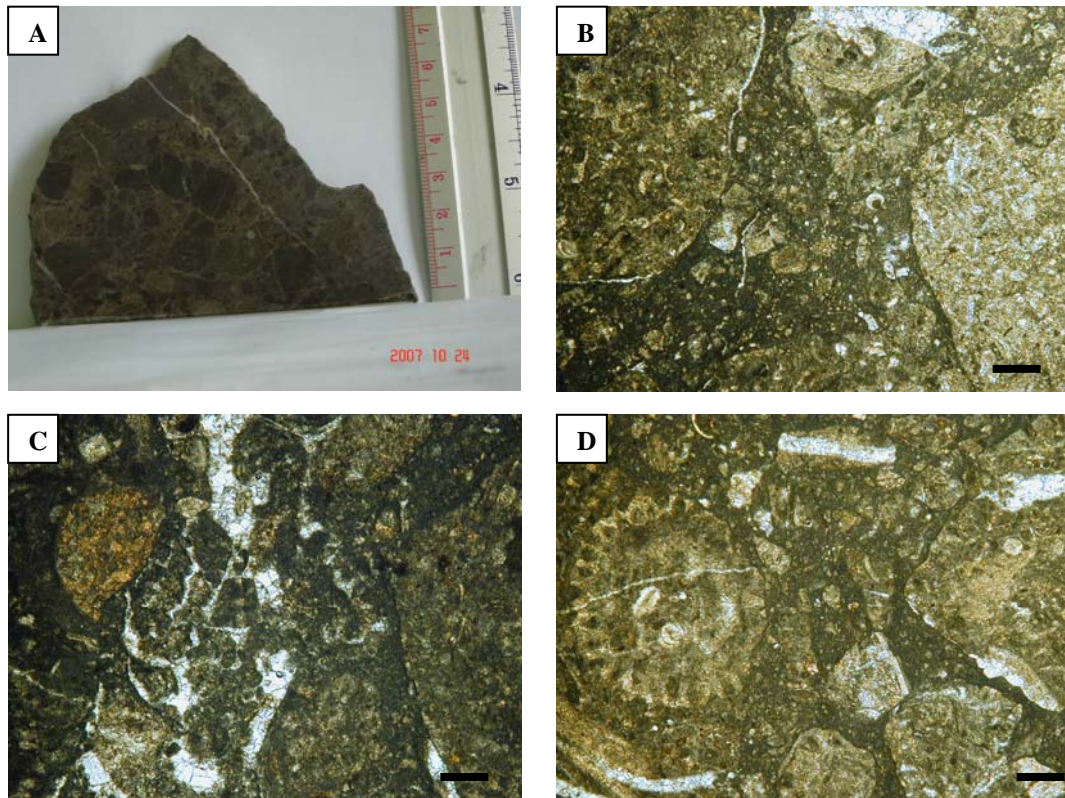


Figure 3.27 A: Rock slab of breccia from lower part of Unit G. B: Photomicrograph of intraformational conglomerate/breccia showing periphery cracking of clast (sample no. A47). C: Photomicrograph of intraformational conglomerate/breccia showing sparry calcite cement between clasts (sample no. A48). D: Photomicrograph of intraformational conglomerate/breccia showing calcareous algae with other fossils in lithoclasts (same sample as B). (All scale bar=500 μm)

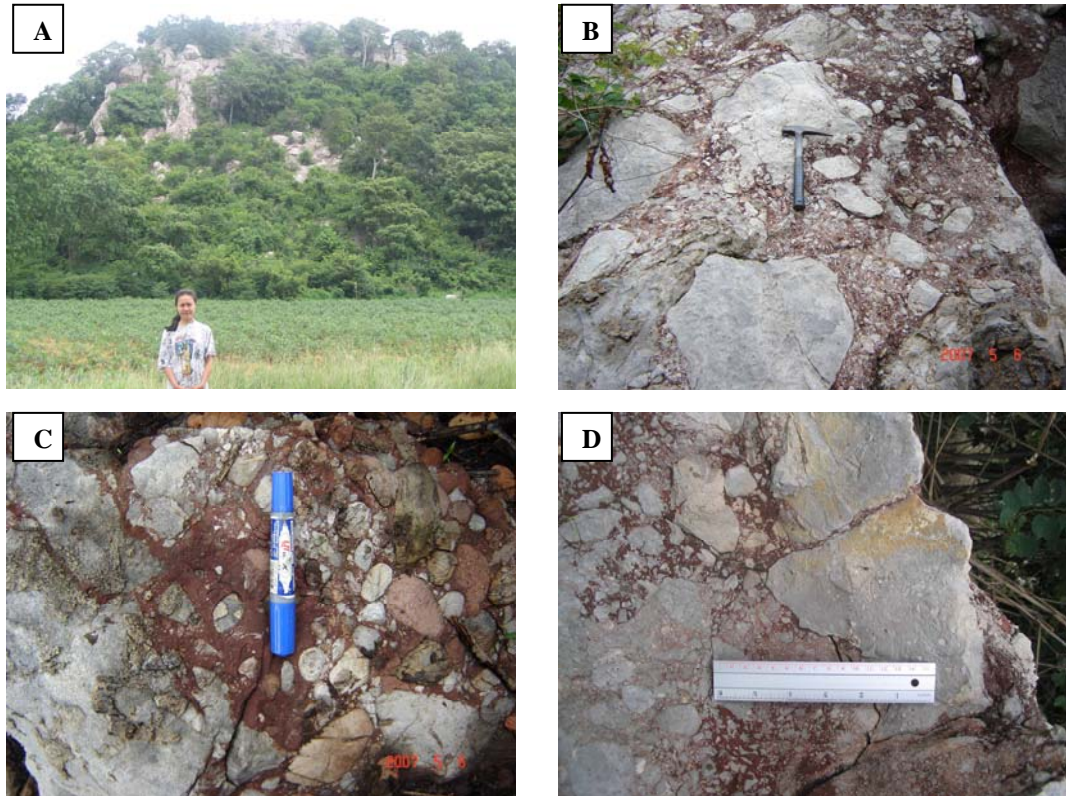


Figure 3.28 A: Field photograph of limestone conglomerate/breccia outcrop of Unit G. B: Outcrop photograph from Unit G showing poorly sorted, polymict conglomerate floated in red matrix. C: Well-rounded clasts in conglomerate from Unit G (marker pen=15 cm). D: Subangular to subrounded clasts from the same unit as C.



Figure 3.29 A: An outcrop of fissure-bearing limestone interval; fissure-fill material is brown in colour with irregular shape. B: Fissure-fill sediment showing lamination with poorly sorted grains texture. C: Another view of an irregular fissure truncated into limestone bed. (Ruler=15 cm)

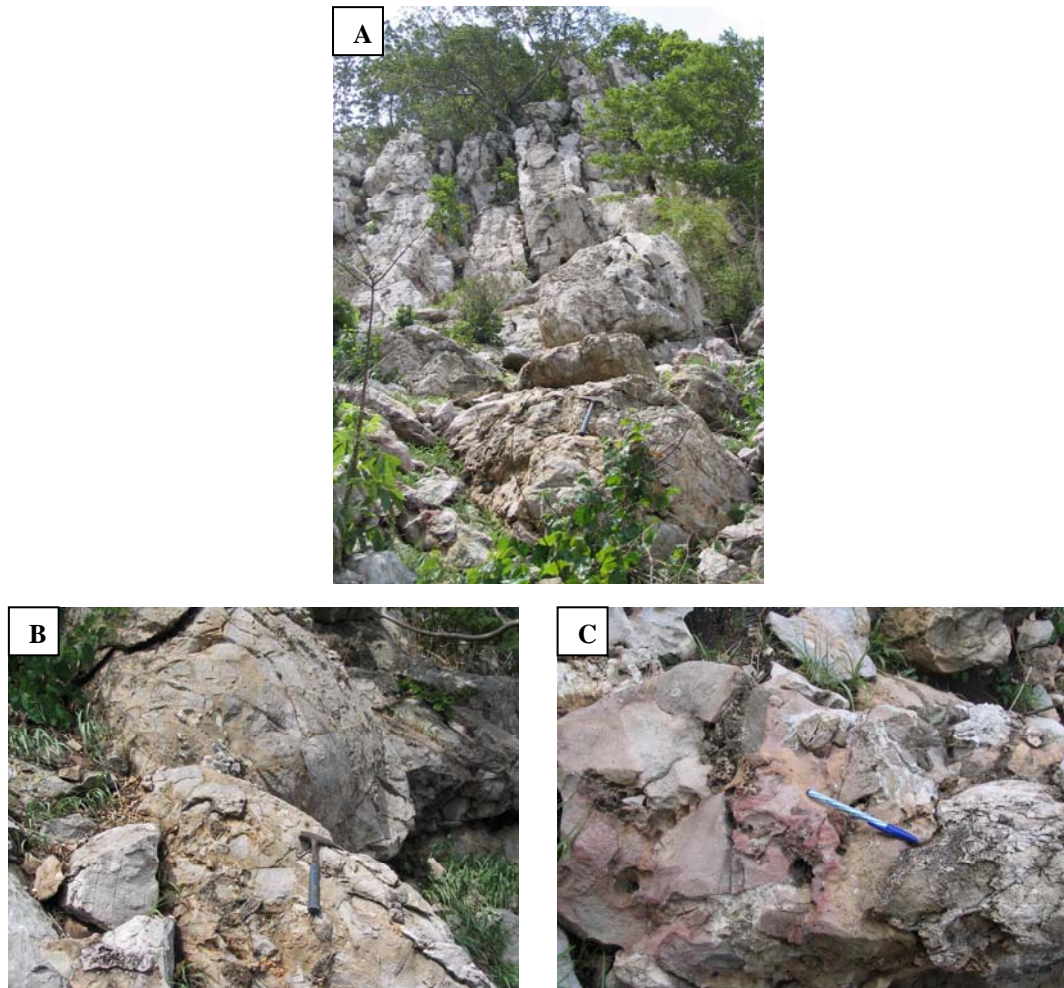


Figure 3.30 A: An outcrop of non-depositional breccia (MF10b1) of Unit C. Breccia is exposed in the lower part of view (geological hammer=30cm). B: Blocks of limestone clasts floated in groundmass showing the high angularity of the clasts (geological hammer=30cm). C: Clasts in breccia showing variety of limestone facies with platform fossils such as coral (lower left). (Pen=15 cm)

oscicles, bryozoans, shell fragments and debris. Chert fragments are also common and have similar texture to nodular or lenticular cherts observed within the sequence. Dolomite clasts have characteristic rough surfaces in this breccia. Size of clasts is variable ranging from 2 cm up to 50 cm. However, most clasts are between 10 cm and 20 cm. They show angular to subrounded shape and are poorly to moderately sorted.

Fissure-infill breccia was deposited as thin laminae. It occurs filling in fissures within host rocks. This lamination is feither planar or wavy parallel to bedding. The lamination is characterized by millimeter to centimeter thick altenation of dark gray and light brown sediments. The sediment is silt and sand size but pebble-size grains are found scattered in the matrix. Cobble- size chert fragments are common in this sediment (e.g. sample no. 811).

Petrographically, this fissure-fill breccia is comprised of strongly recrystallized shell fragments or clasts floating in calcisiltite/dolosiltite matrix (e.g. sample no. 814). These clasts are poorly sorted, low fitting with angular to rounded shape. Some clasts can be determined as crinoid elements and thin bivalve shell. In sample no 811, the sediment infill comprises abundant poorly sorted, angular chert fragments floating in calcisiltite/dolosiltite matrix. This sediment occurs within a paleocalcliche bed. This paleocalcliche is characterized by dominant nodular fabrics, grains coated by micrite, and crinoidal fragments. Fossils are rare; only crinoid elements and very rare micritised fusulinids were observed. Circumgranular cracking surrounding nodular fabrics is common.

Table 3.1 Summary of microfacies types, subfacies, their characteristics and key fossils.

Microfacies Types	Subfacies and characteristics	Fossils
MF1. Lime Mudstone/ wackestone	MF1a. Lime mudstone; peloids, coarse intraclasts, with few bioclastic grains dispersed in mud matrix, grading into dolomite or fenestral mudstone in some intervals.	Ostracods, smaller foraminifers (e.g. <i>Langella</i> sp., <i>Globivalvulina</i> sp., <i>Neohemigordius grandis</i> , <i>N. japonica</i> , <i>Hemigordius</i> sp., and <i>Agathammina</i> sp.), sponge spicules.
	MF1b. Fenestral mudstone; irregular fenestral fabric in lime mudstone groundmass with minor bioclastic grains and peloids, commonly dominated with lime mudstone.	Ostracods, calcispheres, small gastropods, smaller foraminifers (e.g. <i>Hemigordius</i> sp., <i>Agathammina</i> sp., <i>Nodosaria</i> sp., <i>Calcitornella</i> sp., and <i>Globivalvulina</i> sp.), algae (<i>Pseudovermiporella</i> sp., and <i>Vermiporella nipponica</i>).
	MF1c. Bioclastic wackestone; bioclastic grains, peloids and intraclasts dispersed in mud matrix.	Ostracods, calcispheres, small gastropods, brachiopods, smaller foraminifers (e.g. <i>Agathammina</i> sp., <i>Hemigordius</i> sp., <i>Globivalvulina</i> sp., <i>Calcitornella</i> sp., and <i>Pseudoendothyra</i> sp.), algae (<i>Pseudovermiporella</i> sp.).
MF2. Laminated bindstone	MF2a. Laminated bindstone; bioclastic grains and peloids with micrite mud in laminated texture, grains orientated parallel to bedding plane, strongly micritised and abraded bioclasts, common fitted fabric with black filamentous matter.	Algae (e.g. <i>Mizzia</i> sp., <i>Vermiporella</i> sp.), smaller foraminifers (miliolids).
	MF2b. Fenestral bindstone with wackestone matrix; laminated texture with alternation of light-gray fenestral layers and dark-gray layers.	Algal fragments, ostracods, miliolids.
MF3. Algal- foram wackestone/ packstone	MF3a. Algal-foram wackestone: smaller foraminifers and algae predominantly with peloids in micrite matrix.	Algae (e.g. <i>Vermiporella</i> sp., <i>Mizzia</i> sp.), smaller foraminifers (e.g. <i>Hemigordius</i> sp., <i>Agathammina</i> sp., <i>Kamurana</i> sp., <i>Pseudoendothyra</i> sp., <i>Globivalvulina</i> sp., <i>Ichthyolaria</i> sp., <i>Eotuberitina</i> sp., and <i>Pachyphloia</i> sp.), ostracods.

Table 3.1 Summary of microfacies types, subfacies, their characteristics and key fossils. (continued)

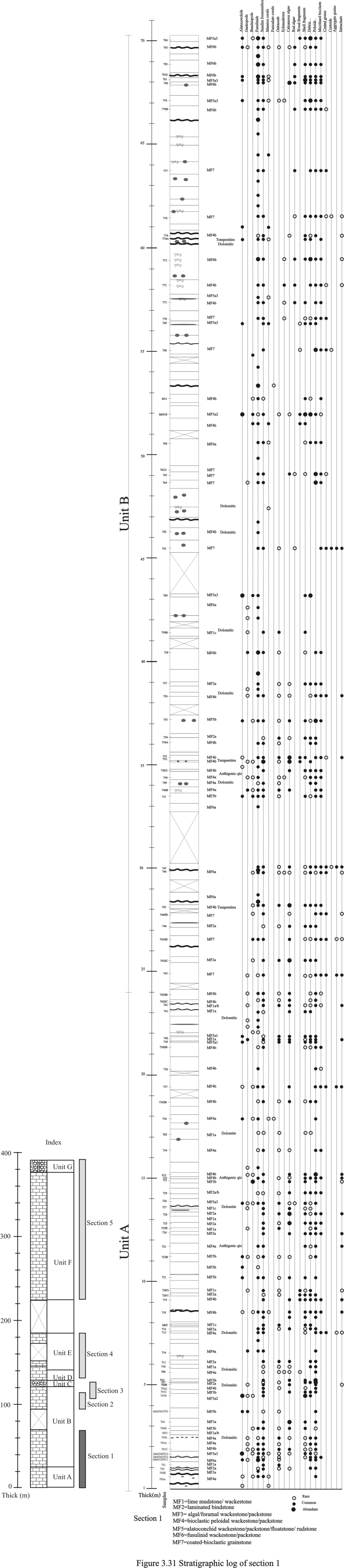
Microfacies Types	Subfacies and characteristics	Fossils
MF3. Algal- foram wackestone/ packstone	MF3b. Algal-foram packstone; algae and smaller foraminifers dominate, packed, grain-supported, poorly to moderately sorted grains, with peloids in micrite matrix.	Algae (e.g. <i>Mizzia</i> sp., <i>Vermiporella</i> sp.), smaller foraminifers (e.g. <i>Hemigordius</i> sp., <i>Agathammina</i> sp., <i>Kamurana</i> sp. and <i>Pseudoendothyra</i> sp.), ostracods, brachiopods, fusulinids (<i>Nankinella</i> sp.).
MF4. Bioclastic peloidal wackestone/ packstone	MF4a. Bioclastic peloidal wackestone; poorly sorted allochems disperse in micrite matrix, algal thallus and fragments, smaller foraminifers, ostracods and other bioclastic fragments or shell debris.	Smaller foraminifers (e.g. <i>Pachyploia</i> sp., <i>Globivalvulina</i> sp., miliolids), fusulinids, algae (e.g. <i>Vermiporella</i> sp., <i>Undarella</i> sp.), ostracods.
	MF4b. Bioclastic peloidal packstone; grain-supported texture with abundant peloids and bioclasts, common grain-in-contacts with poorly to moderately sorted grains.	Algae (e.g. <i>Mizzia</i> sp.), smaller foraminifers (e.g. <i>Pachyploia</i> sp., miliolids), small gastropods, ostracods, fusulinids (<i>Nankinella</i> sp.).
MF5. Alatoconchid wackestone/ packstone/ floatstone	MF5a1. Thin-shell alatoconchid rudstone; thin alatoconchid shell fragments packed in bioclastic peloidal packstone matrix.	Alatoconchids, algae, ostracods, smaller foraminifers.
	MF5a2. Thick-shell alatoconchid rudstone; large alatoconchid shell and shell fragments packed in calcarenite matrix.	Alatoconchids, ostracods, smaller foraminifers.
	MF5a3. Thick-shell alatoconchid floatstone; large alatoconchids floated in calcarenite matrix.	Alatoconchids, brachiopods, ostracods, spicules, smaller foraminifers.
	MF5b1. Alatoconchid biostrome with peloidal wackestone matrix; alatoconchids floated in peloids predominating over skeletal grains in micrite.	Alatoconchids, smaller foraminifers: <i>Protonodosaria</i> sp., <i>Calcitornella</i> sp., <i>Nodosaria</i> sp. <i>Diplosasphaerina</i> sp. <i>Tuberitina</i> sp., some miliolids, Algae: <i>Pseudovermiporella</i> sp., small gastropods.

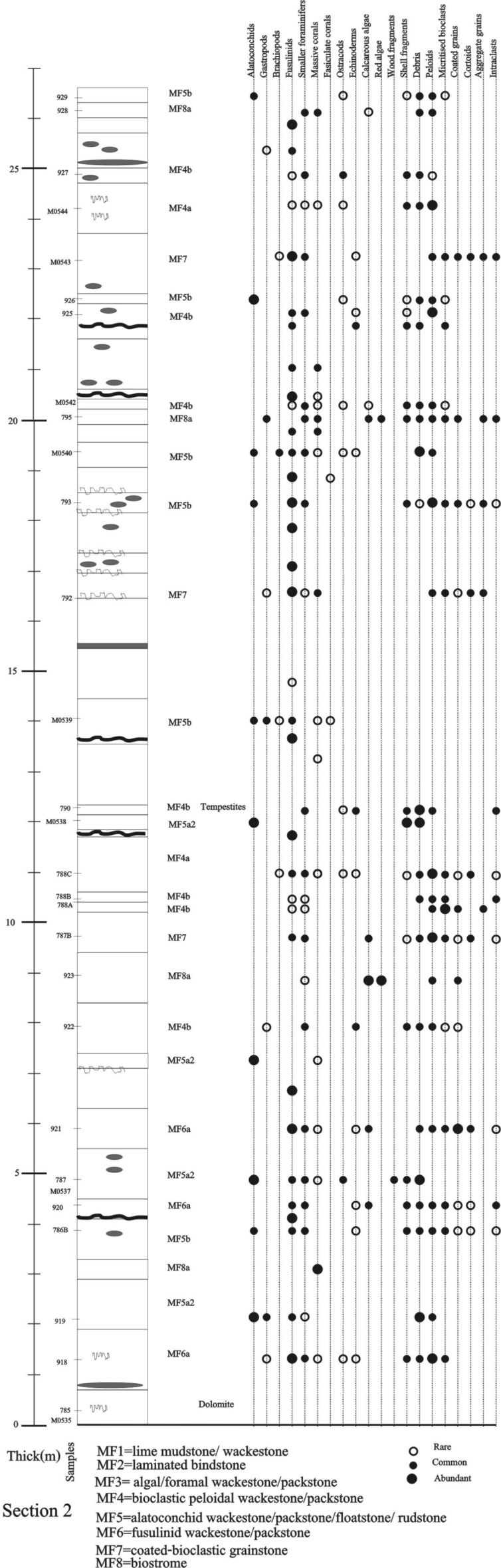
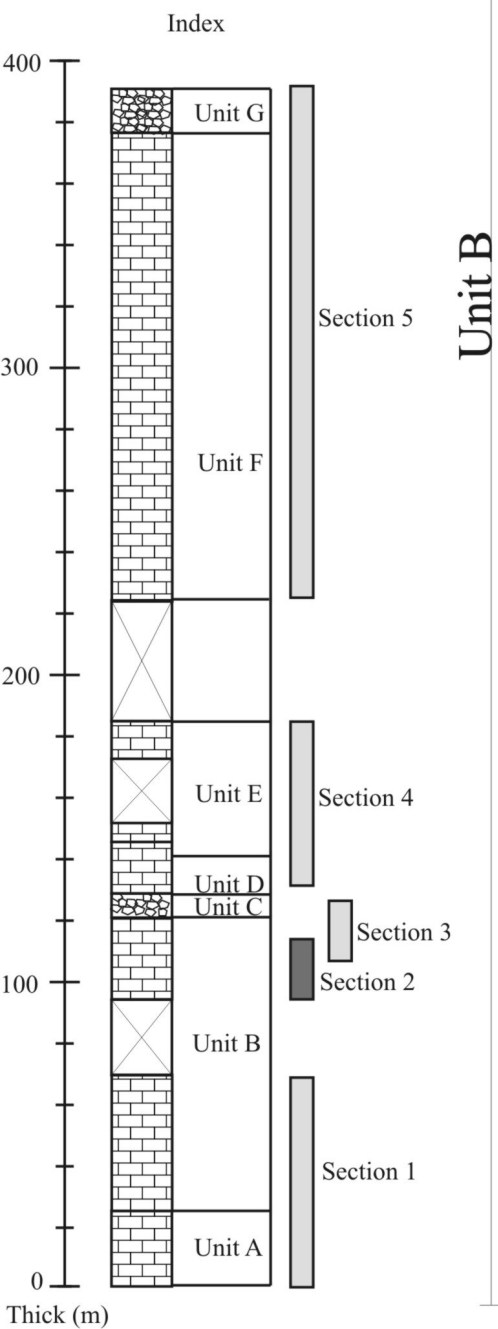
Table 3.1 Summary of microfacies types, subfacies, their characteristics and key fossils. (continued)

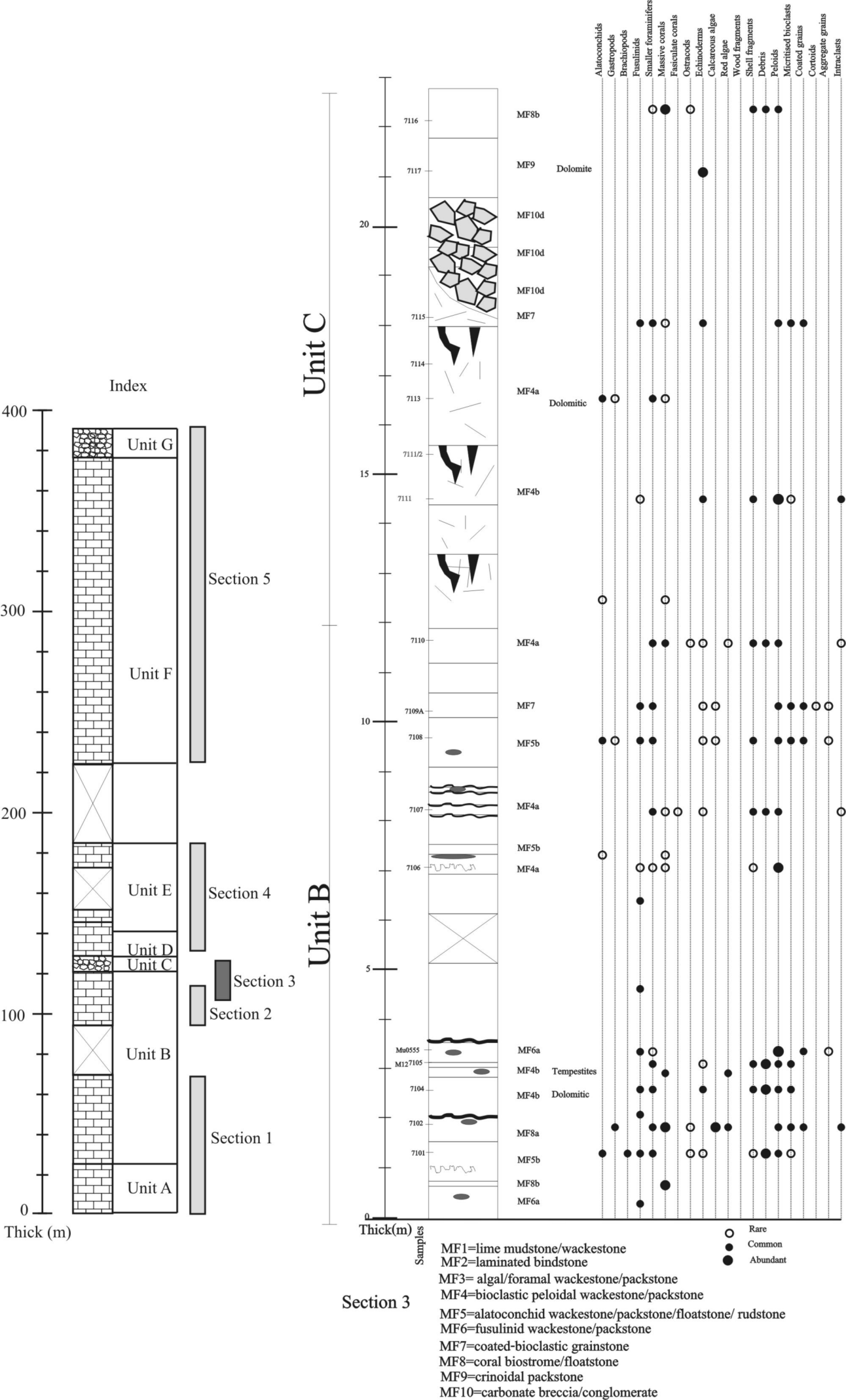
Microfacies Types	Subfacies and characteristics	Fossils
MF6. Fusulinid wackestone/ packstone/ grainstone	MF6a. Fusulinid wackestone; fusulinid dominant and dispersed in peloidal bioclastic wackestone matrix.	Fusulinids: <i>Verbeekina verbeeki</i> , <i>Neoschwagerina</i> sp. <i>Sumatrana</i> sp., and <i>Nankinella</i> sp., smaller foraminifers: <i>Tetrataxis</i> sp., <i>Pseudoendothyra</i> sp., <i>Globivalvulina</i> sp., <i>Agathammina</i> sp., <i>Hemigordius</i> sp., <i>Eotuberitina</i> sp., and others.
	MF6b. Fusulinid packstone; fusulinid dominant and packed with bioclastic fragments, debris and peloids.	Fusulinids: <i>Colania douvillei</i> , <i>Verbeekina verbeeki</i> , <i>Lepidolina</i> sp., <i>Yabeina</i> sp. and <i>Conodofusiella</i> sp., smaller foraminifers: <i>Agathammina</i> sp., <i>Kamurana</i> sp., <i>Tuberitina</i> sp. <i>Pachyphloia</i> sp., and <i>Cribogenerina</i> sp.
	MF6c. Fusulinid grainstone; fusulinid dominant with dacycladacean algae, coated grains with common oncoilitic structure in sparry cement.	Fusulinids: <i>Lepidolina</i> sp., <i>Yabeina</i> sp., and <i>Chusenella</i> sp. Algae (e.g. <i>Mizzia velebitana</i> .)
MF7. Coated bioclastic grainstone	Micritized or coated grains with common micrite envelopes, silt-size grains, well rounded, good sorting, grain-supported fabric with common grain-in-contact.	Smaller foraminifers (e.g. <i>Nodosaria</i> sp., <i>Protonodosaria</i> sp., <i>Pachyphloia</i> sp., <i>Tuberitina</i> sp., <i>Calcitornella</i> sp., <i>Deckerella</i> sp. <i>Texuralia</i> sp., and <i>Globivalvulina</i> sp.), red algae (<i>Undarella</i> sp.)
MF8. Coral biostrome/floatstone	MF8a. Coral biostrome; corals in growth position with mudstone and bioclastic wackestone matrix.	Algae (e.g. <i>Tubiphytes</i> sp.), smaller foraminifers (e.g. <i>Tuberitina</i> sp.)
	MF8b. Coral floatstone; reworked massive coral heads with bioclastic peloidal wackestone matrix.	Crinoid fragments, shell fragments, red algae fragments, smaller foraminifers, ostracods

Table 3.1 Summary of microfacies types, subfacies, their characteristics and key fossils. (continued)

Microfacies Types	Subfacies and characteristics	Fossils
MF9. Crinoidal packstone	Densely packed crinoid elements in packstone matrix.	crinoid elements
MF10. Carbonate breccia/ conglomerate	MF10a. Mass mass-flow breccia; polymict, angular to rounded clasts with calcarenite/doloarenite groundmass.	fragment of fusulinids (e.g., <i>Sumatrina</i> sp.)
	MF10b. Intraformational conglomerate/ breccia; centimeter-size subangular to rounded limestone/dolomite lithoclasts in calcisiltite groundmass.	absent
	MF10c. Polymict channel conglomerate; bimodal polymict carbonate clasts, with red calcarenite/doloarenite groundmass.	absent
	MF10d. Solution-collapse breccias; polymictic clast-supported breccias overlying sediment-filled fissures. Different lithologies of breccia clasts such as bioclastic limestones, dolomites and chert fragments.	absent







CHAPTER IV

PALEONTOLOGY

4.1 General background on alatoconchid bivalves

Alatoconchids are the largest known fossil bivalves and are restricted to the Permian period. They have peculiar morphology in comparison to conventional bivalves. Most notably, they have a vertical commissural plane, a dorsal ridge along the commissural plane, and wing like flanges (Fig. 4.1). In some respects, the alatoconchids are similar to *Corculum* the recent Pacific bivalve. However, there are major difference in morphology, size, shell thickness and shell structure of the alatoconchids. General morphology of these bivalves was first formally described on the basis of Japanese fossils by Ozaki (1968). Subsequently, these bivalves have been described and revised several times as new discoveries and research have been come to light (e.g. Termier et al., 1973; Runnegar and Gobbett, 1975; Kochansky-Devidé, 1978; Yancey and Boyd 1983; and Yancey and Ozaki, 1986). According to Yancey and Boyd (1983) and Yancey and Ozaki (1986), the alatoconchids belong to the family Alatoconchidae (Termier et al., 1973) within the superfamily Ambonychiacea (Miller, 1877). Two subfamilies have been recognized including subfamily Saikraconchinae (Yancey and Ozaki, 1986) and subfamily Alatoconchinae (Termier et al., 1973). Subfamily Saikraconchinae contains genus *Saikraconcha* (Yancey and Boyd, 1983) and subgenus *Dereconcha* (Yancey and Boyd, 1983). These alatoconchids share some common characteristics in having a small cardinal area,

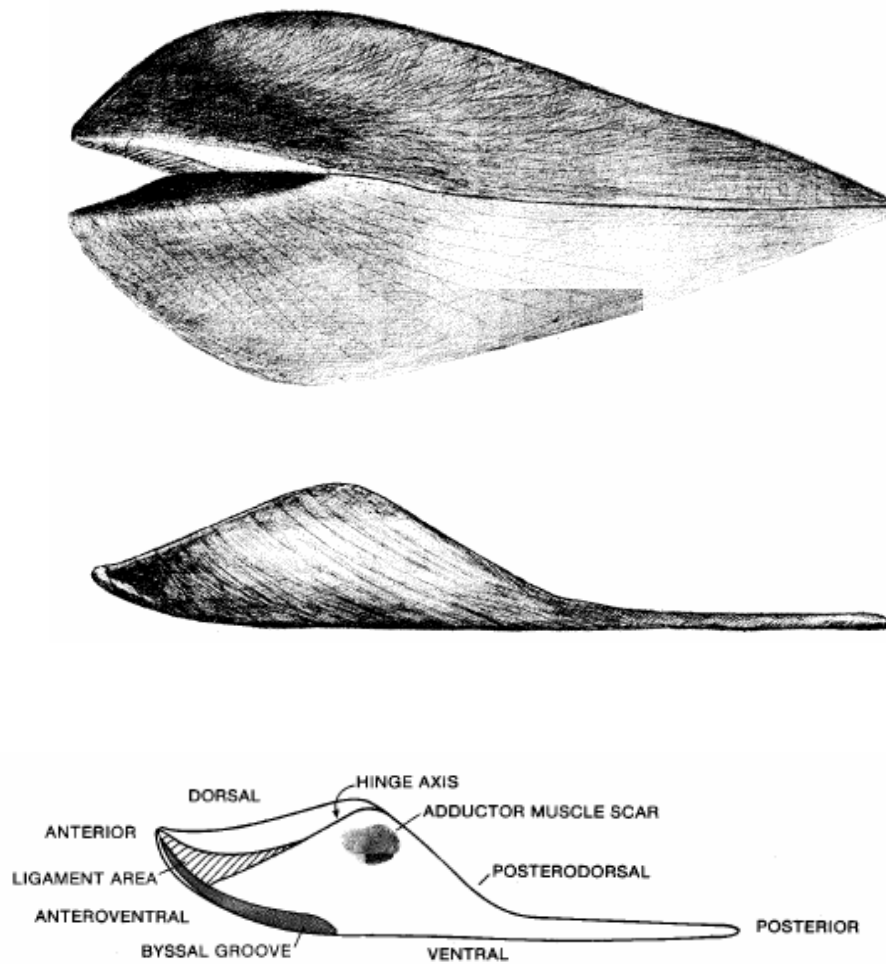


Figure 4.1 Reconstruction of alatoconchids (*Shikamaia (Tanchintongia) perakensis*).

A: Dorsal view. B: Lateral view. C: Internal view with terminology. (after Yancey and Boyd, 1983)

simple ligament pattern, ligament groove subparallel to the hingeline and significantly involving almost all of the cardinal area, and a large byssal collar (Yancey and Ozaki, 1986). Subfamily Alatoconchinae includes genus *Shikamaia* (Ozaki, 1968) and subgenus *Alatoconcha* (Termier et al., 1973). This family is characterized in having the ligament groove restricted to the lower half of the cardinal area, a prominent byssal groove, and a small to absent byssal collar. Further information and more details on the systematic classification of these bivalves is available in the literature mentioned above.

4.2 Morphology and taxonomy of alatoconchids

In order to study the morphology of alatoconchids from Khao Somphot locality, natural random sections of these bivalves were studied in the field. More than 31 selected individuals of alatoconchids were measured, photographed and described. They are embedded within intact limestone bed and are extremely difficult to extract. Whole specimens were impossible to collect for the purposes of this study. They appear in both reworked and life positions (see detail in section 3.3.5). However, representative fragments of some specimens were collected in order to study key aspects of their morphology in detail in the laboratory. These samples were selected, extracted and described. They include selected subsamples of both articulated and disarticulated alatoconchid shells. Morphological descriptions of these specimens are presented in this section. Taxonomic identification is based entirely on available material (Appendix A). Accordingly, identifications are restricted to Family or Genus level only due to lack of morphological information and the difficulty of extraction. Further study and more information on alatoconchid morphology is still needed in

order to solve some aspect of their taxonomy and variability, especially at specific level. In brief, this section provides results of my investigation thus far on alatoconchid morphology.

SYSTEMATIC PALEONTOLOGY

Class BIVALVIA

Order: PTERIOIDA Newell, 1965

Superfamily AMBONYCHIACEA Miller, 1877

Family ALATOCONCHIDAE Termier, Termier and Lapparent 1973

Subfamily SAIKRACONCHINAE Termier, Termier and Lapparent 1973

Genus SAIKRACONCHA Boyd and Newell, 1979

Saikraconcha cf. tunisiensis

Plate 1, Figs. 1-6; Plate 3, Figs. 3-6; Plate 5, Fig. 7; Plate 7, Fig. 3; Plate 9, Fig. 5

Saikraconcha tunisiensis Yancey and Boyd, 1983, p. 512-516, pl. 64, figs.7-11.

Description: Incomplete and broken specimens. Some articulated fragments showing equivalved shell; compressed and high dorsal crest along plane of commissure; gradually rising from beaks; curvature with semi-circular ridge dorsal crest (Appendix A: Pl. 1, Figs. 1, 4; Pl. 7, Fig. 3); alate shape of wing-like flanges extending from base of dorsal crest to lateral shell edge of both valves; short and small appressed anterior part (Pl. 1, Figs. 2, 4); down-turned beaks (Pl. 1, Figs. 1, 2, 4-5); massive infilled umbone, dorsal niche narrow and forming out-bowed elliptical shape on slope of dorsal crest (Pl. 1, Figs. 1, 5); large byssal collar located along commissural plane of ventral side (Pl. 3, Figs. 3, 6; Pl. 7, Fig. 3; Pl. 9, Fig. 5); shell thickness relatively

thin; large body cavity located mainly along commissural plane at the center of antero-posterior path; triangular shape in transverse section along dorsal-ventral plane of both valves (Pl. 1, Figs. 3, 6; Pl. 3, Figs.4-5).

Remarks: These specimens have a high semicircular dorsal crest. This feature is distinctive and differs from that of all other known alatoconchids. The dorsal niche as found in these specimens can be observed in *Alatoconcha vampira* but the latter differs in having a prominent wedge shaped, larger and wider dorsal niche than the former. Moreover, the dorsal niche in *A. vampira* originates anterior of the beak margin and extends up toward the dorsal crest, but in these specimens it originates further behind the beak and extends up around the same point along the slope of the dorsal crest. However, downturned beak character of the Khao Somphot material can be compared to that of *Saikraconcha* (*Saikraconcha tunisiensis*). A large byssal collar is observed in some specimens and is the common characteristic of subfamily Shikraconchinae. Due to a lack of cardinal information for this material (because of extraction problems) it is not possible to classify to species level with confidence. However, it is reasonable to consider them as *Saikraconcha* cf. *tunisiensis*.

Subfamily ALATOCONCHINAE Termier, Termier and Lapparent 1973

Genus SHIKAMAIA Ozaki, 1968

Shikamaia cf. *perakensis*

Plate 2, Figs. 1-5; Plate 4, Figs 1-6; Plate 6, Fig. 7

Tanchintongia perakensis Runnegar and Gobbett, 1975, p. 316-320, pl. 45, figs.1-7;
pl. 46, figs, 1-9.

Shikamaia (*Tanchintongia*) *perakensis* Yancey and Boyd, 1983, pl. 62, figs.1-10.

Description: Incomplete articulated and disarticulated specimens, most of them showing anterior part with missing beaks and wings; large shell with massive infilled anterior; parts of shell wings project from both valves showing dense, thick shell wall; densely packed fine-growth lines forming thick shell wall with more than 2 cm thick of wing around anterior part (Pl. 2, Figs. 3-4); small cavity occurs in a narrow area in this part; slightly to largely diverse anterodorsal margin close to apical end of anterior (Pl. 4, Figs. 3-4; Pl. 6, Fig.7), but strongly appressed at abapical end of anterior (Pl. 2, Figs. 1-2); high dorsal crest along plane of commissure; large body cavity infilled with dark gray matrix; partly observed duplivincular ligament groove showing as incised curvature lines located in lower half of cardinal area; ligament groove aligned with high angle to the hinge line in the anteroventral part; small and prominent byssal groove placed beneath ligament area (Pl. 4, Figs. 3-6); byssal groove connected to central cavity at the abapical end of the cardinal area; high slope angle (45°) between dorsal margin and ventral surface; small byssal collars.

Remarks: These specimens can be placed in the Genus *Shikamaia* on the basis of the ligament structure. High angle between dorsal margin and ventral surface indicates high dorsal crest without elongate shape of cardinal area. These characters can be compared to *Shikamaia (Tanchintongia) perakensis*. The low dorsal crest and elongate shape of the cardinal area in *Shikamaia akasakaensis* precludes designation of the Khao Somphot material as *Shikamaia akasakaensis*. *Shikamaia (Alatoconcha) vampyra* has a low angle between the hinge line and ventral shell surface and has a large, wedge shaped dorsal niche. However this specimen has an appressed to slightly divergent anterior margin and lacks a large dorsal niche as prominent as in *S. (A.) vampyra*. As a result, this specimen is best identified as *Shikamaia*

(*Tanchintongia*) cf. *perakensis*. However, more information is needed before a more confident species determination can be assigned.

Alatoconchidae gen. indet.

Plate 3, Figs 1-2; Plate 5, Figs. 1-5; Plate 6, Figs. 1-6; Plate 7, Fig. 1-2, 5-8; Plate 8, Figs. 1-8; Plate 9, Figs. 1-4, 1-8; Plate 10, Figs. 1-8; Plate 11, Figs 1-8;

Plate 12, Figs. 1-6

Description: Incomplete articulated and disarticulated shells and shell fragments, large wing-like flanks with dorsal ridge, triangular shape in cross section along dorsal-ventral direction, thick shell more than 1 cm thick, similar in thickness of dorsal and ventral shells, narrow body cavity infilled with dark gray matrix.

Remarks: Due to fragmental and poor condition of preservation of incomplete specimens with lack of significant information for taxonomic determination, these specimens can not be confidently assigned to a taxonomic level below family.

4.3 Key foraminifers and algae

In the study locality, there is prolific occurrence of foraminifers including fusulinids, smaller foraminifers, and calcified algae. These fossils can be observed in almost all intervals except in limestone breccias/conglomerate and encrinite limestones.

This study has not addressed taxonomy of foraminifers or algae. Most of them have been identified and listed to only generic level. This section aims to provide some information on the occurrence of both fossil groups. Foraminifers (fusulinids and smaller foraminifers) are used as a major tool for geochronological purposes and

paleoenvironmental interpretation. Fossil algae include members of red algae (Rhodophyceae) and green algae (Chlorophyceae). These algae are used mainly for paleoenvironment interpretation, which is discussed in Chapter V.

The key fusulinid genera (Appendix B) observed in the study area include: *Yabeina*, *Lepidolina*, *Colania*, *Verbeekina*, *Chusenella*, *Sumatrina*, *Conodofusiella*, *Nankinella*, *Dunbarula*, *Minojapanella* and *Neoschwagerina* (Plates 13-23). Smaller foraminifers (Appendix B) include the genera: *Globivalvulina*, *Nodosaria*, *Protonodorasia*, *Deckerella*, *Climacammina*, *Cribrogenerina*, *Pachyphloia*, *Lasiodiscus*, *Langella*, *Geinitzina*, *Diplosphaerina*, *Tuberitina*, *Eutuberitina*, *Umbellina*, *Bisphaera*, *Tetrataxis*, *Calcitornella*, *Bradyna*, *Kamurana*, *Agathammina*, *Hemigordius*, *Neohemigordius* (Plates 24-28). Diagnostic features of these fossils are used for determination and are based mainly on Moor's treatise on invertebrate palaeontology, Part C. The algae (Appendix C) include: *Mizzia*, *Vermiporella*, *Gyroporella*, *Tubiphytes*, *Anthracoporella*, and *Undarella* (Plates 29, 30). Characteristics of these algae can be compared to algae from Khao Phlong Phrab area, central Thailand (Endo, 1969).

CHAPTER V

INTERPRETATION AND DISCUSSION

5.1 Depositional environments

In term of environmental interpretation, the microfacies information and paleontological analysis clearly indicate that carbonate rocks in the study locality were deposited in shallow marine conditions. This result is compatible with previous studies of Permian carbonate sedimentology in the Khao Khwang platform of central Thailand (e.g. Chonglakmani and Fontaine, 1990; Wielchowsky and Young, 1985; Fontaine et al., 2002; Titirananda, 1976; Altermann, 1989). Microfacies study reveals that texture, structure and composition of these carbonates are characteristic of tropical shallow marine carbonate environments. Fossil assemblages are typical of Tethyan fauna and flora. The paleontological data have enhanced the interpretation and validation of the depositional environment interpretation determined from microfacies analysis. The interpretation of depositional environment in this thesis has benefited from and is compatible with a substantial body of research by concerned with previous work, microfacies analysis, depositional models and standard microfacies (e.g. Flügel 2004; Wilson, 1975; Reeckmann and Friedman, 1982).

The study locality in this thesis includes peritidal and subtidal environmental domains. Sediment accumulation in these domains was interrupted by two major sea level falls during that time indicated by unconformity (Tab. 5.1). These domains can be further divided into several sub-environments which are described as follows.

Table 5.1 Summary of lithologic units with brief explanations, microfacies types, some fusulinids and algae, and their depositional environment interpretation. Unconformity is located in Unit C and Unit G.

Lithologic Unit	Description of lithology	Microfacies	Fusulinids	Algae	Interpretation
G	Thickly to very thickly bedded intraformational limestone breccia and red matrix polymict limestone conglomerate	MF10b,c			Peritidal channel/ subaerial
F	Thickly to very thickly bedded fusulinid-bearing limestones, with rare occurrence of alatoconchids, corals, gastropods, brachiopods, thinly bedded argillaceous limestone and laminated limestone intercalated in some interval.	MF4 MF5a3,b1 MF7 MF6a,b	<i>Lepidolina</i> sp. <i>Yabeina</i> sp. <i>Dunbarula</i> sp. <i>Nankinella</i> sp. <i>Minojapanella</i> sp..	<i>Mizzia velebitana</i> <i>Undarella</i> sp. <i>Anthracoporella</i> sp.	Near shore subtidal
E	Thickly bedded fusulinid-bearing limestone with alatoconchid-bearing limestone intercalations in upper part, coral biostrome in lower and middle part.	MF4 MF5a2,a3,b1 MF6a MF7 MF8a,b MF10a	<i>Sumatrana</i> sp. <i>Yabeina</i> sp. <i>Conodofusiella</i> sp. <i>Chusenella</i> sp. <i>Verbeekina verbeeki</i> <i>Nankinella</i> sp.	<i>Mizzia velebitana</i> <i>Vermiporella nipponica</i> <i>Undarella</i> sp.	Subtidal
D	Thickly to very thickly bedded crinoidal limestone or encrinites, dolomite in some beds	MF9			Subtidal normal marine
C	Fissure-bearing limestone with fissure fill sediments and collapse breccia, dolomite common in upper part	MF10d			Subaerial; karstification and collapse breccia
B	Thickly bedded fusulinid-bearing limestones with alatoconchid-and coral-bearing limestones, chert nodules common, dolomite, argillaceous and laminated limestone less common.	MF1c MF2a MF4 MF5a1,a2,a3,b1 MF6a,b MF7 MF8a	<i>Conodofusiella</i> sp. <i>Lepidolina</i> sp. <i>Colania</i> sp. <i>Verbeekina verbeeki</i> <i>Neoschwagerina</i> sp.	<i>Gyroporella</i> sp. <i>Mizzia velebitana</i> <i>Tubiphytes</i> sp. <i>Undarella</i> sp. <i>Vermiporella</i> sp.	Subtidal
A	Medium to thickly bedded limestones with thinly to medium bedded argillaceous limestone and laminated limestone intercalations, conspicuous alatoconchid coquinites, dolomite and chert nodules common.	MF1a,b,c MF2a,b MF3a,b MF4 MF5a1,a2,a3,b1 MF6a	<i>Verbeekina verbeeki</i> <i>Nankinella</i> sp. <i>Neoschwagerina</i> sp.	<i>Vermiporella</i> sp. <i>Mizzia</i> sp.	Peritidal

5.1.1 Peritidal domain

The peritidal domain is consists of three zones including supratidal, intertidal and shallow subtidal zones (Folk, 1973; Wright, 1984). The terms supratidal, intertidal and subtidal are in favor by geologists which are ecologically comparable with supralittoral, littoral and sublittoral respectively (Flügel, 2004). The supratidal zone is situated in a high prolonged subaerial area that is occasionally flooded by high energy events such as storms. The intertidal zone is located between low and high tide-influenced areas. The shallow subtidal zone is located in shallow marine setting just below low tide zone. In this study, four main microfacies types are represented by these sub-environments (Fig. 5.1). Microfacies that related to peritidal environment include: lime mudstone/wackestone faicies (MF1a; b; c), bindstone facies (MF2a; b), algal-foram wackestone facies (MF3a), and carbonate breccia/conglomerate facies (MF 10b; c; d). Detail on microfacies interpretation and depositional environment of the peritidal domain is discussed below.

5.1.1.1 Depositional environment of lime mudstone (MF1a)

This microfacies indicates intertidal environment. It shows characteristics of tidal flats with good preservation of restricted fossils such as miliolids, ostracods and gastropods. Intraclasts are produced by re-sedimentation processes of semi-lithified to lithified sediments introduced by wave or current action. Some bioclastic fragments and shell debris are reworked or transported grains. In some intervals, this facies shows dolomite-rich and fenestral fabric caps. These features can be compared with present-day analogues involving the development of thin dolomitic crusts in tidal flat environments (Shin et al., 1969).

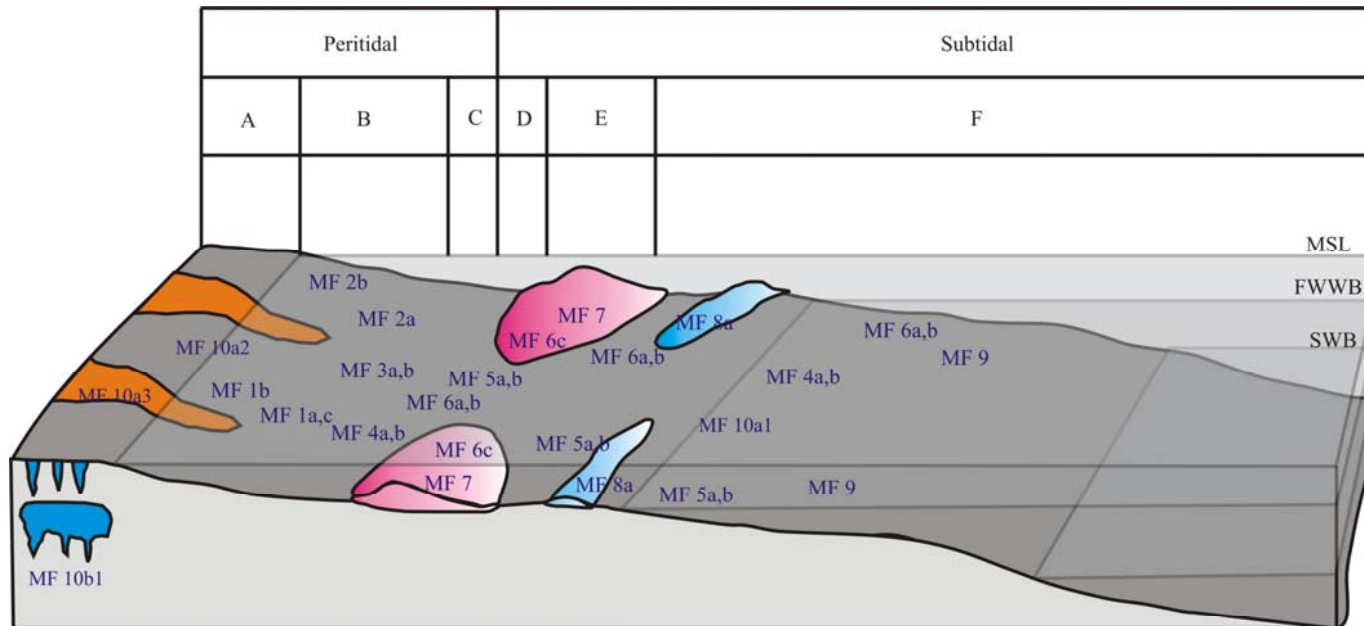


Figure 5.1 Microfacies types and depositional model of the study area in upper most part of Khao Somphot sections. A=supratidal; B=intertidal; C=shallow subtidal with restricted condition; D=subtidal with semi-restricted condition; E=internal bioclastic shoal or barrier bar; F=sheltered lagoon with open marine circulation; MSL=mean sea-level; FWWB=fair-weather wave base; SWB=storm wave base. Explanation of microfacies types and symbols see in text.

5.1.1.2 Depositional environment of fenestral mudstone (MF1b)

Fenestral mudstone is interpreted as tidal mud accumulation in tidal flats within the intertidal environment. Isolated grains in fenestral voids indicate partial breakdown fenestral roof. Fenestral fabric was formed in this area by drying and wetting of sediments. This microfacies can be compared with peritidal flat facies with fenestral mudstone/wackestone of the Permian fusuline-calcareous algal biofacies in central Thailand recognized by Dawson and Racey (1993).

The existence of fenestral fabric or birdseyes generally indicates intertidal environments. In this study, based mainly on rock structure, texture and composition, fenestral fabric is interpreted as shrinkage phenomena (cracks and pores) within intertidal sediments. These features are developed by desiccation and shrinkage processes (Shinn, 1968). They can be correlated with loferite structures described from the Triassic Lofer beds of Austrian Alps by Fischer (1964). In addition, it can be compared with fenestral fabrics of the Middle Triassic Latemar Carbonate (Goldhammer et al., 1987). Birdseyes, fenestrae and loferites in muddy carbonates are more or less synonymous and are commonly observed and associated with upper intertidal- to-supratidal environments (Shinn, 1983).

5.1.1.3 Depositional environment of wackestone (MF1c)

This facies differs from algal-foram facies (MF3) by its higher content of lime mud and relatively lower bioclastic content. It has a more argillaceous texture than the previous fenestral mudstone facies (MF1b). This facies shares some similarities in texture to the lime mudstone facies (MF1a) but differs in containing slightly higher allochemical content. The existence of dolomite-rich caps in some intervals also reveals some similarities to MF1a. Both of these facies can be related to

present-day analogues of thin dolomitic crust developments in tropical tidal flat environments (Shin et al., 1969).

The depositional environment of this facies is interpreted as intertidal. It can be correlated with intertidal sediment below supratidal flats of the Persian Gulf (Wright, 1984). It can also be compared to ostracod wackestone facies of the Triassic peritidal dolostone of *Trigonodus*-Dolomite (Schauer and Aigner, 1997). In addition, the occurrence of restricted fossils including miliolids, gastropods, and well-preserved ostracods indicates restricted-water condition (Flügel, 2004). Intraclasts form by re-sedimentation of semi-lithified to lithified sediments as a function of storm wave or current processes. Some of the bioclastic fragments and shell debris were derived from nearby environments by current or wave action.

5.1.1.4 Depositional environment of laminated bindstone (MF2a)

This microfacies can be correlated with algal mat development as thin shallow subtidal or intertidal environments. Algal tubes are responsible for binding or trapping sediments. Shell fragments and debris were transported to this area by normal tide in normal condition. Additionally, sediment may also derived by wave or current action during high-energy events (Hardie and Ginsburg, 1977; Wanless et al., 1988). The original fabric of this facies is usually obliterated by mechanical compaction. A resultant densely packed packstone texture (diagenetic packstone) is common in this facies. This type of diagenetic alteration is common in microbial mats (Park, 1976; 1977). This facies shares similar texture and composition with dolomitic algal mats of the peritidal flat facies described by Dawson and Racey (1993).

5.1.1.5 Depositional environment of fenestral bindstone (MF2b)

This facies forms when bindstone facies is alternately exposed to subaerial and subaqueous conditions. Fenestral fabric develops in the intertidal or supratidal zone when fluids retreat or escape from the sediments leaving void space referred to as “fenestral pore” or “birds’ eyes” (Shinn, 1968; Fisher, 1964).

In this study, the depositional environment of this facies is interpreted as intertidal, and it develop along side the bindstone facies. However, the former (MF2a) is located slightly shallower than the latter (MF2b). Bioclastic components and fragments in this facies (MF2b) indicate intertidal rather than supratidal. By contrast, in supratidal settings bioclastic grains are normally lacking or almost absent. The intercalation of fenestral bindstone and bindstone facies probably indicates a small-scale fluctuation of sea-level within the peritidal domain. Filamentous matter observed in this facies is interpreted as algal in origin.

5.1.1.6 Depositional environment of algal-foram wackestone (MF3a)

Depositional environment of this facies is shallow subtidal zone with restricted to semi-restricted water circulation. This interpretation is supported by the occurrence of moderate fossil diversity with miliolids and other smaller foraminifers, dasycladacean algae and ostracods. This fossil association indicates restricted shallow subtidal environment. It can be correlated with characteristics of semi-restricted lagoon environment interpreted for the Kimmeridgian of the central Swiss Jura studied by Colombié and Strasser (2005). The existence of drusy calcite cement with crystal size increasing toward the center of void space indicates influence of near-surface meteoric water or burial environments (Flügel, 2004). Large peloid

content with poorly sorted, sub-angular to sub-rounded indicates shape reworking of semi-lithified or non-lithified sediments.

**5.1.1.7 Depositional environment of intraformational
conglomerate/ breccia (MF10b)**

This type is interpreted as intraformational tidal-channel conglomerate/breccia. This facies relates to upper intertidal to supratidal environment (Wright and Azerédo, 2006). The absence of fossils in matrix indicates supratidal environment. Lithoclasts were eroded from underlying strata of this carbonate platform as indicated by fossils in lithoclasts. Circumgranular cracks and vianlets indicate occasional subaerial exposure of this deposit (Flügel, 2004). This deposit can be correlated to intraformational conglomerate/breccias (Fischer, 1964). Characteristics of this facies can be compared with intraclastic argillaceous micrite of peritidal facies of the Dachstein-type carbonate in Hungary (Hass, 2004). This has been interpreted as tidal flat-tidal channel lag deposit formed during prolonged exposure of the platform. The existence of an overriding limestone conglomerate/breccia bed indicates continuous sea-level falls.

**5.1.1.8 Depositional environment of polymict channel
conglomerate (MF10c)**

This conglomerate is interpreted as a bimodal channel conglomerate. It relates to reworking of underlying strata and was deposited in channels (Shinn 1986). The conglomerate has larger clasts in comparison to the underlying unit (MF10b). This evidence indicates close proximity to source area revealing continuous sea-level falls in upper part of peritidal environment.

5.1.1.9 Depositional environment of solution-collapse breccia

(MF10d)

This collapse breccia indicates local paleokarst. This facies shows non-continuous deposition of paleokarstic features (Choquette and James, 1988). Irregular surface development of host rocks with fissures and fills indicates erosion of the carbonate platform. This erosional process occurred during subaerial exposure of the platform during periods of sea-level lowstand. This resulted in development of karstification features including caves. Sediments were derived from underlying beds and filled in these fissures. Clasts containing chert, crinoid and bivalve fragments accumulated in groundmass. Weak compaction of poorly sorted clasts and high angularity indicate in-situ accumulation. Additionally, other evidence of subaerial exposure is the existence of paleocaliche. Circumgranular cracking around nodular fabrics indicate desiccation due to subaerial exposure. Normally, the matrix of this facies is unfossiliferous. However, crinoid fragments and micritised fusulinids are present as individual grains. They must be derived by either erosion of underlying beds or transported in by storm events. With cave collapse, large debris clasts accumulated on the cave floor, derived from the cave roof or wall. The facies characteristics can be compared with Fammenian karst breccia of Middle to Upper Paleozoic carbonates of the Bolsoi Karatau Mountains, Russia (Zempolich et al., 2002). The relationship of this collapse breccia with overlying encrinite bed shows some characteristic similarities to paleokarst in Mississippian limestone, New Mexico (Meyers, 1988).

5.1.2 Subtidal domain

The subtidal domain is located deeper than the shallow subtidal zone of the

peritidal domain. It includes a deeper subtidal lagoon zone and an internal bioclastic shoal zone. In this study, subtidal lagoon zone contains algal-foram packstone facies (MF3b), bioclastic peloidal facies (MF4a; b), alatoconchid facies (MF5a1; a2; a3; b1), fusulinid facies (MF6a; b), coral facies (MF8a; b), crinoidal facies (MF9) and mass-flow breccia facies (MF10a). Internal shoal comprise of coated bioclastic grainstone facies (MF7) and fusulinid grainstone facies (MF6c). Depositional environment and microfacies interpretation of the subtidal domain is discussed below.

5.1.2.1 Depositional environment of algal-foram packstone (MF3b)

This facies was deposited in a subtidal environment around or below fair-weather wave base (FWWB). Geopetal structure with good preservation of grains indicates in-situ accumulation. This facies can be compared with sheltered lagoon environment described by Colombié and Strasser (2005). Microstylolites and packed fabric indicate post-burial pressure dissolution and physical compaction. Squeezing relicts of insoluble material indicate diagenetic alteration as well. This implies that the original texture is probably had more sparsely distributed grains. However, it is possible to determine bioclastic packstone origin by the occurrence of abundant coarse bioclastic grains. It should be mentioned that in the original texture of this facies coarse bioclastic grains occupied more than 50% of the sediment before diagenetic compaction.

5.1.2.2 Depositional environment of bioclastic-peloidal wackestone/ packstone (MF4a; b)

The origin of peloids is probably related to disintegration of algae and/or micritization of skeletal grains. Irregularity in shape and poorly to moderate sorting of peloids support this interpretation. The occurrence of algal fragments and

erosional relicts of algal thallus are also the evidence for this interpretation of the origin of peloids. Micrite or carbonate mud probably has a common algal origin associated for the peloids. It involves algal activity, disintegration and micritization. This facies is interpreted as subtidal deposit and can be correlated with subtidal peloidal facies recognized in Devonian carbonate sequence in south China (Chen et al., 2001).

Minor shell debris content indicates transportation of this component from relatively higher energy shallower water setting to lower energy quieter environments. Some fusulinid tests were transported from other depositional environments as indicated by erosion and micritization of tests. However, crushed fusuline tests are related to post-burial compaction effects during the lithification process (Meyers, 1980).

5.1.2.3 Depositional environment of thin-shell alatoconchid

rudstone (MF5a1)

This facies is interpreted as storm deposit or tempestite. It contains derived thin-shell fragments of allochthonous or even parautochthonous materials and forms thin-shell coquinites. These thin shell fragments were derived from immature alatoconchids (juvenile). This alatoconchid bed can be compared with crudely graded bioclasts from calcareous tempestites in Upper Muschelkalk limestones (Aigner, 1982a). This style of deposit can accumulate under various high energy conditions including intertidal and subtidal environments. Large shells can be moved from lower shoreface settings and are deposited higher up on beach or tidal flat settings by storms (Kreisa, 1981). However, in this study, tempestite (MF5a1) is interpreted as an intertidal deposit based mainly on microfacies of matrix. In addition, thin to medium

bedded tidal flat mudstone (MF1a) which occurs between two tempestite beds, indicates intertidal environment. This special association of facies reveals the environment of these tempestites as well. Diagenetic compaction overprints the original texture of the rock but it can still be observed and estimate.

5.1.2.4 Depositional environment of thick-shell alatoconchid

rudstone (MF5a2)

Based mainly on rock texture and grain components, this facies is inferred to be a storm deposit or tempestite. Allochemical components were transported under high energy conditions and deposited when the energy decreased. Depositional environment is located between fair-weather wave base (FWWB) and normal storm base (NSB). Large alatoconchid shell indicates proximal tempestites which closed to the alatoconchid living site or parautochthonous deposit. It can be compared to proximal shell beds of calcareous tempestites (Aigner, 1982a; Seilacher and Aigner, 1991). Infiltration fabric formed during the waning phase when debris and fragments dropped into larger individual shells (Kreisa and Bambach, 1982). Black skeletal debris and filaments are algal derived, as shown by relicts of algal structure in these materials. These materials are the organic source of the black bituminous color of the rock. Moreover black carbonized or bituminous wood fragments are interpreted as storm derived terrigenous materials. Fossil wood fragments can be observed in other facies as well including mudstone, wackestone and bindstone facies. This evidence suggests that this carbonate platform was located close to land. Microfabric of matrix can be correlated with that of rudist breccias described from Cretaceous carbonate platforms and ramps (Cestari and Satorio, 1995)

5.1.2.5 Depositional environment of thick-shell alatoconchid

floatstone (MF5a3)

Alatoconchid shell concentrations with various directions of shell orientation indicate reworking and transportation. However, the original habitat must have been relatively close to the depositional site as indicated by the mixed accumulation of articulated valves with comparable numbers of single valves and broken shells. This accumulation is interpreted as a parautochthonous proximal tempestite deposit. The shell beds exhibit undulatory scoured bases and immediately overlie fusulinid beds. Undulatory scoured-base indicates storm erosion prior to large shell deposition under storm peak condition (Aigner, 1982a). This facies differs from alatoconchid rudstone (MF5a2) in having lighter color and lesser compaction of alatoconchids than the latter. Note that this floatstone was rapidly deposited during single high energy event or storm. This interpretation is supported by variation of shell condition and orientation without condensed concentration. Large bivalve shells behaved as clasts and were reworked by high energy. This situation can be compared with chert nodules in tempestite chert breccias described from the Middle Mississippian limestone, Illinois basin (Carozzi and Gerber, 1978). Good preservation of undulating scour base along with fusuline imbrication indicates non-disturbance from subsequent later high energy events. These characteristics can be further compared with immediate burial (type A) of storm-generated coquinas (Jeffery and Aigner, 1982). The underlying fusuline bed performed as preexisting bed or substrate. Depositional environment of this fusulinid facies is interpreted as open lagoon and/or locally, subtidal lagoon with semi-restricted or open water circulation located around or below fair-weather wave base. From this relationship, it can be inferred that

alatoconchid floatstone facies was deposited near to or even within the same environment as the fusulinid facies. This result reveals spatial facies variations within the carbonate environment. Microfacies characteristics of these samples indicates storm deposit (Bakush and Carozzi, 1986).

**5.1.2.6 Depositional environment of alatoconchid biostrome
with peloidal wackestone matrix (MF5b1)**

Depositional environment of this limestone facies is within a subtidal lagoon setting or below fair-weather wave base. Water energy in this environment is relatively quiet. This interpretation is supported by the occurrence of micrite and characteristics of peloids. The existence of drusy calcite and microsparite cements indicates aggrading neomorphism which is compatible with the existence of micritic patches. Original interstitial space was occluded mainly by micrite matrix over sparry calcite cement. This environment was favored by alatoconchids. Evidence includes common observation of these fossil embedded in the rock in life-position or growth-position without significant evidence of erosion or reworking. Moreover, texture of the rock also supports less agitated condition as mentioned above. This facies can be correlated with alatoconchid bivalve biostromal facies described from the Permian Limestone of north Palawan Block, Philippines (Kiessling and Flügel, 2000). In addition, it can be compared with subfacies C of the megalodont limestone of the Lofer facies in Dachsteinkalk, Austria (Goldhammer et al., 1990).

Microfabric of samples no 721 and 722b is similar to that found in sample no. 705 but differs in having larger content of bioclastic grains. Depositional environment of this facies is interpreted as subtidal environment located at or below fair-weather wave base with relative quiet conditions. Large amounts of micrite and

peloids support the interpretation of a low energy environment. It should be noted that water depth below fair-weather wave base and in normal conditions, micritic mud is relatively unaffected by winnowing processes. However, small shell fragments can be transported from other areas by wind current and deposited in this environment when current energy drops.

5.1.2.7 Depositional environment of fusulinid wackestone

(MF6a)

Depositional environment of this microfacies is subtidal and below fair-weather wave base, located mainly in lagoon with normal marine circulation. This interpretation is supported by the occurrence of predominant micrite and peloid content indicative of quiet conditions (Flügel, 2004). Micritised and encrusted grains indicate microbial activities in this environment. Well-preserved micritised and coated grains with lobate outline also support in-situ deposition. However, some fusulinids with worn or abraded tests, and fusulinid fragments, indicate transportation or reworking before final deposition. On the other hand, some well preserved fusulinids indicate in-situ deposition. This facies can be compared with fusulinid floatstone/wackestone/packstone facies described from Permian limestone, north Palawan, Philippines (Kießling and Flügel, 2000). Furthermore, it shares some similarities to fusulinid wackestone/packstone facies described from inner platform Murghabian limestone, central Thailand (Dawson and Racey, 1993). It can also be compared with matrix-supported fine calcirudite of unit KD3 of the Khoa Khad Formation, central Thailand (Thambunya, 2005).

Microbial organisms including algae and/or bacteria may be responsible for micritisation of carbonate grains. Relicts of micrite patches indicate

aggrading neomorphism which formed pseudosparite or microsparry cement. The original intergranular material was probably occluded mainly by micrite.

5.1.2.8 Depositional environment of fusulinid packstone/ grainstone (MF6b; c)

Depositional environment of this microfacies is interpreted as near shore with moderately agitated water located between inner shoals within an open lagoon or semi-restricted lagoon. Evidence of worn and broken tests of fusulinids with other skeletal fragments reveals reworking and transportation. High diversity of bioclastic skeletal material indicates high variety of source components. Small fragmental bituminous or carbonized matter is probably derived from algal disintegration. These bioclastic fragments and shell debris were transported into this environment by wave or current and accumulated on a relatively low relief sea bottom. Abraded and micritic fusulinids indicate transportation. Additionally, high concentration of fusulinids in fusulinid packstone indicates occasional storm events. Scour-and-fill structures observed in the field support this interpretation (Aigner, 1982b). This microfacies can be correlated with inner platform, back reef of the Permian fusuline-algal biofacies in central Thailand (Dawson and Racey, 1993). It shares some similarities to packed biomicrite of the Nam Maholan Formation (Assavapatchara, 1998). Moreover, it can be correlated with grain-supported fine calcirudite of unit KD3 of the Khoa Khad Formation (Thambunya, 2005).

5.1.2.9 Depositional environment of coated bioclastic grainstone (MF7)

This microfacies displays characteristics of bioclastic inner shoal deposits. This shoal is located between semi-restricted lagoon and open lagoon above

fair-weather wave base (internal shoal). Rounded and micritised grains indicate reworking and transportation. Good washing and well sorting of allochems support constant agitated water of high energy area. This facies can be compared with skeletal grainstones of platform margin sand shoal of the Pha Nok Khoa platform (El Tabakh and Utha-Aroon, 1998). It can be further correlated with bio-grainstone with micritised bioclasts (MF12) described from an Upper Triassic intra-platform carbonate basin in Slovakia (Tomašových, 2004). In comparison with fusulinid facies (MF6), this facies is related to a depositional environment with more agitated and more constant water energy. The former (MF6) was located in relatively less agitation area water environment.

5.1.2.10 Depositional environment of coral biostrome (MF8a)

This biostrome is located below fair weather wave base with normal marine circulation. This microfacies (including sample no. 928, 802, 923) represents the core facies of biostrome. Biostromes produced by massive coral are classified as framestone and is characterized by a rigid three dimensional framework. In contrast, tabulate corals produce bafflestone. These buildups form during sea-level high stands. They can be correlated with mini-mounds described by Flügel and Krainer (1992).

Evidence that is indicative in-situ deposition of biostrome includes growth-position of reef-building organisms and well preserved geopetal structure. Note that well sorted peloids in sample no. 923 are interpreted as fecal pellets. In-situ accumulation is also supported by microborings.

Sample no. 801 contains an alatoconchid in life position. The rock texture is bioclastic packstone (Dunham, 1962). Allochemical constituents dominate more than 50% in this texture. It is poorly sorted with angular to rounded bioclasts,

peloids, fragments and debris. Microstylolites were also observed in this facies. The common intercalation of alatoconchid bed and coral bed indicate some relationship of these organisms in this environment.

5.1.2.11 Depositional environment of coral floatstone (MF8b)

In some cases as mentioned earlier, coral heads are found in reworked position. Storm energy is interpreted as a major factor influencing this deposit. Under high-energy conditions of a storm event, coral heads were relocated from their living site and transported down slope and deposited under quieter conditions. This case is interpreted as a parautochthonous deposit located closed to source area below fair-weather wave base. Reworked coral heads indicative of storm deposit also occur in the same interval of the Khao Tham Yai area further north of this study area (Fontaine et al., 2002). It can be compared with late Middle Ordovician prasopora-bearing event beds described from central Pennsylvania (Cuffey, 1997).

When sea-level dropped a relative shallower and more restricted environment established in this area. Bioclastic peloidal wackestone with restricted fossils and authigenic quartz support this interpretation. Note that coral heads formed as lag deposits during this time. Abundant occurrence of nodular and lenticular cherts in this interval reveals a near coast environment. Subaerial exposure with collapse breccia indicates successive sea-level change during this time.

5.1.2.12 Depositional environment of crinoidal packstone

(encrinites) (MF9)

Moderately sorted crinoidal packstone is interpreted as flank facies of mound, whilst poorly sorted crinoidal packstone is inferred to relate to the upper core facies of the mound. The characteristics of these crinoidal packstones can be

compared with Early Carboniferous mud mound deposits in Sacramento Mountain, New Mexico (Ahr, 1989). It can be further correlated with crinoidal biosparrite of unit KC2 of the Khao Khad Formation, central Thailand (Thambunya, 2005). These crinoidal packstones were deposited in relatively deeper parts of this environment in comparison to other facies types. Characteristics of this facies type indicate parautochthonous deposits that accumulated under a slope of low topographic relief below normal storm wave base.

5.1.2.13 Depositional environment of mass-flow breccia

(MF10a)

This breccia is interpreted as a local mass-flow deposit. It was deposited below fair-weather wave base under and probably gravity triggered by a high energy event. Evidence of a high energy event indicates an immediately underlying alatoconchid floatstone bed (sample no. A63). This alatoconchid bed shows characteristics of reworking and transportation. High facies variation of clasts of this breccia indicates erosion and transportation of material from different parts of this carbonate platform. Subsequent compaction and pressure solution enhance fitness of clasts. This mass flow breccia can be compared with Early Permian polymict depositional carbonate breccias described from the Southern Alps (Flügel and Flügel-Kahler, 1980).

5.2 Age constraints

In terms of geochronological constraint, fusuline biostratigraphy (and hence taxonomy) is used as the principal method for establishing age. However, description of fusuline taxonomy is beyond the scope of this study. Consequently, most of the

fusulines mentioned in this study have been determined only to generic level without providing description (see more information in section 4.3). The aim of fusulinid study in this thesis is to provide essential biostratigraphic age information for the studied sections. As a result, the *Lepidolina-Yabeina* zone has been determined. This fusulinid zone indicates a Midian age (Middle Permian) on the basis of well-established fusuline biostratigraphy documented from the Permian system in Transcaucasia (Jin et al., 1997). This age is correlated with the Capitanian stage of the approved Permian chronostratigraphic subdivisions of the Permian Subcommittee, ICS (Tab. 5.2). Moreover, the occurrence of other fusulinids including *Conodofusiella* sp. and *Dunbarula* sp. strengthens the age evaluation of the Khao Somphot sequence studied herein.

5.3 Paleoenvironment of alatoconchids

In order to evaluate the nature of alatoconchid environment, field data, microfaeces and paleontology are integrated, interpreted and discussed. In the first step, it is important to differentiate between autochthonous and allochthonous beds. Autochthonous beds represent the original habitat of these organisms. As mentioned in section 3.2.5 and section 5.1, alatoconchid beds can be categorized into two major lithofacies types; alatoconchid floatstone/rudstone facies (MF5a) and alatoconchid biostromal facies (MF5b). The former represents an allochthonous deposit while the latter indicates an autochthonous deposit. Microfacies analysis of limestones and paleontology of both alatoconchids and associated fossils are essential for deducing the paleoenvironment of these bivalves.

Table 5.2 Chronostratigraphic subdivision scheme for the Permian system.

(modified after Jin et al., 1997).

SERIES	STAGES	SELECTED FOSSIL ZONES			Polarity	Ma
		Ammonoids	Conodonts	Fusulinids		
Triassic	Griesbachian	<i>Ophiceras</i> <i>Otoceras</i>	<i>Hindeodus parvus</i>			251.0 ±3.6
Permian	Lopingian	Changhsingian	<i>Pseudotirotilites</i> <i>Paratirotilites</i> - <i>Shevyrevites</i> <i>Iranites</i> - <i>Phisonites</i>	<i>Clarkina changxingensis</i> <i>C. subcarinata</i>	<i>Palaeofusulina sinensis</i>	
		Wuchiaopingian	<i>Araxoceras</i> - <i>Konglingites</i> <i>Anderssonoceras</i> <i>Roadoceras</i> <i>Doulingoceras</i>	<i>C. orientalis</i> <i>C. leveni</i> <i>C. dukouensis</i> <i>C. postbitteri</i>	<i>Nanlingella simplex</i> - <i>Conodofusiella kwangiana</i>	253.0 ±0.3
	Guadalupian	Capitanian	<i>Timorites</i>	<i>Jinogondolella altudaensis</i> <i>J. postserrata</i>	<i>Lepidolina</i> <i>Yabeina</i> <i>Polydiexodina shumardi</i>	
		Wordian	<i>Waagenoceras</i>	<i>J. asserata</i>	<i>Neoschwagerina craticulifera</i>	264.1 ±2.2
		Roadian	<i>Demorezites</i> <i>Stacheoceras discoidale</i>	<i>J. nankingensis</i>	<i>Praesumatrina neoschwagerinoides</i> <i>Cancellina cutalensis</i> <i>Armanina</i>	Hilawarra Reversal
	Cisuralian	Kungurian	<i>Pseudovidrioceras dunbari</i> <i>Propinacoceras busterense</i>	<i>Mesogondolella idahoensis</i> <i>Neostreptognathodus pnevi</i> - <i>N. exculptus</i>	<i>Misselina claudiae</i> <i>Brevaxina dyhrenfurthi</i>	
		Artinskian	<i>Uraloceras fedorowi</i> <i>Aktubinskia notabilis</i> - <i>Artinkia artiensis</i>	<i>N. pequopensis</i> <i>Sweetognathus whiteri</i>	<i>Pamina</i> <i>Charalowschwagerina vulgaris</i>	272.2 ±3.2
		Sakmarian	<i>Sakmarites inflatus</i> <i>Svetlanoceras strigosum</i>	<i>M. bisselli</i> <i>S. primus</i> <i>Streptognathodus postfusus</i>	<i>Robustoschwagerina schellwieni</i> <i>Sphaeraschwagerina sphaerica</i>	280.3 ±2.6
		Asselian	<i>S. serpentinum</i> <i>S. primore</i>	<i>S. constrictus</i> <i>S. Isolatus</i>	<i>S. moelleri</i> - <i>P. fecunda</i> <i>S. vulgaris</i>	290.6 ±3.0
	Carboniferous	Gzhelian	<i>Shumardites confessus</i> - <i>Enulites plummeri</i>	<i>S. wabaunsensis</i> <i>S. elongatus</i>	<i>Daixina robusta</i> - <i>D. bosbytauensis</i> <i>T. struckenbergi</i>	300.3 ±3.2

From this study, it is clearly evident that alatoconchids exist within the context of a shallow marine carbonate environment. They were lagoonal organisms and their habitat was within the subtidal lagoon mainly, but also in semi-restricted lagoon settings along the leeward-side of internal shoals. The unusual bivalve morphology with large, thick shells and expansive wing-like flange features typical of alatoconchids, is compatible with an epifaunal habit rather than infaunal. According to uniformitarian approach, the morphological characters of the alatoconchids can be compared with those of modern bivalve families such as the Ostreidae, Tridacnidae and Isognomonidae. On this basis, these bivalves are interpreted to be epifaunal suspension-feeders. The flat ventral shell surface served functionally for supporting, resting or reclining, on soft muddy substrates (Yancey and Boyd, 1983). This interpretation is consistent with the bioclastic peloidal wackestone matrix of the alatoconchid biostrome facies describing herein. The limestone texture indicates relative deep lagoonal waters, relatively quiet conditions, and a soft muddy lagoonal floor substrate.

The paleoenvironmental setting of Permian alatoconchid bivalves has been variously interpreted by previous workers. They were originally considered to be reef organisms. They are interpreted herein as bank-setting fauna based mainly on their morphology and the sedimentology of their habitat substrate (Termier et al., 1973). These large “winged” bivalves seem to have preferred a relatively loose/soft sediment surface rather than a reef-top environment (Yancey and Boyd, 1983). Most of the observed alatoconchid localities documented from Malaysia, Japan, Afghanistan and Tunisia are hosted in fine-grained sedimentary rocks. In Malaysia and Tunisia, the

rocks are light colored, poorly sorted bioclastic packstone suggestive of moderate- to high- energy environment (Runnegar and Gobbett, 1975). By contrast, dark-gray lime mudstone/wackestone in Japan and Afghanistan indicates low-energy environment (Isozaki, 2006; Termier et al., 1973). In the Philippines, gregarious alatoconchid accumulation has been interpreted as a lateral-limited biostrome (Keissling and Flügel, 2000). Paleogeographically, the family Alatoconchidae appears to have been restricted mainly in the Paleotethyan realm between the Cimmerian and Cathaysian continents.

Lithofacies of alatoconchid-bearing limestones at Khao Somphot is closely similar to that found in Malaysia and the Philippines as mentioned above. In addition, the high organic content with bituminous color of the limestones is similar to that observed in the Japanese alatoconchid locality. In the Philippines, the alatoconchid-bearing strata are parts of the Minilog Formation in North Palawan. This formation is Wordian-Capitanian in age, based on the occurrence of fusulinids including neoschwagerinids and verbeekinids. Lithofacies of this formation can be compared to that of found in the Indochina Block (e.g., Wiedchosky and Young, 1985; Dawson and Racey, 1993; El Tabakh and Utha-aroon, 1998). However, the latter differs in having a broader microfacies spectrum. The Minilog Formation is speculated to have been part of the Indochina Block during the Carboniferous and Permian periods. It was separated during Middle Permian and collided with the South China during Late Cretaceous time. Associated fossils in the alatoconchid beds are phylloid algae and diverse mollusk fragments. The existence of alatoconchid shells in high concentration suggests gregarious life habit leading to production of lateral limited biostromal beds with associated baffling or trapping of sediments. In some cases, alatoconchid beds

overlie fusulinid beds and underlie dacycladacean beds. This associated vertical succession may indicate shallowing upward sequence. Alatoconchids are generally located in agitated environments as indicated by worn shells with imbrication structures. Generally, the fusulinid facies is located below fair-weather wave base and the dacycladacean facies is located in shallower settings, while the alatoconchid facies is between them (Kiessling and Flügel, 2000). This information and interpretation is consistent with some alatoconchid intervals observed in this study. In addition, observation herein show more than one lithofacies of alatoconchid-bearing beds (see previous section). Alatoconchid habitats were located in both subtidal semi-restricted lagoon, and open lagoon. In the open lagoon, they are associated with coral biostromal facies slightly above fair-weather wave base and with fusulinid facies below fair-weather wave base.

In West Malaysia, the alatoconchid locality is within the H.S. Lee Formation. The rock sequence in this formation can be correlated to the lower part of the Artinskian stage (early Leonardian). The age is indicated by the occurrence of the *Pseudofusulina ambigua* zone. Paleomagnetic evidence indicates relatively low paleolatitude for the Malay Peninsular during that time (Haile and McElhinny, 1972). Alatoconchids are associated with Tethyan fauna including fusulinids and gastropods (Runnegar and Gobbett, 1975). In this respect, the Malaysian fauna can be compared with the alatoconchid fauna in the Khao Somphot area. However, the interpretation of a high-energy habitat for alatoconchids by Runnegar and Gobbett (1975) for the Malaysian occurrence is inconsistent with the nature of the matrix which consists of fine sediment. All observations from Khao Somphot indicate a low-energy habitat.

In Japan, two localities have been documented from Akasaka and Kamura. The sequence at Akasaka is within the *Parafusulina* zone while the latter was found in the *Neoschwagerina-Lepidolina* zone. These zones indicate Kubergandian (Roadian) and Murghabian-Midian (Wordian-Capitanian) ages respectively. Alatoconchid-bearing limestone sequences in both localities share the same tectono-sedimentary origin and history but they accumulated on different seamounts within the mid-Panthalassa Ocean. Lithofacies from these two outcrops are similar with black to dark gray massive limestone, lime mudstone and wackestone with relatively high carbon content (bituminous facies). The bivalve habitat is interpreted as shallow lagoon with quiet conditions (Isozaki, 2006). At Khao Somphot, the carbonate sequence accumulated on a continental platform. This is very different in tectonic setting from that interpreted for the Japanese localities. However, they nevertheless show some similarities in lithofacies and indicate relatively quiet subtidal lagoon conditions.

The triple association of the Alatoconchidae, Waagenophyllidae and Verbeekinidae was noted by Isozaki (2006). He also noted the simultaneous abrupt extinction or diversity decline of these three groups at the end of late Middle Permian. This event is correlated with global cooling (onset of ice house condition). He suggested a symbiotic relationship of these three groups of organisms with algal symbionts, restricted to warm tropical environments and low latitudes. In Indochina Block of Thailand, there is no record of shallow marine carbonate strata at the end of Permian time. However, terrigenous strata with fossil wood (e.g., *Gigantopteris* sp. and *Glossopteris* sp.) ranging in age from Dzhulfian to Dorashamian (Upper Permian) have been recorded from the Phetchabun area, central Thailand (Chonglakmani and

Fontaine, 1990; Rigby, 1998). This evidence coincides with a global sea-level fall as recorded in the global sea-level curve (e.g., Vail et al., 1977; Hallam, 1984). The triple relationship observed in Japan is also observed at Khao Somphot. The decline of alatoconchids is observed within the *Lepidolina*-*Yabeina* Zone and also be related to abnormal growth of *Lepidolina* sp. (lower part of Unit F). This abnormal growth is related to environmental stress during that time. This peculiar characteristic of *Lepidolina* can be found in Khao Tam Yai area located further north of the Khao Somphot (Fontaine, 2002). It can be inferred that the end of late Middle Permian was a time of relatively high physical environmental changed that affected the living condition of alatoconchids and other organisms. This phenomenon may have caused the extinction of alatoconchids during that time, together with other organisms. This phenomenon can be compared with the beginning of the end-Permian global mass extinction (e.g. Isozaki, 2006).

Numerous associated organisms occur within the study area such as bellerophon mollusks, foraminifers, corals, ostracods, calcareous algae and echinoderms, all indicative of warm shallow marine environment. This interpretation can be correlated with the study of Yancey and Boyd (1983). The occurrence of calcareous green algae (dasycladaceans) suggests photic zone depositional environment. Some coralline red algae (e.g. *Tubiphytes* sp.) are characterized as encrusting organisms. These organisms are responsible for small biostrome construction in the thesis area. They can be framebuilders, binders and cementing agents together with corals, alatoconchids and other reef-builders. The co-occurrence of these organisms in the same intervals reveals some biological interaction within the biostromal community. The alatoconchid shell structure consists of an inner granular

calcite layer and outer prismatic calcite crystal layers (see section 3.2.5). The prismatic layer may be an adaptation for photosynthesizing symbionts such as zooxanthellae. This translucent crystal can focus and enhance light intensity and be exploited by symbionts scattered within the mantle of the alatoconchid animal. This symbiotic strategy is significant for a number of modern bivalves (such as Tridacnidae) and may be the cause of extinction of some large bivalves such as rudists and megalodontids (Vogel, 1975). The findings of this study are not incompatible with these ideas. The disappearance of Alatoconchidae, Waagenophyllidae and Verbeekinidae in the Khao Somphot locality is observed in Unit F. This unit can be correlated to upper part of the Midian stage. In addition, some organisms display prolific occurrence in this unit such as *Lepidolina*, *Yabeina*, *Nankinella*, *Dunbarula*, *Climacammina*, and *Mizzia*. However, it is beyond the scope of this thesis for further explore and determine of the cause of this phenomenon.

5.4 Sequence stratigraphy and relative sea-level fluctuation

The aim of this section is to provide some preliminary data related to sequence stratigraphy of the study sections, and offer some views on sea level change during that time.

Two major intervals of geological unconformity are recognized at Khao Somphot locality. They are related to subaerial exposure of the platform and include karstification and collapse breccia (Unit C) and intraformational breccia with channel conglomerate (Unit G) (Tab. 5.2). Collapse breccia is inferred to have developed during sea-level low stand during middle to late Midian time. The intraformational breccia with overlying channel conglomerate were initiated by successive sea-level

fall during late Midian time. These features can be correlated with 3rd order cycles. Their timing and duration are compatible with the global sea-level curve (Vail et al., 1977; Ross and Ross, 1987) (Fig. 5.2). During the Permian period, one of the significant successive sea level falls occurred during Kubergandian to Midian (Middle Permian) and terminated in Midian time. In addition, small-scale limestone sequences have been recognised in the stratigraphic record of the study sections. These sequences are inferred to be 5th order parasequence. They are represented by thickly bedded limestones and medium to thickly bedded dolomite or dolomitic limestone couplets, thickly bedded limestones and thinly to medium bedded argillaceous limestone or laminated limestone couplets. Microfacies study was used to confirm composition and texture of the rocks (section 3.2). Two main types of parasequence were differentiated including peritidal and subtidal parasequences. Both parasequences contain several parasequence types (Fig. 5.3). The observed peritidal parasequence types are characterised mainly by intertidal facies overlain by subtidal facies. These parasequences are most pronounced in Unit A. The intertidal facies include tidal flat mudstone, fenestral mudstone, laminated bindstone, fenestral bindstone and dolomitic limestone. This peritidal sequence can be compared to an ideal section of Lofer Cycles (Fig. 5.4) (Fisher, 1964). Subtidal parasequences comprise four main types of deeper subtidal facies which are directly overlain by shallower facies. They comprise alatoconchid biostrome overlain by grainstone, coral biostrome overlain by coated grainstone, fusulinid wackestone overlain by fusulinid grainstone, and crinoidal packstone overlain by fusulinid packstone. These parasequences are dominant in Unit B, Unit D, Unit E and Unit F. Among them Unit F exhibits the most excellent preservation of fusulinid wackestone overlain by fusulinid grainstone.

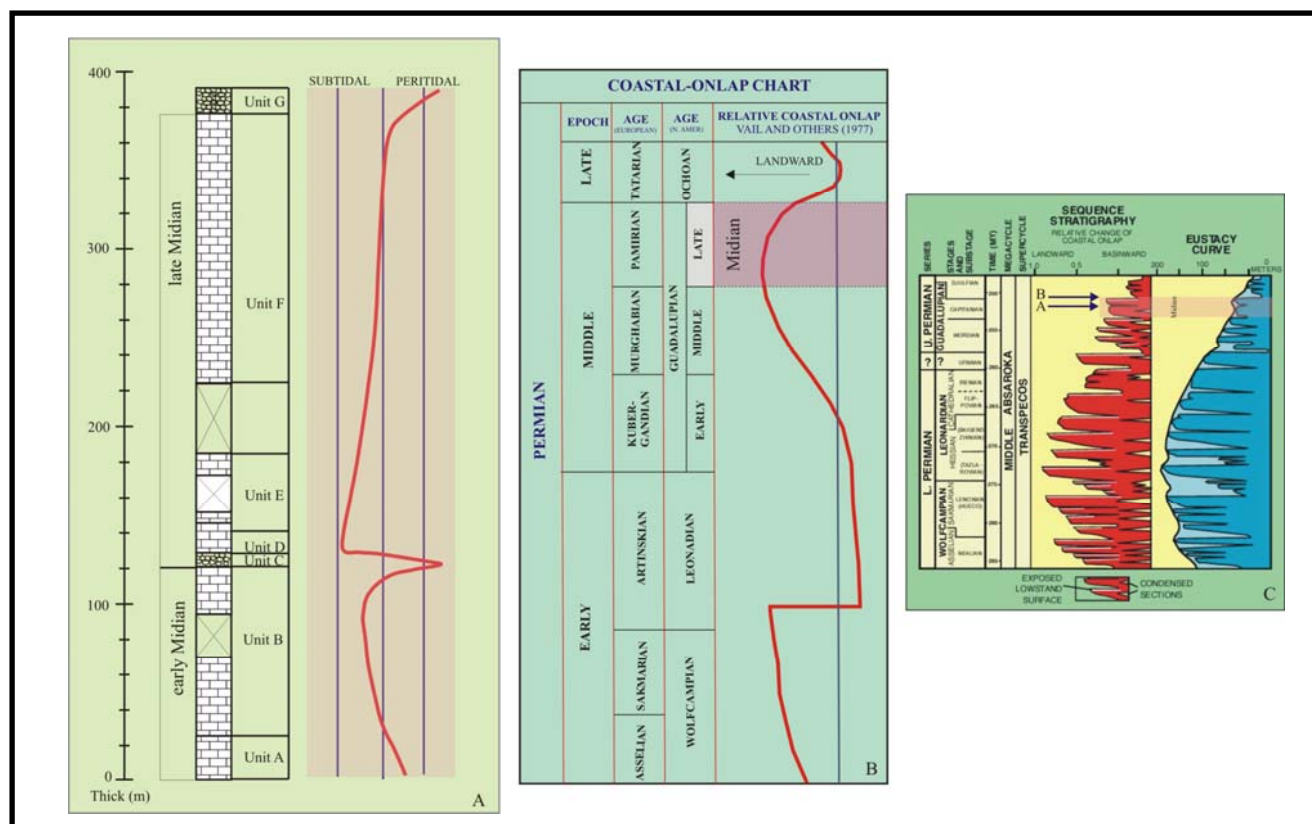


Figure 5.2 A: Relative sea-level curve with stratigraphic unit from this thesis study. B: Coastal-onlap chart of the Permian showing relative sea-level fall during late Middle Permian (modified after Welchowsky and Young, 1985). C: Coastal-onlap curve and eustasy curve of the Permian showing two events of relative sea-level fall (marked by arrows) during Capitanian (Midian) time (modified after Ross and Ross, 1985). Sea-level fall in A can be correlated with B and C.

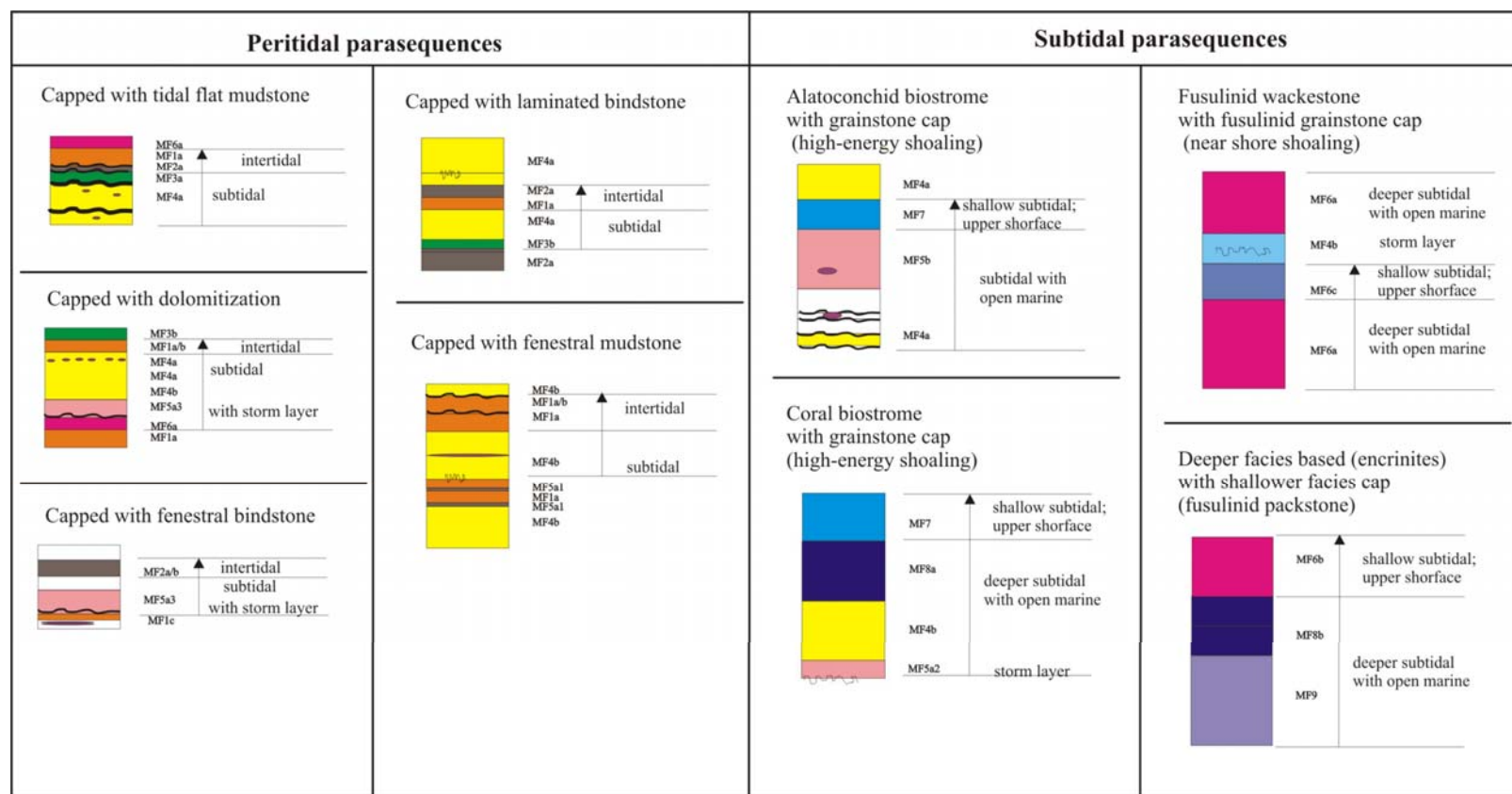


Figure 5.3 Parasequence types observed in the upper part of the Khao Somphot sections. Abbreviations and symbols as in Fig. 5.2 and Fig. 3.31.

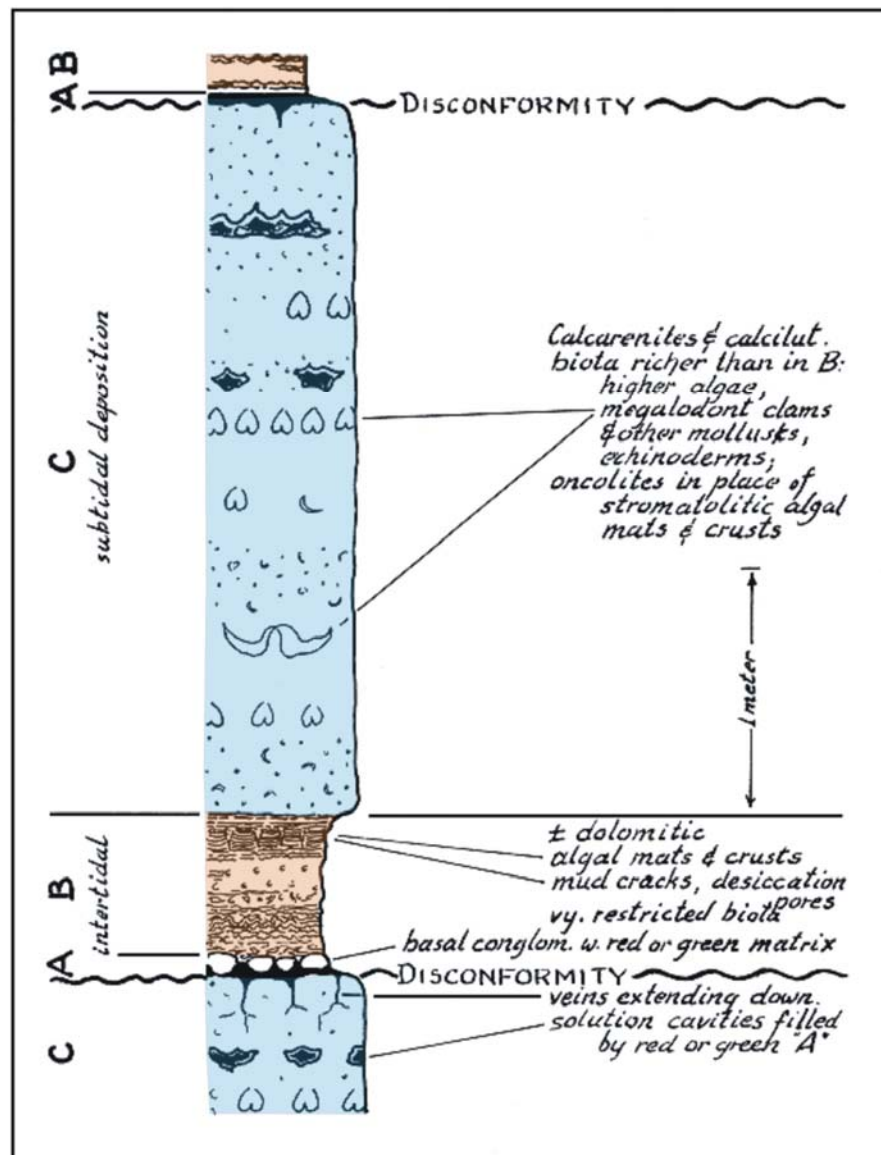


Figure 5.4 An ideal Lofer cycle showing subtidal deposit capped by intertidal deposit.

Disconformity is located on top of subtidal deposit with or without basal conglomerate. (after Fischer, 1964)

Crinoidal facies overlain by fusulinid facies was found between Unit D and E. The rest of these parasequence types are located mainly in Unit B and E. Sediments in peritidal and shallow lagoon environment normally display well stratified sequences in vertical succession. This evidence reflects small scale sea-level oscillations which are driven by the Milankovitch cycle (Fischer, 1986; 1991). The evidence of karstification with overprinting of some facies (e.g., fenestrae and dolomite) suggest allocyclic controlled sedimentary processes rather than autocyclic. However, autocyclic effects are believed to have some effect (Strasser, 1991).

5.5 Diagenesis

There are several diagenetic features observed both in outcrop and at microscopic scales. They include stylolites, crushed fusulinid tests, condensed fabrics, dolomite rhombs, nodular and lenticular cherts, authigenic quartz and shear fractures. These features are caused by several processes including mechanical compaction, pressure solution and stylolitization, dolomitization, silicification and micritization.

5.5.1 Mechanical compaction

Evidence of mechanical compaction in thin-section include observation of crushed fusulinid tests (e.g. sample no. 723, 746), and condensed fabric or diagenetic packstone (e.g. sample no. 726, 739, 743). Crushed fusulinid or miliolid tests to be broken and rearranged without significant transportation (Fig. 5.5). Condensed fabric is more pronounced in some samples of laminated bindstone. It is associated with large abundance of bioclastic grains with densely packed texture. Grain fracturing is common in these samples. Most of them are arranged parallel to bedding plane. Some grains are protruded normal to bedding plane. This feature is associated with

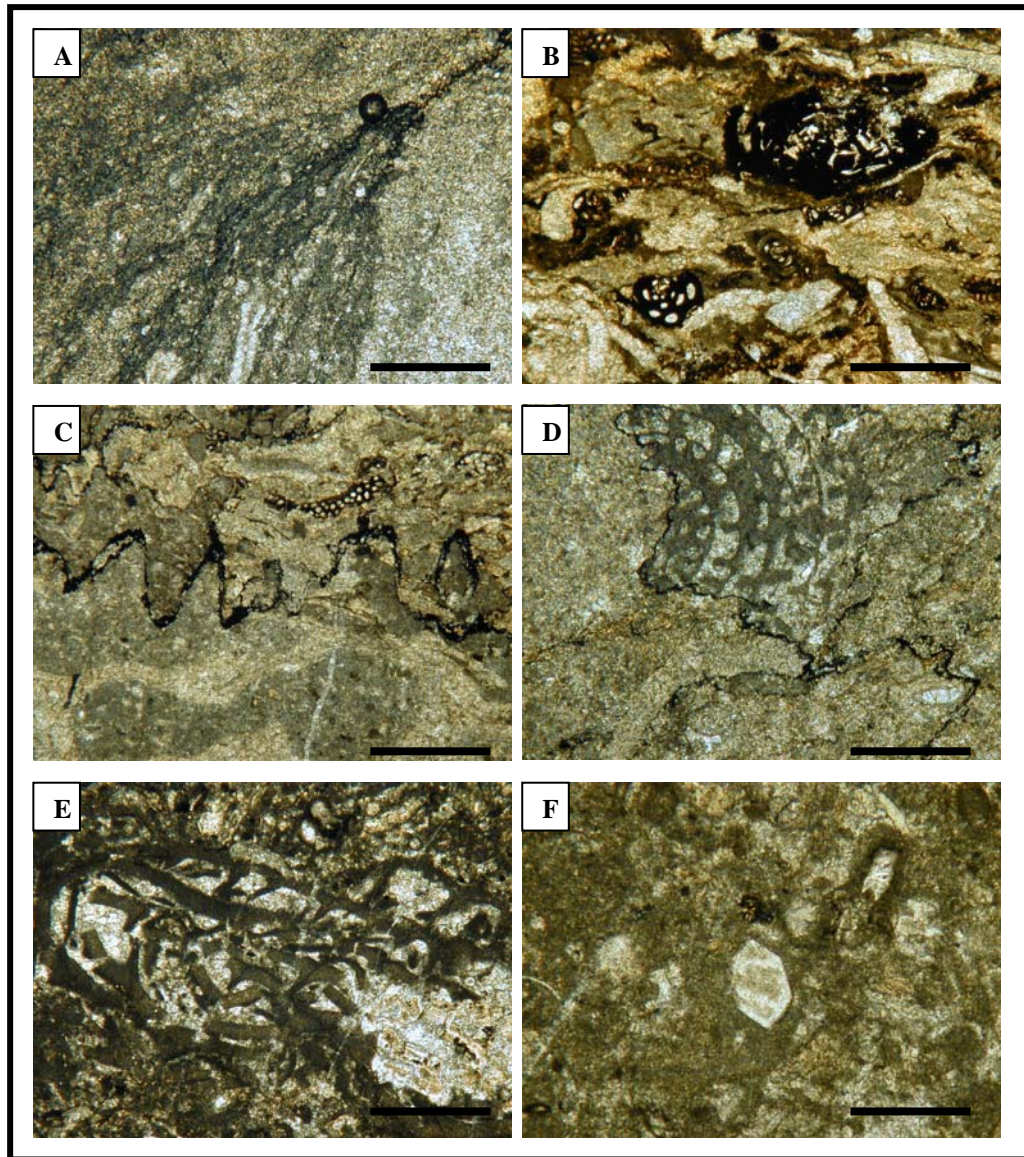


Figure 5.5 A: Photomicrograph of horse-tail spray of insoluble seams caused by compaction in mud-supported limestone texture. B: Photomicrograph showing crushed miliolid tests cause by strong compaction. C: Photomicrograph showing sutured stylolite. D: Photomicrograph showing stylobreccia. E: Photomicrograph of selective silicification in the internal chamber of fusulinid tests. F: Authigenic quartz crystal. (All=PPL). (All scale bar=500 µm)

multi-grain, non-parallel reticulate non-sutured seams. This feature causes by reduction of rock volume and porosity by overburden pressure. It indicates after burial diagenesis. This process is generally followed by chemical process of pressure solution and stylolization (Meyers, 1980; Logan 1984). Original matrix of the rock was soft indicated by some grains protruded normal to bedding plane.

5.5.2 Pressure solution and stylolitization

According to field observation, sutured stylolites are found common in this study area. They were observed most frequently in thickly to very thickly bedded limestones. This stylolite can be found throughout all studied sections and it is more profound in upper part of section two.

Based on field observation and microscope study, stylolite seams are common in both mud-supported and grain-supported texture (Fig. 5.5). In mud-supported texture, it is commonly developed non-sutured seams. Whilst in grain-supported texture limestones, it commonly exhibits sutured seams.

Non-sutured seams compose of irregular anastomosing set with hose-tail structure (e.g. sample no. 735). This seam developed in mudstone texture. Multi-grain, non-parallel reticulate non-sutured seams are found in diagenetic laminated bindstone.

Sutured seams consist of single small (e.g. sample no. 702b, 703c1, 738) or large amplitudes (e.g. sample no. 756a). In sample 702b, stylolite is form as singular set with arranged parallel to bedding plane. It separates underlying laminated bioclastic bindstone and overriding dolomitic limestone. In addition, it was found separate grains between two sides of seam in packstone texture (e.g. sample no. 703c1, 738). In some interval, strong stylolitization cause stylobreccia (sample no.

M11). In this sample, it shows densely packed bioclastic packstone fabric formed stylobreccia. This stylobreccia is characterized by non-parallel reticulate seams with multiple grain-contacts. In some case, it was determined as multi-grain, non-parallel reticulate sutured seam (sample no. 741).

These stylolite seams were produced following mechanical compaction process. Sutured seams are more common in coarse-grain limestones. Grain-rich carbonate can be stylolized under less than 30 meter depth (Railsback, 1993). Non-sutured seams or solution seams are common in fine-grain or mud-rich limestones including lime mudstone, wackstone, packstone and weakly cemented grainstone (Ricken, 1987). These solution seams develop in limestone which contain significant amount of insoluble residue (clay, organic matter). Solution seams can be either pre- or post-burial in their origin (Bose et al., 1996).

5.5.3 Dolomitization

In the field, some of dolomitized beds can be preliminarily observed as roughly elephant-skin rock surface. There are two main types of dolomites observed in this locality including millimicron-size inequigranular, non-rhombic hypidotopic dolomite and millimicron-size inequigranular rhombic poikilotopic dolomite (Fig. 5.6). In samples no. 817, it is characterized by inequigranular, non-rhombic crystal, tightly packed subhedral to anhedral, straight and lobate boundaries with some crystal face junctions, hypidotopic fabric. Grains range between 0.05 and 0.1 mm. This sample can be classified as millimicron-size inequigranular, non-rhombic hypidotopic dolomite (Friedman, 1965). Note that this sample was collected from bed in crinoids dominated interval.

For sample no. 701, it displays fine-grained dolomite crystals. It shows

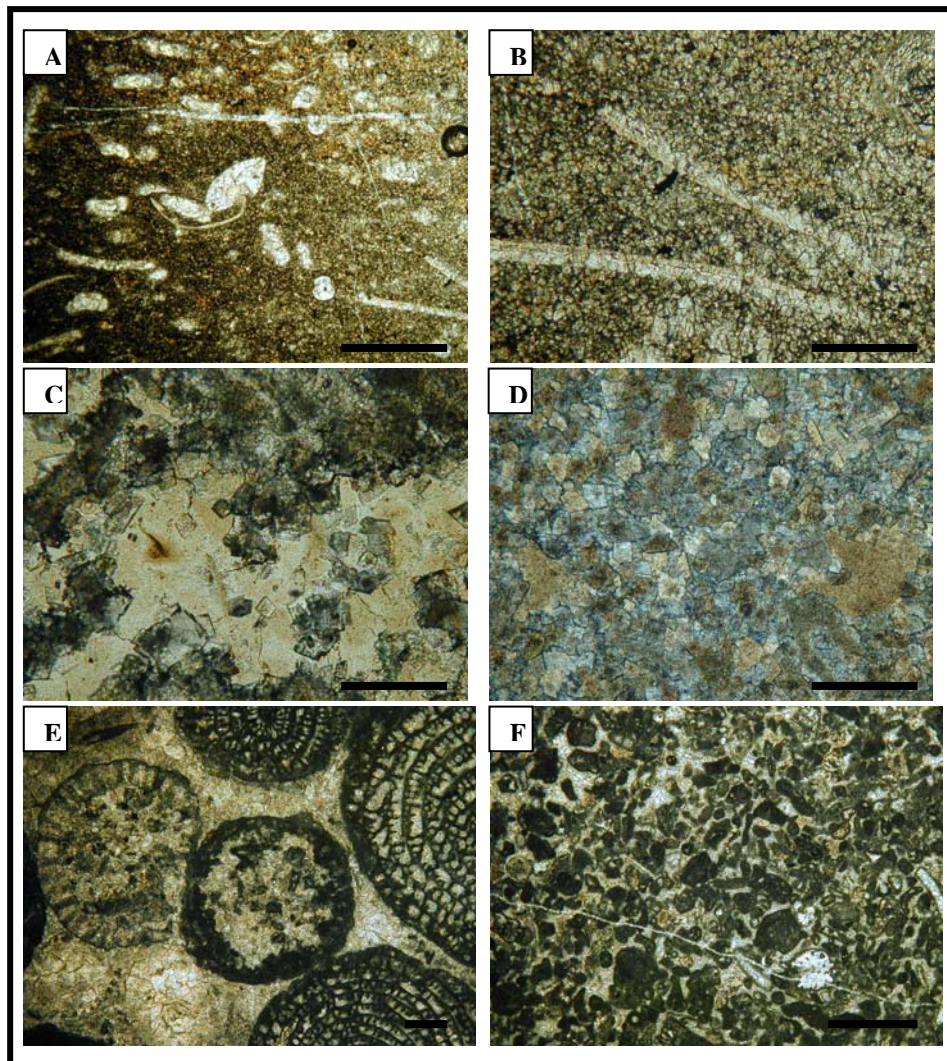


Figure 5.6 A-B: Photomicrograph of fine-grained inequigranular hypidiotopic dolomite (PPL). C: Photomicrograph of selective silicification and inequigranular rhombic poikilotopic dolomite. D: Photomicrograph of inequigranular rhombic poikilotopic dolomite. E: Photomicrograph of fusulinid grainstone facies showing micrite envelopes at grain margins of algae and fusulinids. F: Photomicrograph of coated grain facies showing cortoids and peloids. (All scale bar=500 μm ; under PPL for all except D, XPL)

inequigranular hypidiotopic, tightly pack, subhedral to anhedral, some crystal face preserved, intercrystalline boundaries lobate and straight. Crystal sizes are measured between 0.02 and 0.005 mm. Ghost structure is common in this sample. This sample can be classified as millimicron-size inequigranular, non-rhombic hypidotopic dolomite (Friedman, 1965).

According to sample no. 764, it exhibits inequigranular with poikilotopic fabric, euhedral rhombic crystals with straight compromise boundaries. Crystal grains were found between 0.05 and 0.1 mm. This sample can be classified as millimicron-size inequigranular rhombic poikilotopic dolomite. In this sample, dolomite rhombs are scattered in silicified patch while the surrounding area is non-silicified or dolomitized.

Sample no. 817 was collected from bed in crinoids dominated interval. This dolomite indicates recrystallization and related to post-burial diagenesis. Mg^{2+} -rich crinoid elements may influence dolomitization history of this sample.

For sample no. 701, in general, crystal fabric and texture of this sample is similar to sample no. 817. But it differs from the latter by having higher numbers of recrystallised restricted fossils with ghost structure. Additionally, this dolomite has finer crystal grains. This dolomite is gradually changed from underlying mudstone. This mudstone contains restricted faunas indicate restricted tidal flat of intertidal environment. Consequently, it can be interpreted that this dolomite formed near-surface relatively early and prior to complete lithification. Mosaic dolomite with very fine to fine crystalline can be developed under hypersaline condition by early dolomitization process (Amthor and Friedman, 1991).

In sample no. 764, it shows selective silicification with large dolomite rhombs. This dolomite fabric was formed under relatively shallow burial condition before complete lithification of carbonate (Jacka, 1974).

5.5.4 Silicification

The products of this process were observed in the field as nodular and lenticular cherts. Lenticular cherts are characterized by thin chert bed intercalated with limestone beds or aligned within any given bed. Nodular cherts can be found in any interval limestone beds. Some of them were observed with some fossils embedded inside their texture. These fossils include fusulinid tests, alatoconchids, corals and gastropods and others. All of them are shown as recrystallized fossils within that nodule. Nodular cherts are more common than lenticular cherts and can be observed throughout the studied sections. The latter was found prominent in the lower part of Unit A.

In thin-sections, silicification evidence can be found as partly silicified fusulinid tests in peloidal wackestone (e.g. sample no. 723). Fusulinids were found as crushed tests with silicified internal chambers. In this sample, authigenic euhedral quartz grains are common and are scattered in micrite matrix (Fig. 5.5). Fossils in this sample are rare.

As mentioned in chapter III, nodular chert is common in the field. This chert contains mainly of fibrous chalcedony caused by silicification process. Silicification is related to climatic condition during the Permian. During this time, weathering and erosion processes produced silica-enriched solution and precipitated around coastal area. Paleoclimatic factors including low Ph, high amount of CO₂ and change in salinity are preferable for silica precipitation (Laschet, 1984). Although, silica

replacement is probably controlled by organic matters but biogenic silica is not considered as a primary source of silica in this process (Altermann, 1989).

Authigenic quartz grains are common in restricted with hypersaline environments associated with micritic limestones (Flügel, 2004). This interpretation is comparable to this thesis data. In sample no. 723, it shows micritic texture with rare fossil and it is overlain by algal mat layers. This evidence can be correlated with the occurrence of authigenic quartzs in the Trypali carbonate unit of Greece (Upper Triassic) which studied by Pomoni-Papaioannou and Karakitsios (2002).

5.5.5 Micritization

Micritization is a process that related to replacement of grain peripheries or the whole grains by crypto- or microcrystalline carbonate crystals. Incomplete micritization produces micrite envelopes such as in cortoids. Complete micritization forms gradual or total alteration of grain such as in peloids (Flügel, 2004).

In thin section, coated grains facies is one of conspicuous evidence for incomplete micritization process. Most of grains are cortoids showing micrite envelopes around grains. In addition, selective micritization such as micritized fusulines and algae in fusulinid grainstone facies, bindstone facies and wackestone facies are introduced by this process. Peloids in peloidal bioclastic facies and other facies are the evidence of complete micritization (Fig. 5.6).

Coated grains indicate shallow marine, warm water environments (Flügel, 2004). Micrite envelopes are commonly related to light dependent boring organisms (Bathurst, 1966).

5.6 Benefit of this study and suggestion for the next research

1. This thesis is the first detailed study on alatoconchids and their environment in Thailand by means of microfacies and paleontology. Information on this topic can be used as guidance for the future work.

2. In Thailand, the occurrence alatoconchids at Khao Somphot locality is the finest known so far. The Khao Somphot could be used as the type section on alatoconchid study.

3. Information of sea-level fall during Median time from this study as indicated by collapse breccia and channel breccia/conglomerate would be more or less importance for possible interval of petroleum reservoir. However, some more research must be conducted before conclusive remark.

4. Black bituminous matrix of limestone especially in Unit A might be more or less significance for petroleum source rock. Carbon content analysis and other related field of studies must be proposed before final conclusion.

5. The study shows that some geological phenomenon occurred in late Midian. It might be correlated with global sea-level falls. Future works on geological and paleontological aspect within this interval from platform to basin in a given regional scale could lead to more clarified understanding on this phenomenon.

6. The fossils in this locality would be preserved, protected and promoted. The area is easy to access by road transportation and could be publicized as a geological park or museum.

CHAPTER VI

CONCLUSION

This thesis study is concerned mainly with the depositional environment of alatoconchid-bearing limestones which in turn reflects paleoenvironment of alatoconchid bivalves. The study sections are represent nearly 400 meters of sequence which is comprised of well bedded limestones located in the upper part of Khao Somphot strata. These sections comprise more than thirty observed alatoconchid beds in the lower through to middle part of the sequence. The results of this study include lithostratigraphic unit differentiation, microfacies and depositional environment of limestones, paleontology and paleoenvironment of alatoconchids, sequence stratification, and geochronological dating by fusulinids. The major conclusions are listed below,

1. Carbonate rocks in the study locality consists of ten major microfacies types and most of them contain subfacies including;

MF1. Lime Mudstone/ wackestone

MF1a. Lime mudstone

MF1b. Fenestral mudstone

MF1c. Bioclastic wackestone

MF2. Laminated bindstone

MF2a. Laminated bindstone

MF2b. Fenestral bindstone

- MF3. Algal-foram wackestone/ packstone
 - MF3a. Algal-foram wackestone
 - MF3b. Algal-foram packstone
- MF4. Bioclastic peloidal wackestone/ packstone
 - MF4a. Bioclastic peloidal wackestone
 - MF4b. Bioclastic peloidal packstone
- MF5. Alatoconchid wackestone/ packstone/ floatstone
 - MF5a1. Thin-shell alatoconchid rudstone
 - MF5a2. Thick-shell alatoconchid rudstone
 - MF5a3. Thick-shell alatoconchid floatstone
 - MF5b1. Alatoconchid biostrome
- MF6. Fusulinid wackestone/ packstone/ grainstone
 - MF6a. Fusulinid wackestone
 - MF6b. Fusulinid packstone
 - MF6c. Fusulinid grainstone
- MF7. Coated bioclastic grainstone
- MF8. Coral biostrome/floatstone
 - MF8a. Coral biostrome
 - MF8b. Coral floatstone
- MF9. Crinoidal packstone
- MF10. Carbonate breccias/ conglomerate
 - MF10a. Mass mass-flow breccia
 - MF10b. Intraformational conglomerate/ breccia

MF10c. Polymict channel conglomerate

MF10d. Solution-collapse breccias.

2. Lithostratigraphic unit of the study locality can be differentiated into seven main units. Lithology, microfacies and depositional environment of these units have been summarized below in ascending order.

Unit A is characterised by medium to thickly bedded limestones with thinly to medium bedded argillaceous and laminated limestone intercalations. It shows prolific occurrence of alatoconchid facies. This unit is located mainly in the peritidal domain with occasional storm influence. Microfacies recognized are: MF1a, b, c, MF2a, b, MF3a, b, MF4, MF5a1, a2, a3, b1, and MF6a.

Unit B comprises thickly bedded fusulinid-bearing limestones with alatoconchid facies and coral facies. It accumulated mainly in subtidal domain around and below fair-weather wave base. Storm layers with alatoconchids are most prolific. Microfacies recognized are: MF1c, MF2a, MF4, MF5a1, a2, a3, b1, MF6a, b, MF7, and MF8a.

Unit C exhibits mainly as fissure fill sediment based collapse breccia. It is designated as MF10d. This unit relates to subaerial exposure of the platform due to sea level fall.

Unit D contains crinoidal packstone mainly assigned as MF9. This unit was deposited below fair-weather wave base in relatively deep water subtidal settings.

Unit E is a thickly bedded limestone with fusulinid facies, alatoconchid facies and coral facies. Microfacies recognized are: MF4, MF5a1, a2, a3, b1, MF6a,

MF7, MF8a, b, and MF10a. This unit was deposited below and around fair-weather wave base in a subtidal lagoon setting with open marine circulation.

Unit F is characterised by thickly to very thickly bedded fusulinid facies with rare occurrence of alatoconchids restricted to the lower part. Microfacies recognized include: MF4, MF5a3, b1, MF6a, b, and MF7. This unit accumulated largely in subtidal near shore settings around and above fair-weather wave base.

Unit G is comprised of intraformational breccia (MF10b) with channel conglomerate (MF10c) overlying and indicates subaerial exposure of the platform.

3. Alatoconchid bivalves in the study area are represented by at least two genera and two species: *Shikamaia* cf. *perakensis* and *Saikraconcha* cf. *tunisiensis*. Their environment is located in subtidal lagoon and semi-restricted lagoon settings.

4. Small scale sea-level fluctuation during Midian time is the main influence controlling meter-scale repeated sedimentary cycles within the study sections. This effect is more prominent in peritidal units than subtidal units.

5. Age dating of the study sections is provided mainly by fusulinids and in particular the occurrence of the *Lepidolina*-*Yabeina* zone along with other key taxa such as *Colania*, *Sumatrina*, *Conodofusiella*, etc. These paleontological determinations indicate a Midian (Capitanian) or late Middle Permian age for the sequence exposed at Khao Somphot.

REFERENCES

REFERENCES

- Ahr, W. M. (1989). Sedimentary and tectonic controls on the development of an Early Mississippian carbonate ramp, Sacramento Mountains area, New Mexico. In P. D. Crevello, J.L. Wilson, J.F. Sarg and J. F. Read (eds.). **Controls on Carbonate Platform and Basin Development** (Spec. Publ. 44: 203-212). Society of Economic Paleontologists and Mineralogists.
- Aigner, T. (1982a). Calcareous tempestites; storm-dominated stratification in Upper Muschelkalk Limestones (Middle Triassic, SW-Germany). In G. Einsele, and A. Seilacher (eds.). **Cyclic and Event Stratification** (pp 180-198). Berlin-Heidelberg.
- Aigner, T. (1982b). Event-stratification in nummulite accumulations and in shell beds from the Eocene of Egypt. In G. Einsele, and A. Seilacher (eds.). **Cyclic and Event Stratification** (pp 248-262). Berlin-Heidelberg.
- Altermann, W. (1989). Facies Development in the Permian Petchabun Basin, Central Thailand. **Verlag Fur Wissenschaft und Bildung**. Berlin.
- Altermann, W.(1991). New Permo-Carboniferous geochemical data from central Thailand: implication for volcanic arc model. **Verlag Fur Wissenschaft und Bildung**. Berlin.
- Amthor, J.E. and Friedman, G.M. (1991). Dolomite-rock textures and secondary porosity development in Ellenburger Group carbonates (Lower Ordovician), west Texas and southeastern New Mexico. **Sedimentology**. 38: 343-362.

- Assavapatchara, S. 1998. **Lithostratigraphy of Upper Paleozoic Carbonate Rocks in the Southern Part of Changwat Loei**. M.S. thesis, Department of Geology, Chulalongkorn University, Thailand.
- Baccelle, L., and Bosellini, A. (1965). Diagrammi per la stima visiva della composizione percentuale nelle rocce sedimentarie. **Annali della Università di Ferrara Sezione IX, Science Geologiche e Paleontologiche**. 1: 59-62.
- Baird, A., Dawson, O., and Vachard, D. (1993). New data on biostratigraphy of the Permian Ratburi Limestone from north Peninsular Thailand. In T. Thanasuthipitak (ed.). **Proceedings of the International Symposium on Biostratigraphy of Mainland Southeast Asia: Facies & Paleontology** (Vol. 1, pp. 243-259). Chiang Mai University, Chiang Mai, Thailand.
- Bakush, S., and Carozzi, A. V. (1986). Sub-tidal storm-influenced carbonate ramp model: Galena Group (Middle Ordovician) along Mississippi River. (Iowa, Wisconsin, Illinois, and Missouri) U.S.A. **Archives Sciences, Genève**. 39: 141-183.
- Barr, S. M., and MacDonald, A.S. (1991). Toward a Late Paleozoic-Early Mesozoic tectonic model for Thailand. **Journal of Thai Geosciences**. 1: 11-22.
- Bathurst, R. G. 1966. Boring algae, micrite envelopes and lithification of molluscan biosparites. **Geological Journal**. 5: 15-32.
- Bose, P.K., Sarkar, S., and Bhattacharya, S. (1996). Dissolution seams: some observations from the Proterozoic Chanda Limestone, Adilabad, India. **Carbonate and Evaporite**. 11: 70-76.
- Boyd, D.W., and Newell, N. D. (1979). Permian Pelycypods from Tunisia. **American Museum Novitates**. 2686.

- Bunopas, S., and P. Vella. (1978). Late Paleozoic and tectonics model. In P. Nutalaya (ed.). **Proceedings of 3rd Regional Conference Geology and Mineral Resources of Southeast Asia** (pp 133-140). Bangkok, Thailand.
- Bunopas, S. (1981). **Paleogeographic history of western Thailand and adjacent parts of south-east Asia: A plate tectonics interpretation**. Ph.D. Dissertation, Victoria University of Wellington, New Zealand. (Reprinted in 1982, Geological Survey Paper 5, Geological Survey Division, Department of Mineral Resources, Bangkok, Thailand).
- Bunopas, S. (1983). Paleozoic succession in Thailand. In P. Nutalaya (ed.). **Proceedings of the Workshop on Stratigraphic Correlation of Thailand and Malaysia** (Vol. 1, pp 39-76). Haad Yai, Thailand.
- Bunopas, S. (1992). Regional stratigraphic correlation in Thailand. In C. Piancharoen (ed-in-chief). **Proceedings of the National Conference on Geologic Resource of Thailand: Potential for Future Development**. Department of Mineral Resources, Bangkok, Thailand.
- Campbell, H. J. (1997). The Middle Permian alatoconchid bivalves of Thailand. In Dheeradirok, P., Hinthong, C., Chaodumrong, P., Puttapiban, P., Tansathien, W., Utha-aroon, C., Sattayarak, N., Nuchanong, T., and Techawan, S. (eds). **Proceedings of the International Conference on Stratigraphy and Tectonic Evolution of Southeastern Asia and the South Pacific (GeoThai'97)** (p 129). Department of Mineral Resources, Bangkok, Thailand.
- Carozzi, V. P. (1993). **Sedimentary Petrography**. Prentice Hall, Englewood cliffs, New Jersey.

- Carozzi, V. P. (1989). **Carbonate Rock Depositional Models: A Microfacies Approach**. Prentice Hall, Englewood cliffs, New Jersey.
- Carozzi, V. P., and Gerber, M.S. (1978). Synsedimentary chert breccia: a Mississippian chert tempestite. **Journal of Sedimentary Petrology**. 48: 705-708.
- Cestari, R. and Sartorio, D. (1995). Rudists and facies of the Periadriatic domain. **Agip**. S. Donato Milanese.
- Charoenpravat, A., Wongwanich, T., Tantiwanit, W, and Theetiparivattra, U. (1984). **Geologic Map of Thailand, sheet NE47-12 Changwat Loei, scale 1: 250,000**. Geological Survey Division, Department of Mineral Resources, Bangkok, Thailand.
- Charoenpravat, A., Chuaviroj, S., Hinthong, C., and Chonglakmani. (1994). **Geologic Map of Thailand, sheet NE47-7 Changwat Lampang, scale 1: 250,000**. Geological Survey Division, Department of Mineral Resources, Thailand.
- Chaodumrong, P. (1992). **Stratigraphy, Sedimentology and Tectonic Setting of the Lampang Group, Central North Thailand**. Ph.D. Dissertation, University of Tasmania.
- Chen, D.Z., Tucker, M.E., Jiang, M.S. and Zhu, J.Q. (2001). Long-distance correlation between tectonic-controlled, isolated carbonate platforms by cyclostratigraphy and sequence stratigraphy in the Devonian of South China. **Sedimentology**. 48: 57-78.
- Chonglakmani, C., and Intarawichitr, K. (1994). The Permian and Triassic sequence of the Kiu Lom dam and Its vicinities, northern Thailand. In Angsuwathana, P., Wongwanich, T., Tanasathen, W., Wongsomsak, S., and Tulyatid, J. (eds.). **Proceeding of the International Symposium on Stratigraphy Correlation**

of Southeast Asia. (IGCP 306) (p 129) Department of Mineral Resources, Bangkok, Thailand.

Chonglakmani, C. (2002). Current status of Triassic stratigraphy of Thailand and its implication for geotectonic evolution. In N. Montajit (ed-in-chief). **Proceedings of the Symposium on Geology of Thailand 2002.** (pp 1-3). Department of Mineral Resources, Bangkok, Thailand.

Chonglakmani, C. (1999). The Triassic system of Thailand: Implications for the paleogeography of southeast asia. In Ratanasathien, B., and Rieb, S.L. (eds.). **Proceedings of the International Symposium on Shallow Tethys (ST) 5.** (pp 486-495). Department of Geological Sciences, Chiang Mai University. Chiang Mai.

Chonglakmani, C. and Fontaine, H. (1990). The Lam Narai-Phetchabun region: a platform of Early Carboniferous to Late Permian age. In P. Charusiri (ed.). **Proceedings of Technical Conference on Development of Geology for Thailand into the year 2000** (pp 39-98). Chulalongkorn University, Bangkok, Thailand,

Chonglakmani, C., and Sattayarak, N. (1984). **Geologic Map of Thailand, sheet NE 47-16 Changwat Phetchabun, scale 1: 250,000.** Geological Survey Division, Department of Mineral Resources, Bangkok, Thailand.

Choquette, P.W., and James, N.P. (1988). Introduction. In N.P. James, and P.W. Choquette (eds.). **Paleokasrt.** (pp 1-20). Springer-Verlag.

Colombié, C. and Strasser, A. (2005). Evolution of a keep-up carbonate platform. **Sedimentology.** 52: 1207-1227.

- Cooper, M. A., Herbert, R., and Hill, G. S. (1989). The structural evolution of Triassic intermontane basins in northern Thailand. In T. Thanasuthipitak, and P. Ounchanum (eds.). **Proceedings of the International Symposium on Intermontane Basins: Geology and Resources.** (pp 231-421). Department of Geological Sciences, Chiang Mai University, Chiang Mai, Thailand.
- Cox, B. M., and Sumbler, M. G. (1998). Lithostratigraphy: principles and practice. In P. Doyle, and M. R. Bennett (eds.). **Unlocking the Stratigraphical Record: Advances in Modern Stratigraphy** (pp 11-28). John Willey & Sons, England.
- Cuffey, R. J. (1997). Prasopora-bearing event beds in the Coburn limestone (bryozoa; Ordovician; Pennsylvania). In C. E. Brett and G. C. Baird (eds.). **Paleontological Events; Stratigraphic, Ecological, and Evolutionary Implications.** Columbia Univ. Press, New York.
- Dawson, A. and Racey, A. (1993). Fusuline-calcareous algal biofacies of the Permian Ratburi Limestone, Saraburi, central Thailand. **Journal of Southeast Asian Earth Science.** 81: 49-65.
- Department of Mineral Resources. (1992). **Lexicon of Stratigraphy names of Thailand.** Geological Survey Division, Bangkok, Thailand.
- Department of Mineral Resources. (1987). **Geological Map of Thailand, on scale 1: 2,500,000.** Geological Survey Division, Bangkok, Thailand.
- Dheeradilok, P., Udomsrisuk, T., Tansuan, V., Jungyusuk, N., Nakanart, A. (1976). **Geologic Map of Thailand, sheet ND47-11, Changwat Nakhorn Pathom, on scale 1: 250,000.** Geological Survey Division, Department of Mineral Resources, Thailand.

- Dunham, R. J. (1962). Classification of carbonate rocks according to depositional texture. In W. E. Ham (ed.). **Classification of Carbonate Rock**. (Vol. 1, pp 108-121). American Association of Petroleum Geologists Memoir.
- El Tabakh, M. and Utha-Aroon C. (1998). Evolution of a Permian carbonate platform to siliciclastic basin: Indochina plate, Thailand. **Sedimentary Geology**. 21: 97-119.
- Embry, A.F, and Klovan, J.E. (1971). A late Devonian reef tract on northeastern Banks Island. N.W.T. **Bulletin of Canadian Petroleum Geology**. 19: 730-781.
- Endo, R. (1969). Fossil algae from the Khao Phlong Phrab district in Thailand. In T. Kobayashi and R. Toriyama (eds.). **Geology and Palaeontology of Southeast Asia** (Vol. 7, pp 33-85).
- Fischer, A.G. (1964). The Lofer cyclothems of the Alpine Triassic. **Kansas Geological Survey Bulletin**. 169: 107-149.
- Fischer, A.G. (1991). Orbital cyclicity in the Mesozoic strata. In: G. Einsele, W. Ricken, and A. Seilacher (eds.). **Cycles and Events in Stratigraphy** (pp 48-62). Springer-Verlag, Germany.
- Fischer, A.G. (1986). Climatic rhythms recorded in the strata. **Annual Review of Earth and Planetary Sciences**. 14: 351-376.
- Fischer, A.G. (1964). The Lofer cyclothems of the Alpine Triassic. **Kansas Geological Survey Bulletin**. 169: 107-149.
- Flügel, E. (2004). **Microfacies of Carbonate Rocks: Analysis, Interpretation and Application**. Springer-Verlag, Berlin.
- Flügel, E. (1982). **Microfacies Analysis of Limestones**. Springer-Verlag, Berlin.

- Flügel, E., and Flügel-Kahler, E. (1992). Phanerozoic reef evolution: Basic questions and a data base. **Facies**. 26: 167-278.
- Flügel, E., and Krainer, K. (1992). Late Carboniferous aulopoid buildups from the Carnic Alps, Italy: Evidence for mound formation by combined organic growth, baffling and sediment infiltration. **Neues Jahrbuch für Geologie und Palaontologie, Monatshefte**. 185: 39-62.
- Folk, R. L. (1959). Practical classification of limestones. **American Association of Petroleum Geologists Bulletin**. 43: 1-38.
- Folk, R. L. (1962). Spectral subdivision of limestone types. In W. E. Ham (ed.). **Classification of Carbonate Rocks** (Vol.1, 1-279). **American Association of Petroleum Geologists Memoir**.
- Folk, R. L. (1973). Carbonate Petrography in the post-Sorbian age. In L. C. Play and Murray, R. C. (eds.). **Dolomitization and Limestone Diagenesis**. (Spec. Publ. 13: 14-48.) Society of Economic Paleontologists and Mineralogists.
- Fontaine, H., Salyapongse, S., and Vachard, D. (1999). New Carboniferous fossils found in Ban Bo Nam area, central Thailand. In C. Khantaprab (ed-in-chief). **Proceedings of the Symposium on Mineral, Energy and Water Resources of Thailand: Towards the year 2000** (pp 39-98). Chulalongkorn University, Bangkok, Thailand.
- Fontaine, H., Salyapongse, S., Tien, N. D., and Vachard, D. (2002). The Permian of Khao Tham Yai area in Northeast Thailand. In N. Montajit (ed-in-chief). **Proceedings of the Symposium on Geology of Thailand 2002** (pp 45-57). Department of Mineral Resources, Bangkok, Thailand.

- Friedman, G. M. (1965). Terminology of recrystallization textures and fabrics in sedimentary rocks. **Journal of Sedimentology Petrology**. 35: 643-655.
- Gatinsky, Y. G., Mishima, A.V., Vinogradov, I.V., and Kovalev, A. A. (1978). The main metallogenic belts of Southeast Asia as a result of different geodynamic conditions interference. In P. Nutalaya (ed-in-chief). **Proceedings of the 3rd Regional Conference on Geology and Mineral Resources of Southeast Asia** (pp 313-318). AIT, Bangkok, Thailand.
- Goldhammer, R.K. Dunn, P.A. and Hardie, L.A. (1990). Depositional cycles, composite sea-level changes, cycle stacking patterns, and the hierarchy of stratigraphic forcing: Example from Alpine Triassic platform carbonates. **Geological Society of America Bulletin**. 102: 535-562.
- Goldhammer, R.K. Dunn, P.A. and Hardie, L.A. (1987). High frequency glacio-eustatic sea-level oscillations with Milankovitch characteristics recorded in Middle Triassic platform carbonates in northern Italy. **American Journal of Science**. 287: 853-892.
- Haas, J. (2004). Characteristics of peritidal facies and evidences for subaerial exposures in Dachstein-type cyclic platform carbonates in the Transdanubian Range, Hungary. **Facies**. 50: 263-286.
- Hahn, L., Koch, K. E., and Witte, K. H. (1986). Outline of the geology and mineral potential of Thailand. **Geologische Jahrbuch**. Reihe B. 59: 3-49.
- Haile, N. S., and McElhinny, M. W. (1972). The potential value of paleomagnetic studies in restraining romantic speculation about the geological history of Southeast Asia. Regional conference on the geology of Southeast Asia. **Geological Society of Malaysia Newsletter**. 34: p16. (Abstract).

- Hallam, A. (1984). Pre-Quaternary sea level changes. **Annual Review of Earth and Planetary Science**. 12: 205-244.
- Hardie, L. A., and Ginsburg, R. M. (1977). Layering: The origin and environmental significance of lamination and thin bedding. In L. A. Hardie (ed.). **Sedimentation on the Modern Carbonate Tidal Flat of Northwest Andros Island, Bahamas**. Johns Hopkins Studies in Geology. Johns Hopkins University Press, Baltimore. 22: 50-123.
- Harrison, D., Chaodumrong, P., and Charusribandhu, M. (1997). Assessment of limestone resources from Suratthani Province, Thailand. In Dheeradirok, P., Hinthong, C., Chaodumrong, P., Puttapiban, P., Tansathien, W., Utha-aroon, C., Sattayarak, N., Nuchanong, T., and Techawan, S. (eds). **Proceedings of the International Conference on Stratigraphy and Tectonic Evolution of Southeastern Asia and the South Pacific (GeoThai'97)** (pp 640-649). Department of Mineral Resources, Bangkok, Thailand.
- Helmcke, D., and Lindenberg, H. G. (1983). New data on "Indosinian" orogeny from central Thailand. **Geologische Rundschau**. 72, 1: 317-328.
- Helmcke, D. (1985). The Permo-Triassic Paleotethys in Mainland Southeast-Asia and Adjacent Parts of China. **Geologische Rundschau**. 74, 2: 215-228.
- Helmcke, D. (1986). On the Geology of the Petchabun Fold-Belt (Central Thailand)- Implication for the Geodynamic evolution of Mainland S.E. Asia (GEOSEA V). **Geological Society of Malaysia Bulletin**. 19: 79-85.
- Helmcke, D. (1994). Distribution of Permian and Triassic syn-orogenic sediments in central mainland SE-Asia. In P. Angsuwathana, T. Wongwanich, W. Tansathien, S. Wongsomsak, and J. Tulyatid (eds.). **Proceeding of the**

International Symposium on Stratigraphic Correlation of Southeast Asia (pp 123-128). Department of Mineral Resources, Bangkok, Thailand.

Hinthong, C., Chuaviroj, S., Kaewyana, W., Srisukh, S., Pholprasit, C., and Pholachan, S. (1985). **Geological map of Thailand scale 1:250,000, sheet Changwat Phra Nakhon Si Ayutthaya (ND 47-8)**. Geological Survey Division, Department of Mineral Resources, Bangkok, Thailand.

Isozaki, Y. (2006). Guadalupian (Middle Permian) giant bivalve Alatoconchidae from a mid-Panthalassan paleo-atoll complex in Kyushu, Japan: a unique community associated with Tethyan fusulines and corals. **Proceeding of the Japan Academy** (Ser B, 82, 1: 25-32).

Jacka, A. D. (1974). Replacement of fossils by length-slow chalcedony and associated dolomitisation. **Journal of Sedimentary Petrology**. 44: 421-427.

Javanaphet, C. (1969). **Geological Map of Thailand on scale 1: 1,000,000**. Department of Mineral Resources, Bangkok, Thailand.

Jeffery, D., and Aigner, T. (1982). Storm sedimentation in Carboniferous limestones near Weston-Super-Mare (Dinantian, SW-England). In G. Einsele, and A. Seilacher (eds.). **Cyclic and Event Stratification** (pp 240-247). Berlin-Heidelberg.

Jin, Y., Wardlaw, B. R., Glenister, B. F., and Kotlyar, G.V. (1997). Permian chronostratigraphic subdivision. **Episodes**. March:10-15.

Kiessling, W. and Flügel, E. (2000). Late Paleozoic and Late Triassic limestones from north Palawan Block (Philippines): microfacies and paleogeographical implication. **Facies**. 43: 39-78.

- Kochansky-Devide, V. (1978). Tanchintongia marine aberrante Permische bivalve in Europa. **Paleontologische Zeitschrift**. 52: 213-218.
- Kozar, M. G., Crandall, G. F., Hall, S. E. (1992). Integrated structural and stratigraphic study of the Khorat Basin, Rat Buri limestone (Permian), Thailand. In C. Piancharoen (ed-in-chief). **Proceedings of the National Conference on Geologic Resource of Thailand: Potential for Future Development** (pp 692-736). Department of Mineral Resources, Bangkok, Thailand.
- Kreisa, R. D. (1981). Storm-generated sedimentary structures in sub-tidal marine facies with examples from the Middle and Upper Ordovician of southwestern Virginia. **Journal of Sedimentary Petrology**. 51: 823-848.
- Kreisa, R. D. and Bambach, R. K. (1982). The role of storm processes in generating shell beds in Paleozoic shelf environments. In G. Einsele, and A. Seilacher (eds.). **Cyclic and Event Stratification** (pp 200-207). Berlin-Heidelberg.
- Laschet, Ch. (1984). On the origin of cherts. **Facies**. 10: 257-290.
- Logan, B. W. (1984). Pressure response (deformation) in carbonate sediments and rocks: analysis and application, Canning Basin. In P. G., Purcell (ed.). **Proceeding of the Geological Society of Australia/Petroleum Exploration society of Australia, The Canning Basin, Western Australia**. (pp 235-251).
- Metcalf, I. (1990). Allochthonous terrane processes in Southeast Asia. **Philosophical Transaction of Royal Society of London**. 331: 625-640.
- Metcalf, I. (2002). Permian tectonic framework and paleogeography of SE Asia. **Journal of Asian Earth Science**. 20: 551-566.

- Meyers, W. J. (1988). Paleokarstic features in Mississippian Limestones, New Mexico. In: N.P. James, and P.W. Choquette (eds.). **Paleokarst** (pp 306-328). Springer-Verlag, N.Y.
- Meyers, W. J. (1980). Compaction in Mississippian skeletal limestones, southwestern New Mexico. **Journal of Sedimentary Petrology**. 50: 457-474.
- Moore, R. (1969). **Treatise on Invertebrate Paleontology** (Part N). The Geological Society of America and the University of Kansas.
- Nakornsri, N. (1981). **Geological Survey Report Number 3. Geology and Mineral Resources of Amphoe Ban Mi (ND47-4) scale 1: 250,000**. Department of Mineral Resources, Bangkok, Thailand.
- Nakornsri, N. (1976). **Geological Map of Amphoe Ban Mi (ND47-4) on scale 1: 250,000**. Department of Mineral Resources, Bangkok, Thailand.
- Newell, N. D. (1965). Classification of the Bivalvia. **American Museum Novitates**. 2206: 1-25.
- Ozaki, K. (1968). Problematical fossils from the Permian limestone of Akasaka, Gifu Prefecture. Yokohama. **Kokuritsu Daigaku Science Report (Sect. 2), Biological and Geological Sciences**. 14: 27-33.
- Park, R. K. (1976). A note on the significance of lamination in stromatolites. **Sedimentology**. 23: 379-393.
- Park, R. K. (1977). The preservation potential of some stromatolites. **Sedimentology**. 24: 485-506.
- Pettijohn, F. J., Potter, P. N., and Siever, R. (1972). **Sand and Sandstone**. Springer-Verlag, Berlin.

- Pia, J. (1933). **Die rezenten Kalksteine**. Mineralogisch Petrographische Mitteilungen, Neue Folge, Ergänzungs band. Leipzig.
- Pirrie, D. (1998). Interpreting the record: facies analysis. In P. Doyle, and M.R.Bennett (eds.). **Unlocking the Stratigraphical Record: Advances in Modern Stratigraphy** (pp 395-420). John Willey & Sons, England.
- Piyasin, S. (1991). Tectonic events and radiometric dating of the basement rocks of Phitsanulok Basin. **Journal of Southeast Asian Earth Science**. 1, 1: 41-48.
- Pomoni-Papaioannou, F., and Karakitsios, V. (2002). Facies analysis of the Trypali carbonate unit (Upper Triassic) in central-western Crete (Greece): an evaporate formation transformed into solution-collapse breccias. **Sedimentology**. 49: 1113-1132.
- Railsback, L. B., (1993). Lithologic controls on morphology of pressure dissolution surfaces (stylolites and dissolution seams) in Paleozoic carbonate rocks from the mideastern United States. **Journal of Sedimentary Petrology**. 63: 513-522.
- Raksaskulwong, L. (2002). Upper Paleozoic Rocks of Thailand. In N. Mantajit (ed-in-chief). **Proceedings of the Symposium on Geology of Thailand** (pp 29-34). Department of Mineral Resources, Bangkok, Thailand.
- Reeckman, A., and Friedman, G. M. (1982). **Exploration for Carbonate Petroleum Reservoir**. John Willey & Son, N.Y.
- Ricken, W. (1987). The carbonate compaction law; a new tool. **Sedimentology**. 34: 571-584.
- Rigby, J.F. (1998). Upper Paleozoic Floras of SE Asia. **Biogeography and Geological Evolution of SE Asia**. 73-82.

- Ross, C. A., and Ross, J. R. P. (1987). Late Palaeozoic sea level and depositional sequences. In Ross, C.A., and Haman, D (eds.). **Timing and depositional history of eustatic sequences, Constraints on seismic stratigraphy** (Vol. 24, pp 137-149). Cushman Foundation for Foraminiferal Research, Special Publication.
- Royal Thai Survey Department. (1992). **Topographic map of Thailand, on scale 1:50,000, sheet 5239II, Ban Wang Hin Ngom.**
- Royal Thai Survey Department. (1986). **Topographic map of Thailand, on scale 1:250,000, sheet ND47-4, Amphoe Ban Mi.**
- Runnegar, B. and Gobbet, D. J. (1975). *Tanchintongia* gen. nov., a bizarre Permian myalinid bivalve from west Malaysia and Japan. **Palaeontology**. 18: 315-322.
- Schauer, M., and Aigner, T. (1997). Cycle stacking pattern, diagenesis and reservoir geology of peritidal dolostones, trigonodus-dolomite, Upper Muschelkalk (Middle Triassic, SW-Germany). **Facies**. 37: 99-114.
- Seilacher, A. and Aigner, T. (1991). Storm deposition at the bed, facies, and basin scale: the geologic perspective. In: *Cycles and Events in Stratigraphy*. G. Einsele, W. Ricken, and A. Seilacher (eds.) pp 249-267. Springer-Verlag, Berlin-Heidelberg.
- Shinn, E. A. (1986). Modern carbonate tidal flats: their diagenetic features. **Quarterly Journal of Colorado School of Mines**. 81: 7-35.
- Shinn, E. A. (1983). Birdseys, fenestrae, shrinkage pores, and loferites: a reevaluation. **Journal of Sedimentary Petrology**. 53: 619-628.
- Shinn, E. A. (1969). Submarine lithification of Holocene carbonate sediments in the Persian Gulf. **Sedimentology**. 12: 109-144.

- Shinn, E. A. (1968). Practical significant of birdseye structures in carbonate rocks. **Journal of Sedimentary Petrology**. 38: 215-233.
- Shinn, E. A., Lloyd, R.M, and Ginsburg, R. N. (1969). Anatomy of a modern carbonate tidal flat, Andros Island, Bahamas. **Journal of Sedimentary Petrology**. 39: 1202-1228.
- Strasser, A. (1991). Lagoonal-peritidal sequences in carbonate environments: autocyclic and allocyclic processes. In G. Einsele, W. Ricken, and A. Seilacher (eds.) **Cycles and Events in Stratigraphy** (pp 709-721). Springer-Verlag, Berlin-Heidelberg.
- Strohmenger, C., and Wrasing, G. (1991). A proposed extension of Folk's textural classification of carbonate rocks. **Carbonate and Evaporite**. 6: 23-28.
- Suntharalingam, T. 1968. Upper Paleozoic Stratigraphy of the Area West of Kampar, Perak. **Geological Society of Malaysia Bulletin**.1: 1-15.
- Termier, H., Termier, G., and Lapparent, A. F. (1973). Grands Bivalves r'ecifaux du Permian sup'erieur de I'Afghanistan central. **Societe Geologique du Nord Annales**. XCIII, 1: 75-80.
- Thambunya, S. (2005). **Lithofacies and Diagenesis of the Khao Khad Formation in the Vicinity of Changwat Saraburi, Central Thailand**. Ph.D. dissertation, Department of Geology, Chulalongkorn University, Thailand.
- Thanasuthipitak, T. (1978). Geology of Uttaradit area and its implications on tectonic history of Thailand. In P. Nutalaya (ed-in-chief). **Proceedings of the 3rd Regional Conference on Geology and Mineral Resources of Southeast Asia** (pp 187-197). AIT, Bangkok, Thailand.

- Tittirananda, O. (1976). **Aspects of Stratigraphy and Palaeontology of the Permian Rat Buri Limestone of Saraburi, Central Thailand**. Ph.D. dissertation, Bedford College, University of London.
- Tomašových, A. (2004). Microfacies and depositional environment of an Upper Triassic intra-platform carbonate basin: the Fatric Unit of the west Carpathians (Slovakia). **Facies**. 50: 77-105.
- Ueno, K. (2003). The Permian fusulinoidean faunas of the Sibumasu and Baoshan blocks: Their implication for the paleogeographic and paleoclimatologic reconstruction of the Cimmerian continent. **Palaeogeography, Palaeoclimatology, Paleoecology**. 193: 1-24.
- Vail, P. R., Mitchum, R.M., and Thompson, S. (1977). Seismic stratigraphy and global changes of sea-level, part 4: global cycles of relative changes of sea-level. **American Association of Petroleum Geologists Memoir**. 26: 83-97.
- Vogel, K. (1975). Endosymbiotic algae in rudists? **Palaeogeography, Palaeoclimatology, Paleoecology**. 17: 327-332.
- Wakita, K., and Metcalfe, I. (2005). Ocean plate stratigraphy in East and Southeast Asia. **Journal of Asian Earth Sciences**. 24: 679-702.
- Wang, X.-D., Ueno, K., Mizuno, Y., and Sugiyama, T. (2001). Late Paleozoic faunal, climatic, and geographic changes in the Baoshan block as a Gondwana-Derived continental fragment in Southwest China. **Palaeogeography, Palaeoclimatology, Paleoecology**. 170: 197-218.
- Wanless, H. R. Tedesco, L. P., and Tyrrell, K. M. (1988). Production of subtidal tabular and surficial tempestites by Hurricane Kate, Caicos Platform, British West Indies. **Journal of Sedimentary Petrology**. 58: 739-750.

- Wieldchowsky, C.C., and Young, J.D. (1985). Regional facies variation in Permian rocks of the Phetchabun Fold and Thrust Belt, Thailand. In P. Thanvarachorn, S. Hokjaroen, and W. Youngme (eds.). **Proceedings on Geology and Mineral Resources Development of the Northeastern Thailand** (pp 41-56). Khon Kaen University, Khon Kaen, Thailand.
- Wilson, J. L. (1975). **Carbonate facies in geologic history**. Springer-Verlag, N. Y.
- Wolfart, R. (1987). Geology of Amphoe Sop Prap (4844I) and Amphoe Wang Chin (4944IV), scale 1:50,000, Thailand. **Geologische Jahrbuch**. Reihe B. 65: 3-52.
- Wright, V. P. (1984). Peritidal carbonate facies models: a review. **Geological Journal**. 19: 309-325.
- Wright, V. P. (1992). A revised classification of limestones. **Sedimentary Geology**. 76: 177-186.
- Wright, V. P., and Azerédo, A. C. (2006). How relevant is the role of macrophytic vegetation in controlling peritidal carbonate facies?: Clues from the Upper Jurassic of Portugal. **Sedimentary Geology**. 186: 147-156.
- Yancey, T.E. (1985). Bivalve of the H.S. Lee Formation (Permian) of Malaysia. **Journal of Paleontology**. 59, 5: 1286-1297.
- Yancey, T.E., and Ozaki, K. (1986). Redescription of the Genus *Shikamaia* and Clarification of the Hinge Characters of the Family Alatoconchidae (Bivalvia). **Journal of Paleontology**. 60, 1: 116-125.
- Yancey, T.E., and Boyd, D. (1983). Revision of the Alatoconchidae: A Remarkable Family of Permian Bivalves. **Palaeontology**. 26, 3: 497-520.

Yancey, T.E., and Stanley, G.D. (1999). Giant alatoform bivalve in the Upper Triassic of western North America. **Palaeontology**. 42, 1: 1-23.

Zempolich, W.G., Cook, H.E., Zhemchuzhnikov, V.G., Zhaimina, V.Y., Zorin, A.Y., Buvtyshin, V.M., Kotova, E.A., Golub, L.Y., Giovannelli, A., Viaggi, M., Lehmann, P.J., Fretwell, N., Alexeiev, D.V., and Lapointe, P.A. (2002). Biotic and abiotic influence on the stratigraphic architecture and diagenesis of Middle to Upper Paleozoic carbonates of the Bolshoi Karatau Mountains, Kazakhstan and the early marine cements and reservoir quality in subsurface reservoirs. In W. G. Zempolich, and H.E. Cook, (eds.). *Paleozoic Carbonates of the Commonwealth of Independent Status (CIS): Subsurface and Outcrop Analogs*. **SEPM special publication** (74: 123-180).

APPENDICS

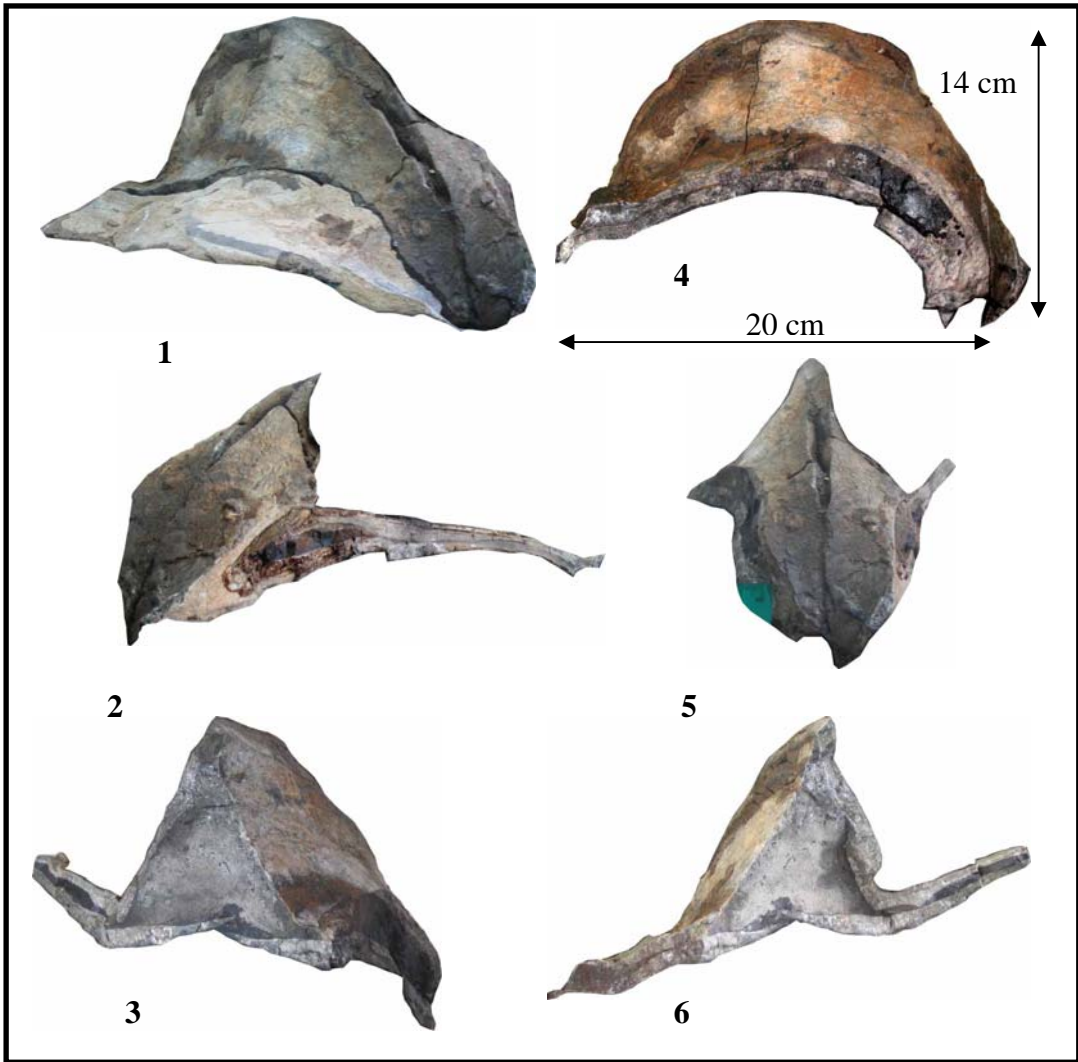
APPENDIX A

ALATOCONCHID BIVALVES

EXPLANATION OF PLATE 1

Figs. 1-6 *Saikraconcha cf. tunisiensis*. 1: oblique external view showing dorsal ridge, wing-like flange of right valve, downturned beaks and narrow dorsal niche along anterior slope of dorsal crest. 2: lateral view of the left valve with anterior part of both valves, left valve show body cavity infilled later by matrix and black chert nodule. 3: interior view showing large body cavity with high dorsal ridge (anterior to the right). 4: lateral view of the right valve showing downturned beaks, high dorsal crest and small body cavity along lateral wing or flange (anterior to the right). 5: an anterior view showing narrow elongate shape of dorsal niche. 6: interior view of the opposite part of fig. 3, showing large and triangular shaped body cavity, high dorsal ridge and wing-like flanges.

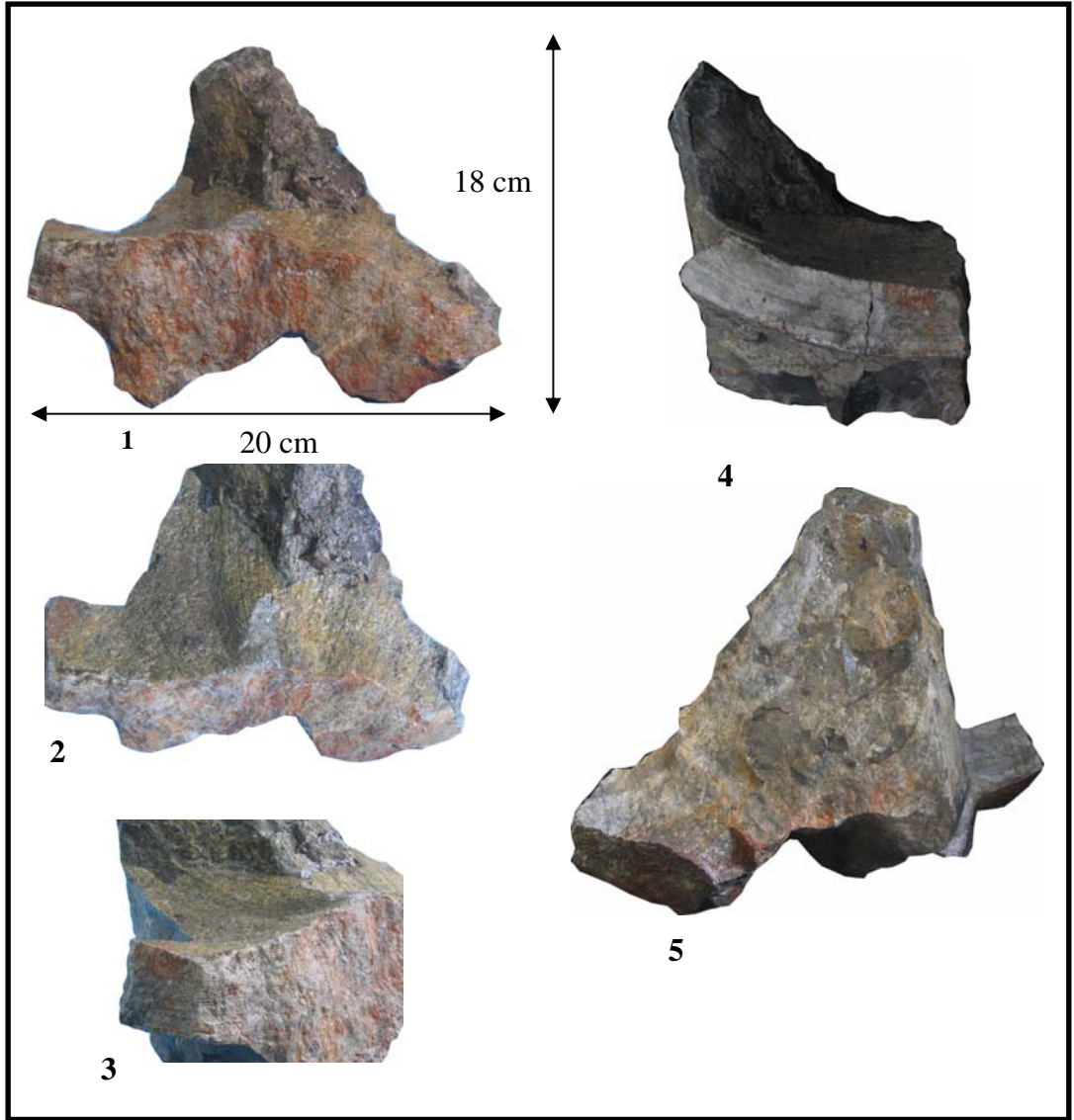
PLATE 1



EXPLANATION OF PLATE 2

Figs. 1-5 *Shikamaia* cf. *perakensis*. 1: anterior view showing massive infilled umbone, appressed anterior. 2: dorsal view of an anterior portion showing ornamentation on ventral surface and appressed cardinal area. 3: lateral view of an anterior part of the right valve showing thick and massive shell wall with fine growth lines (anterior to the right). 4: Lateral view of an anterior part of the right valve showing thick and massive shell wall, high slope on the left showing development of dorsal crest (anterior to the right). 5: interior view of abapical end of cardinal area showing large body cavity with high dorsal ridge and part of wing-like flanges.

PLATE 2



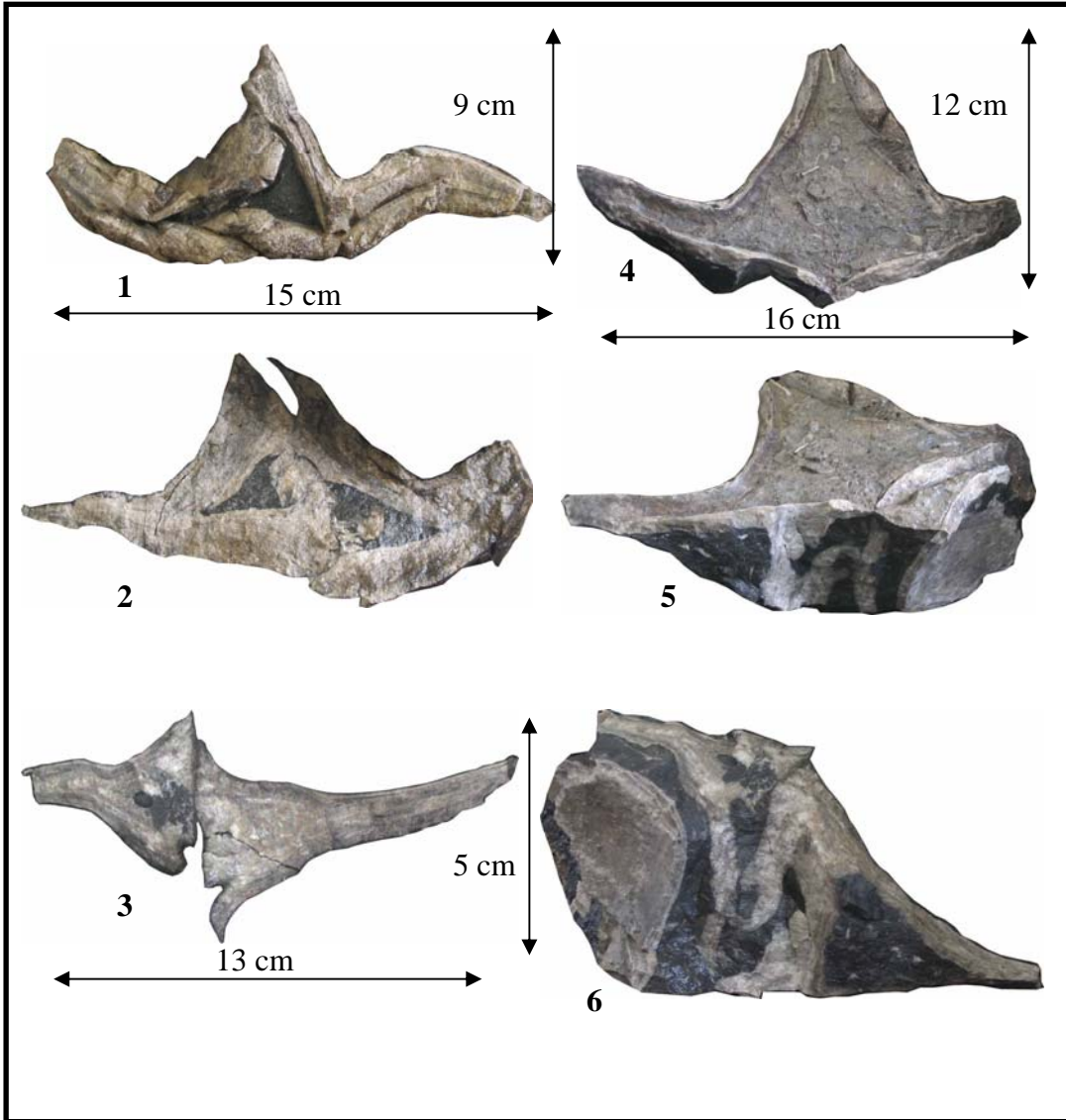
EXPLANATION OF PLATE 3

Figs. 1-2 *Alatoconchidae* gen. indet. 1: posterior view of articulated specimen, thick wing-like flange, apparently triangular shape body cavity in cross-section, ventral part of the right valve rest on the left valve, edge of the left valve lost.

2: anterior view of the same specimen as 1 (opposite view of 1), showing thicker shell wall in both valves.

Figs. 3-6 *Saikraconcha* cf. *tunisiensis*. 3: an anterior portion showing massive infilling umbone with low dorsal ridge and appressed cardinal areas, byssal groove and byssal collar located along ventral surface. 4: internal view showing large body cavity. 5: oblique ventral view showing small byssal groove as small ovoid opening, shell fragment of another bivalve adhering below the right valve. 6: oblique ventral view of the opposite side of fig. 5, showing byssal collar on the right valve and byssal groove on the left one.

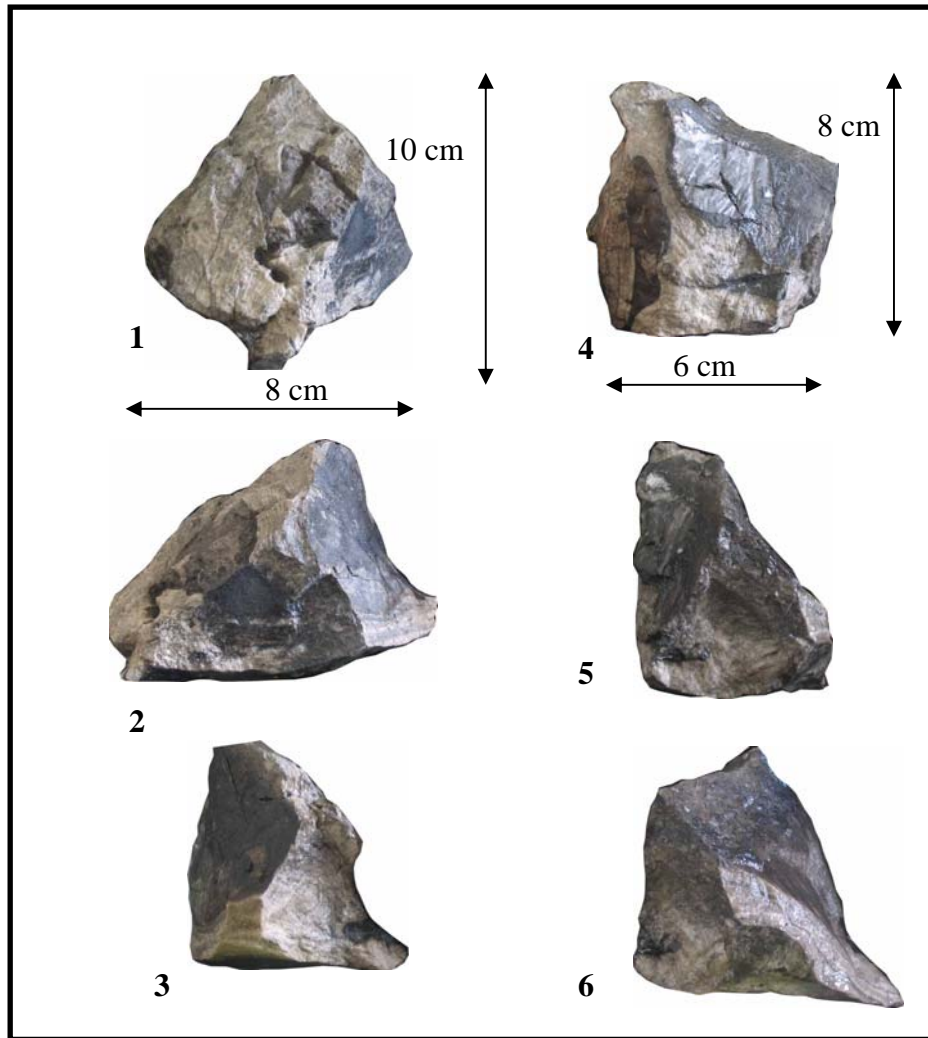
PLATE 3



EXPLANATION OF PLATE 4

Figs. 1-6 *Shikamaia* cf. *perakensis*. 1: broken, incomplete articulated shell illustrating abapical part of an anterior region, densely infilled umbone with small area of body cavity, byssal groove on left valve, small byssal collar. 2: side view of the same specimen as 1, showing thick shell wall on the right valve. 3: piece of left valve showing massive umbone with fine growth lines, prominent byssal groove above ventral surface. 4: abapical end of cardinal area showing massive umbone with part of byssal groove above ventral surface, curvature ligament occupying lower half of cardinal area below hinge line, small body cavity developed on abapical end of cardinal area. 5: anterior view showing flat ventral surface and ridge shape along dorsal region, small byssal groove located above ventral surface. 6: oblique lateral view of the same specimen as in figs. 4 and 5 showing part of thick wing-like flange developed beside umbonal region.

PLATE 4



EXPLANATION OF PLATE 5

Fig. 1: Oblique cross-section of an articulated shell showing an anterior part, shell orientated in life position, alate with wing-like flanges on both valves, high dorsal ridge, byssal groove located on ventral side, small byssal collar placed beneath byssal groove (pen for scale=15 cm of total length).

Fig. 2: Tracing of Fig. 1.

Fig. 3: Oblique cross-section of an articulated shell showing an anteroposterior portion, slightly triangular shape alatoconchid with internal body cavity (marker pen for scale=15 cm).

Fig. 4: Tracing of Fig. 3.

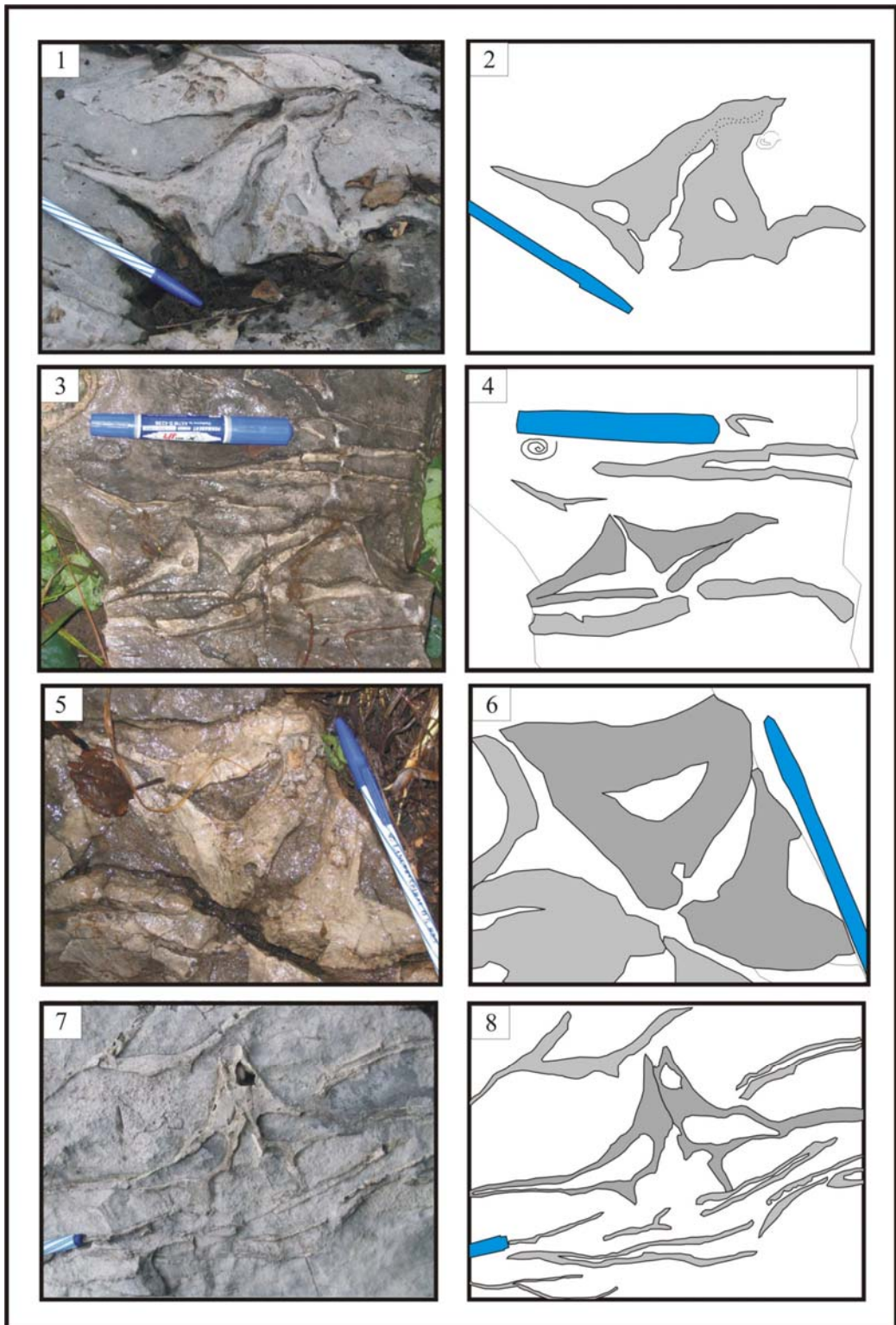
Fig. 5: Oblique cross-section of an articulated shell showing an anteroventral view close to abapical end of cardinal area, partly observed internal cavity, prominent byssal groove on both valves located slightly above ventral surface, (pen for scale=15 cm of total length).

Fig. 6: Tracing of Fig. 5.

Fig. 7: Cross-section of an articulated shell showing an anterior portion along the dorsal-ventral plane, prominent byssal groove and large byssal collar in the ventral part, body cavity partly developed on both valves, dorsal crest with sharply pointed top (pen for scale=15 cm of total length).

Fig. 8: Tracing of Fig. 7.

PLATE 5



EXPLANATION OF PLATE 6

Fig. 1: Oblique cross-section of an articulated shell along dorsal-ventral part of anteroposterior region, wing-like flanges on both valves, prominent dorsal ridge, lower part of body cavity on both valves occluded by small chert nodules (pen for scale=15 cm of total length).

Fig. 2: Tracing of Fig. 1.

Fig. 3: Cross-section of articulated shell along an anterior region close to the beaks, massive infilled shells without body cavity, appressed beaks and small dorsal niche between valves (pen for scale=15 cm).

Fig. 4: Tracing of Fig. 3.

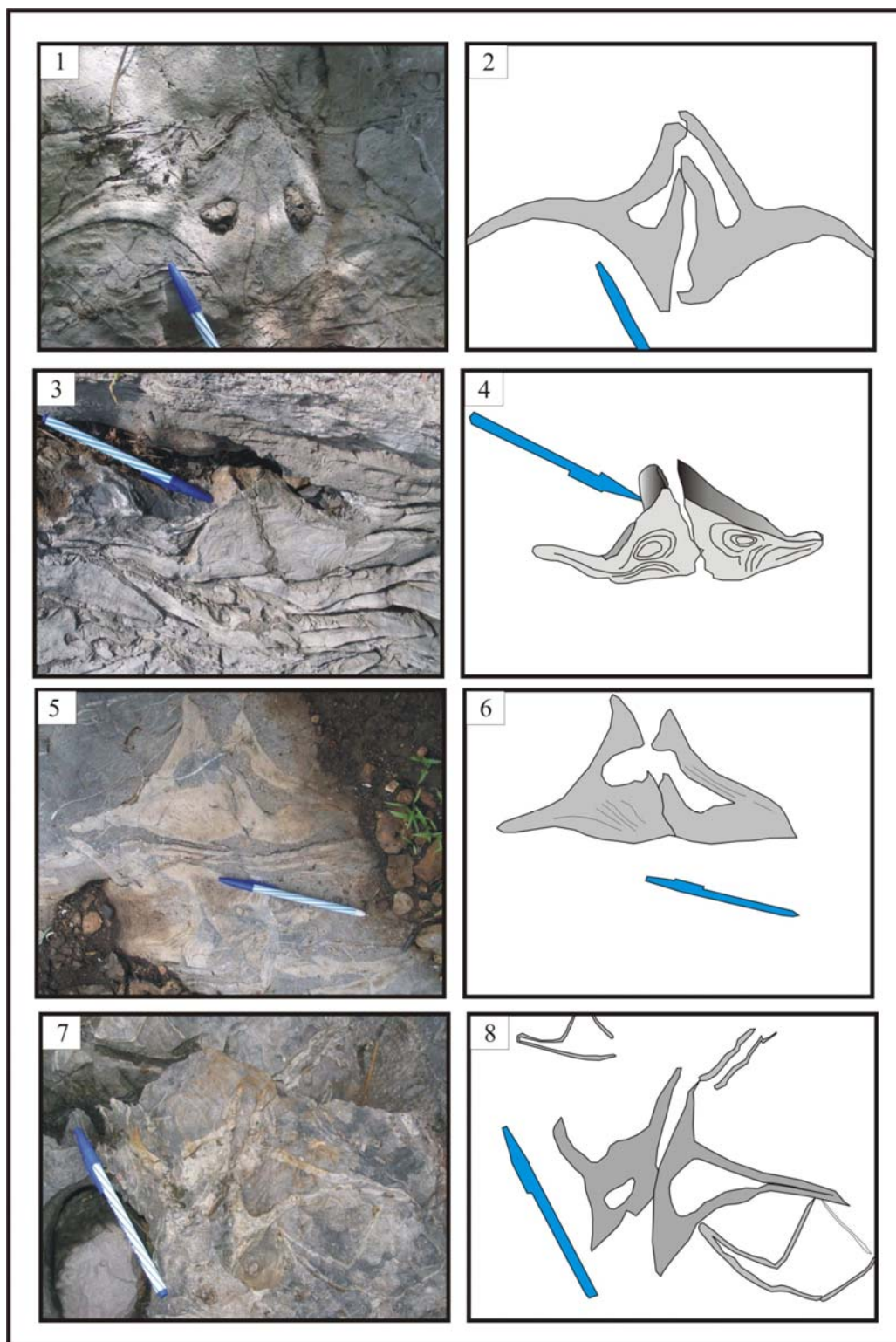
Fig. 5: Oblique cross-section of an articulated shell along dorsal-ventral portion of an anteroposterior region, large and thick shell with short wing-like flange (pen for scale=15 cm).

Fig. 6: Tracing of Fig. 5.

Fig. 7: Oblique section of dorsal view of an articulated shell, well defined dorsal crest, divergent beaks (specimen at center). This specimen can be compared to *Shikamaia perakensis* based on their similarity in divergent beaks, large shell with prominent dorsal crest. Other specimens on lower right and upper left of view showing relative thinner shell walls of articulated specimens, anteroposterior region with large body cavity, triangular in cross-section along both valves (pen for scale=15 cm).

Fig. 8: Tracing of Fig. 7.

PLATE 6



EXPLANATION OF PLATE 7

Fig. 1: Oblique cross-section along dorsal-ventral plane of an anterior region, wing-like flanges, massive infilled umbone, small byssal groove slightly above ventral surface (pen for scale=15 cm of total length).

Fig. 2: Tracing of Fig. 1.

Fig. 3: Large articulated shell showing cross-section along an anterior part, prominent and high dorsal crest forming ridge-like structure, thick shell wall along dorsal ridge, ventral and dorsal shell wall having same thickness along both wing-like flanges, byssal groove located above large byssal collars, right valve broken and missing wing terminal, presence of byssal collars enables this specimen to be compared with Genus *Shikraconcha* (pen for scale=15 cm of total length).

Fig. 4: Tracing of fig. 3.

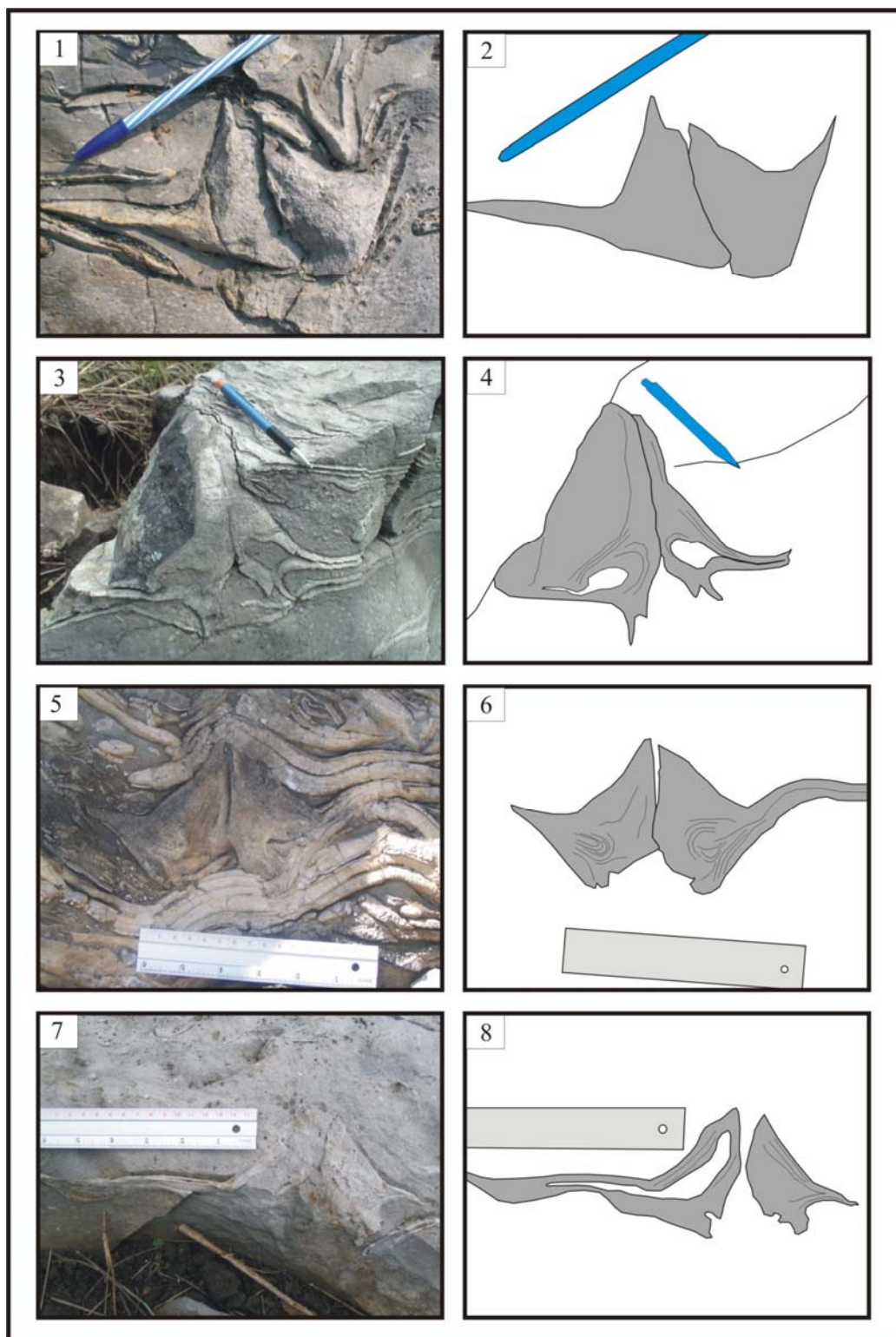
Fig. 5: Oblique cross-section of an anterior region close to the beaks, massive infilled umbone without body cavity, appressed shell along anterior part, prominent dorsal ridge on both valves along commissural plane, wing-like flanges, small byssal groove, circular growth lines at center of umbone (ruler for scale=15 cm).

Fig. 6: Tracing of Fig. 5.

Fig. 7: Oblique cross-section of an articulated shell along abapical end of cardinal area showing byssal groove developed on both valves, clearly observed wing-like flange with partly developed body cavity on left (ruler for scale=15 cm).

Fig. 8: Tracing of Fig. 7.

PLATE 7



EXPLANATION OF PLATE 8

Fig. 1: Slightly oblique cross-section of an articulated specimen showing an anteroposterior region, wing-like flanges on both valves with a prominent dorsal ridge along commissural plane, triangular shaped body cavity, with flat ventral surface (pen for scale=15 cm of total length).

Fig. 2: Tracing of Fig. 1.

Fig. 3: Cross-section of an articulated shell closed to abapical end of an anteroposterior portion, ventral shell wall with same thickness as dorsal shell wall, high dorsal ridge exhibiting a prominent ridge along dorsal margin, wing-like flanges extending laterally to terminal edge of the shell, with flat ventral surface (pen for scale=15 cm of total length).

Fig. 4: Tracing of Fig. 3.

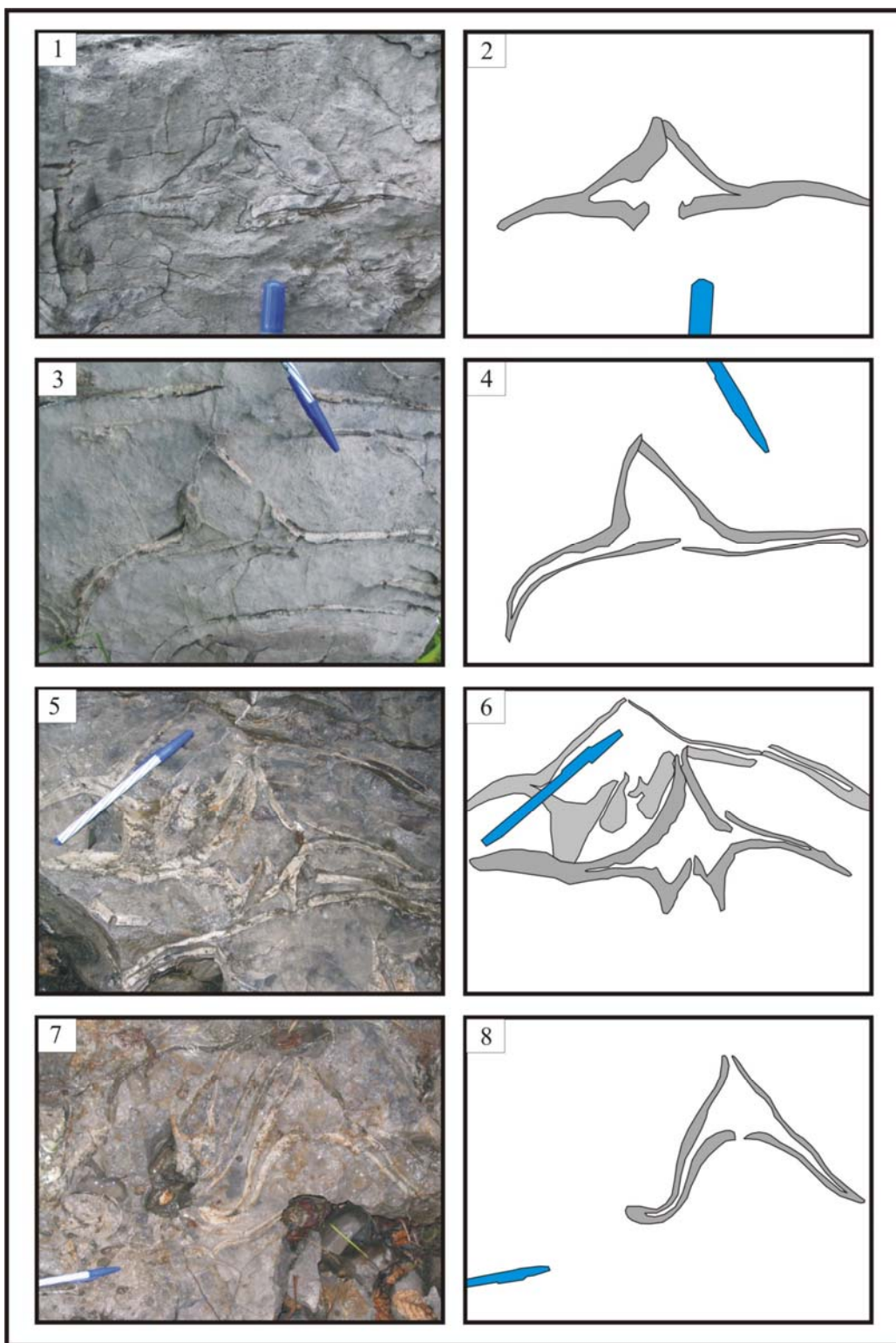
Fig. 5: Slightly oblique cross-section of articulated shells, high dorsal ridge, wing-like flanges, large body cavity, large byssal collars on both valves ventrally; this specimen can be compared to Subfamily Shikraconchinae based on the occurrence of large and prominent byssal collars (pen for scale=15 cm of total length).

Fig. 6: Tracing of Fig. 5.

Fig. 7: Cross-section of an articulated shell closed to abapical end of anteroposterior portion, abnormal orientation of wing-like flanges (possibly due to post-burial compaction) high dorsal ridge with inferred flat ventral surface, large body cavity, same thickness of dorsal and ventral shell walls (pen for scale=15 cm of total length).

Fig. 8: Tracing of Fig. 7

PLATE 8



EXPLANATION OF PLATE 9

Fig. 1: Oblique lateral-section along a single valve showing position of shell close to lateral edge of the valve (geological hammer as scale=30cm in total length).

Fig. 2: Tracing of Fig. 1.

Fig. 3: Oblique cross-section of the area closed to abapical end of an anteroposterior portion, triangular shape of large body cavity (pen for scale=15 cm of total length).

Fig. 4: Tracing of Fig. 3.

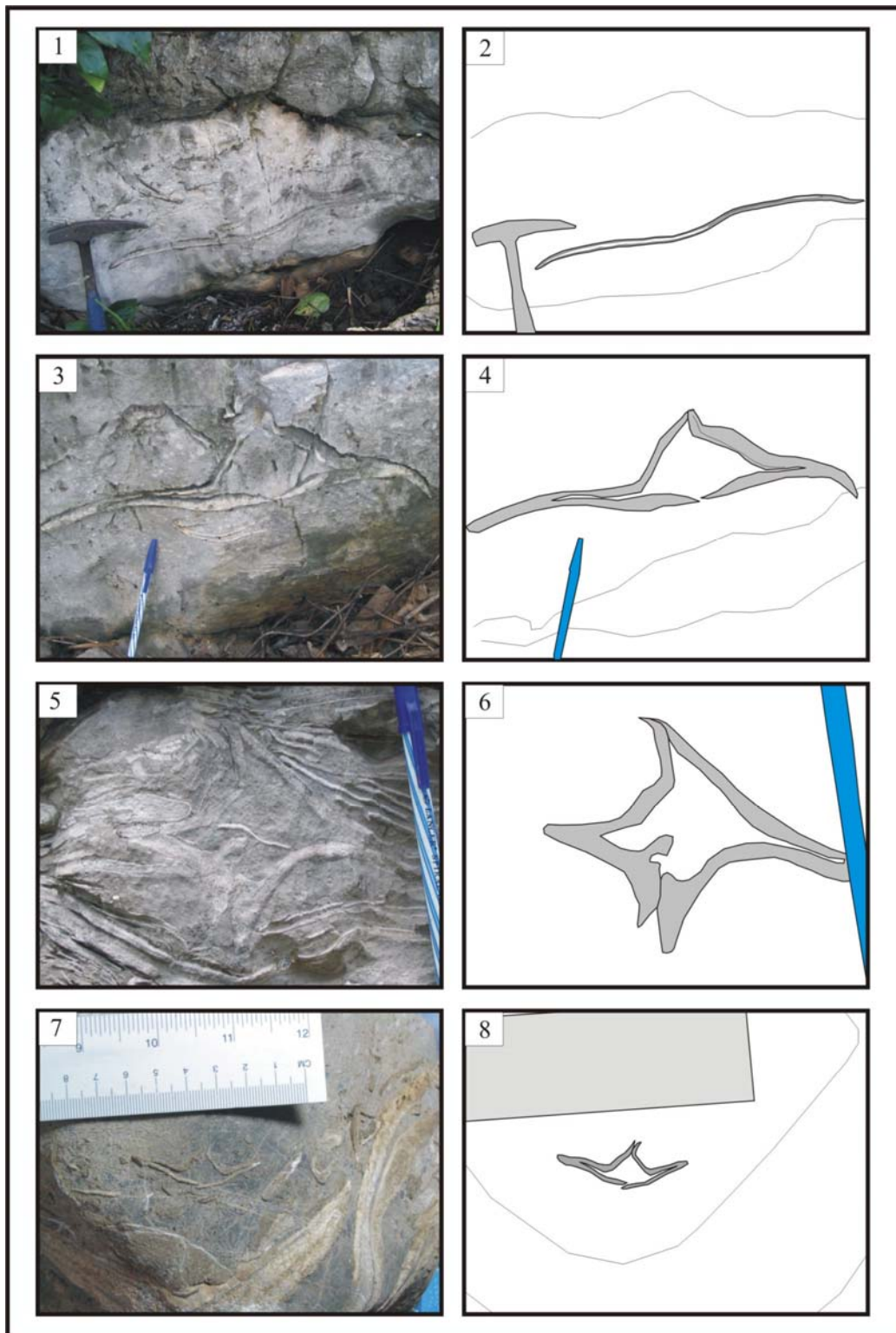
Fig. 5: Oblique cross-section of apical part of an anteroposterior region, prominent byssal collars on ventral side of both valves, byssal groove located above byssal collars, ridge shape dorsal margin, wing-like flanges (pen for scale=15 cm of total length).

Fig. 6: Tracing of Fig. 5.

Fig. 7: Cross-section of juvenile articulated shell, 3 cm width of each valve, wing-like flanges, prominent dorsal ridge as found in adult shell.

Fig. 8: Tracing of Fig. 7.

PLATE 9



EXPLANATION OF PLATE 10

Fig. 1: Oblique cross-section of an articulated shell, anteroposterior portion showing large body cavity, wing-like flanges, high dorsal ridge along commissural plane, byssal groove located at ventral part of the shell (ruler for scale=15 cm).

Fig. 2: Tracing of Fig. 1.

Fig. 3: Oblique cross-section of an articulated shell, view closed to abapical end of anteroposterior region, large body cavity, thin shell wall on both dorsal and ventral sides, prominent dorsal ridge, wide and flat ventral surface (pen for scale=15 cm).

Fig. 4: Tracing of Fig. 3.

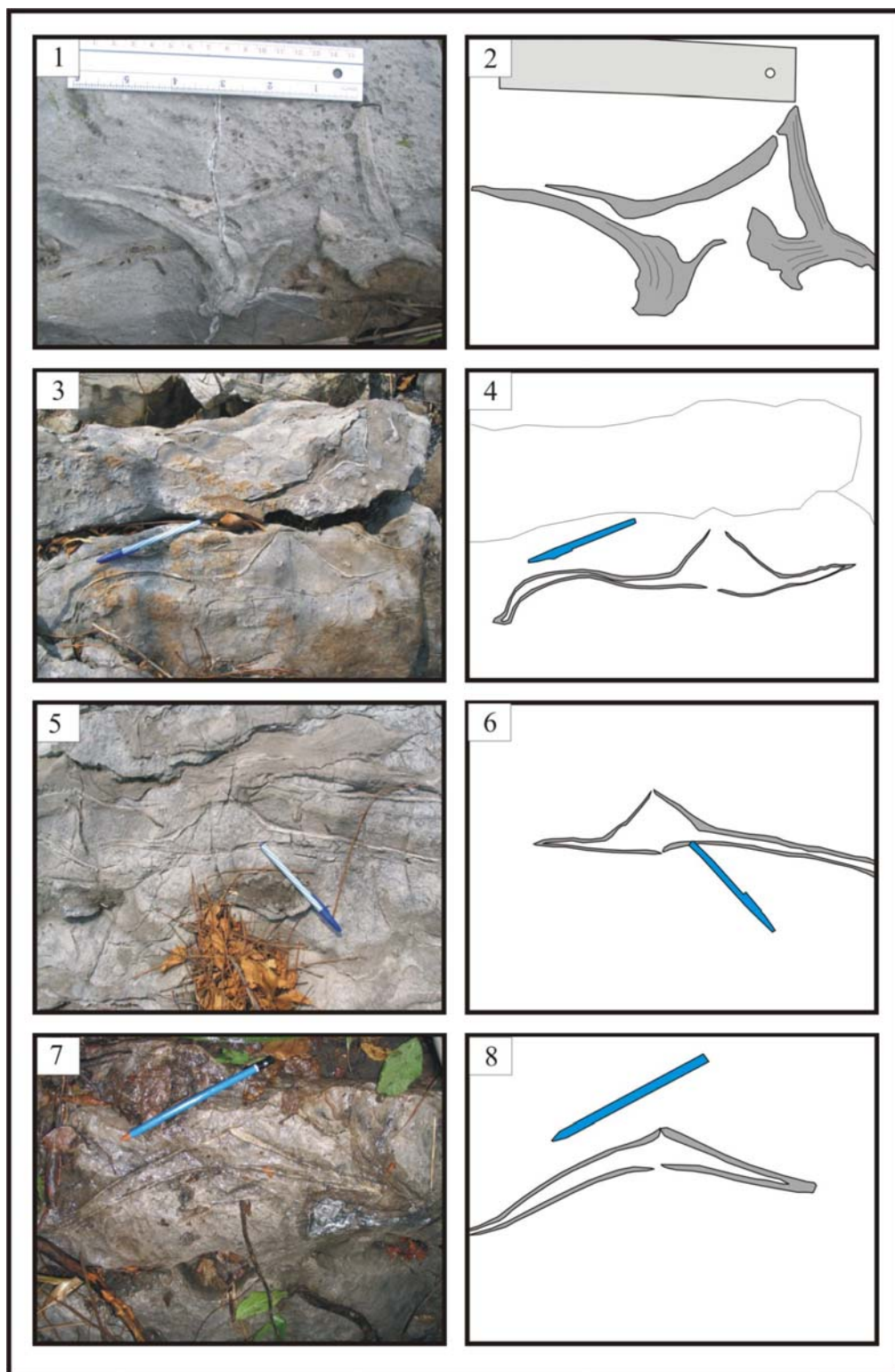
Fig. 5: Oblique cross-section similar to fig. 3 showing another side of random section, (pen for scale=15 cm)

Fig. 6: Tracing of Fig. 5.

Fig. 7: Oblique cross-section of posterior region cutting along dorsal-ventral plane, very low dorsal ridge, wing-like flanges, large body cavity (pen for scale= 15 cm).

Fig. 8: Tracing of Fig. 7.

PLATE 10



EXPLANATION OF PLATE 11

Fig. 1: Oblique cross-section of large articulated shell close to abapical end of anteroposterior region, wing-like flanges extend laterally on both valves, prominent and low dorsal ridge along commissural plane, thin shell with large body cavity (pen for scale=15 cm).

Fig. 2: Tracing of Fig. 1.

Fig. 3: Lateral-section of a single left valve showing slightly upturned beak, short cardinal area, massive and thick shell wall, high dorsal crest, low and flat posterior region, relatively small body cavity (pen for scale=15 cm).

Fig. 4: Tracing of Fig. 3.

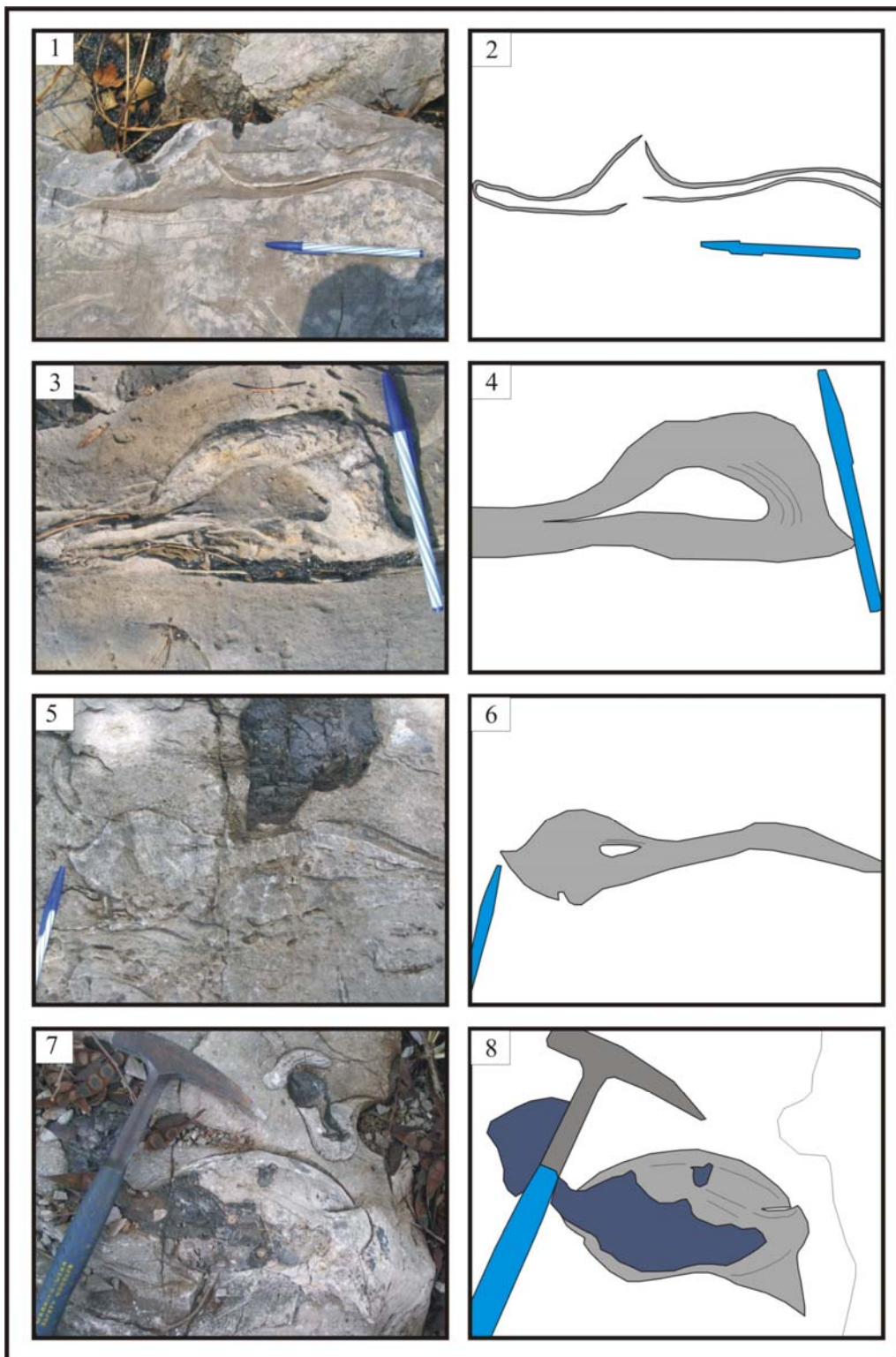
Fig. 5: Lateral-section of a single right valve showing massive and thick shell wall, short cardinal area (pen for scale=15 cm of total length).

Fig. 6: Tracing of Fig. 5.

Fig. 7: Dorsal view of an articulated specimen showing ellipsoidal shape, appressed and terminated beaks, black chert nodule developed on dorsal surface (geological hammer for scale=30 cm of total length).

Fig. 8: Tracing of Fig. 7.

PLATE 11



EXPLANATION OF PLATE 12

Fig. 1: Oblique cross-section of an articulated shell showing dorsal ridge crest along commissural plane, wing-like flanges on both valves extending to the lateral edge of the shell, byssal groove located just above ventral surface (pen for scale=15 cm).

Fig. 2: Tracing of Fig. 1.

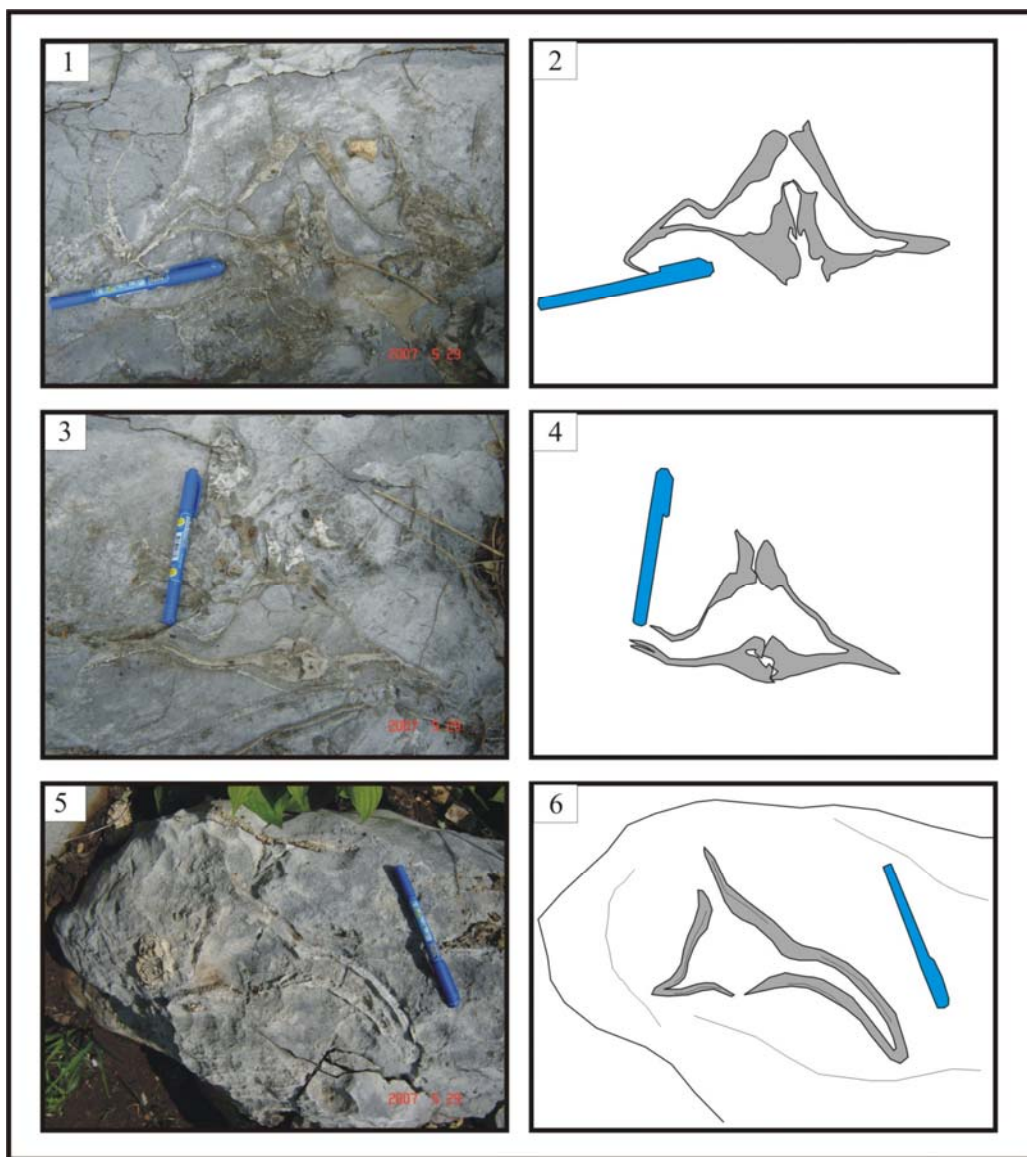
Fig. 3: Oblique cross-section of an articulated shell showing nearly triangular shape of body cavity, thin dorsal shell wall but thick along dorsal ridge, large body cavity, small byssal groove (pen for scale=15 cm).

Fig. 4: Tracing of Fig. 3.

Fig. 5: Oblique cross-section of an articulated shell, large body cavity, high dorsal ridge (pen for scale=15 cm).

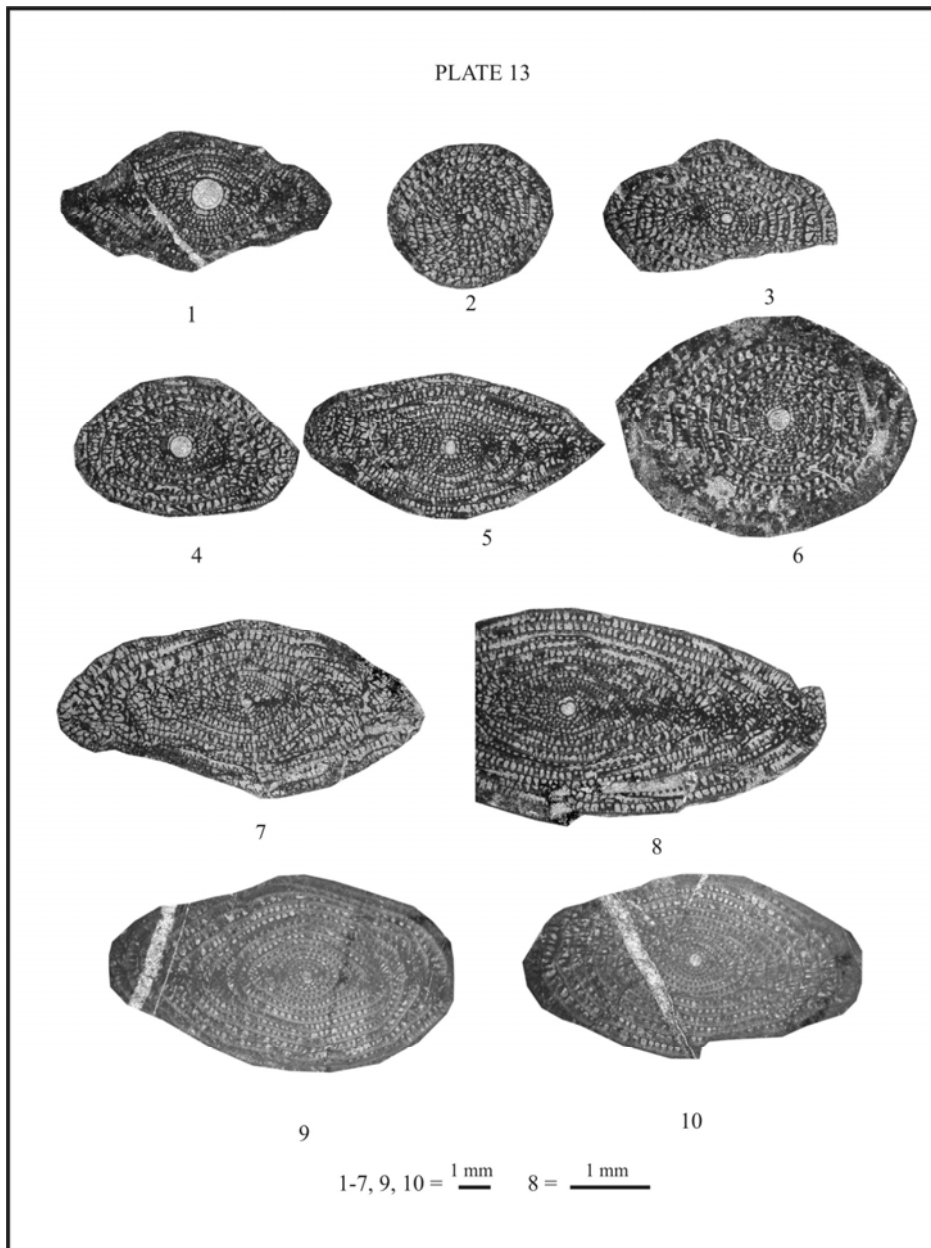
Fig. 6: Tracing of Fig. 5.

PLATE 12



APPENDIX B

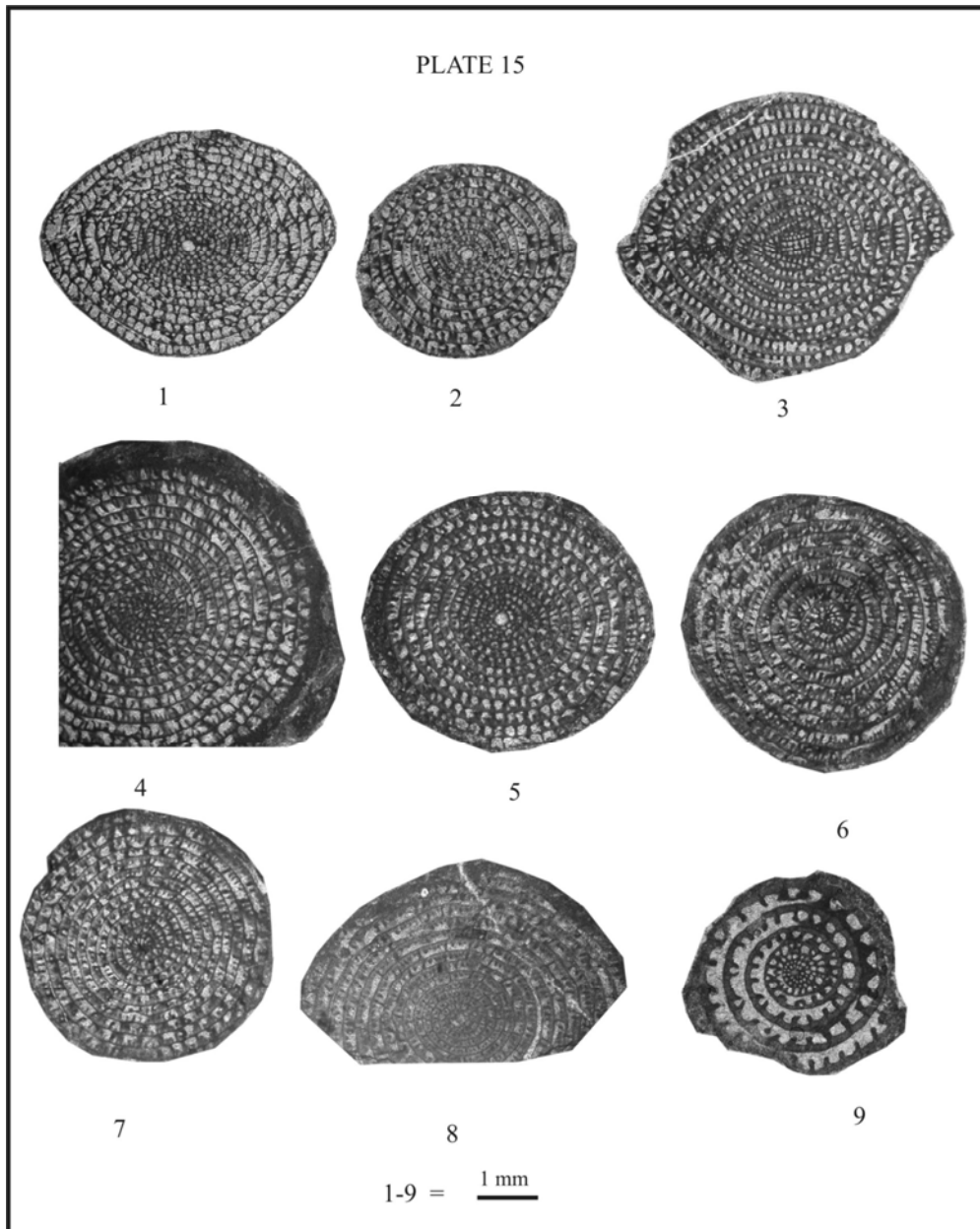
KEY FUSULINIDS AND SMALLER FORAMINIFERS



EXPLANATION OF PLATE 13

Figs. 1, 2, 5, 7, 8: *Lepidolina* sp.

Figs. 3, 4, 6, 9, 10: *Yabeina* sp.

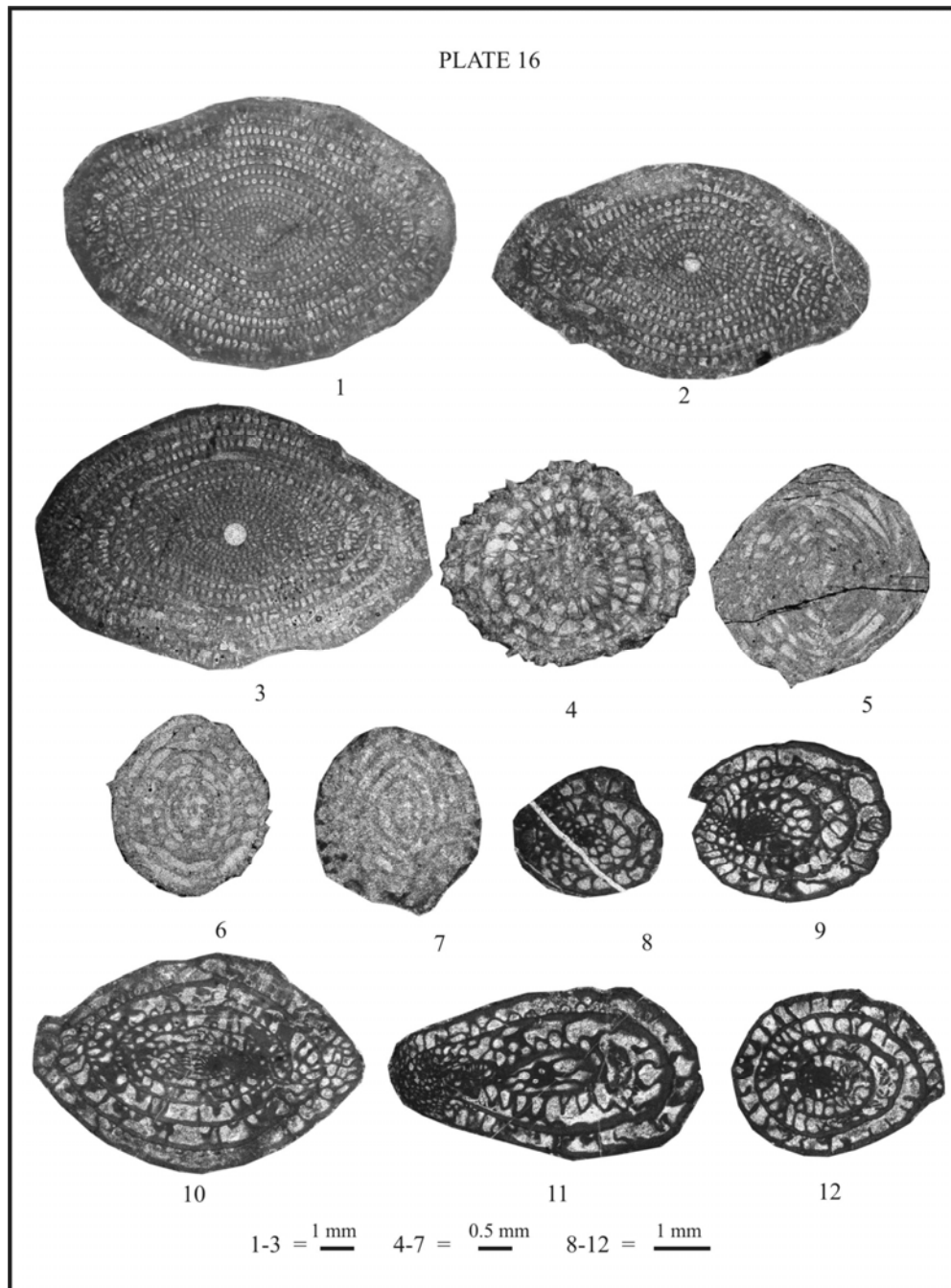


EXPLANATION OF PLATE 15

Figs. 1-3, 5: *Yabeina* sp.

Figs. 4, 6, 7, 8 : *Lepidolina* sp.

Fig. 9: *Chusenella* sp.

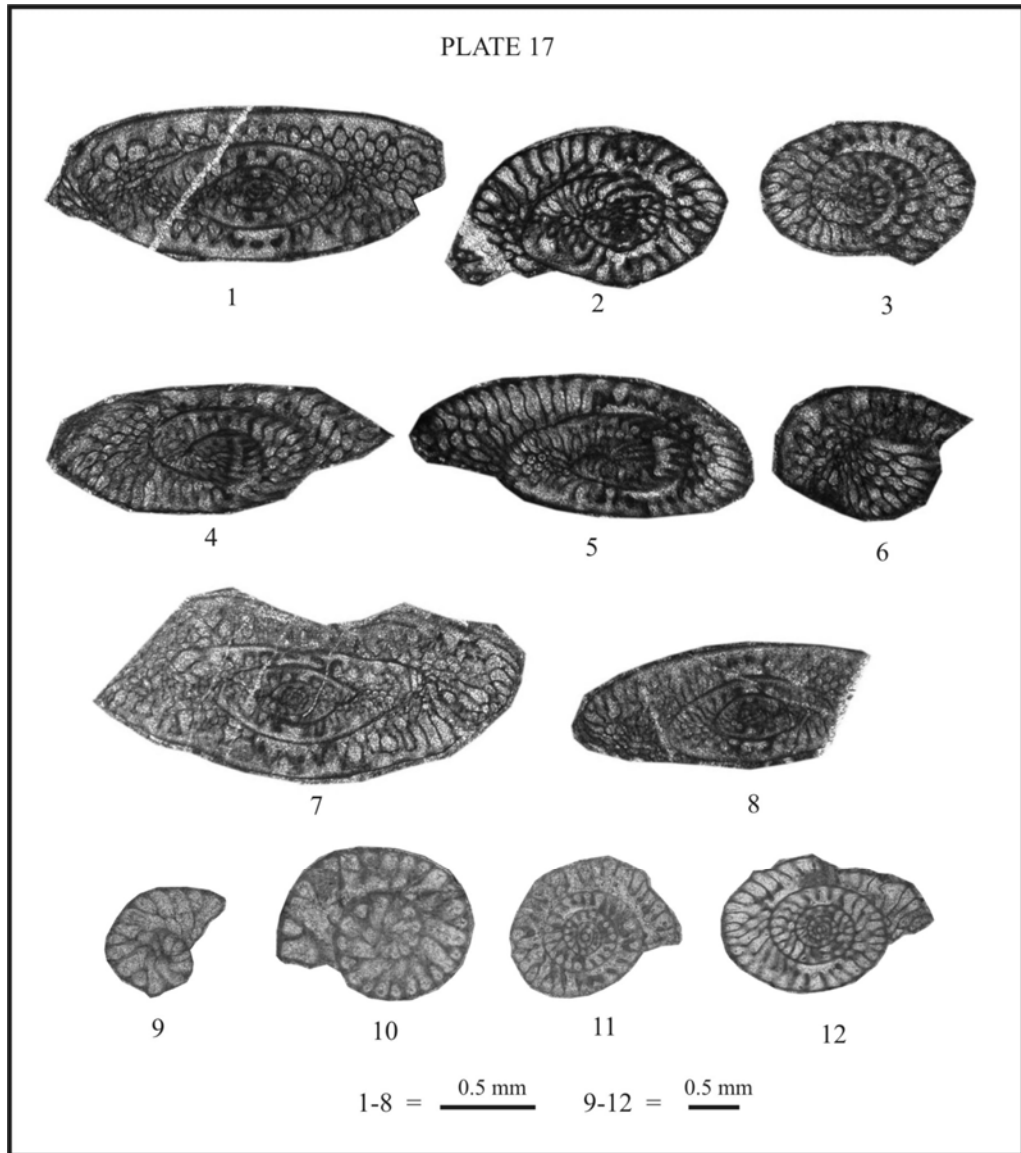


EXPLANATION OF PLATE 16

Figs. 1-3: *Lepidolina* sp.

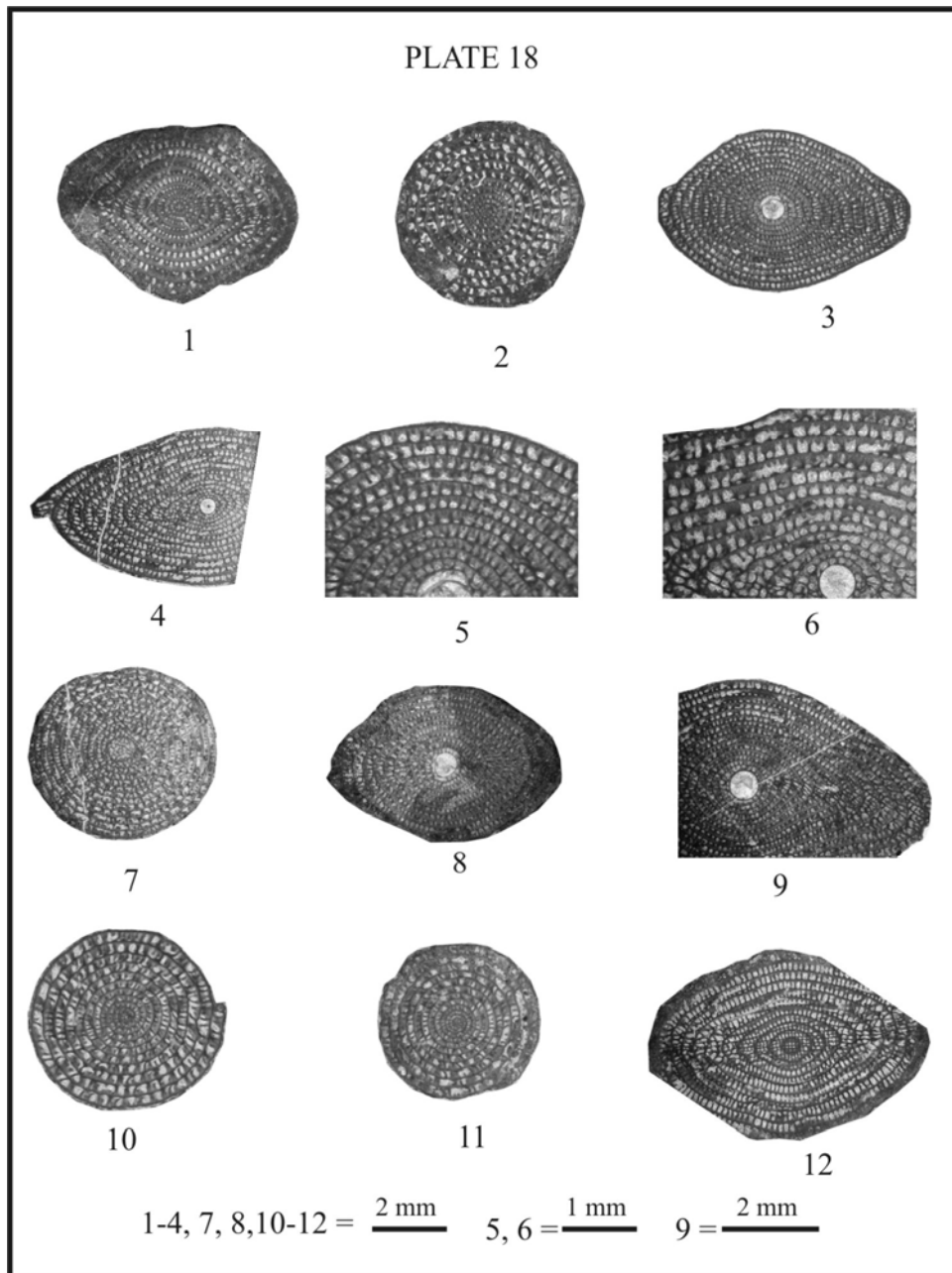
Figs. 4-7: *Nakinella* sp.

Figs. 8-12: *Chusenella* sp.



EXPLANATION OF PLATE 17

Figs. 1-12: *Dunbarula* sp.



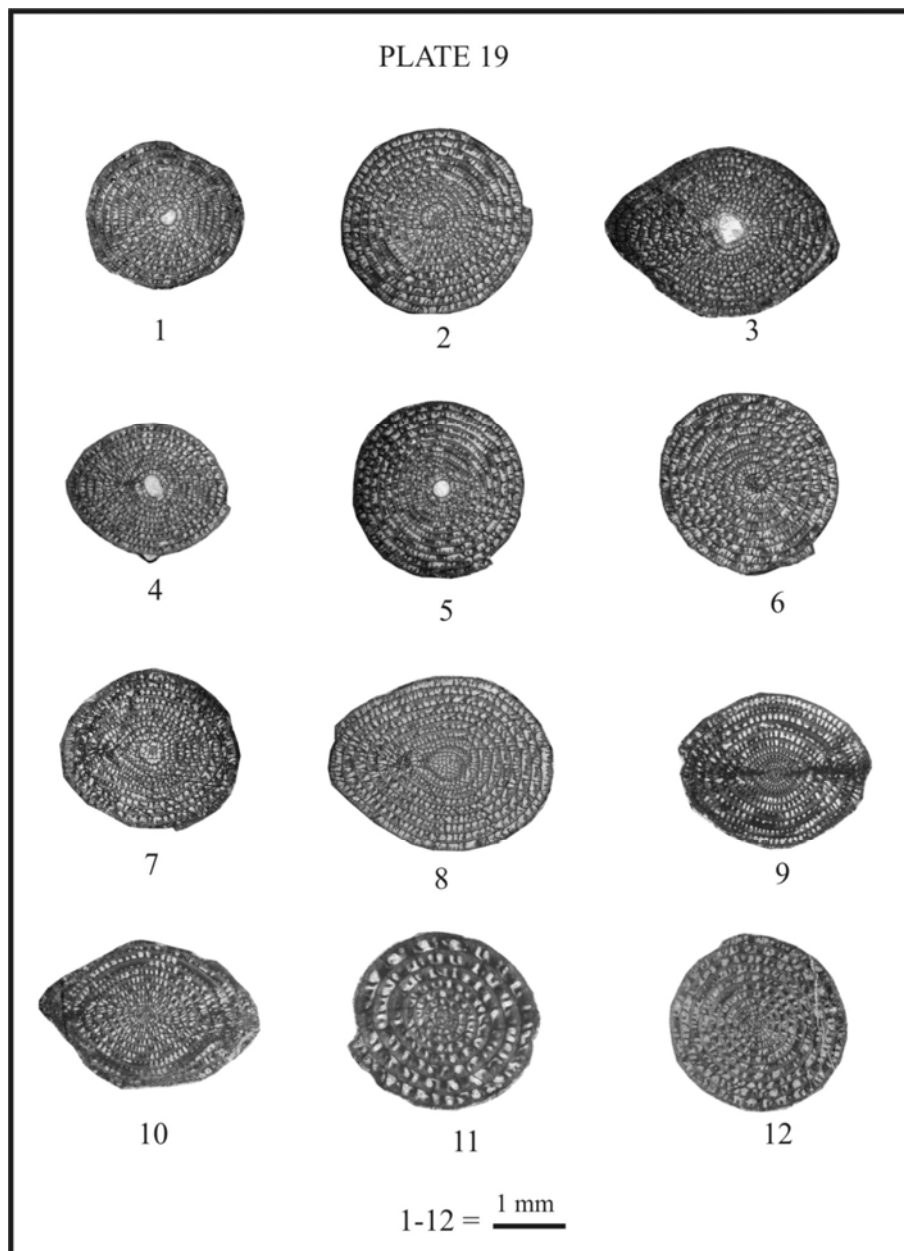
EXPLANATION OF PLATE 18

Figs. 1, 2: *Neoschwagerina* sp.

Figs. 3-6, 8: *Colania* sp.

Figs. 7, 9: *Lepidolina* sp.

Figs. 10-12: *Yabeina* sp.



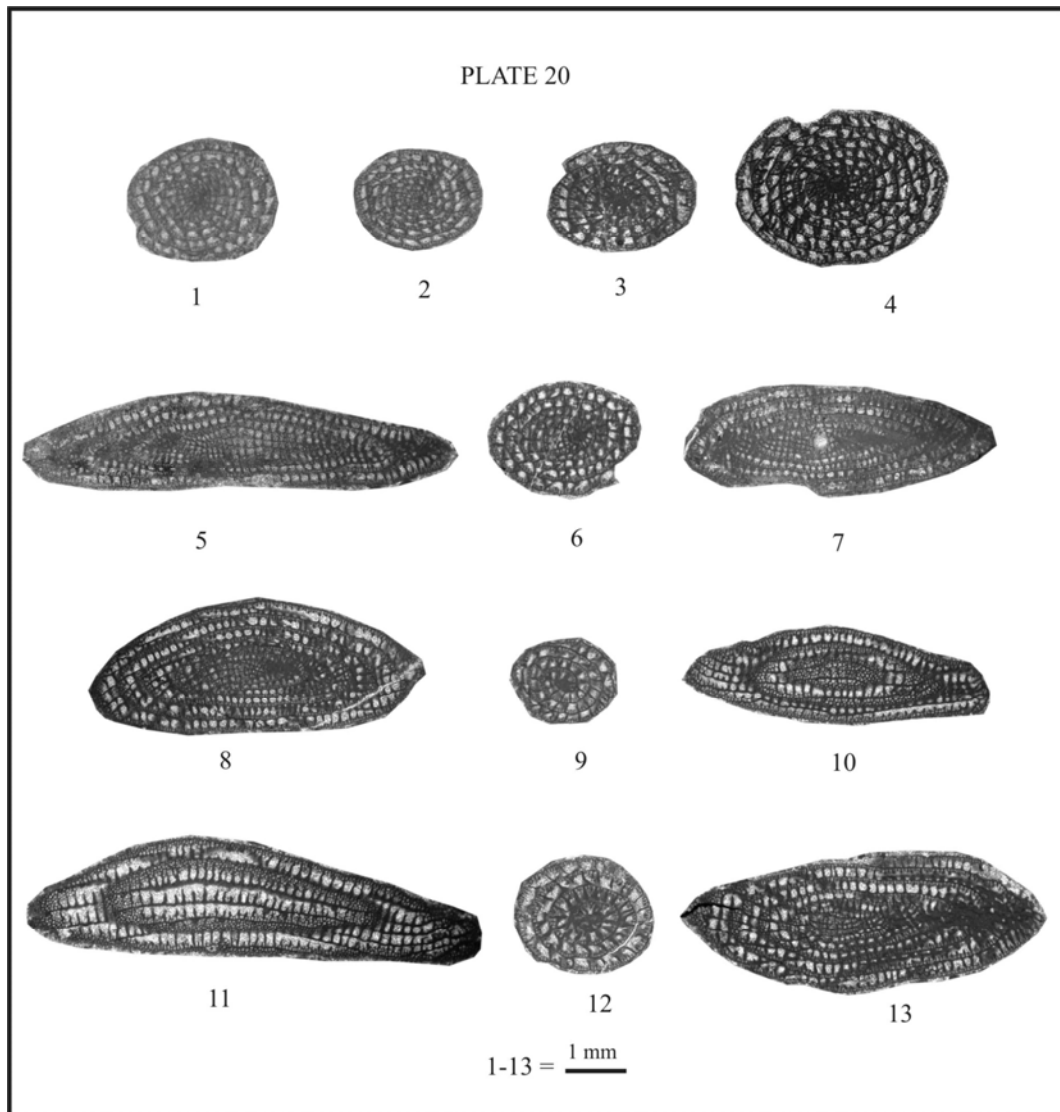
EXPLANATION OF PLATE 19

Figs. 1, 2: *Neoschwagerina* sp.

Figs. 3-6, 8: *Colania* sp.

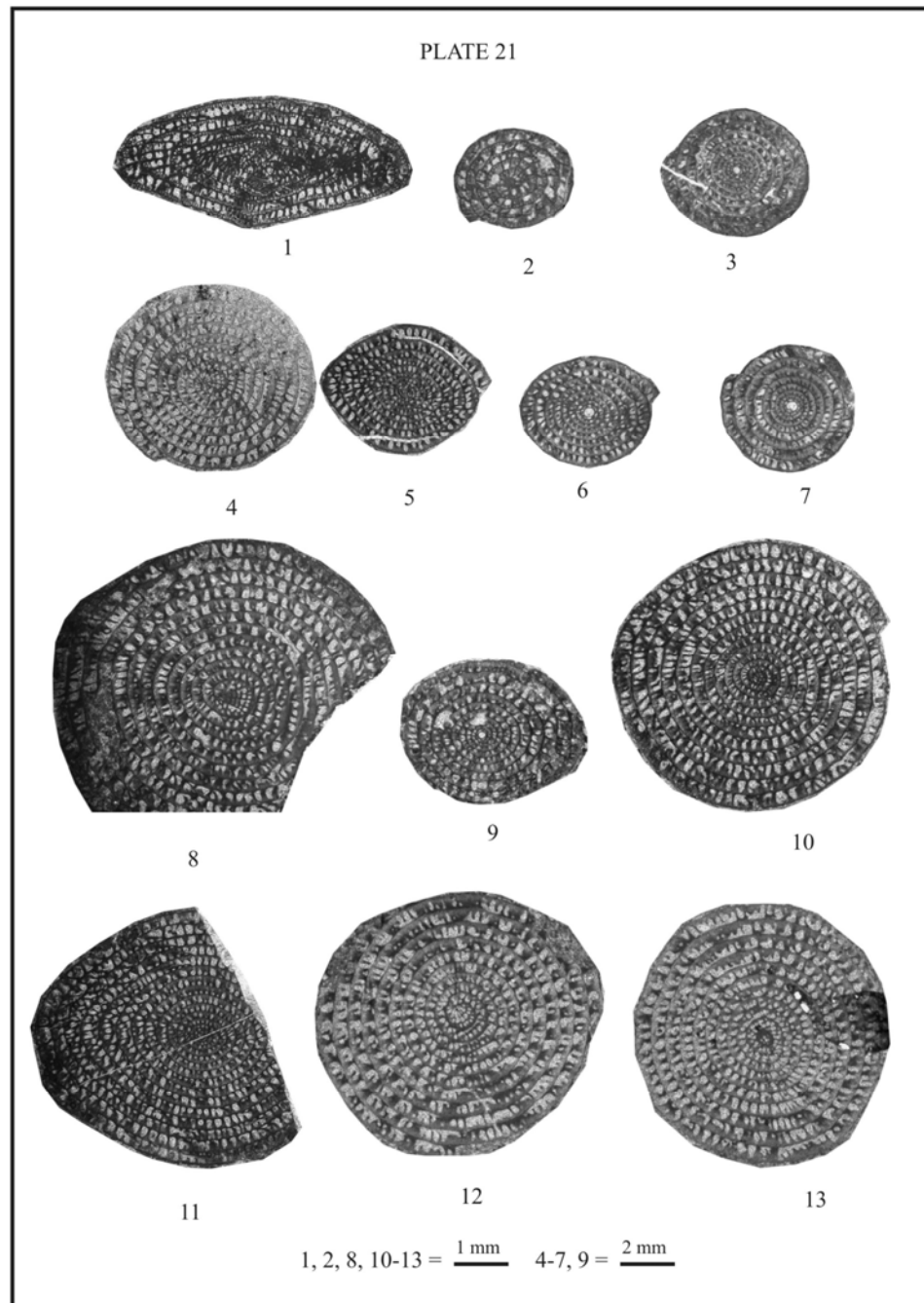
Figs. 7, 9: *Lepidolina* sp.

Figs. 10-12: *Yabeina* sp.



EXPLANATION OF PLATE 20

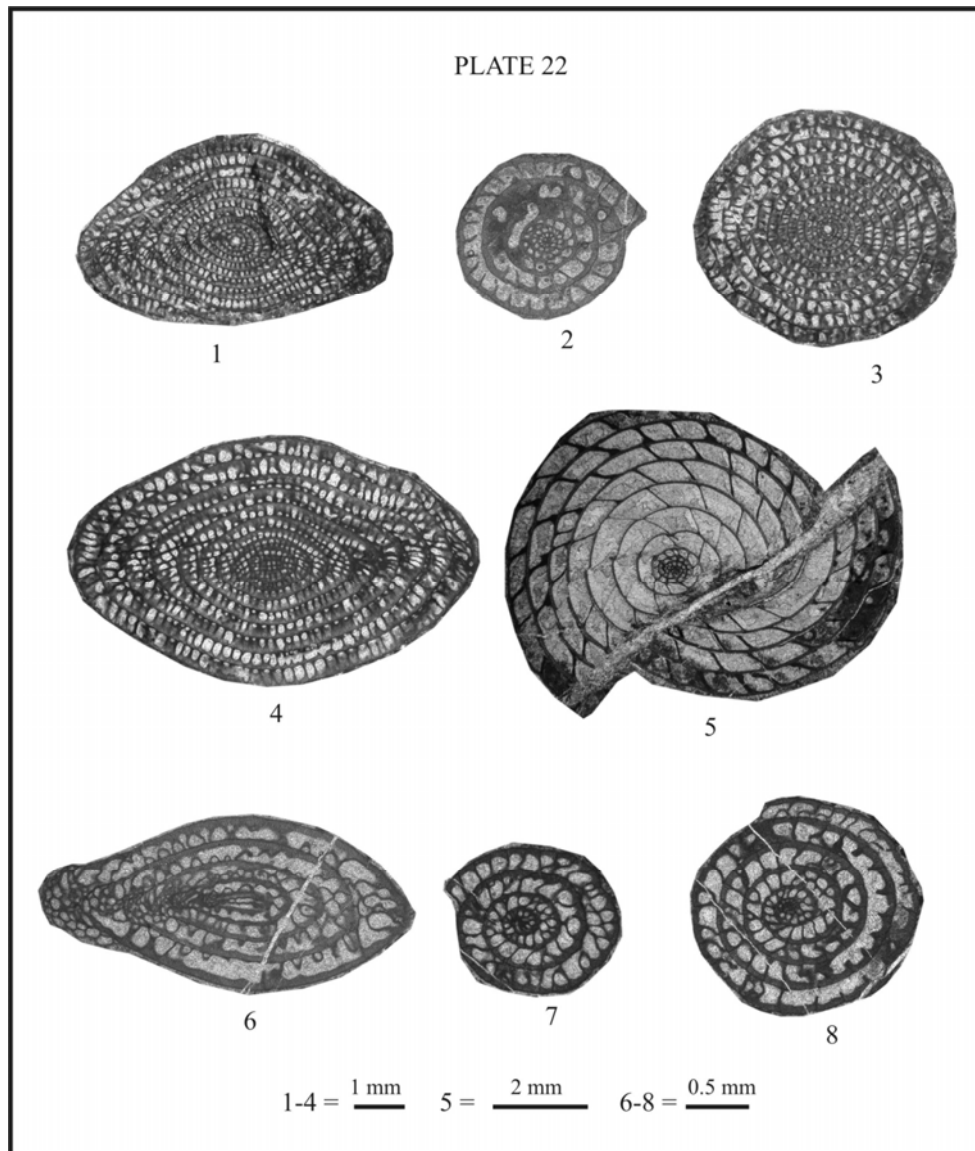
Figs. 1-13: *Sumatrina* sp.



EXPLANATION OF PLATE 21

Figs. 1, 2: *Sumatrina* sp.

Figs. 3-13: *Yabeina* sp.

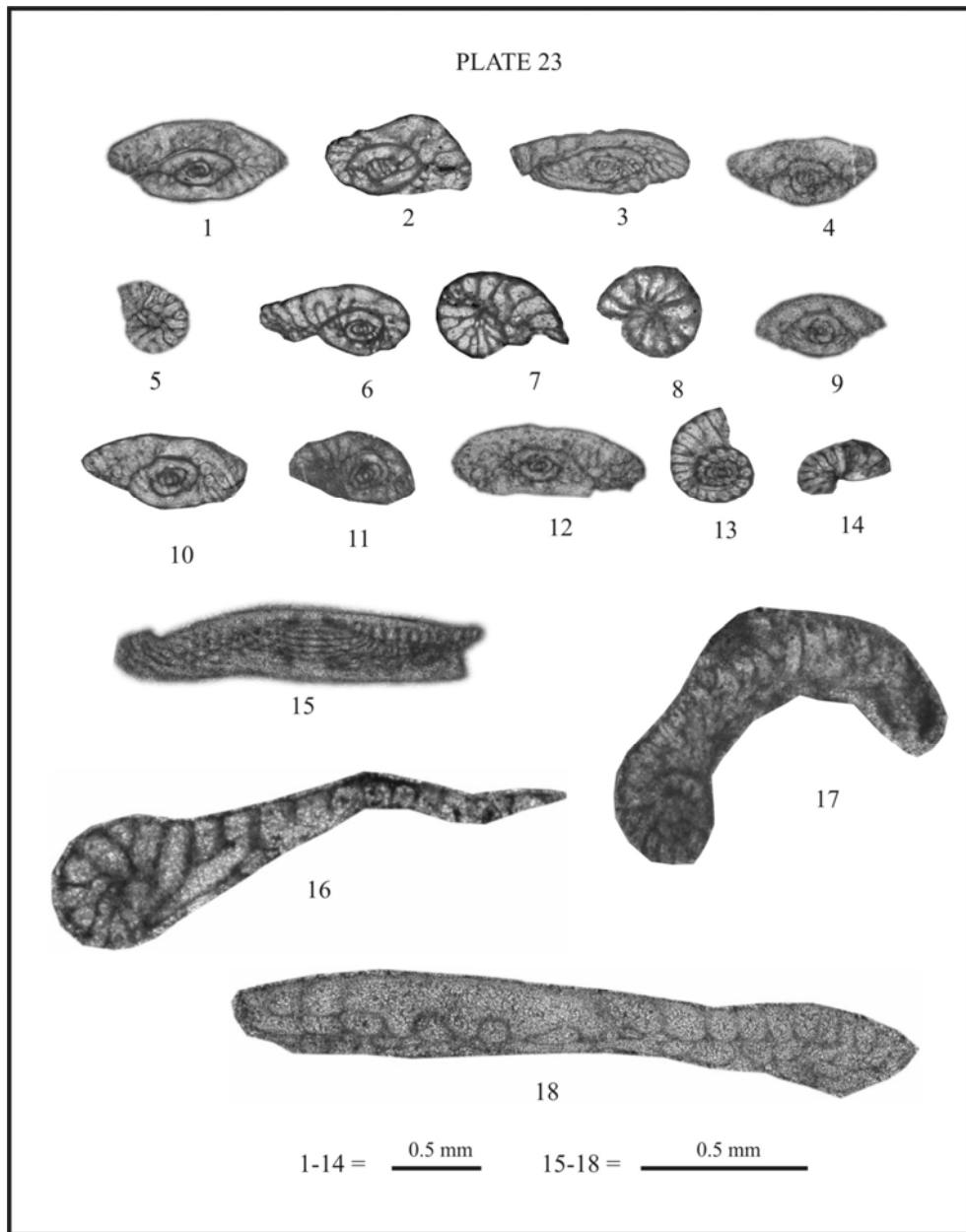


EXPLANATION OF PLATE 22

Figs. 1, 3, 4: *Yabeina* sp.

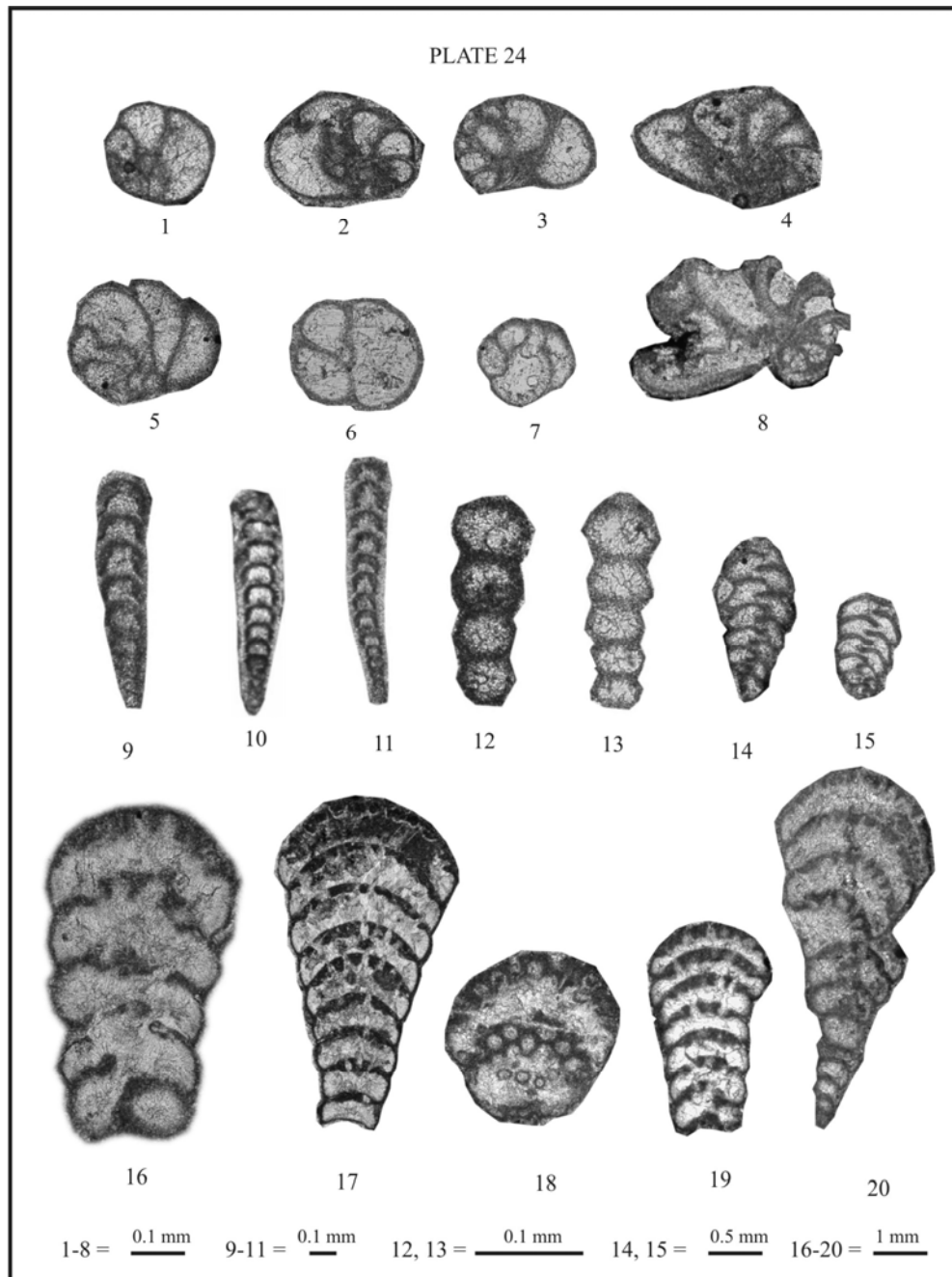
Figs. 2, 6-8: *Chusenella* sp.

Fig. 5: *Verbeekina* sp.



EXPLANATION OF PLATE 23

Figs. 1-18: *Conodofusiella* sp.



EXPLANATION OF PLATE 24

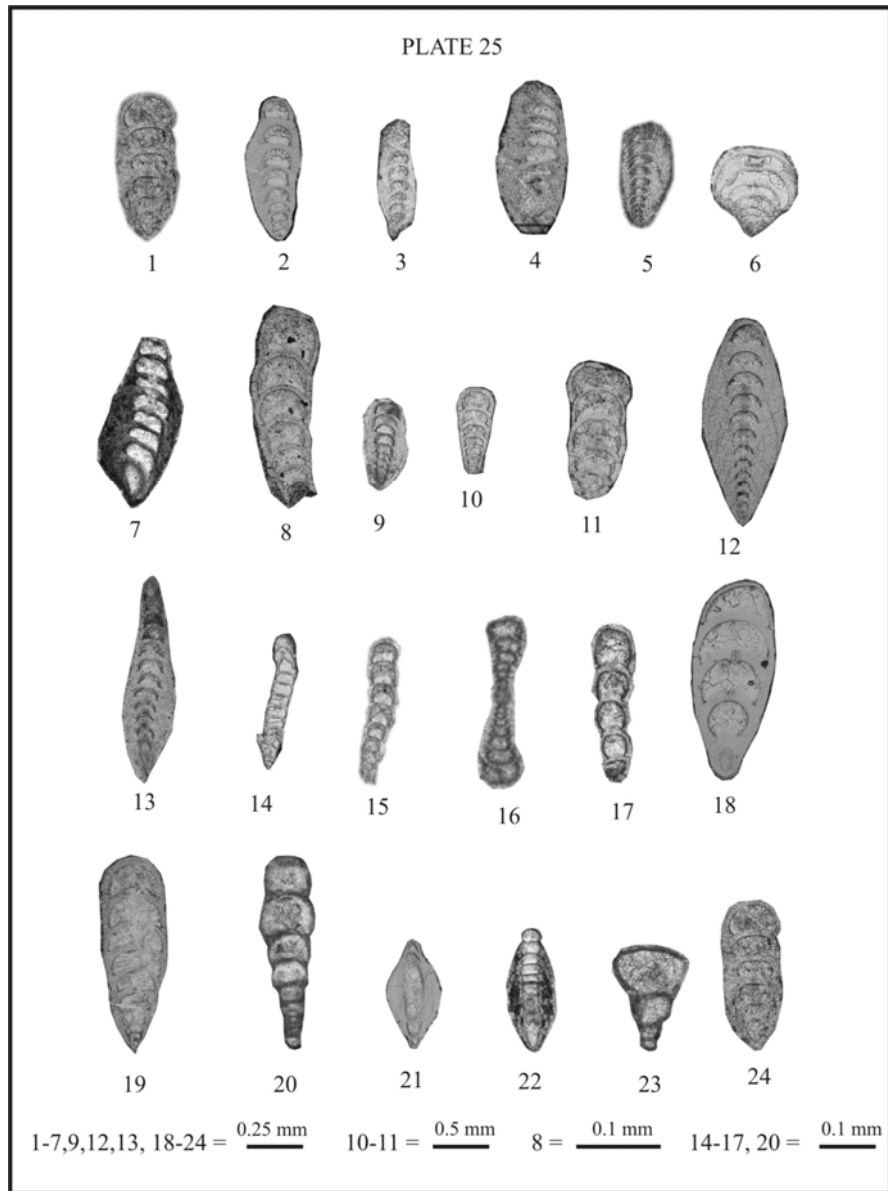
Figs. 1-8: *Globivalvulina* sp.

Figs. 9-13: *Nodosaria* sp.

Figs. 14, 15: *Dagmarita* sp.

Figs. 16, 19: *Climacammina* sp.

Figs. 17, 18, 20: *Cribrogenerina* sp.



EXPLANATION OF PLATE 25

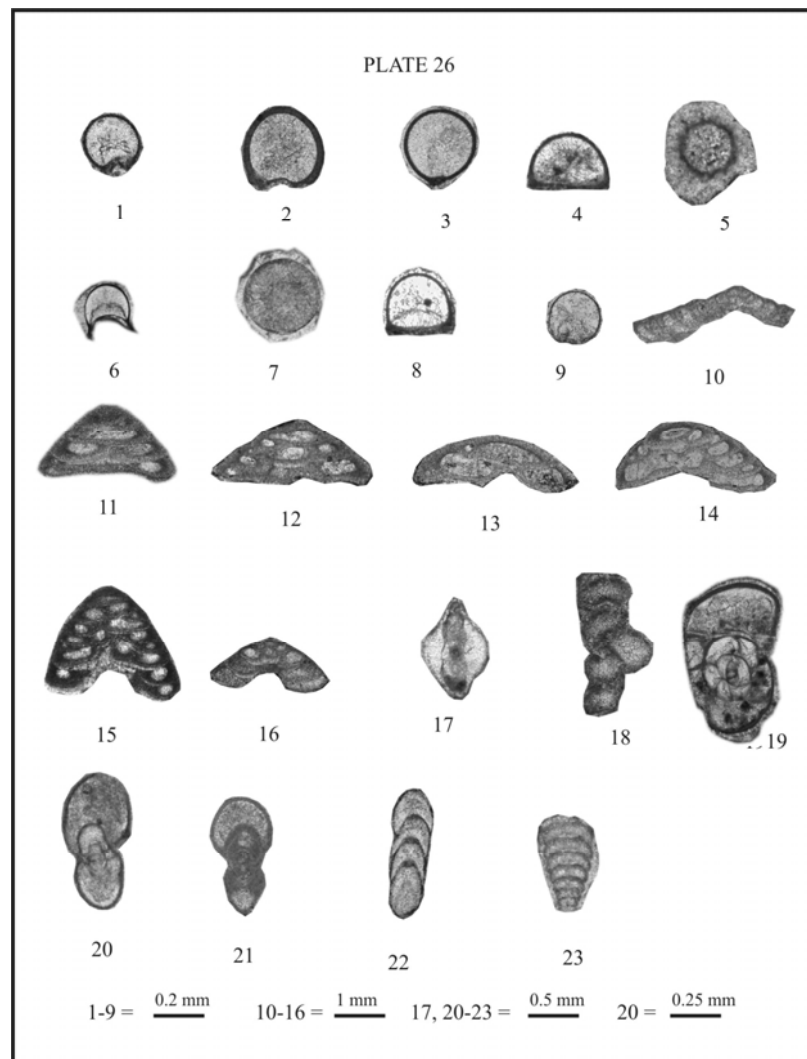
Figs. 1-5, 7, 9, 12, 13, 21, 22, 24: *Pachyphloia* sp.

Figs. 6, 23: *Geinitzina* sp.

Figs. 8: *Protonodosaria* sp.

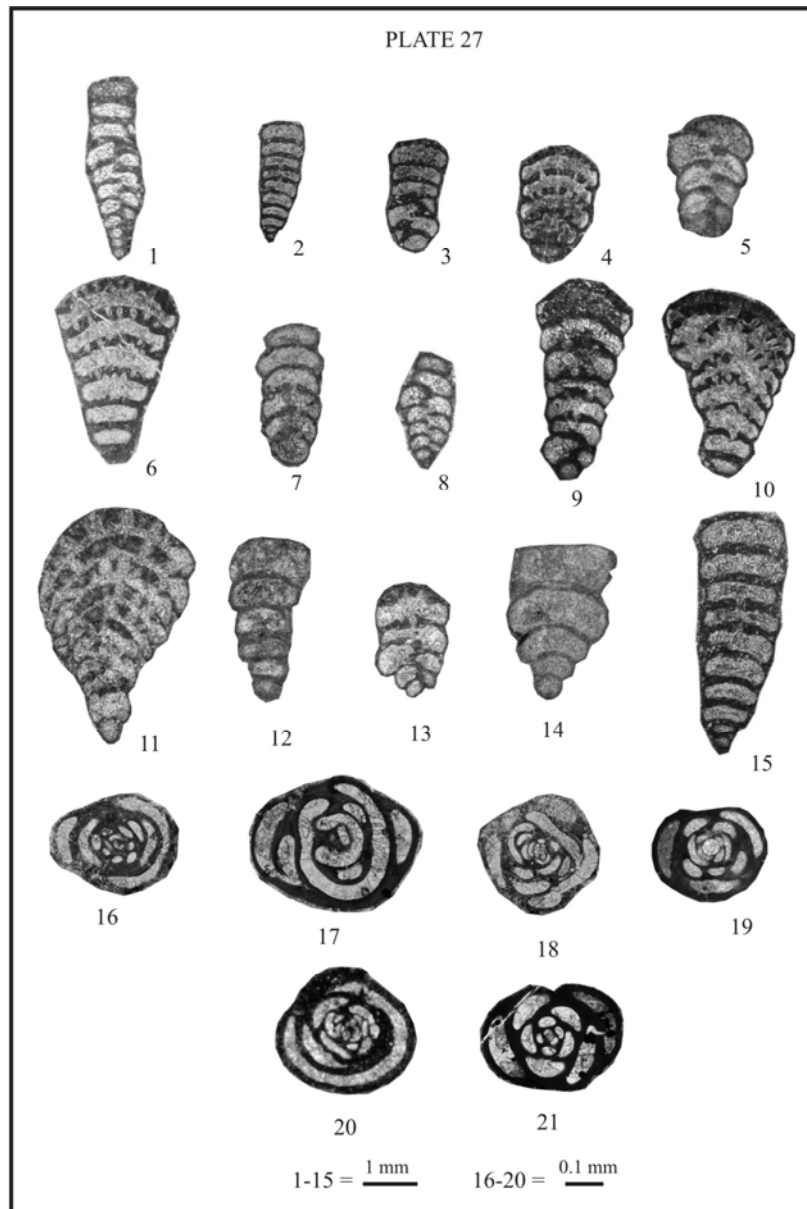
Figs. 10, 11, 18, 19: *Langella* sp.

Figs. 14, 15, 17, 20: *Nodosaria* sp.

Fig. 16: *Lasiodiscus* sp.

EXPLANATION OF PLATE 26

- | | |
|--|--------------------------------------|
| Figs. 1, 3, 9: <i>Diplosphaerina</i> sp. | Fig. 18: <i>Calcitornella</i> sp. |
| Figs. 2, 4, 8: <i>Tuberitina</i> sp. | Fig. 19: <i>Bradyna</i> sp. |
| Fig. 5: <i>Umbellina</i> sp. | Fig. 20: <i>Pseudokahlerina?</i> sp. |
| Fig. 6: <i>Eutuberitina</i> sp. | Fig. 21: <i>Neoendothyra?</i> sp. |
| Fig. 7: <i>Bisphaera</i> sp. | Fig. 22: <i>Fronkina</i> sp. |
| Figs. 10-16: <i>Tetrataxis</i> sp. | Fig. 23: <i>Geinitzina?</i> sp. |
| Fig. 17: <i>Pachyphloia</i> sp. | |



EXPLANATION OF PLATE 27

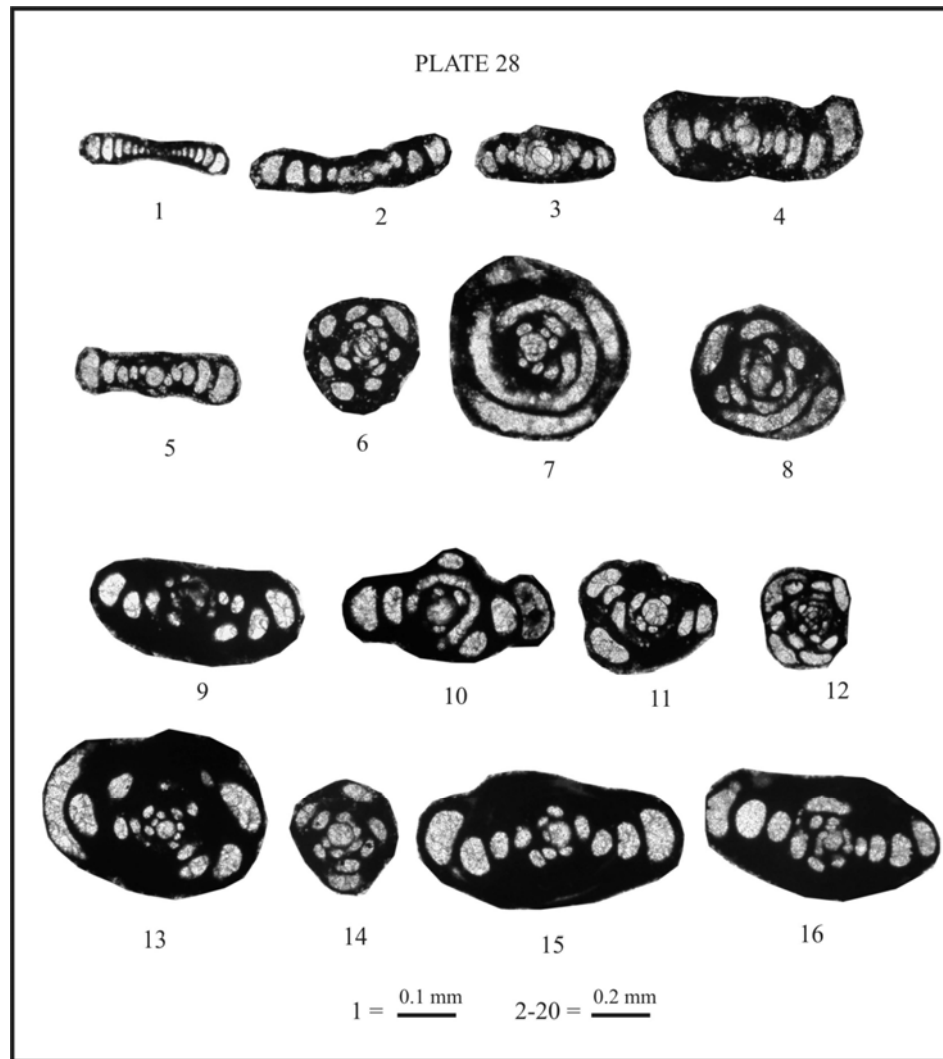
Figs. 1, 3, 5, 7, 8: *Deckerella* sp.

Figs. 2, 4, 9, 12-15: *Climacammina* sp.

Figs. 6, 10, 11: *Cribrogenerina* sp.

Figs. 16-18, 20: *Kamurana* sp.

Figs. 19-21: *Agathammina* sp.



EXPLANATION OF PLATE 28

Fig. 1: *Hemigordius* sp.

Figs. 2, 3, 4, 5, 7: *Neohemigordius grandis*.

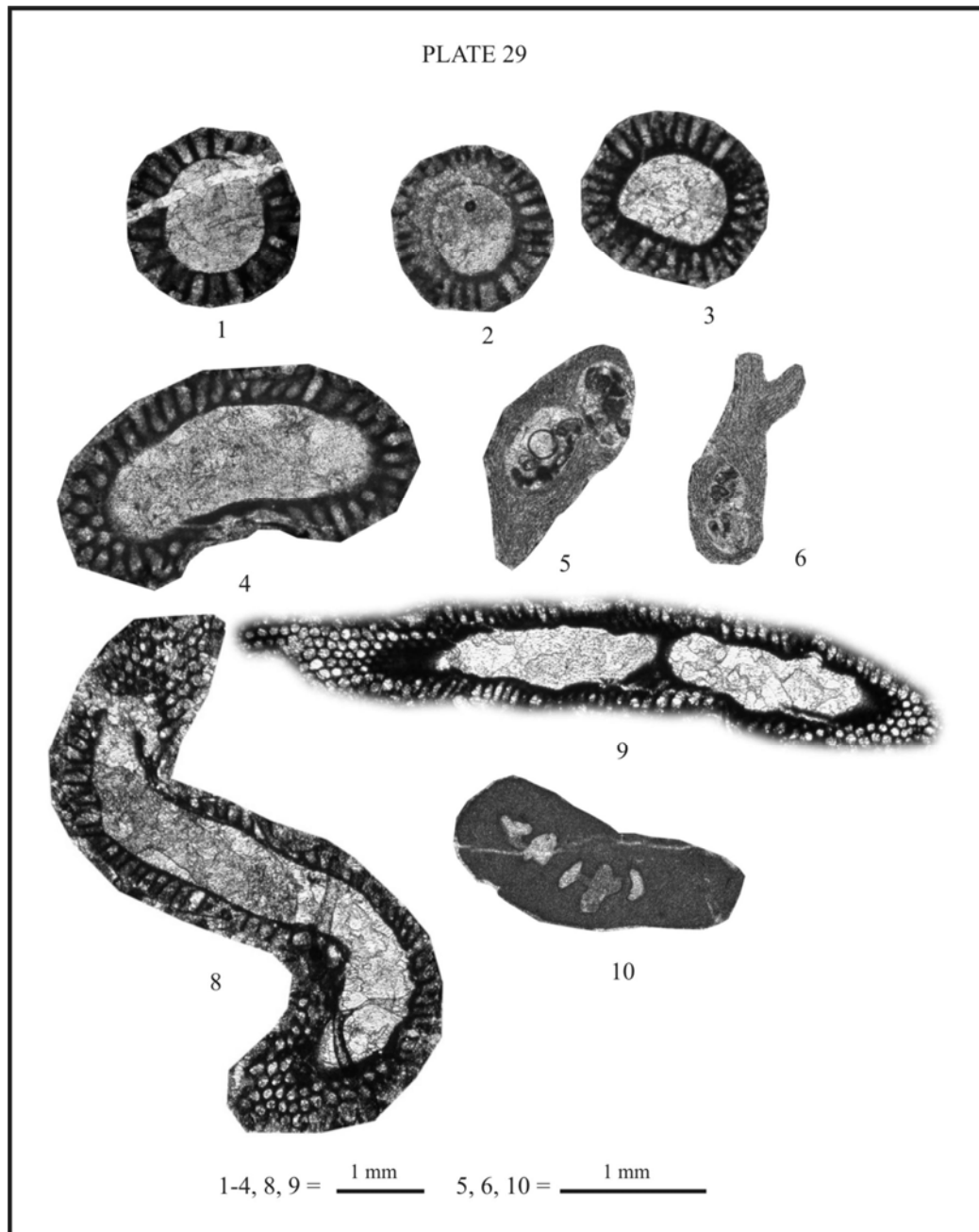
Figs. 6, 12, 13: *Kamurana* sp.

Figs. 8, 11, 14: *Agathammina* sp.

Figs. 9, 10, 15, 16: *Neohemigordius japonica*.

APPENDIX C

KEY ALGAE

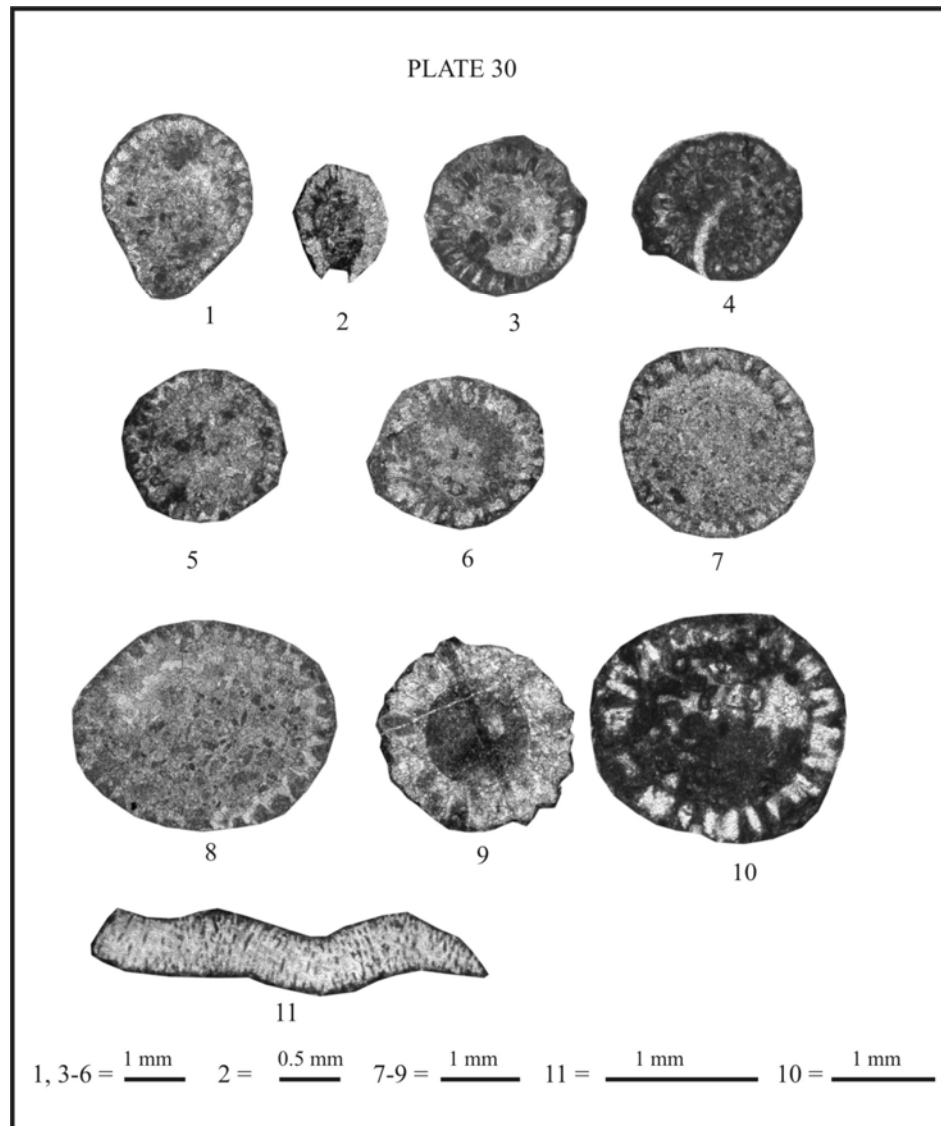


EXPLANATION OF PLATE 29

Figs. 1-4, 8, 9: *Vermiporella nipponica*.

Figs. 5, 6: *Undarella* sp.

Fig. 10: *Tubiphytes* sp.



EXPLANATION OF PLATE 30

Figs. 1-4, 5, 6, 10: *Mizzia* sp.

Figs. 7-9: *Gyroporella* sp.

Fig. 11: *Anthracoporell*

CURRICULUM VITAE

The author was born in January, 1976 in North-eastern province of Udon Thani. He completed high school level from Udonpittayanukool School in 1994. In 1998, he graduated degree of B.Sc. (Geotechnology) from Department of Geotechnology, Faculty of Technology, Khon Kaen University. During 1998-1999, he worked as a geotechnical engineer and a geologist for Siam Tone Co, Ltd. and Ten Consultant Co, Ltd. After that he did continue his higher study in Geology at Department of Geology, Faculty of Science, Chulalongkorn University. Consequently, he completed degree of M.Sc. (Geology) in 2003. Since October, 2003, he has undertaken his PhD at Suranaree University of Technology with a scholarship from Mahasarakham University. Recently, the author is a lecturer at Department of Biology, Faculty of Science, Mahasarakham University and researcher at Palaeontological Research and Education Centre of that university.